

From the: Munich Medical Research School,  
Ludwig Maximilians University



Dissertation  
zum Erwerb des Doctor of Philosophy (Ph.D.)  
an der Medizinischen Fakultät der  
Ludwig-Maximilians-Universität zu München

***Ventral striatal fMRI in affective and psychotic disorders:  
A transdiagnostic approach using resting state and task  
functional resonance imaging, clinical and genetic data***

vorgelegt von:  
Christopher Eberle

aus:  
Augsburg, Deutschland

Jahr:  
2021

---

Mit Genehmigung der Medizinischen Fakultät der  
Ludwig-Maximilians-Universität zu München

<b>First evaluator (1. TAC member):</b>	Prof. Dr. Nikolaos Koutsouleris
<b>Second evaluator (2. TAC member):</b>	Prof. Dr. Dr. Elisabeth Binder
<b>Third evaluator:</b>	Prof. Dr. Michael Ingrisch
<b>Fourth evaluator:</b>	Priv. Doz. Dr. Elisabeth Kaufmann

**Dean: Prof. Dr. med. Thomas Gudermann**

date of the defense:

07.10.2021



## Table of content

<b>Table of content</b> .....	<b>5</b>
<b>Abstract</b> .....	<b>7</b>
<b>List of figures</b> .....	<b>9</b>
<b>List of tables</b> .....	<b>11</b>
<b>List of abbreviations</b> .....	<b>13</b>
<b>1. Introduction</b> .....	<b>15</b>
1.1 Need of a better classification system of psychiatric diseases.....	15
1.2 The reward system as a potential source of biomarkers .....	27
1.3 Imaging genetics as a translational approach in biomedical research.....	40
1.4 Resting state fMRI .....	45
1.5 Aims and scope of this study .....	51
<b>2. Endophenotype potential of the nucleus accumbens</b> .....	<b>53</b>
2.1 Importance and approaches of early detection of SCZ .....	53
2.2 Methods.....	58
2.3 Results.....	64
2.4 Discussion .....	71
2.5 Conclusion .....	75
<b>3. Using fMRI activation during reward anticipation to characterize the reward system across diagnostic boundaries</b> .....	<b>77</b>
3.1 Reward anticipation as a source of biomarkers in multiple networks.....	77
3.2 Methods.....	79
3.3 Results.....	84
3.4 Discussion .....	142
3.5 Conclusions.....	152
<b>4. General Discussion</b> .....	<b>153</b>
4.1 Overall Summary .....	153
4.2 The potential of reward processing in psychiatry .....	154
4.3 The diminution of the phenomenological reduction .....	154
4.4 The potential of neurobiological measures to overcome the classification of verbally reported symptoms .....	155
<b>References</b> .....	<b>157</b>

**Acknowledgements.....201**

**Affidavit .....203**

**Confirmation of congruency .....205**

**Publication .....207**

## Abstract:

The effective clinical management of psychotic and affective disorders still represents a major challenge in psychiatry. Due to the high prevalence of these disorders and the subjective suffering, they cause a massive burden for the health system and society, and improvement in diagnostic and treatment strategies is urgently sought. In consideration of the literature, there are two promising avenues for this endeavour: On the one hand, particularly regarding schizophrenia (SCZ), early detection of high risk states or disease manifestation is crucial for the eventual treatment success. On the other hand, the heterogeneity of psychotic and affective disorders as well as blurry boundaries between the associated clinical syndromes often leave the diagnosis, which is the foundation of an evidence based treatment selection, on shaky ground. At the neurobiological level, several lines of evidence underline the role of the ventral striatum, particularly the nucleus accumbens (NAcc), for the pathophysiology of psychosis and more generally reward processing. Disturbed reward processing in turn is related to anhedonia, a core symptom of major depressive disorder (MDD), bipolar disorder (BD) and also SCZ.

Against this background, this thesis aimed to unravel the potential of ventral striatal brain circuits as a source of biomarkers of psychotic and affective disorders. For this purpose, two sub-studies were performed: Firstly, we studied the impact of a validated polygenic risk score (PGRS) for SCZ, childhood adversity (CA) as widespread environmental factor and their interaction on resting state (RS) fMRI measures and NAcc seed connectivity in 253 healthy controls (HC) and compared these patterns with fully expressed disease in 23 patients with SCZ. Consistent with previous reports, SCZ patients showed strong regional functional connectivity density (FCD) increases in subcortical nuclei, particularly in the NAcc, compared with HC. Furthermore, in the HC sample, a positive association between the FCD of the NAcc and both the PGRS and the interaction between PGRS and CA was found. Fine-mapping exhibited increased connectivity between the NAcc and visual association cortices for high levels of both PGRS and the PGRS-by-CA interaction. Taken together, this study showed that in HC, high PGRS for SCZ affects both global and regionally specific connectivity of the NAcc in a similar pattern as observed in SCZ patients, and that this effect was already amplified even by a history of very mild CA. This latter observation strengthened the notion that environmental factors need consideration in imaging genetics studies.

Secondly, we examined the neural underpinnings of reward anticipation (RA) in MDD, BD and SCZ as studied by fMRI. This study revealed that aberrantly low striatal activation during RA is typical of SCZ, whereas the response of this network appeared to be preserved in MDD and BD. Interestingly, two further large-scale brain networks involved in RA – the salience network and the default mode network showed both transdiagnostic and further disease-specific alterations: While the salience network was found to be impaired primarily in SCZ patients, all patient groups revealed deficits in the suppression of the default mode network. Among hub regions of all three networks that were further differentiated in an early and a late response period, levels of anhedonia were correlated with the extent of the (early) hippocampal deactivation failure across diagnostic boundaries.

In sum, both investigations confirm the possibility to use fMRI to probe the functional status of the ventral striatum. The first study underlines the centrality of striatal regions in the pathophysiology of psychosis as these alterations already emerged in healthy individuals at high genetic risk for developing SCZ, particularly when including unspecific environmental risk to the model. Hyperconnectivity of this region in SCZ during the resting state matched with a blunted response during the RA task. The latter study showed that at least two further large-scale brain networks are impaired in both psychotic and affective disorders during RA, indicating a potential of reward processing as a source of imaging phenotypes or biomarkers to characterize patients of the respective disease spectrum.



## List of figures

- Figure 1.** The limbic dopaminergic pathways.
- Figure 2.** Aberrant salience hypothesis.
- Figure 3.** Levels of analysis and the respective measurement precision illustrated with an example of schizophrenia.
- Figure 4.** Number of studies tagged “resting-state” and “fMRI” in PubMed between 1990 and 2020.
- Figure 5.** Basic principle of seed-based RS fMRI.
- Figure 6.** NAcc mask.
- Figure 7.** Proof-of-concept group averages.
- Figure 8.** Comparison of FCD between HC and SCZ.
- Figure 9.** PGRS effects at the level of FCD and NAcc seed analyses.
- Figure 10.** Effects of PGRS.
- Figure 11.** Trial sequence of the reward anticipation task.
- Figure 12.** Temporal dissection of the stimulus presentation in three 2 s segments.
- Figure 13.** Atlas-based segmentation of basal ganglia.
- Figure 14.** Task-positive BOLD amplitude effects of RA (full 6 s) in HC.
- Figure 15.** Task-negative BOLD amplitude effects of RA (full 6 s) in HC.
- Figure 16.** Task-positive BOLD amplitude effects during early RA in HC.
- Figure 17.** Task-negative BOLD amplitude effects of early RA in HC.
- Figure 18.** Task-positive BOLD amplitude effects of late RA in HC.
- Figure 19.** Task-negative BOLD amplitude effects of late RA in HC.
- Figure 20.** Violation of regressor orthogonality in combined early/late RA 1<sup>st</sup> level models.
- Figure 21.** Differences between task effects in the early and late RA phases.
- Figure 22.** Final ROI selection based on activation and deactivation during 6 s of RA.
- Figure 23.** Task effects of RA in patients with MDD.
- Figure 24.** Task effects of early RA in patients with MDD.
- Figure 25.** Task effects of late RA in patients with MDD.
- Figure 26.** Task effects of RA in patients with BD.
- Figure 27.** Task effects of early RA in patients with BD.
- Figure 28.** Task effects of late RA in patients with BD.
- Figure 29.** Task effects of RA in patients with SCZ.
- Figure 30.** Task effects of early RA in patients with SCZ.
- Figure 31.** Task effects of late RA in SCZ.
- Figure 32.** Panoramic overview of RA task effects per diagnostic group.
- Figure 33.** F-contrast of RA effects.
- Figure 34.** Group differences in RA (6 s of stimulus presentation) between MDD and HC.
- Figure 35.** Group differences in RA (6 s of stimulus presentation) between BD and HC.
- Figure 36.** Group differences in RA (6 s of stimulus presentation) between SCZ and HC.
- Figure 37.** F-contrast of early RA effects.
- Figure 38.** Group differences in early RA between SCZ and HC.
- Figure 39.** F-contrast of late RA effects.
- Figure 40.** Group differences in late RA between MDD and HC.
- Figure 41.** Group differences in late RA between SCZ and HC.
- Figure 42.** BOLD activation in peak voxels of temporal DMN hubs.
- Figure 43.** Significant time main effect in the right anterior insula.
- Figure 44.** BOLD deactivation in temporal DMN hubs.
- Figure 45.** Significant time effect of the mesencephalic cluster.
- Figure 46.** BOLD activation in the left hippocampal cluster during early RA.

**Figure 47.** Correlation between BDI-based anhedonia scores and the left hippocampal cluster contrast value during early RA.

**Figure 48.** Group effects of RA in the left NAcc.

**Figure 49.** Group effects of RA in the left putamen.

**Figure 50.** Group effects in the left pallidum.

**Figure 51.** Time effect of RA in the left and right NAcc.

## List of tables

- Table 1.** Comparison of the criteria for MDD according to ICD-10 and DSM-5.
- Table 2.** Comparison of the criteria for manic episodes according to ICD-10 and DSM-5.
- Table 3.** Positive, negative, and general symptoms of the PANSS.
- Table 4.** Comparison of the diagnostic criteria of SCZ according to DSM-5 and ICD-10.
- Table 5.** Clinical and demographic characteristics of study participants.
- Table 6.** CTQ severity classes\* of healthy subjects.
- Table 7.** Comparison von FCD<sub>voxel</sub> between HC and patients.
- Table 8.** Seed analysis of the NAcc: Effects of PGRS and PGRS-by-CA.
- Table 9.** Demographic and clinical characteristics participants.
- Table 10.** Anhedonia and total score of the BDI.
- Table 11.** Overall RTs and RTs by trial type ('money', 'verbal').
- Table 12.** Task-positive effects of RA (full 6 s) in healthy controls ( $p_{\text{voxel.FWE}} < 0.05$ ;  $k > 10$ ).
- Table 13.** Task-negative effects of RA (full 6 s) in healthy controls ( $p_{\text{voxel.FWE}} < 0.05$ ;  $k > 10$ ).
- Table 14.** Task-positive effects of early RA in healthy controls ( $p_{\text{voxel.FWE}} < 0.05$  ( $k > 10$ )).
- Table 15.** Task-negative effects of early RA in healthy controls ( $p_{\text{voxel.FWE}} < 0.05$ ;  $k > 10$ ).
- Table 16.** Task-positive effects of late RA in healthy controls ( $p_{\text{voxel.FWE}} < 0.05$ ;  $k > 10$ ).
- Table 17.** Task-negative effects of late RA in HC ( $p_{\text{voxel.FWE}} < 0.05$ ;  $k > 10$ ).
- Table 18.** Contrasting 'RA<sub>early</sub> > RA<sub>late</sub>' in HC ( $p_{\text{voxel.FWE}} < 0.05$ ).
- Table 19.** Contrasting RA<sub>early</sub> < RA<sub>late</sub> in HC ( $p_{\text{voxel.FWE}} < 0.05$ ;  $k > 10$ ).
- Table 20.** Task-positive and negative effects of RA in MDD ( $p_{\text{voxel.FWE}} < 0.05$ ;  $k > 10$ ).
- Table 21.** Task-positive and negative effects of early RA in MDD ( $p_{\text{voxel.FWE}} < 0.05$ ;  $k > 10$ ).
- Table 22.** Task-positive and task-negative effects of late RA in MDD ( $p_{\text{voxel.FWE}} < 0.05$ ;  $k > 10$ ).
- Table 23.** Task-positive and negative effects of RA in BD ( $p_{\text{voxel.FWE}} < 0.05$ ;  $k > 10$ ).
- Table 24.** Task-positive and negative effects of late RA in BD ( $p_{\text{voxel.FWE}} < 0.05$ ;  $k > 10$ ).
- Table 25.** Task-positive and negative effects of RA in SCZ ( $p_{\text{voxel.FWE}} < 0.05$ ;  $k > 10$ ).
- Table 26.** Task-positive and -negative effects of early RA in SCZ ( $p_{\text{voxel.FWE}} < 0.05$ ;  $k > 10$ ).
- Table 27.** Task-positive effects of late RA in SCZ ( $p_{\text{voxel.FWE}} < 0.05$ ;  $k > 10$ ).
- Table 28.** F-contrast of RA between diagnostic groups ( $p_{\text{voxel}} < 0.005$ ,  $p_{\text{cluster.FWE}} < .10$ ).
- Table 29.** Regions showing group differences in RA in directed T-contrasts ( $p_{\text{voxel}} < 0.005$ ;  $p_{\text{cluster.FWE}} < 0.05$ ).
- Table 30.** F-contrast of early RA between diagnostic groups ( $p_{\text{voxel}} < 0.005$ ,  $p_{\text{cluster.FWE}} < .10$ ).
- Table 31.** T-contrasts of early RA effects between patient groups and HC ( $p_{\text{voxel}} < 0.005$ ;  $p_{\text{cluster.FWE}} < 0.05$ ).
- Table 32.** F-contrast of late RA between diagnostic groups ( $p_{\text{voxel}} < 0.005$ ,  $p_{\text{cluster.FWE}} < .10$ ).
- Table 33.** T-contrasts of the late RA phase between the patient groups and HC ( $p_{\text{voxel}} < 0.005$ ;  $p_{\text{cluster.FWE}} < 0.05$ ).
- Table 34.** Dynamic characteristics (early vs. late RA phase) in all 14 ROIs and 6 atlas regions.
- Table 35.** Group main effects, time main effects and group-by-time effects in peak voxels.
- Table 36.** Pairwise post hoc T-tests group-by-time interaction effects.
- Table 37.** Group main effects, time main effects and group-by-time effects in cluster ROIs.
- Table 38.** Post hoc time-by-group effects in cluster ROIs investigated separately per patient group.
- Table 39.** Specificity interrogation of single categories, the total score of the BDI-II, the anhedonia score and the inverse score.
- Table 40.** Group main effects, time main effects and group-by-time effects activation in atlas/segmentation based pre-defined VS regions.
- Table 41.** Group-by-time effects in atlas- and segmentation-based VS regions.



## List of abbreviations

**AAL** Automated Anatomical Labelling  
**AI** anterior insula  
**ACC** anterior cingulate cortex  
**CA** childhood adversity  
**CSF** cerebrospinal fluid  
**CTQ** Childhood Trauma Questionnaire  
**EPI** echo-planar image  
**fMRI** functional magnetic resonance imaging  
**FWE** family-wise error  
**GM** grey matter  
**GWAS** genome-wide association studies  
**HIP** Hippocampus  
**ICA** Independent Component Analysis  
**IFG** inferior frontal gyrus  
**MRI** magnetic resonance imaging  
**NAcc** nucleus accumbens  
**PANSS** Positive and Negative Syndrome Scale  
**PCC** posterior cingulate cortex  
**PET** positron emission tomography  
**PFC** prefrontal cortex  
**PGRS** polygenic risk score  
**QC** quality control  
**RA** reward anticipation  
**RS** resting state  
**SCZ** schizophrenia  
**SD** standard deviation  
**SFG** superior frontal gyrus  
**SMA** supplemental motor area  
**SPECT** single photon emission computed tomography  
**STG** superior temporal gyrus  
**VTA** ventral tegmental area  
**WM** white matter



# 1. Introduction

## 1.1 Need of a better classification system of psychiatric diseases

### 1.1.1 Mental health as a core issue of the health system

Mental disorders are regarded as the core health challenge of the 21<sup>st</sup> century (Wittchen et al., 2011). Several statistics point to the widespread prevalence of mental diseases: For example, more than 10% of the worldwide population is suffering from a mental disorder, and over a third of the total EU population is affected each year (Patel & Saxena, 2014; Wittchen et al., 2011). Furthermore, a recent meta-analysis proposed that the lifetime prevalence of mental diseases within the general population in middle- and high-income countries is over 50% (Trautmann et al., 2016). Besides the difficulties in school achievement and professional career which typically follow severe mental health issues, an elevated mortality risk is a common feature of multiple psychiatric disorders (Walker et al., 2015). This accounts, among other diseases, for schizophrenia (SCZ) (Cuijpers et al., 2014; Saha et al., 2007), major depressive disorder (MDD) (Gilman et al., 2017; Wulsin et al., 1999) and bipolar disorder (BD) (Crump et al., 2013). This increased general mortality in psychiatric diseases has often been attributed to an unhealthy lifestyle (Chesney et al., 2014; Walker et al., 2015), including poor diet, physical inactivity, chronic disease, tobacco smoking (Prochaska et al., 2017), or substance abuse (Kavanagh et al., 2002; Regier, 1990). In addition, numerous psychiatric conditions are linked to an increased risk of suicide, for example MDD, SCZ, BD as well as borderline personality disorder and anorexia nervosa (Chesney et al., 2014; Hor & Taylor, 2010).

Apart from the often dramatic impact on the lives of those affected, their relatives and their social and work-related environment, there is a robust body of evidence suggestive of high incisive consequences of mental disorders on the social system: In 2016, 7% of all global burden of disease as measured in DALY (a measurement capturing the amount of years lost due to disability and premature mortality) and 17% of years lived in disability were related to mental health illnesses (Rehm & Shield, 2019). The resulting financial expenses are enormous, although estimated costs naturally vary depending on the type of disorder, populations investigated, sources of costs considered, lack of data and analytical framework (Trautmann et al., 2016). Based on data from 2010, the global economic costs of mental disorders were estimated at \$2.5 trillion worldwide (Trautmann et al., 2016), whereas they amounted to €798 billion in European countries (Gustavsson et al., 2011). Furthermore, due to demographic changes and longer life expectancy, these expenses are projected to double until 2030 (Patel & Saxena, 2014). Moreover, further additional costs incurred for the healthcare system can be grouped into two types (Gustavsson et al., 2011): Firstly, direct non-medical costs, encompassing social services, special accommodation or informal care. Secondly, indirect costs, including production losses caused by work absence, early retirement and mortality. Regarding indirect costs, Insel et al. (2008) assumed that mental illnesses cause US\$193.2 billion in lost earnings each year. Taken together and bearing societal changes in mind, mental disorders can be considered as a core health challenge

of this century (Roehrig, 2016; Wittchen et al., 2011), which in turn underlines the urgency of improvement in treatment and prevention.

Affective and psychotic disorders are among the most common mental diseases (Kessler et al., 2005). Although technical advances led to remarkable insights into their pathophysiology and effective therapeutic strategies, treatment outcomes often remain poor (Cuijpers et al., 2020; Myers, 2010). Given that an appropriate diagnosis is the basis for treatment selection and therefore the key to a successful therapy, high rates of under- and misdiagnosis in psychotic and affective disorders (Coulter et al., 2019; Mukherjee et al., 1983; Joyce, 1984; Rost et al., 1998; Verhaak et al., 2006; Vermani et al., 2011) point to difficulties in current classification systems and are likely to be a major contributing factor to the efficacy-effectiveness gap in psychiatry.

### 1.1.2 Current conceptual delimitation of psychotic and affective disorders

The current nosology of psychotic and affective disorders, as defined in DSM-5 and ICD-10, is based on Emil Kraepelin's *Zweiteilungsprinzip* (two entities principle), by which he 'crystallized *dementia praecox* and *manic-depressive psychosis* from an amorphous mass of madness' in 1919 (Brockington & Leff, 1979). Although this so-called Kraepelian dichotomy represents a major advance in psychiatry from the historical perspective, the validation of these nosological categories was limited (Craddock & Owen, 2005): Firstly, prototypical presentations of BD and SCZ were thought to 'breed true', as family studies revealed an increased risk for SCZ but not for BD in relatives of SCZ patients, and vice versa in respective studies of BD. Secondly, in cases with typical clinical presentations, SCZ and BD can mostly be clearly distinguished from one another. Thirdly, as Kraepelin already acknowledged that some symptoms are not specific to one mental disease, he proposed that only the consideration of the course of the illness allows valid classifications (Ebert & Bär, 2010). In particular, Kraepelin suggested that *dementia praecox* is associated with a gradual and progressive cognitive decline, while *manic-depressive psychosis* is predominantly characterized by episodic courses with periods of intermittent functional decline as well as phases of full recovery (Grof et al., 1995; Prossin et al., 2010).

Although the terminology of *dementia praecox* and *manic-depressive psychosis* changed to SCZ and BD respectively, today's psychiatric practice and research is still strongly influenced by the fundamentals of the Kraepelian dichotomy. Moreover, the Kraepelian dichotomy offers great advances for clinical practice, such as providing a common language for clinicians or facilitating diagnosis of often complex clinical phenomena (Craddock & Owen, 2005). However, considering the aforementioned high rates of misdiagnosis, the question arises as to what extent this 'amorphous mass of madness' (Brockington & Leff, 1979) fits within the form of today's nosology that is still based on Kraepelin's dichotomy. As a background for the present work, three major representatives of the spectrum, namely MDD, BD, and SCZ, are briefly outlined below with regard to key characteristics.



### *Major depressive disorder (MDD)*

MDD has been reported to be the most frequent mental disorder in the general population (Stein et al., 2020). With about 350 million people affected each year (Marcus et al., 2012) and a lifetime prevalence of over 16% (Kessler et al., 2007), MDD is among the largest contributors to the overall disease burden (Murray et al., 2012; Stein et al., 2020). The severe clinical condition is generally characterized by persistently lowered mood affecting many aspects of an individual's life. At the psychological level, clinical manifestations include anhedonia (lack of reactivity to pleasurable stimuli), decreased self-esteem, rumination, feelings of guilt, sorrow, impaired decision-making, anxiety and hypochondria (Cooper et al., 2018; Hamilton, 1986; Leykin et al., 2011). At the physiological level, MDD is inter alia marked by insomnia, weight loss and fatigue (Stevens & Rodin, 2011). Moreover, in particularly severe cases of depression, psychotic features, such as delusions, hallucinations or depressive stupor, can be present. A further aggravating factor is that depressive episodes are often accompanied by an elevated suicidal risk (Hawton et al., 2013).

To justify the diagnosis of MDD, both ICD-10 and DSM-5, the two most common diagnostic manuals, list a set of symptoms that must be present concurrently for a minimum of 2 weeks (American Psychiatric Association, 2013; World Health Organization et al., 1992). Given that sadness and grief are natural emotional reactions to losses or sad events, the time criterion is particularly important to demarcate MDD, which can occur spontaneously or, if occurring to certain events, persists beyond a normal period (Gelenberg, 2010). **Table 1** compares the criteria of the current diagnostic manuals. In the DSM-5, at least five out of these symptoms are required to diagnose MDD. In addition, these symptoms must lead to clinically significant distress or an impairment in social, occupational or other parts of a person's life (American Psychiatric Association, 2013). Similarly, the ICD-10 also requires a minimum of four of the listed symptoms. However, three thresholds define further degrees of severity. Since ICD-10 and DSM-5 demand only a selection of the symptoms in **Table 1**, both manuals allow heterogeneity within the diagnostic category (Goldberg, 2011). For example, if a patient has hypersomnia, increased body weight and psychomotor retardation, this person obtains the same depression score as another patient who suffers from insomnia, has weight loss and is agitated, although these symptoms are contrary.

**Table 1. Comparison of the criteria for MDD according to ICD-10 and DSM-5.**

DSM-5 <sup>1</sup>	ICD-10 <sup>2</sup>
<ul style="list-style-type: none"> <li>• Depressed mood most of the day, nearly every day</li> <li>• Markedly diminished interest or pleasure in all, or almost all, activities most of the day, nearly every day</li> <li>• Significant weight loss when not dieting or weight gain, or decrease or increase in appetite nearly every day</li> <li>• Insomnia or hypersomnia nearly every day.</li> <li>• psychomotor agitation or retardation nearly every day</li> <li>• Fatigue or loss of energy nearly every day</li> <li>• Feelings of worthlessness or excessive or inappropriate guilt nearly every day</li> <li>• Diminished ability to think or concentrate, or indecisiveness, nearly every day</li> <li>• Recurrent thoughts of death, recurrent suicidal ideation without a specific plan, or a suicide attempt or a specific plan for committing suicide</li> </ul>	<ul style="list-style-type: none"> <li>• Depressed mood</li> <li>• Markedly diminished interest or pleasure in activities</li> <li>• Reduced ability to concentrate and sustain attention or marked indecisiveness</li> <li>• Beliefs of low self-worth or excessive or inappropriate guilt</li> <li>• Hopelessness about the future</li> <li>• Recurrent thoughts of death or suicidal ideation or evidence of attempted suicide</li> <li>• Significantly disrupted sleep or excessive sleep</li> <li>• Significant changes in appetite or weight</li> <li>• Psychomotor agitation or retardation</li> <li>• Reduced energy or fatigue</li> </ul>

<sup>1</sup>DSM-5: Diagnostic and Statistical Manual of Mental Disorders (American Psychiatric Association, 2013).

<sup>2</sup>ICD-10: International Classification of Diseases (World Health Organization et al., 1992).

### *Bipolar disorder (BD)*

BD, formerly known as manic depression, is a recurrent affective disorder characterized by particularly marked mood shifts. Depressive episodes in BD are equally defined as in MDD. In contrast to depressive disorders, the essential feature of BD is that the medical history includes at least one distinct manic phase, making (hypo-)mania the unique hallmark of the disease (Belmaker, 2004). In mania, patients persistently exhibit elevated, euphoric and sometimes even dysphoric mood states. Furthermore, these states are often accompanied by an uncontrollable excitement, increased energy, pressure of speech and a reduced need for sleep (Cerimele et al., 2013). Increased optimism, which is often present, impairs the patient's judgement and, in combination with a lack of social inhibitions, may foster high-risk behaviours. In some cases, BD patients may also show delusions or extreme flight of ideas, making their speech incomprehensible (Cerimele et al., 2013). Hypomania describes a milder form of mania, albeit hypomanic symptoms are still noticeably deviant from the behaviour of healthy people. Although far-reaching impairments may be observed in hypomania, they do not cause severe disruptions of the patient's everyday life or social rejection as in acute mania (Cerimele et al., 2013).

In episodes of mixed features, patients exhibit rapid mood shifts between mania and depression (Muneer, 2017). Both ICD-10 and DSM-5 distinguish two subtypes of BD (American Psychiatric Association, 2013; World Health Organization et al., 1992): While BD-I patients experience depressive and full-blown manic episodes, those patients with BD-II only exhibit hypomanic phases.

The diagnosis according to the current manuals is thus composed of the diagnostic criteria of depressive (see **Table 1**) and (hypo)manic episodes. **Table 2** lists the criteria of a manic episode according to ICD-10 and DSM-5, respectively. To fulfill the criteria of a manic episode, both diagnostic manuals require a minimum of three of the mentioned symptoms.

**Table 2. Comparison of the criteria for manic episodes according to ICD-10 and DSM-5.**

DSM-5 <sup>1</sup>	ICD-10 <sup>2</sup>
<ul style="list-style-type: none"> <li>• Inflated self-esteem or grandiosity</li> <li>• Decreased need for sleep</li> <li>• More talkative than usual or pressure to keep talking</li> <li>• Flight of ideas or subjective experience that thoughts are racing</li> <li>• Distractibility, as reported or observed</li> <li>• Increase in goal-directed activity or psychomotor agitation</li> <li>• Excessive involvement in activities that have a high potential for painful consequences</li> </ul>	<ul style="list-style-type: none"> <li>• Increased activity or motor restlessness</li> <li>• Increased talkativeness</li> <li>• Flight of ideas or subjective feeling of racing thoughts</li> <li>• Loss of normal social inhibition, resulting in behavior inappropriate to the circumstances</li> <li>• Decreased need for sleep</li> <li>• Excessive self-esteem or delusions of grandeur</li> <li>• Distractibility or persistent change of activities or plans</li> <li>• Impulsive reckless behavior, the risk of which the individual does not recognize</li> <li>• Increase in sexual drive or sexual indiscretion</li> </ul>

<sup>1</sup>DSM-5: Diagnostic and Statistical Manual of Mental Disorders (American Psychiatric Association, 2013).

<sup>2</sup>ICD-10: International Classification of Diseases (World Health Organization et al., 1992).

Analogous to MDD, the individual clinical picture of BD patients can vary over a broad range within the diagnostic boundaries. Given that BD also comprises mood states of opposite polarity to depressive symptoms, this diagnostic category is particularly marked by heterogeneity.

The estimated overall lifetime prevalence of the disease in the general population is around 1% (Bebbington & Ramana, 1995). However, prevalence rates vary slightly between BD-I and BD-II,

with the latter being less common (Baliki et al., 2013). Over the years, further epidemiological differences between these subtypes have been identified: While the mean age-of-onset of BD-I is under 25 years, BD-II was found to manifest slightly later (Merikangas et al., 2011). Furthermore, BD-I has a higher prevalence in males than females, whereas this ratio is reversed in BD-II (Merikangas et al., 2011).

Due to the particularly heterogenous nature of BD, the body of literature on the course of the disease is also complex: First of all, Saunders and Goodwin (2010) suggest that BD is a lifelong disorder. A 40-year follow-up study reported that only 16% did not experience a symptomatic episode during the last five years, whereas more than 50% still had recurrent phases of the disease (Angst, 1980). Moreover, several predictors of poor syndromic recovery have been identified, including medical comorbidities, nonadherence to medical treatment, lower socioeconomic levels and the lower age of onset (DelBello et al., 2007; Leboyer et al., 2005). Furthermore, BD patients with mixed features are likely to have worse symptoms and outcomes, more episodes throughout their lifetime and higher rates of comorbidities (Fagiolini et al., 2015). While these factors are important for predicting individual disease trajectories, the widely varying outcomes reflect the heterogeneity of the group.

Taken together, BD is a severe psychiatric disorder with particularly multifaceted clinical presentations. This high diversity emphasizes that it is necessary to differentiate the distinct subtypes of BD when it comes to the selection of the most suitable treatment and in psychiatric research.

### *Schizophrenia (SCZ)*

The international prevalence of SCZ approaches 1% and its annual incidence is about 1.5 in 10.000 people (McGrath et al., 2008). SCZ represents a group of severe clinical disorders characterized by fundamental disturbances in cognition and perception and blunted or inappropriate affects (World Health Organization et al., 1992). In a large-scale, cross-cultural study carried out in 9 countries, 97% of patients with SCZ were characterized by a lack of insight (Sartorius et al., 1972). Further, around 70% of SCZ patients revealed psychotic symptoms, whereas 66% presented symptoms of flattened affect. Although psychotic symptoms like hallucinations and delusions are easy to detect, they are not exclusive to SCZ and therefore, their classification can be challenging.

Traditionally, symptoms of SCZ are divided into two main opposite groups, namely positive and negative symptoms (see **Table 3**) (Möller, 1995). Over time, cognitive impairment has received increasing recognition and is now considered as source of a third group of symptoms (Weickert et al., 2000). As Möller (1995) already noted, the assignment of clinical signs into positive and negative symptom groups varies across different authors, even though there seems to be agreement on the core of the syndrome. In favour of a uniform conceptualization, one practically useful description of psychotic symptoms is based on the Positive And Negative Syndrome Scale (PANSS) developed by Kay et al. (1987) which has also been applied in the framework of this thesis. **Table 3** details the positive, negative and general symptoms as defined in the PANSS.

**Table 3. Positive, negative, and general symptoms as defined in the PANSS\*.**

Positive symptoms	<ul style="list-style-type: none"> <li>• Delusions</li> <li>• Conceptual disorganization</li> <li>• Hallucinatory behaviour</li> <li>• Excitement</li> <li>• Grandiosity</li> <li>• Suspiciousness</li> <li>• Hostility</li> </ul>
Negative symptoms	<ul style="list-style-type: none"> <li>• Blunted affect</li> <li>• Emotional withdrawal</li> <li>• Poor rapport</li> <li>• Passive-apathetic social withdrawal</li> <li>• Difficulty in abstract thinking</li> <li>• Lack of spontaneity &amp; flow of conversation</li> <li>• Stereotyped thinking</li> </ul>
General symptoms	<ul style="list-style-type: none"> <li>• Somatic concern</li> <li>• Anxiety</li> <li>• Guilt feelings</li> <li>• Tension</li> <li>• Mannerisms &amp; posturing</li> <li>• Depression</li> <li>• Motor retardation</li> <li>• Uncooperativeness</li> <li>• Unusual thought content</li> <li>• Disorientation</li> <li>• Poor attention</li> <li>• Lack of judgement &amp; insight</li> <li>• Disturbance of volition</li> <li>• Poor impulse control</li> <li>• Preoccupation</li> <li>• Active social avoidance</li> </ul>

\*Positive And Negative Symptom Scale (Kay et al., 1987).

The wide range of features of the disease mirrors the multifaceted clinical presentation of SCZ. For many years, diagnostic manuals acknowledged the resulting heterogeneity of SCZ by defining clinical subtypes of the disease. In ICD-10, the category of SCZ (F20) includes paranoid, hebephrenic, catatonic, undifferentiated SCZ, post-schizophrenic depression, residual, simple, other and unspecified SCZ (World Health Organization et al., 1992). Among the aforementioned, paranoid SCZ (33.6%) and residual SCZ (32.1%) are the most prevalent disorders of the F20-group (Deister & Marneros, 1993).

Until its fourth edition, the DSM also differentiated between subtypes. However, these have been eliminated from the current 5<sup>th</sup> edition due to their low level of stability, reliability and validity (Tandon et al., 2013; Tandon & Maj, 2008). Instead, a more dimensional assessment is preferred to better address the heterogeneity of SCZ (Barch et al., 2013). **Table 4** displays diagnostic criteria of SCZ according to DSM-5 and ICD-10. According to DSM-5, two out of five symptoms need to be present for a significant portion of the time and for at least six months (American Psychiatric Association, 2013). To fulfill the diagnosis of SCZ according to ICD-10, at least one of the first category or at least two of the second category need to be present for most of the time for at least one month (World Health Organization et al., 1992).

**Table 4. Comparison of the diagnostic criteria of SCZ according to DSM-5 and ICD-10.**

DSM-5 <sup>1</sup>	ICD-10 <sup>2</sup>
<ul style="list-style-type: none"> <li>• Delusions</li> <li>• Hallucinations</li> <li>• Disorganized speech</li> <li>• Grossly disorganized or catatonic behaviour</li> <li>• Negative symptoms</li> </ul>	<ul style="list-style-type: none"> <li>• At least one of the following:               <ul style="list-style-type: none"> <li>○ Echoing/insertion/withdrawal/broadcasting of thought</li> <li>○ Delusional perceptions</li> <li>○ Hallucinatory voices</li> <li>○ Impossible delusions of some kind</li> </ul> </li> <li>• At least two of the following:               <ul style="list-style-type: none"> <li>○ Persistent hallucinations in any modality</li> <li>○ Incoherence or irrelevant speech</li> <li>○ Catatonic behaviour</li> <li>○ Negative symptoms</li> </ul> </li> </ul>

<sup>1</sup>DSM-5: Diagnostic and Statistical Manual of Mental Disorders (American Psychiatric Association, 2013).

<sup>2</sup>ICD-10: International Classification of Diseases (World Health Organization et al., 1992).

Taken together, this overview of the nosology not only shows that the Kraepelian dichotomy is still reflected in the modern classification systems, but also that each diagnostic group is characterized by heterogeneity at the phenomenological level. Moreover, transdiagnostic symptomatic overlaps become apparent that have also been thematized in the literature, including psychotic symptoms (e.g., paranoia) in affective disorders (Goodwin & Jamison, 2007; Keck et al., 2003) or affective symptoms (e.g., anhedonia) in SCZ (Andreasen, 1982; Buckley et al., 2009; Schultze-Lutter et al., 2007). Furthermore, a 35 year long cohort study confirmed a substantial overlap of the clinical picture between BD and SCZ (Larsen et al., 2009). At the clinical level, symptom overlaps represent major challenges for our current classification system as both ICD-10 and DSM-5 are often based on verbally reported symptoms and observed behaviour instead of genetical, behavioural and neurobiological data. At the scientific level, the remaining uncertainty of diagnostic classification hampers the neurobiological characterization of clinical groups and thus the establishment of biomarkers.

### 1.1.3 Psychotic and affective disorders as part of a continuous spectrum

In light of this phenomenological heterogeneity within and between affective and psychotic disorders, Häfner et al. (2005) suggested that these disorders could be seen in a hierarchical model of preformed dimensional psychopathological patterns. Besides conceptual overlaps, both clinical reality and genetic research findings corroborate this assumption.

#### **Clinical reality as a challenge for Kraepelin's dichotomy**

Several observations in clinical practice point to shortcomings of the current categorical classification of affective and psychotic disorders: Firstly, psychiatric comorbidities are a widespread phenomenon (Pincus et al., 2004) which puts the strict dichotomous view into question, in addition to the symptom overlap between the diseases. Of relevance to this thesis, for example, it has been estimated that comorbid depression occurs in 50% of psychotic patients (Buckley et al., 2009). Furthermore, previous evidence suggests that depressive symptoms, together with anxiety, are related to psychotic symptom severity, distress and content, prognosis and relapse (Hartley et al. 2013). Moreover, approximately 19% of people fulfilling the criteria for a depressive episode additionally experience psychotic symptoms (Ohayon & Schatzberg, 2002).

Secondly, Kendler et al. (1998) were able to define six different subtypes of psychotic disorders, namely classic schizophrenia, major depression, schizophreniform disorder, bipolar-schizomania, schizodepression, and hebephrenia based on a latent class analysis. Comparing these data-driven subgroups indicates that the psychotic spectrum comprises patients that are closer to the core of psychotic (i.e. positive) symptoms as well as others presenting a rather affective psychopathology, even beyond mania.

Thirdly and in harmony with this notion of symptom-based subtypes of Kendler et al. (1998), some individuals exhibit a mixture of both psychotic and affective symptoms, either concurrently or at times throughout their disease. Nevertheless, as they do not clearly meet the criteria of either SCZ or BD, these patients exhibiting this heterogeneous symptom pattern are falling between the dichotomous categories. Consequently, the diagnosis of such clinical pictures not only stands on shaky ground, but also directly challenges the Kraepelinian dichotomy. Kasanin (1933) was among the first to target this issue by introducing schizoaffective disorder as an independent disease standing apart from SCZ and BD. However, despite its large overlap with both SCZ and BD (Laursen et al., 2009), schizoaffective disorder accounts for 10-30% of inpatient admissions for functional psychosis (Azorin et al., 2005). Furthermore, schizoaffective disorder is considered to be among the most misdiagnosed illnesses in psychiatry (Malaspina et al., 2013). In line with this, Nurnberger et al. (1994) reported a poor reliability, weak validity, and low stability of the diagnosis. In order to compare schizoaffective patients with neighbouring diagnoses, Brockington & Leff (1979) separated a sample of 119 psychotic patients according to the presence of either manic or depressive symptoms. While the group of psychotic patients with depressive symptoms was heterogeneous, psychotic patients with manic symptoms appeared to be rather similar to BD than SCZ.

In sum, clinical presentations not only point towards major weaknesses of dichotomous categories in the psychotic-affective spectrum, but also draw an image of a rather smooth transition between the two spectra. Furthermore, the diagnosis of schizoaffective disorder bridges the gap between SCZ and BD.

### **The genetic relationship between psychotic and affective disorders in a nutshell**

Genetic research has also provided evidence that these groups cannot be clearly distinguished from each other. According to a review on family studies (Craddock et al., 2005), familial co-aggregation was found between schizoaffective disorder and both BD and SCZ and, in line with the clinical overlap mentioned above, between BD and SCZ. These findings are in clear contradiction with the 'breed true' assumption of BD and SCZ as two distinct disorders. Furthermore, findings from a twin study suggest that genetic risk factors for schizoaffective disorder are shared with genetic influences on both SCZ and mania (Cardno & Owen, 2014).

Mounting evidence stemming from research on genetic risk variants corroborates the image of disease continuum: Besides disease-specific genetic factors, MDD, BD, and SCZ share a common polygenic component (Green et al., 2010; Schulze et al., 2014). This indicates that each of these psychiatric conditions might represent a different manifestation of a general and shared psychopathology. Moreover, multiple psychotic experiences (auditory and visual hallucinations and delusions of persecution) were found to be genetically correlated with both SCZ and MDD (Barkhuizen et al., 2020).

Taken together, accumulating findings from different scientific disciplines contrast the traditional concept of homogeneous psychotic and affective categories. Instead, evidence indicates an underlying continuous affective-psychotic spectrum which is bridged by bipolar disorder, particularly mania. Genetic research also provided evidence that the groups cannot be clearly distinguished from each other.

### **Consequences of the mismatch between theoretical classifications and clinical reality**

Although ICD and DSM have been constantly revised over the years, the previous chapter has shown that the classification of psychotic and affective disorders remains challenging. The linguistic philosopher Wittgenstein described the mismatch between theoretical concepts and clinical reality with a metaphor: He wrote that "the classifications made by philosophers and psychologists are as if one were to classify clouds by their shape" (Wittgenstein, as cited by Jablensky et al., 2016). On the one hand, clouds have unclear boundaries, get shifted by invisible air streams and sometimes merge together. On the one hand, weather forecasts are mostly based on observation and prediction of their movement whereas their inner physical and chemical structures remain invisible to the unaided eye (Jablensky, 2016). Central aspects of this metaphor seem to be transferable to the current psychiatric nosology: Affective and psychotic disorders have blurred boundaries and show symptomatic overlaps between each other (see chapter 1.1.3). Moreover, in analogy with forecasts in Wittgenstein's allegory, the question arises whether important aspects are neglected by the attempt of fitting mental illnesses into a traditional model based on Kraepelin's dichotomy.



With this metaphor in hand, it is easier to understand complaints about the inadvertent replacement of the phenomenological gestalt of psychopathologies by generalizing classifications in psychiatry (Park, 2019). In reference to the growing authority of the DSM in the U.S., Andreasen (2007) described this trend as 'the death of phenomenology' in psychiatry, stating a steady decline of individuality, while other sources underlined the importance of a patient's unique characteristics to clinical treatment (Ozomaro et al., 2013).

Given the heterogeneity of mental disorders, general classifications might often miss individual needs and consequently foster to entail prolonged suffering. Although two patients may share the same diagnosis, the actual underlying pathophysiology might vary substantially and thus require different treatment approaches. However, even though current psychiatric nosology is increasingly criticized, possible solutions have often proven elusive (Nesse & Stein, 2012).

#### **1.1.4 The general trend towards dimensional diagnostic models in psychiatry**

Despite reasonable arguments, such as uncertainty and reduced individuality of diagnoses, classification systems are necessary at several levels, including facilitating clinical diagnosis, invoicing psychiatric treatments or providing a common language for clinicians for the effective exchange of information. However, frequent revisions of diagnostic criteria will not resolve the problems of disease group heterogeneity, comorbidity and fuzzy boundaries defining pathology (Nesse & Stein, 2012). Insel et al. (2010) stated that 'categories based on clinical consensus fail to align with findings from clinical neuroscience and genetics', and therefore restrain the development of new treatments targeting actual pathophysiological mechanisms. To overcome this barrier, neurobiological and genetic findings could be translated into clinical practice, for example by establishing biomarkers of groups of diseases.

The *Research Domain Criteria* (RDoC) project (Insel et al., 2010) represents another similar, yet slightly different promising approach to increase biological validity in clinical practice, as it views both mental health and illness as different functional stages of psychological and biological domains. According to Insel et al. (2010), three assumptions are fundamental to the RDoC project: Firstly, mental disorders are conceptualized as a type of brain disorders. While neurological illnesses can be identified with lesions, mental illnesses reflect disorders of brain circuits. Secondly, neuroscience holds tools that allow the detection of such anomalies within brain circuits. Thirdly, genetical techniques and other neuroscientific tools are capable of providing biosignatures which possibly augment clinical symptoms as the major basis of diagnostics (Insel et al., 2010).

On the one hand, the perspective on mental diseases as brain disorders also implies an insufficiency of clinical signs and verbally conveyed symptoms based on a patient's self-report as a valid source for psychiatric diagnostics. On the other hand, dysfunctions in neural circuitries provide implications for several domains, for example cognition, emotion, and behavior. Each of these domains is representing a continuum from normal to severely ill. Moreover, this dimensional approach to mental disorders cuts across traditional diagnostic boundaries and aims to identify both disorder-specific and common

pathomechanisms (Nusslock & Alloy, 2017). Consequently, the RDoC project counteracts the problems of heterogeneity, comorbidity and diagnostic overlaps by focussing on individually present dysfunctions.

In general, the RDoC model is based on 'dimensions of observable behavior and neurobiological measures' that are referred to as constructs (Morris & Cuthbert, 2012). These constructs are grouped under six neurophysiological domains (Ross & Margolis, 2019): (1) negative valence system; (2) positive valence system; (3) cognitive systems; (4) social processes; (5) arousal and regulatory system; (6) sensorimotor. Each of these superordinate domains reflects both a conceptual typology of functions and empirical relationships among activity in related brain circuitries (Morris & Cuthbert, 2012). The long-term aims of the RDoC project include the validation of tasks in order to apply them in clinical trials, identification of treatment targets, definition of clinical subgroups for better treatment selections and to foster the translation of research findings into changes in clinical decision making (Morris & Cuthbert, 2012).

In summary: In the recent years, evidence suggestive of shortcomings of the current nosology of mental disorders has accumulated, particularly with regard to the classification of affective and psychotic disorders based on Kraepelin's dichotomy. Due to the translational gap between psychiatric research and clinical practice, both high levels of subjective suffering and related costs to health care systems have not improved to an extent that the advances in neurobiological understanding of these disorders might actually allow. Overcoming this translational gap could improve diagnostics, course prediction and individualized treatments strategies in favour of the individual wellbeing of people affected and the burden on society.

## 1.2 The reward system as a potential source of biomarkers

Reward processing is an important part of our everyday life and an essential factor to enhance our wellbeing as underlying mechanisms are involved in directing behaviours towards positive stimuli and to avoid harm. In addition, dysfunctional reward processing is a prominent transdiagnostic characteristic in multiple psychopathologies, including affective disorders, impulse control disorders and anhedonic symptoms in SCZ (Zald & Treadway, 2017). Considering this centrality, the neurocircuits underlying the reward system are potential target systems for the development of biomarkers for the characterisation of mental disorders. Accordingly, reward-related aspects also receive ample attention in the above mentioned RDoC conceptualization, as reward processing is reflected in different constructs, for instance 'reward learning' as part of the 'positive valence system' domain. The following chapter sets out to overview reward-related research, techniques to quantify reward processing and literature on the reward system in psychopathology.

### 1.2.1 Reward processing in psychological research

Not only in the context of the RDoC project, but with a long tradition in psychological research, reward processing has gained significant attention. From an evolutionary standpoint, rewards can be characterized as stimuli encouraging certain behaviors that help animals to survive (Schultz, 2016). These stimuli can be either innately rewarding (e.g., sex, food), known as intrinsic rewards, or learnt to be associated with a positive outcome, known as extrinsic rewards (e.g., money, recognition) (Wilson et al., 2018). The phenomenon of extrinsic rewards has been well described in the classical psychological principle 'law of effect' by Edward Thorndike (Gray, 2010). This principle states that “responses that produce a satisfying effect in a particular situation become more likely to occur again in that situation, and responses that produce a discomforting effect become less likely to occur again in that situation” (Schacter et al., 2015). Through iterative learning processes, such associations between salient stimuli and positive outcomes are established and strengthened. This explains a longstanding interest in reward processing in psychological research. However, reward processing is a multifaceted construct comprising a whole range of subprocesses.

### 1.2.2 Subprocesses of reward processing

In research, reward processing represents an umbrella term that comprises different subprocesses. Keren et al. (2018) distinguish between the following four stages of reward processing: First, the *prediction* stage: This stage relates to the recognition of objects as potentially rewarding, based on a subject's knowledge. In experimental designs, the prediction phase is commonly captured by using key stimuli in order to induce subjects to anticipate positive or negative outcomes. The monetary incentive delay (MID) task as presented by Knutson et al. (2001) (further described and applied in chapter 3) can be considered as test focussing on this reward subprocess. The second stage relates to the *decision* between reward oriented or punishment avoiding actions. This stage is also an important component of human executive function encompassing the estimation of the actual costs for attaining

the reward. In translational work, aspects of this phase are captured by asking participants to choose from different possibilities. In order to examine the complex interplay between the processes of cognition and motivation, Bechara et al. (1994) introduced a paradigm that was later termed Iowa Gambling Task. As a highly sensitive measure, it has been widely applied in clinical studies (Bechara et al., 1994; Li et al., 2010). The *action* stage as third stage relates to the efforts made to either obtain a reward or avoid punishment (Keren et al., 2018), including motivational aspects. Translationally, this stage refers to the phase of an experiment in which an action is required, such as pressing a button to receive a reward. The fourth and last stage of this conceptualization relates to experiencing reward-related outcomes which is sometimes referred to as reward *consumption*. It also entails the consolidation of these experiences to be able to access them in later reward processing situations. In translational terms, this stage corresponds to the outcome phase including wins and losses.

Taken together, the characterization of neural correlates of reward processing requires the differentiation of respective subprocesses, as, for example, dysfunctions might only affect the prediction stage of reward processing, while the functioning of other components is preserved.

### 1.2.3 Research techniques to measure reward processing

Over the years, research on the reward system underwent a remarkable evolution and became a multifaceted scientific field for itself. For this research, different methodological approaches to quantify reward processing have been elaborated which are briefly outlined in the following.

#### *'Paper & Pencil'*

Several self-report assessments have been developed to operationalize either reward-related behaviour or respective personality traits. Among the most prominent self-report measures are the BIS/BAS-scales developed by Carver and White (1994). These scales are based on Gray's Reinforcement sensitivity theory (1990) according to which three orthogonal systems subserve human cognition and emotion: A behavioural inhibition system (BIS), a behavioural approach system (BAS), and a fight/flight system. A total of 24 Likert-scaled items measure BIS and BAS. While BIS is quantified by one subscale, three subscales target the BAS, namely a Drive scale (addressing pursuit of desired goals), a Fun Seeking scale (reflecting desires for new rewards/willingness to approach potentially rewarding events) and a Reward Responsiveness scale (targeting positive responses to occurring or anticipated rewards) (Carver & White, 1994).

Another measurement tool based on Gray's reinforcement sensitivity theory is the Sensitivity to Punishment and Sensitivity to Reward Questionnaire (SPSRQ) by Torrubia and colleagues (2001). While the Sensitivity to Punishment scale measures individual aspects of the BIS, the Sensitivity to Reward scale addresses individual differences in sensitivity related to the BAS.

Besides questionnaires directly focussing on reward-related behaviour and its biological substrates, temperaments indirectly associated with reward processing can also be assessed. For example, Cloninger took reward processing into account in two of his prominent personality scales, as 'reward dependency' is one of the quantified traits in both the Tridimensional Personality Questionnaire (Cloninger, 1991) and the Temperament and Character Inventory (Cloninger & Svrakic, 1994).

### *Functional magnetic resonance imaging*

The discovery of the BOLD signal as a tool for investigating in vivo brain functioning by Ogawa et al. (1990) constituted a milestone in brain research. Initially, investigations of the human brain were focussing on task-related activation. By contrasting the BOLD signal during task and with the BOLD signal at baseline, it can be concluded that the difference ('contrast') represents activation specifically associated with the task. Consequently, by using reward-related paradigms, this non-invasive functional resonance imaging (fMRI) technique allows the investigation of neuronal substrates of reward processing. Richards and colleagues (2013) distinguish three types of fMRI reward tasks: Firstly, passive reward related tasks do not require any activity in order to obtain the rewards. For example, in the slot-machine task (Van Leijenhorst et al., 2010), individuals see three slot machines, each of which displays seemingly random pictures. If all slot machines present the same image at the end of a trial, the participant gets rewarded. Secondly, in instrumental reward tasks, certain behaviour, for example a button press, is required to achieve a reward. Similar to tasks in Karen and colleagues' decision stage (2018), the third group requires the participants to choose between different rewarding options. Examples include the Pirates Paradigm (Galvan et al., 2006) that consists of a memory challenge, the Cake Gambling Task (van Leijenhorst et al., 2006) in which subjects need to make a perceptual judgement, and the MID task (Knutson et al., 2001) in which a button press is required after following a brief flash.

### *Nuclear medical techniques*

Based on the administration of radiopharmaceuticals, imaging techniques of nuclear medicine allow the *in vivo* investigation of biochemical processes at the synapses. As described in the following chapter, dopaminergic pathways in the brain play a key role in the context of reward processing. Therefore, methods of nuclear medicine that focus on dopaminergic transmission could be used to capture biochemically specific aspects of reward processing. Specific tracers for either positron emission tomography (PET) or single photon emission computed tomography (SPECT) readout are available to study dopaminergic signal transmission, for example  $^{123}\text{I}$ -FPCIT-SPECT and  $^{18}\text{F}$ -Dopa-PET to study the integrity of nigrostriatal neurons, or  $^{123}\text{I}$ ]IBZM-SPECT and  $^{11}\text{C}$ ]Racloprid-PET to study the striatal D2-receptor density.

### 1.2.4 Neural substrates and anatomy of the reward system

Over 60 years ago, Olds and Milner (1954) were among the first to explore a neural system underlying positive reinforcement in the mammalian brain. By implanting needle electrodes at various points in rat brains, they enabled these animals to stimulate themselves by pressing a lever. Highest scores of electrical self-stimulation were located in the medial forebrain bundle. Generally, these fibres are part of a projection system originating in several neighbouring nuclei located in the mesencephalon, a region of high density of dopaminergic neurons (Björklund & Dunnett, 2007). In harmony with this preliminary finding, subsequent work consistently reported a link between reward processing and the dopamine system (Arias-Carrión & Pöppel, 2007; Berridge & Robinson, 1998; Miller et al., 1990; Pessiglione et al., 2006). However, since dopamine transmission is influencing various circuitries, the association between this neurotransmitter and reward processing is more complex.

In general, dopaminergic neurons are a heterogeneous group of at least five distinct G protein-coupled subtypes mediating diverse physiological actions (Missale et al., 1998). Mainly localized to midbrain areas, dopaminergic neurons form different mesencephalic nuclei, namely the ventral tegmental area (VTA), substantia nigra pars compacta, and noradrenergic brainstem nuclei in the locus coeruleus. As these nuclei in turn project to multiple brain regions, they contribute to several levels of behavioural, cognitive and emotional functioning (Aston-Jones & Waterhouse, 2016; Haber & Knutson, 2010).

From the VTA, two major dopaminergic projections descend to cortical and subcortical regions after passing the medial forebrain bundle: The first (mesolimbic) pathway mainly targets the ventral striatum (VS), most importantly the nucleus accumbens (NAcc), while other axons form synapses in the amygdala and hippocampus (Grace, 2000; Hernandez et al., 2006; Stott & Ang, 2013; Willis & Haines, 2018). Several cognitive functions associated with regions of the mesolimbic pathway are also related to reward processing, for example controlling behavioural arousal, modulating reinforcement properties, and experiencing emotion ("The limbic (emotional) system," 2009; Wise & Rompre, 1989). For this reason, components of the mesolimbic pathway are widely considered part of the reward circuitry. Dopaminergic neurons of the second (mesocortical) pathway mainly project to the prefrontal cortex (PFC) and adjacent structures relevant to executive functions, ability to focus and effort learning (Hauser et al., 2017; Ledonne & Mercuri, 2017; Travis, 2003). Furthermore, Knutson et al. (2003) suggest that the medial PFC is involved in tracking monetarily rewarding outcomes. Hence, alongside the mesolimbic pathway, mesocortical dopamine projections also contribute to the processing of reward signals.

It adds to the immense complexity that these two dopaminergic pathways are closely interlinked via glutamatergic projections. Generally, dopamine neurons were found to establish functional glutamatergic synapses in addition to terminals releasing dopamine (Trudeau, 2004). Furthermore, after receiving dopaminergic input from the VTA, glutamatergic projections of the hippocampus, amygdala and the medial PFC target the NAcc (Kable & Glimcher, 2009; Pierce & Kumaresan, 2006). Therefore, dopaminergic projections of the mesocortical pathway indirectly contribute to NAcc activity, too. In-

terestingly, LeGates et al. (2018) observed activity-dependent plasticity at the hippocampus-NAcc synapses and suggested that the strength of this connection plays an important role in reward-related behaviour. Neurochemical transmission within the mesocorticolimbic pathways is visualized in **Figure 1** below.

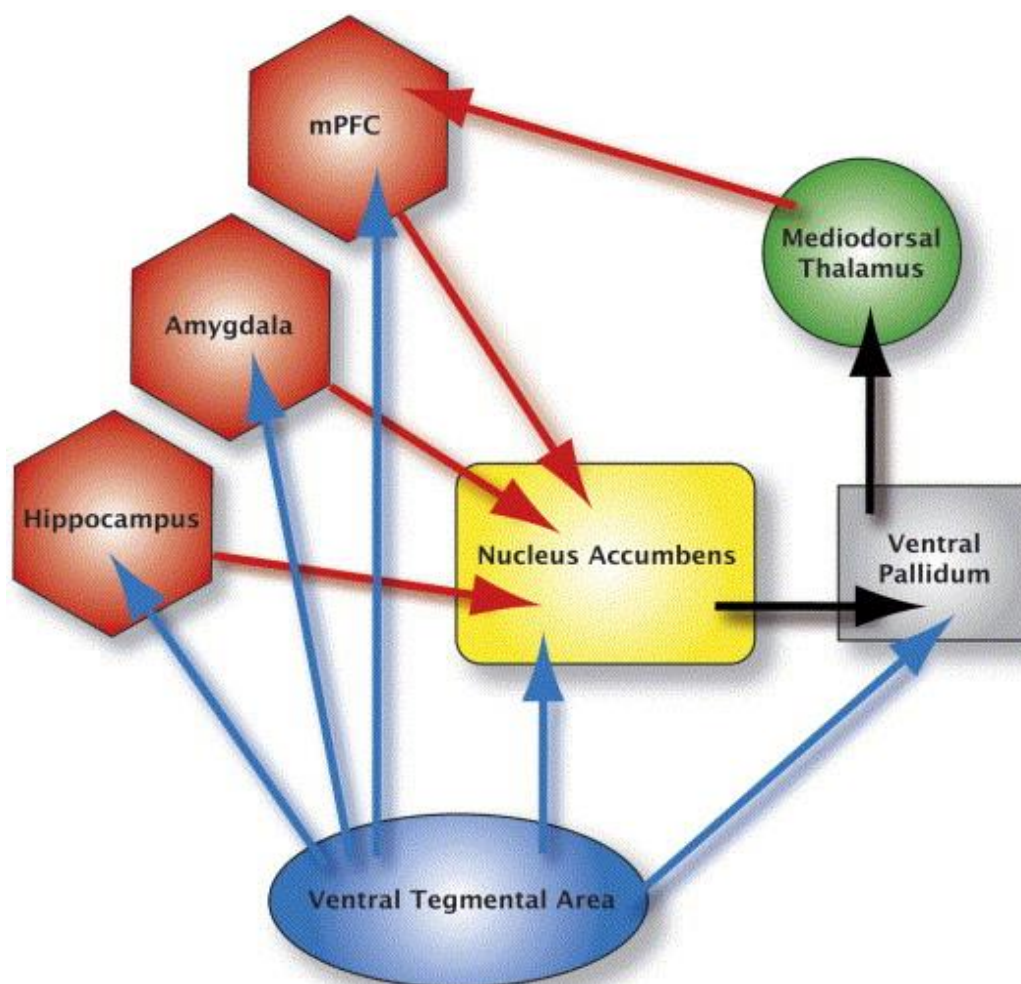


**Figure 1. The limbic dopaminergic pathways.** The VTA dopaminergic neurons travel to other areas in the brain via several pathways. The mesocortical pathway projects to widespread areas, including the medial PFC, amygdala and hippocampus. The mesolimbic pathway projects from the VTA to limbic structures, most importantly the NAcc. In addition, glutamatergic projections of the hippocampus, amygdala and the medial PFC target the NAcc. A third VTA projection reaches out to the ventral pallidum. Figure reprinted with permission from Pierce & Kumaresan (2006).

Taken together, experimental animal research on mesocorticolimbic pathways further support a key role of dopamine in reward-related functions. Beyond this, a central role of the VS, particularly the NAcc, has now been established by neuroimaging evidence, pointing to involvement of the VS in both reward anticipation (RA) and reward outcome (Diekhof et al., 2012; Oldham et al., 2018). Findings of an association between striatal regions and addiction – a psychiatric condition involving disturbed

reward processing – corroborate this notion (Apicella et al., 1991; Daniel & Pollmann, 2014; Kalivas et al., 2005; Schultz et al., 1992). Due to its centrality within a reward circuitry, dopamine has been termed 'reward transmitter' (Wise & Rompre, 1989). Another observation relevant for a network based approach as often pursued in neuroimaging comes from a human PET study that discovered a close relationship between the mesolimbic dopamine system and the salience network (McCutcheon et al., 2019). This cingulate-insular network is central to detecting behaviourally meaningful environmental stimuli and suggests a connection between the reward system and basic cognitive processes.

In conclusion, a dopaminergic reward pathway originating in the brain stem and encompassing limbic circuitry, with the VS/NAcc as a key relay structure, underlies reward processing in humans. Furthermore, regions of a second mesocortical dopaminergic pathway, including medial PFC, amygdala, and the hippocampus, allow to top-down-regulate the reward pathway via glutamatergic projections to the NAcc.

### **1.2.5 The reward system and psychopathology**

#### **Conceptual associations between reward and mental disorders**

In recent years, evidence accumulated that dysfunctional reward processing is a common feature in a variety of psychiatric disorders (Zald & Treadway, 2017) and the reward system has thus become a commonly investigated target in psychiatric research (Dichter et al., 2012). In general, reward processing comprises a whole series of clinically relevant psychological constructs: These include, for example, motivation, anticipation, salience, satiety and pleasure (Whitton et al., 2015). In fact, some of these features are even directly listed amongst diagnostic criteria of different mental disorders and thus bridge directly between reward processing and psychopathology (Whitton et al., 2015; Zald & Treadway, 2017). Examples include symptoms of anhedonia (e.g. decreased interest or pleasure in activities), particularly in affective and psychotic disorders, or the phenomenon of craving in addiction as well as impulse control disorders, or, in turn, the absence of valuation of social reward signals in schizoid personality disorder and autism. Against this background, physiological underpinnings of these functions seem a potential source of transdiagnostic biomarkers in psychiatry. It is thus comprehensible that the RDoC project considers reward processing as a domain of its own (Insel et al., 2010).

#### **Nuanced models of reward-related deficiencies**

In general, the reward system can be impaired in several ways. Most commonly, reward dysfunctions are viewed as simple states of hyper- or hypo-reward processing. In many cases, however, such simplified models struggle to sufficiently explain the complex reward-related characteristics in psychiatric disorders. To further enhance and systematize the understanding of the broad variety of alterations in reward processing, Zald and Treadway (2017) distinguished four models: Firstly, the maladaptive



scaling hypothesis proposes that the valuation of rewards depends on the availability of optional rewards and a person's individual preference. On the one hand, specific rewards can act as an anchor causing a devaluation of other available rewards. This particularly applies to addictions, as certain rewards (such as drugs or gambling) might be strongly reinforced while other, less risky and more healthy alternatives are downscaled. On the other hand, unlike strong desires due to high anchors, flat scaling leads to an attenuated ability to differentiate between available rewards, which may affect an individual's motivation negatively. In brief, the maladaptive scaling hypothesis helps to understand shifts in the subjective valuation of certain rewards.

The second type of reward disturbances assumes a deficit in dopamine transfers and resembles the principle of Pavlovian conditioning (Zald & Treadway, 2017). While dopaminergic cells usually fire phasically in response to both primary and conditioned rewards (Wolfram Schultz, 1998), they can also start respond to cues preceding reinforcers instead of the reward itself over time (Tripp & Wickens, 2008; Zald & Treadway, 2017). If reward-predicting stimuli are overly equated with the actual reward, such conditioning might result in a hypersensitivity of the reward system.

The third model does not assume one general valuation system, but rather postulates competing sub-components (Zald & Treadway, 2017). According to Rangel et al. (2008), three distinct subsystems contribute to valuation processes: A habitual system (automatic responses), a Pavlovian system (conditioned, stimulus-triggered responses), and a goal-directed system (computing action-outcome associations and evaluating rewards associated with these outcomes). The advantage of this model is the distinction of reward domains. For example, a person may have difficulties in evaluating possible outcomes positively (goal-directed system) due to anhedonia, while the reward processing of the other two subsystems may be unaffected. Therefore, this conception helps to better understand at first sight contradictory research findings of reward processing.

The fourth model proposes that weighting reward and cost parameters may be subject to distortions (Zald & Treadway, 2017). For example, instantly available discounts might result in both, *hyper*responsiveness to immediate rewards and *hypo*responsiveness to delayed rewards. This example particularly illustrates the sensitivity of different reward parameters, including magnitude and probability. Consequently, this hypothesis can be used to explain seemingly inconsistent findings of hyper- and hypo-sensitivity to rewards in the same disease, for example as observed attention-deficit/hyperactivity disorder (Plichta et al., 2009). SCZ patients often show a similar pattern: Although value and cost are often well estimated, SCZ patients often focus on the most salient feature and fail to consider other alternatives which might be more likely (Zald & Treadway, 2017). Therefore, such minimal or suboptimal utilisation of information from other parameters fosters oversensitivity to extremes, as in the case in paranoia.

These different models of reward disturbances not only underline the complexity of reward-related dysfunction, but also help to construct experiments to study this multifaceted phenomenon that is

widely present across psychiatric diseases. In addition, these nuanced models hold important implications for transdiagnostic research on the reward system, for example when it comes to the comparison of previous findings from different studies or in the selection of suitable paradigms.

### **Symptoms arising from disturbed reward system and neural underpinnings of reward processing in major psychiatric diseases**

#### *MDD: Linking anhedonia and reward dysfunctions*

In DSM-5, anhedonia is one out of two symptoms required for the diagnosis of MDD (American Psychiatric Association, 2013). Moreover, anhedonia has also been linked to reward-related constructs, such as reward valuation, decision-making, anticipation, reinforcement learning and motivation (Der-Avakian & Markou, 2012). Furthermore, it has been suggested that especially in the presence of anhedonia, MDD is characterized by a reduced ability to modulate behavior in response to intermittent rewards – a state possibly associated with blunted phasic firing of dopamine neurons (Whitton et al., 2015).

Given the centrality of anhedonia in MDD and its association to dopamine, it is not surprising that a large number of neuroimaging studies have focussed on dopamine-rich mesocorticolimbic pathways in MDD. In general, there is accumulating evidence for a blunted VS response (including the caudate NAcc) in depressed patients (Pizzagalli et al., 2009). A meta-analysis comprising 32 experiments has corroborated the assumption of striatal disturbances in MDD, showing reduced activity in the bilateral caudate head and the left putamen relative to HC (Keren et al., 2018). Moreover, attenuated VS response during RA has also been found to predict the emergence of depressive symptoms and disorder (Morgan et al., 2013; Stringaris et al., 2015) and depression symptom severity (Satterthwaite et al., 2015). Furthermore, RS experiments have suggested an association between diminished functional connectivity (FC) within the reward system, most notably the left VS, and depressive symptom load (Satterthwaite et al., 2015). In addition, a longitudinal study indicated that striatal FC also predicts future risk for depressive disorder (Pan et al., 2017). Interestingly, decreased VS activation during a reward task was observed in never-depressed adolescents at high risk for MDD (Gotlib et al., 2010). However, reports of altered VS activation in MDD are not entirely consistent. In contrast to findings of decreased VS response in MDD, Knutson et al. (2008) reported that unmedicated depressed patients were able to sufficiently recruit the NAcc during RA. Although patients in this sample were shown to suffer from severe symptoms of depression, they still had the capacity to experience positive arousal during RA. Against the background of a relationship between anhedonia and striatal activation, the absence of anhedonia may explain normal VS functioning in this specific sample. Together, merging evidence underlines the importance of striatal regions in MDD, particularly with regard to the course of the disease. However, other findings indicate that this association might more specifically depend on anhedonia, and contradictive findings in general point to the heterogeneity of MDD.

Beyond a relationship between striatal alterations and the symptom spectrum of MDD, other patterns of aberrant activation have been reported. According to a coordinate-based meta-analysis, MDD patients exhibit reward-related hyperresponsiveness of the orbitofrontal cortex (Ng et al., 2019). Given that depression is associated with both reduced reward responsiveness in the VS and that decreased RS frontostriatal network connectivity (Drysdale et al., 2017), hyperactivation of prefrontal regions may indicate heightened inhibitory control over subcortical regions, which in turn may lead to anhedonia (Ng et al., 2019). Besides alterations in prefrontal and striatal regions, MDD is linked to enhanced activity of the anterior cingulate cortex (ACC) during RA (Dichter et al., 2012; Knutson et al., 2008; Quevedo et al., 2017), a region that has been associated with reward-based decision making (Bush et al., 2002). In line with this, a meta-analysis reported that acute depressive states are characterized by downregulated glutamate levels primarily in the ACC (Luykx et al., 2012).

Taken together, previous literature implicates three major reward-related alterations in MDD relative to HC: A *hypo*activation in the VS, in particular in the NAcc and a *hyper*activation in the orbitofrontal cortex. Besides this, aberrant ACC activation was noted. Consistently, Hall et al. (2014) suggested a sensitivity of NAcc, PFC, and ACC during reward processing to the impact of disease burden and recurrent episodes of depression.

#### *BD: Hyperresponsiveness of the reward system*

Manic states are characterized by impulsive decision-making and risk-taking behaviours (American Psychiatric Association, 2013), hence one could expect that elevated dopamine-levels underlie and cause (hypo-)mania. Consistent with this hypothesis, dopamine agonists were observed to induce mania-like behaviors in healthy subjects (Jacobs & Silverstone, 1986). Moreover, more recent findings suggest *low* striatal D2-type receptor availability in impulsivity (London, 2020). Since this behavioural trait is a core feature of mania, this finding could lend indirect support to the hypothesis that manic states are also related to impaired dopamine signalling.

On this basis, the question arises whether models of a hypersensitive reward system can be applied to manic BD patients, and whether BD patients in euthymic or depressive mood states exhibit equal, distinct or no impairments of the reward system at all. Over the years, multiple neuroimaging studies have approached this topic. In the presence of (hypo-)mania, patients with BD revealed reduced VS activity during both anticipation (O'Sullivan et al., 2011) and reward outcome (Abler et al., 2008). In contrast, adolescent BD patients in current manic phases exhibited a different pattern of decreased activation during RA, particularly located to the dorsolateral PFC (Urošević et al., 2016). Regarding euthymic BD patients, equivocal observations of VS activation were reported in the context of reward processing: On the one hand, euthymic BD-II patients had increased reward-related VS activation during RA compared to HC, while this effect did not appear in euthymic BD-I patients (Caseras et al., 2013). Conversely, BD-I patients showed higher VS responses to positive outcomes than BD-II patients. Together these findings emphasize the complexity (e.g., state dependency, reward-phase-dependency) of reward-related dysfunctions in BD. Furthermore, a recent study on euthymic BD patients found

reduced engagement of prefrontal regions during reward processing (Macoveanu et al., 2020). Another neuroimaging study on euthymic BD patients reported elevated engagement of the ACC during RA (Kollmann et al., 2017). In patients with current euthymic to mildly depressed states, Trost et al. (2014) reported decreased bottom-up responsiveness to immediate priorly conditioned reward stimuli within the mesolimbic reward system, particularly in the VS.

By comparing depressed BP patients with unipolar depressed patients, disorder-specific abnormalities within the reward circuitry emerged: Chase et al. (2013) demonstrated reward-related hyperactivation within the ventrolateral PFC in patients with BD-I compared with MDD. Of note, the ventrolateral PFC has been linked to processing salient emotional stimuli (Dolcos et al., 2004). Furthermore, increased responses of this region have been suggested to reflect arousal in BD during RA (Whitton et al., 2015). Interestingly, Whitton and colleagues (2015) provided support for the distinctive role of the PFC by merging results from two separate meta-analyses of magnetic resonance spectroscopy, one on MDD and one on BD: While patients with MDD exhibit reduced brain glutamate levels (Luykx et al., 2012), the opposite effect was observed in patients with BD (Gigante et al., 2012).

In summary, several lines support neural dysregulations during reward processing in patients with BD, though results are in part inconsistent. Besides different affective states in BD, contradictory findings of striatal responses may be due to different methodological approaches: Firstly, studies reporting elevated VS activation in BD mostly employed card guessing games while studies using MID tended to report reduced striatal activation. Secondly, BD samples are often rather small, which is probably a result of both the heterogeneous nature of BD and the difficulty to measure manic patients. Thirdly, although paradigms were often adapted from the same original study, slight variation can be observed, for instance variation of RA duration or lack of neutral/loss trials. Given that impulsivity, a main characteristic of mania, is elevated in both euthymic (Swann et al., 2003) and depressed BD patients (Frye et al., 2007) while VS activation is partly mediated by glutaminergic input from the PFC (Pierce & Kumaresan, 2006), reduced prefrontal activation in BD might reflect impairments of top-down control of the VS. Lee et al. (2017) corroborate the notion of the PFC as a key region in BD by reporting reduced prefrontal grey matter (GM).

### *SCZ: Dopamine hypothesis and aberrant salience*

The dopamine hypothesis has been among the most prominent and enduring models of SCZ. While the original version of this hypothesis supposed a general excessive dopamine-dependent neuronal activity (leading to positive symptoms), it was reconceptualized by integrating subcortical hyperdopaminergic states (Howes & Kapur, 2009). However, due to major advances in genetics, imaging and molecular biology, a third version of the hypothesis followed, which further differentiated the dopamine-related pathomechanisms by assuming four distinct components contributing to the clinical presentation of SCZ (Howes & Kapur, 2009): First, the interaction of multiple factors, particularly fronto-temporal dysfunction, drug use, stress, genetic predisposition, and cause as dysregulation of dopamine release. Second, while former models focused on D2-receptors in SCZ, *presynaptic* dopamine release gained growing attention in this most recent version of the dopamine hypothesis.

Third, dysregulated dopaminergic modulation is associated with psychosis in general. The exact pathology depends on the weighting of the factors named above as well as the socio-cultural context. Fourth, altered dopamine release might bias the appraisal of stimuli and thus leading to 'aberrant salience' to meaningless stimuli (leading to positive symptoms), whereas SCZ patients lack an adequate response to relevant rewarding stimuli at the neural level (Howes & Kapur, 2009; Whitton et al., 2015). This might also foster negative symptoms in SCZ. **Figure 2** illustrates dopaminergic processes in the model of aberrant salience.

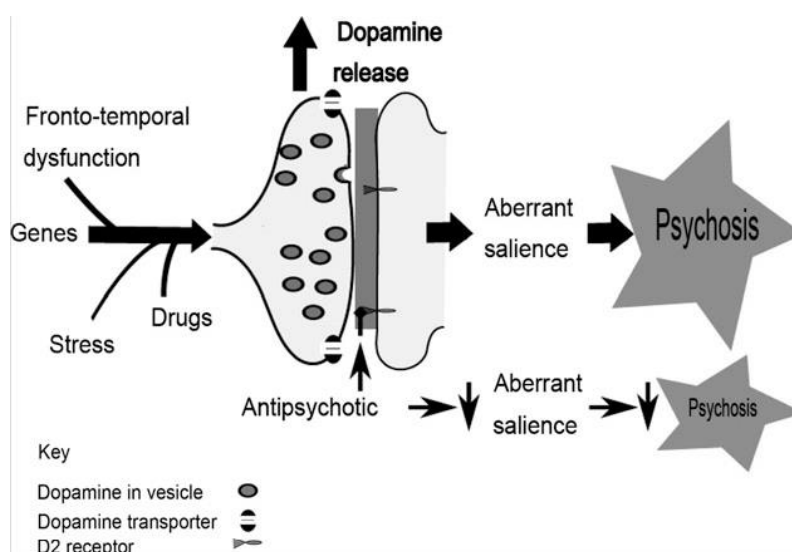


**Figure 2. Aberrant salience hypothesis.** Multiple risk factors interact and lead to striatal dopamine dysregulation, which alters the appraisal of stimuli and may result in psychosis. Current antipsychotics aim to downstream the primary dopaminergic dysregulation. Reprinted with permission from Howes & Kapur (2009).

Over the years, multiple studies found supporting evidence for the aberrant salience model in SCZ. A meta-analysis including eleven striatal (caudate and putamen) [ $^{11}\text{C}/^{18}\text{F}$ ]-DOPA uptake PET studies reported a 14% increase in striatal dopamine synthesis capacity compared to healthy subjects (Fusar-Poli & Meyer-Lindenberg, 2013). Furthermore, overactive dopamine functioning was found correlated with symptom severity and neurocognitive dysfunction in patients with SCZ (Howes et al., 2009).

In the light of the dopamine hypothesis, subregions of the dopamine-rich mesocorticolimbic pathways, particularly the VS, have been intensely examined in SCZ by using fMRI combined with paradigms triggering dopamine release. A recent coordinate-based meta-analysis of neuroimaging studies corroborated reduced activation of a fronto-striatal network during RA (Leroy et al., 2020). Regarding striatal responses to reward, a growing number of imaging studies reported reduced VS response in patients with SCZ during RA (Chung & Barch, 2016; Juckel et al., 2006; Kirsch et al., 2007; Schlagenhauf et al., 2008; Subramaniam et al., 2015). Moreover, severity of negative symptoms was found to be negatively associated with the VS activation (Juckel et al., 2006).

Furthermore, the impact of antipsychotic drugs on reward processing has also been investigated as they target dopaminergic functioning. Reduced VS activity was found in both unmedicated schizophrenics (Juckel, Schlagenhauf, Koslowski, Wüstenberg, et al., 2006) and SCZ patients currently treated with typical neuroleptics (Juckel, Schlagenhauf, Koslowski, Filonov, et al., 2006). Interestingly, patients with only mild hyperactivation of the reward circuitry before atypical antipsychotic monotherapy were likely to improve in negative symptom scores while their reward-related activity decreased over time (Nielsen et al., 2018). In contrast, patients showing reduced striatal neural activation prior to the treatment turned out to be rather treatment resistant, whereas their striatal activation profile normalized over time. According to a recent study, SCZ patients exhibiting dopaminergic dysfunction responded better to antipsychotic treatments than those predominantly characterized by other neurochemical pathomechanisms (Vanes et al., 2018). A recent fMRI study on SCZ examining corticostriatal functional connectivity reported reduced connectivity between the putamen and both the medial PFC and the salience network (Karcher et al., 2019). The salience network has before been shown to be dysregulated itself in SCZ (White et al., 2013). Given the importance of the salience network for the appraisal of stimuli, such studies demonstrate point towards a connection between the dopaminergic hypothesis and the ‘aberrant salience’ hypothesis.

Besides that, it has been shown that patients reveal blunted neural prediction errors to rewarding cues (Morris et al., 2012) as well as exaggerated prediction error learning for meaningless cues (Morris et al., 2013). Furthermore, learning about non-predictive cues was associated with severity of positive symptoms. Given these findings, Whitton et al. (2015) concluded that salience attribution, which usually optimizes the allocation of attention, is impaired in SCZ and that this impairment is for the most part associated with altered striatal functioning.

Further supporting evidence for the hypothesis of aberrant salience derives from self-report studies of negative symptoms in SCZ: Paradoxically, it has been demonstrated that patients with SCZ report similar levels of positive emotion to current feelings compared to HC, whereas non-current feelings are valued more negatively (Strauss & Gold, 2012). This discrepancy suggests that negative symptoms rather reflect beliefs related to low pleasure experiences that surface when patients retrieve non-current feelings than actual real-world pleasurable experiences. In this respect, the quality of anhedonia in SCZ may differ conceptually from MDD, even though the clinical presentation may appear similar. Differences to MDD are also noticeable in motivational aspects of anhedonia: In contrast to MDD, patients with SCZ show no deficiencies in effort expenditure, but decreased allocation of more effort for higher magnitude or higher probability rewards (Barch et al., 2014; Gold et al., 2013). This abnormal effort-cost computation was associated with the presence of negative symptoms (Gold et al., 2013).

Merging evidence from behavioural, molecular imaging and neuroimaging implies a coherent overall picture of enhanced striatal dopamine release underlying positive symptoms of psychosis and blunted striatal response being related to negative symptoms, as assumed by the aberrant salience hypothesis.

Overall, the high prevalence of reward-related alterations across psychopathologies of the affective-psychotic spectrum indicates that experimental imaging data on the reward subsystems might improve our understanding of these pathologies at the neurobiological level.

### 1.3 Imaging genetics as a translational approach in biomedical research

As the search for biological factors influencing cognitive and emotional aspects of mental illness became popular in the 20<sup>th</sup> century, and with molecular techniques advancing fast, genetics moved to the forefront of psychiatric research. This led to tremendous progress in the illumination of the genetic architecture of psychiatric disorders. Since about 70% of an individual's genes are expressed in the brain, variability of genetic information as for example carried by functional polymorphisms, may affect how information is processed (Hariri et al., 2006). With the overarching goal to examine how genetic variants may give rise to different brain phenotypes, including pathological conditions, imaging genetics was established as a synthetic research approach combining neuroimaging and genetics.

#### 1.3.1 Basic principle of genetic information and microarrays in a nutshell

The rapidly evolving field of imaging genetics particularly relies on molecular genetics. A fundamental assumption in molecular genetics is that 99.4% of the DNA is identical between any two humans, whereas around 0.6% varies individually (1000 Genomes Project Consortium et al., 2015). The DNA is an informational molecule that is constructed as two double stranded helices made of around 3 billion nucleotides. Each nucleotide has a backbone that consists of sugar, to which nucleobases are attached, including Adenin, Guanin, Cytosine and Thymine. Furthermore, nucleotide bases are complementary to each other, for instance Adenin only binds with Thymine while Guanin only binds with Cytosine. Most of the DNA is identical between individuals, but single positions of the double stranded helices of a DNA sequence can be variable among humans. These single nucleotide polymorphisms (SNPs) are inherited and heritable variants barely change over generations (Thomas et al., 2011). An individual's genome roughly consists of around 4-5 million SNPs (1000 Genomes Project Consortium et al., 2015). While the vast majority of SNPs is functionally silent, some SNPs actively influence protein structure or expression (Alwi, 2005). Besides a large number of SNPs which are shared in the human population, certain SNPs are rather unique and form the basis of diversity in health and disease.

The current state-of-the-art technology for the investigation of SNPs is microarrays that allows to measure polymorphisms on a large scale of up to about 1 million per probe. Such high throughput techniques have become the technological basis for genome-wide association analyses, posing new statistical challenges. In cases of SNPs not being contained on a chip, meanwhile imputation techniques allow for a reliable indirect estimation of the respective genotypes due to the correlation structure in the population.

#### 1.3.2 Heritability and genetics of psychiatric disorders

At the beginning of the 20<sup>th</sup> century, first family studies, i.e. twin and adoption studies, were conducted, forming the basis for genetic research into psychiatric diseases (Smoller et al., 2019). Twin studies compare concordance rates between monozygotic and dizygotic twins that were raised in the same family. If the concordance rate in MZ is below 100%, an environmental influence on the phenotype is implied. Over the years, a growing body of family studies revealed consistent evidence that



genetics represent an important factor in various psychiatric syndromes (Cross-Disorder Group of the Psychiatric Genomics Consortium et al., 2013; Kendler & Eaves, 2007).

In MDD, a meta-analysis of six twin studies estimated a heritability rate of around 37% (Sullivan et al., 2000). A few years later, a large sample twin study estimated a similar heritability of 38%. Moreover, a study on opposite-sex twin pairs indicated that personality as well as failures of interpersonal relationship were etiologically more important in women, whereas externalizing psychopathology, greater sensitivity to stressors, and prior depression had a stronger impact on liability to major depression in men (Kendler & Gardner, 2014). In SCZ, a recent twin study reported heritability estimates of 79% (Hilker et al., 2018), while those of bipolar patients were ranging between 70-90% (Barnett & Smoller, 2009; Smoller & Finn, 2003).

For more than a decade, genome-wide association studies (GWAS) – that is the parallel association analysis of all polymorphisms – have facilitated the discovery of complex traits in genetics, their links to diseases and their translation toward new therapeutics by identifying genotype-phenotype associations (Visscher et al., 2017). For instance, a large meta-analysis of GWAS on depression identified 178 genetic risk loci as well as 223 independently significant SNPs of relevance for the disease (Levey et al., 2020). Genetic risk loci have also been identified for psychosis. In their cutting-edge paper, Ripke et al. (2014) found 108 loci that meet genome-wide significance for the SCZ.

These genetic risk variants have been applied in a multitude of psychiatric studies. For example, Jonas et al. (2019) showed that the genetic risk for SCZ was also linked to poorer course of disease severity, cognitive deficits and willpower in psychotic patients. Interestingly, this work group was also able to show that among patients with a mixture of affective and non-affective symptoms at initial admission, high SCZ PGRS scores predicted those whose diagnosis would later develop into a non-affective psychosis. These results suggest that a PGRS for SCZ is related to the actual core of psychotic disorders. For BD, 30 loci associated with an increased risk for the disease have been yielded recently (Stahl et al., 2019). By analysing over 50.000 patients of BD or SCZ, Ruderfer et al. (2018) were able to identify 114 genome-wide significant loci associated with synaptic and neuronal pathways that are related to both BD and SCZ.

This brief overview shows that among the affective disorders BD has a higher heritability than MDD. Moreover, evidence of the genetic overlap between SCZ and BD reflects the blurry boundary between psychotic and affective disorders.

### **1.3.3 The endophenotype concept**

Until the 1970s, two different concepts were coupled to examine the heritability of aberrant brain morphology and functioning in psychiatric diseases: Firstly, the term genotype implies a genetic constitution of an individual and can be measured by techniques of molecular biology, including DNA sequencing and polymerase chain reaction (Gottesman & Gould, 2003). Secondly, a phenotype describes any observable characteristic of an individual, such as morphological or physiological appear-

ance. A phenotype is understood as results of the interaction between its genotype and the environment. While some genotypes give rise to specific phenotypes in monogenic diseases following Mendelian Laws, this simple connection does not account for diseases with more complex genetics (Province et al., 2001). The key problem with genotypes is that epigenetic markers have the ability to persist during development while still being transmitted to a descendant (Esteller, 2008; Portela & Esteller, 2010). Consequently, the same genotype has the potential to give rise to a broad variety of phenotypes, and in turn, the same phenotype can arise from different genotypes (Gottesman & Gould, 2003). Moreover, the number of genes involved in a phenotypic expression is related to both complexity of the phenotype and difficulty of the analyses of underlying genes. Therefore, with increasing genetic complexity of psychiatric disorders, their phenotypic classification is not the optimal base for investigating genetic underpinnings (Gottesman & Gould, 2003).

To overcome the limitations of phenotype-based classifications in psychiatry, Gottesman et al. (2003) introduced the endophenotype concept to psychiatric research, which received increasing attention ever since. As a term adapted first applied in the biology of grasshoppers (John & Lewis, 1966), endophenotypes were originally defined as internal phenotypes that are biologically measurable by using biochemical tests or microscopy (2003). Ozomaro et al. (2013) compiled the key points of endophenotypes in modern research as follows: 'The endophenotype should segregate with the illness in the population, and co-segregate with the illness within families; it should be heritable and more prevalent in affected than in unaffected families; it should not depend on whether the illness is currently clinically manifested; and finally, it should be specific to the illness and capable of being reliably measured'.

In general, endophenotypes can be regarded as a link between genotypes and phenotypes. More specifically, they represent physiological/pathophysiological core processes, and only shifts of several of them may result in the clinical phenotype. Moreover, endophenotypes can be specified at different levels of analysis, for instance in neurophysiology, self-report, biochemistry, neurocognition, or assorted other outcomes (Beauchaine & Constantino, 2017). Nevertheless, it is crucial that the investigated marker is genetically vulnerable, however, it is also supposed to be easier to quantify than the phenotype itself. One aim of the endophenotype concept is thus a higher measurement precision compared to phenotype measures, which tend to have a high degree of measurement prediction error (Beauchaine & Constantino, 2017). In contrast, in the ideal case of equally distributed dichotomous genetic vulnerability, the measurement precision of genotypes would be particularly high. By bridging measures of genotypes and phenotypes, endophenotypes harbour the potential to improve the weak measurement prediction of phenotypes. In psychiatry, the concept has experienced a renaissance in evolutionary psychiatry that fuses physiology and pathophysiology, claiming that the same traits that bear a disease risk may be beneficial from an evolution point of view (Keller et al., 2018). **Figure 3** shows the relations between genotypes, endophenotypes and phenotypes as well as their measurement precision illustrated with an example.

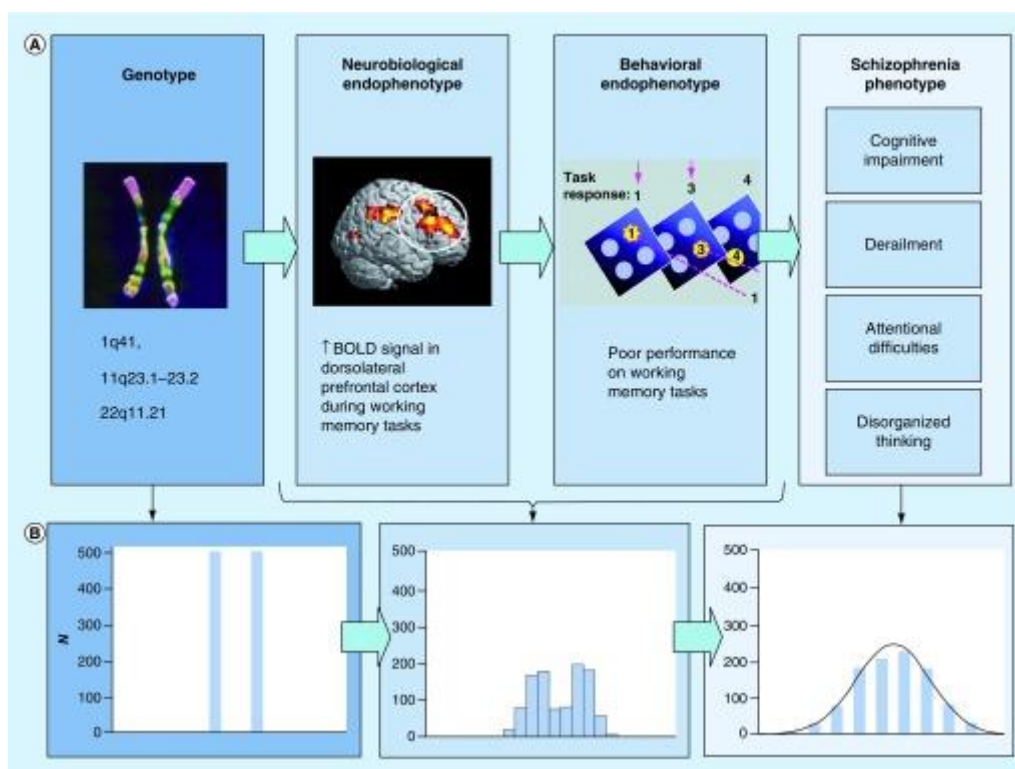


**Figure 3. Levels of analysis and the respective measurement precision illustrated with an example of schizophrenia. (A)** Relations between the concept of genotypes, endophenotypes and phenotypes. **(B)** Measurement precision of different levels of analysis. The genotype level graph on the left shows an ideal measurement precision of an equally distributed, dichotomous genetic trait in a sample of 1000 participants. The middle graph shows a large statistical power of an endophenotype quantification. The graph on the right depicts a quantification of a phenotypic expression with a 50% error. Reprinted with permission from Beauchaine & Constantino (2017).

To this day, endophenotypes for numerous psychiatric diseases have been established, including Alzheimer’s disease (Reitz & Mayeux, 2009), attention deficit hyperactivity disorder (Pineda et al., 2011), alcoholism (Salvatore et al., 2015), anxiety disorder (Bas-Hoogendam et al., 2016), autism (Mahajan & Mostofsky, 2015), BD (Glahn & Burdick, 2011), MDD (Goldstein & Klein, 2014) and SCZ (Allen et al., 2009), and contributed to a better understanding of the biological mechanisms underlying the diseases. Within the next few years, endophenotypes are likely to become an even more important component in psychiatric research as they hold the potential to overcome the weak biological validity of phenotypic classifications.

### 1.3.4 Specific imaging genetic results on affective and psychotic disorders

The combination of genetics and neuroimaging represents a promising approach to understand the influence of genetic variations on the human brain to improve our understanding of the impact of brain-relevant polymorphism on behaviour (Bigos & Weinberger, 2010). Imaging genetics covers sev-

eral different research areas and techniques: On the one hand, for the search of genes, imaging markers get extracted from cords and run across either the whole genome or a subset of genes to find new associations. On the other hand, predefined genetic markers can be applied to examine their relation to a known imaging marker to actually validate genetic markers.

Although various brain phenotypes have been shown to be heritable, the detection of genes associated with either structure or functioning of the brain is quite challenging due to small effect sizes and high costs of MRI measurements, which, together, leads to a lack of power (2012). The ENIGMA (*'The Enhancing Neuroimaging Genetics through Meta-Analysis'*) consortium, an international alliance of researchers, aims to overcome issue by integrating data from over 70 institutions in order to address research questions in neuroscience, genetics, and medicine (Thompson et al., 2014). Among the gene search studies of ENIGMA, all of which yielded remarkable insights into genetic effects on the human brain, three studies deserve special mention as they represent a project cascade: First, Stein et al. (2012) discovered SNPs which were strongly associated with hippocampal volume, the first imaging marker analysed at this scale. The hippocampus is not only an important region for learning (Maguire et al., 2000), spatial and episodic memory (Burgess et al., 2002), and stress regulation (Snyder et al., 2011), but also plays an important role in several psychiatric diseases, including SCZ (Heckers & Konradi, 2002), BD (Frey et al., 2007) and MDD (Caetano et al., 2007; MacMaster et al., 2008). In addition to the SNP linked to hippocampal volume, another intergenic variant revealed an association with intracranial volumes that was investigated in parallel (Stein et al., 2012). Secondly, Hibar et al. (2015) used the entire set of subcortical structures to identify five novel intergenic loci influencing the volumes of the putamen and the caudate nucleus. These regions are important hubs within the reward circuitry (see chapter 1.2) and are also linked to various brain disorders, including SCZ (Ebdrup et al., 2010; Luo et al., 2019), and BD (Hwang et al., 2006) and MDD (Krishnan et al., 1992; Sacchet et al., 2015). Thirdly, Grasby et al. (2020) recently analysed genetic influences on cortical structure parameters. Thereby, they identified 175 loci with effects on regional surface area and 10 loci associated with regional thickness. While not directly linked to disease, these studies stand out due to their statistical power and demonstrate that a certain amount of structural brain variability is directly related to genetic variability. Work is ongoing here to enhance disease *specificity* of brain markers.

## 1.4 Resting state fMRI

### 1.4.1 Origin of RS fMRI and typical observations in associated data

The brain comprises a large number of regions specialized on certain functions, such as processing sensory input, learning, memory, attention or movement execution. Although this model is implying that specialized brain areas are recruited for specific functions, these regions actually communicate with each other constantly, even in the absence of a cognitive demand or an external goal. Together, they form a complex, integrative whole-brain network 'in which information is continuously processed and transported between structurally and functionally linked brain regions' (van den Heuvel & Hulshoff Pol, 2010). While this view corresponds to our fundamental understanding of the functionality of the brain, the discoveries behind it are fairly recent.

After a few years of task-based fMRI studies, it was revealed that task-related shifts in BOLD signals are not limited to increases. Biswal et al. (1995) were the first to report observations of a high synchronicity in low-frequency fluctuations (0.01-0.08 Hz) between the left and right primary motor cortex at rest. This discovery built the foundation for later RS measurements and initiated a new research area in neuroimaging which has since broadened rapidly. Advances in functional neuroimaging provided new tools to analyze interactions between brain regions and consequently enhanced examinations of functional connectivity (FC) (van den Heuvel & Hulshoff Pol, 2010). FC is defined as temporal coherence in the high amplitude, low-frequency neuronal signals among anatomically separated brain areas (Friston et al., 1993; Greene et al., 2016). It can be understood as the level of parallel activity and can be found in the absence of any explicit task (van den Heuvel & Hulshoff Pol, 2010). FC may also change during certain tasks or stimuli – psychophysiological interaction analysis is one example, how such modulations of FC over time can be quantified (Di et al., 2017; Schöpf et al., 2010). Dynamical causal modelling (DCM) takes this one step further and analyzes directionality and influences of nodes on FC between other nodes, allowing to model computational units of the brain (Friston et al., 2003).

At rest, a set of functionally connected regions referred to as the *default mode network* (DMN) emerges with the peculiar property of a higher amplitude compared with a task condition (Raichle et al., 2001). DMN regions typically deactivate during attention-demanding tasks (Fox et al., 2005). This stereotypical deactivation pattern tends to be very robust with regard to its anatomical extension, but this widespread deactivation pattern may vary in anatomical detail, depending on the exact task (Sheline et al., 2009). However, the DMN is not only deactivating as one network – the DMN (through FC) is also bound together to a network, even in the absence of a task. Parker and Razlighi (2019) have demonstrated that task-negative (amplitude) effects and FC are two different but overlapping neurophysiological processes. The question then arose, if the DMN, as found during rest, can also be activated by specific conditions. It was suggested that functions of the DMN are mainly self-referential in nature, such as to empathize with others to understand their desires and intentions, but also to remember the past and to plan the future. Such internal processes are a counterpart to mental activity

directed towards the outside world. In general, Buckner (2008) distinguishes two subsystems of the DMN: The most robust components mainly comprise midline regions, including medial PFC, most rostral parts of the ACC, precuneus, PCC, retrosplenial cortex, and the lateral parietal cortex (Marchetti et al., 2012). Apart from that, both hippocampi as well as both parahippocampal cortices form a second subsystem (Li et al., 2014).

Over the years, RS fMRI has been established as a central technique to characterize the human brain due to its effectiveness, simplicity, and non-invasiveness (Chao-Gan & Yu-Feng, 2010; Smitha et al., 2017). In contrast to task-based fMRI, the disadvantage of RS fMRI lies in the lack of an a priori hypothesis about neuronal activity.

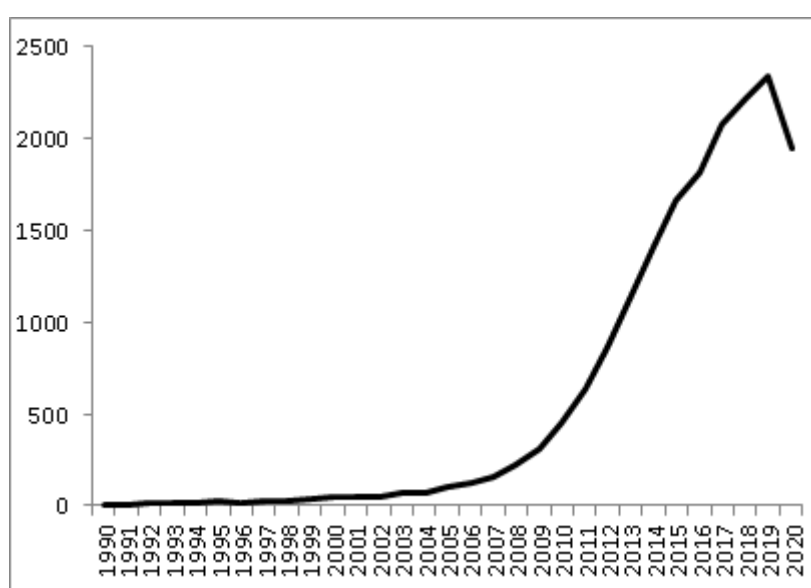


Figure 4. Number of studies tagged “resting-state” and “fMRI” in PubMed between 1990 and 2020.

## 1.4.2 Statistical approaches to RS fMRI data

### Seed analysis

Most straightforward, a RS time-series of a specified seed region (the minimal version of which is a single voxel) can be cross-correlated with either time-series of a second voxel or region, or the time-series of all other regions or voxels (Chao-Gan & Yu-Feng, 2010). Seed regions can for example be a priori defined brain area or a selection based on an activated area from a task-dependent fMRI analysis (van den Heuvel & Hulshoff Pol, 2010). A high correlation of the seed voxel with other voxels during rest implies a strong FC between them. Correlating a seed region with all other voxels of the brain results in a so-called seed-based FC map showing all FCs of a seed region within the brain. **Figure 5** schematically illustrates the basic principle of seed-based analysis of RS data. Here, 'RS' refers to a state without explicit cognitive task, yet different definitions of this state exist (e.g., eyes-open vs.

eyes-closed). Generally, seed analysis can also be performed during task-dependent fMRI either before or after removal of task-related amplitude changes. Although these statistical approaches are compelling for their simplicity and interpretability, their application to whole-brain examinations usually requires a predefined region of interest (ROI) (Smitha et al., 2017).

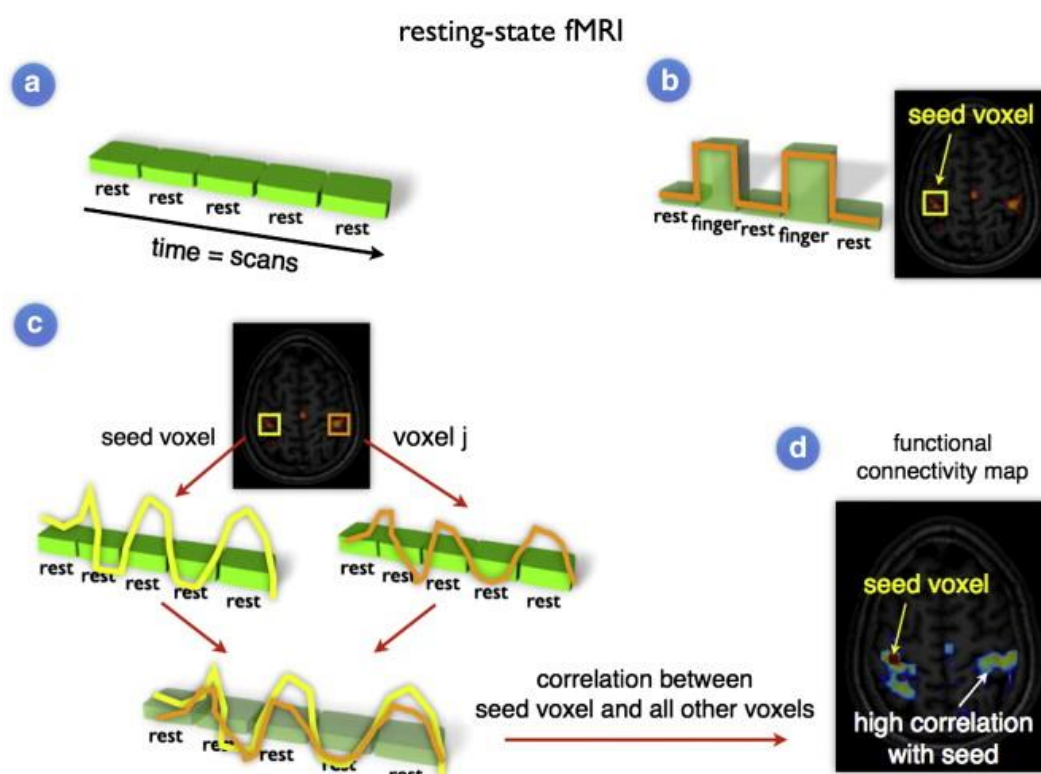


**Figure 5. Basic principle of seed-based RS fMRI.** (a) As in task-based fMRI, the BOLD signal gets measured during a RS fMRI measurement. (b) Prior to the examination, a task-based fMRI experiment can be used to select a ROI  $j$  (here a voxel in the motor network). (c) The FC connectivity between two regions can be calculated by cross-correlating time-series of a predefined seed voxel and a voxel  $j$ . (d) By correlating the time-series of a seed voxel and all other voxels, all functional connections of a seed voxel can be calculated. The resulting FC map displays regions that are highly correlated with the seed voxel. Reprinted with permission from van den Heuvel & Hulshoff (2010).

### Principle of functional connectivity density mapping

Even after many years of insight-enhancing RS studies, new methods are still being discovered to investigate the great potential of RS data sets. More recently, Tomasi et al. (2010) introduced functional connectivity density (FCD) as a highly effective data-driven approach which examines the number of both local or global FCs of a specific voxel by using Pearson's correlation. A high FCD value of a given voxel indicates that this voxel has a large number of FCs to other voxels (or a high average FC intensity) throughout the entire brain and thus suggests a central functional role of the respective region the

voxel is located in (Zhuo et al., 2014). Moreover, FCD is an effective technique that takes full advantage of the native resolution of fMRI data and provides FC maps with a high spatial resolution (3 mm isotropic) (Tomasi & Volkow, 2010). With higher resolution (e.g., 2 mm isotropic) the procedure becomes computationally more challenging: Even if restricted to GM, the round 30.000 voxels result in a matrix with 925 million elements, requiring a tile-wise calculation. The resulting FCD maps have a typical regional maximum in the posterior cingulate and precuneus area that correspond to high glucose metabolism as measured by FDG-PET (Pourhassan Shamchi et al., 2018). Further, local maxima of a FCD map reflect hub areas of typical RS networks (Tomasi & Volkow, 2011). FCD maps can thus be understood as an integral of FC in a single map, emphasising the integrating nature, yet collapsing the detailed information to which other voxels a voxel is connected.

### **Independent component analyses of RS fMRI data**

The self-organisation of the brain's activity in communicating networks is strongly present in the RS. Thus, methods that extract latent components such as independent component analysis (ICA) are attractive to identify functional networks in RS fMRI data (Beckmann et al., 2005; Damoiseaux et al., 2008). Both an individual RS fMRI dataset and data from a whole group can be analysed using ICA (de Vos et al., 2018; Schöpf et al., 2010). ICA results in both maps of components (at the group and the individual level), and the corresponding BOLD time course of these networks. Thus, both voxel-wise analyses of the anatomical extension of functional networks ('*intra*-network FC') and analyses of the interplay between networks ('*inter*-network FC') are typical secondary analysis steps.

#### **1.4.3 RS fMRI findings in MDD, BD and SCZ**

Due to its effectiveness, simplicity, and non-invasiveness as particular advantages, RS fMRI decisively facilitates the examination of critical patient groups, such as paediatric populations or even unconscious patients (Smitha et al., 2017). This is particularly true when compared with task-dependent fMRI that requires cooperation and cognitive ability to perform the task. RS fMRI has proven as an effective tool to identify network alterations in affective and psychotic disorders. Recently, 12 RS fMRI studies all presenting a voxel-wise analysis in MDD and control groups have been meta-analysed (Ma et al., 2019): Depressive patients exhibited increased FC in the left hippocampus, left amygdala and left middle frontal gyrus, whereas decreased FC was found in the left lingual gyrus, left middle occipital gyrus, right middle frontal gyrus and right cuneus. Moreover, illness duration was reported to be associated with hyperactivation in the left parahippocampus and hypoactivation in parts of the cerebellum. Furthermore, Kim et al. (2016) detected a relationship between FC within the affective network (comprising amygdala, orbitofrontal cortex, pallidum and the insular cortex) and depressive mood in adolescent depression.

There is also a considerable amount of literature on abnormal brain functioning in BD at rest. First of all, a recent meta-analysis compared acute and remitted states of BD regarding different patterns of intrinsic functioning of large-scale brain networks and reported that acute phases of BD were also related to impaired FC within the affective network compared to remission (Y. Wang et al., 2020).



However, the literature on RS fMRI experiments in BD is not entirely consistent in itself. For example, a recent seed-based RS study (Syan et al., 2018) showed altered FC in the to the ventrolateral PFC, cingulate cortex, amygdala and medial prefrontal cortex in patients with BD.

In SCZ, several imaging studies reported diffuse hypoconnectivities in multiple brain regions, including the left insula, right superior temporal gyrus, the DMN (including the right medial PFC, left precuneus and ACC), the self-referential network (including the right superior temporal gyrus) and the right pre-central gyrus (Brandl et al., 2019). Moreover, SCZ patients had a lower hemispheric asymmetry of FC compared with healthy subjects (Agcaoglu et al., 2018). Notably, Arbabshirani et al. (2014) addressed the challenge of making a machine learning based diagnosis of SCZ by classifying 195 SCZ patients and 175 healthy subjects using RS measures and with an accuracy of 85%. Aligning with the dopamine hypothesis of SCZ, enhanced FC between the NAcc and association cortices was shown to correlate with hallucinations as key symptom of psychosis, particularly with the degree of complexity of the hallucinations (Rolland et al., 2015).

Of particular relevance for this thesis, several transdiagnostic RS studies have been carried out on brain functions at rest in patients of the psychotic-affective spectrum and shed light on both possible commonalities and differences between diagnostic categories. Kühn and Gallinat (2013) investigated RS activity in both SCZ and MDD and found opposing activation in the ventromedial PFC for the two disorders, with hypoactivation in SCZ and hyperactivation in MDD. On the one hand, the ventromedial PFC is related to self-referential processes (D'Argembeau, 2013). On the other hand, dysfunctional self-reference is present in both MDD (Sheline et al., 2009) and SCZ (Meer et al., 2010). Consequently, findings of opposing activation in the ventromedial PFC align well with different expressions of impaired self-reference in both disorders (Kühn & Gallinat, 2013). Interestingly, comparing RS measures in SCZ and BD revealed a connection between the fronto-occipital network and the anterior DMN, which was not only common to both disorders, but also was correlated with positive psychotic symptoms, indicating a transdiagnostic endophenotype of psychosis (Meda et al., 2012).

Taken together, RS fMRI is a powerful with simple data acquisition and different analysis techniques allowing the detection of abnormalities of large-scale brain networks. Furthermore, RS fMRI findings on psychotic and affective patient groups corroborate the notion of a more continuous clinical spectrum with blurred boundaries between the clinical conditions.



## 1.5 Aims and scope of this study

The current nosology of psychiatric diseases has several weaknesses, particularly in psychotic and affective disorders, and could thus hinder the development of personalized treatments in favour of an optimal outcome. Diagnostics in psychiatry is hitherto still mainly based on subjective self-reports, while biological pathomechanisms and phenotypic heterogeneity of clinical presentations are not adequately taken into account. The high individual suffering for both people affected as well as their relatives and the enormous societal burden make improvements in the current classification of mental illness an urgent topic.

One aim is to introduce a biologically more valid reconceptualization of mental disorders that overcomes the limitation of verbally reported symptoms. Recent initiatives, first and foremost the RDoC project, seek to identify and use such endophenotypes that reflect transdiagnostic pathomechanisms mechanisms and a dimensional approach to the heterogeneity of clinical presentations. This thesis calls into question whether RS and task-dependent fMRI measures of the reward system hold the potential to provide markers for a biologically based characterization of psychotic and affective disorders.

The first goal was to evaluate the endophenotype potential of NAcc RS FC in patients with SCZ. Therefore, we examined whether genetic and environmental risk factors affect FC markers of this key region of the reward system at the level of RS fMRI. The second goal was to characterize neural processes underlying reward processing in MDD, BD, and SCZ. Due to the versatility of reward processing, we focussed on the anticipation phase (rather than the consumption phase) of the MID task by Knutson et al. (2001). Inspired by pupillometric findings of Schneider et al. (2018), we additionally dissected the RA phase in different time windows to disentangle presumed subprocesses reward prediction from reward-related arousal and attentional processes.



## 2. Endophenotype potential of the nucleus accumbens

Content of this chapter has been published as: Eberle C, Peterse Y, Jukic F, Müller-Myhsok B, Czamara D, Martins J, et al. **Endophenotype Potential of Nucleus Accumbens Functional Connectivity: Effects of Polygenic Risk for Schizophrenia Interacting with Childhood Adversity.** *J Psychiatry Brain Sci.* 2019;4:e190011. <https://doi.org/10.20900/jpbs.20190011>.

### 2.1 Importance and approaches of early detection of SCZ

#### 2.1.1 Prognosis of SCZ and relations to therapy compliance

The first acute episode of SCZ usually manifests in late adolescence or early twenties (Gogtay et al., 2011). In this regard, Kirkbride et al. (2006) identified a gender difference: While the risk of onset in men peaks in the age band 20 to 24 years, the highest incidence in females was found to be between the ages of 25 and 29. Furthermore, the distribution of age at first illness in female patients also has a flatter curve relative to men. Regarding this, literature suggests the later onset of SCZ in women to be related to the neuromodulatory effect of oestrogen on D2 receptors and a generally increased vulnerability threshold in women (Häfner et al., 1994). Moreover, in terms of prevalence, men are slightly more often diagnosed with SCZ than women (Abel et al., 2010). In general, courses of the disease range from an almost complete recovery after a single acute episode to severe, non-remitting courses accompanied by development of marked social and cognitive impairments (Jablensky, 2012). Although treatment approaches are continuously improving, the prognosis of SCZ often remains poor. Empirical studies suggest that the prognosis for the course of the disease roughly follows a 'rule of thirds' (Myers, 2010): Around one third of the patients diagnosed with SCZ might experience only one episode from which they recover completely. Another third of those affected might recover partially, i.e., these patients exhibit an episodic course with recurrent psychotic episodes and only partial remission, requiring psychosocial support (Jablensky, 2011). Lastly, some patients fail to respond to treatment and continuously suffer from exacerbations of the disease (Faden & Citrome, 2019). These statistical numbers further underline the sorrowful nature of SCZ and remind of the Kraepelian dichotomy between relapsing-remitting and progression-type of disease. Moreover, the chronicity in two-thirds of the patients represents a major factor causing the disproportionately high medical and rehabilitation costs compared to other chronic diseases (Desai et al., 2013).

A major hindrance to an ideal treatment regime is the loss of reality, including false perceptions and beliefs (Larson et al., 2010). As a core symptom of SCZ, loss of reality fosters the lack of both disease insight and trust in the good intentions of the practitioners and consequently has negative impact on the therapy compliance. Choosing a treatment that is tailored to the individual patient may also enhance the patient's confidence in practitioners and thus improve therapy adherence.

Nevertheless, it is not only important to give the accurate diagnosis and offer an individual therapy strategy, but also to treat psychotic symptoms at the earliest possible stage. Several lines of evidence

suggest an association between the duration of untreated psychotic symptoms and therapy outcome, including worse functional disabilities, greater symptom severity, poorer quality of life and higher rates of resistance of antipsychotic treatment (Barnes et al., 2008; Larson et al., 2010; Marshall et al., 2005; Perkins et al., 2005). Unfortunately, however, a long-term study indicates that the first treatment is commonly preceded by a year-long period of psychotic symptoms (Loebel et al., 1992). Therefore, there is much room for improvement as early treatment is likely to enhance the clinical and functional outcome of first episode psychosis. The detection of SCZ at an early stage is thus essential to lower subjective suffering, the risk of chronicity and the resulting burden for the healthcare system.

### **2.1.2 Genetic, developmental and environmental risks for schizophrenia**

Since early detection of SCZ is pivotal for the course of the disease (Larsen et al., 2011), it is important to reconsider what is known on its aetiology. According to the stress-vulnerability model of SCZ, onset and course of SCZ result from multiple factors (Zubin, 1975): On the one hand, as pointed out in the first chapter, twin studies (Sullivan et al., 2003) and family studies (Freedman et al., 2001; Lichtenstein et al., 2006) suggest a high heritability of the illness. On the other hand, there is accumulating evidence that a wide range of environmental factors are associated with psychotic outcomes, such as growing up in an urban environment, cannabis abuse, minority group position and the exposure to early life adversity (e.g., childhood abuse, emotional neglect, bullying), particularly during critical phases of brain development (Matheson et al., 2013; van Dam et al., 2012; van Os et al., 2010). Moreover, several studies indicate an association between severe childhood experiences, including sexual abuse, chronic victimization and disrupted attachment relationships, and several positive symptoms during adulthood, for example hallucinations and paranoia (Bentall et al., 2012; Bentall & Fernyhough, 2008; Daalman et al., 2012; Read et al., 2005; Varese et al., 2012).

### **2.1.3 Brain alterations related to SCZ**

#### **Brain patterns in established SCZ**

In order to detect these preliminary symptoms despite their often inconspicuous nature, the question arises whether risk factors or the prodromal phase are already accompanied by brain abnormalities and, if so, whether these abnormalities are similar to the ones found in the fully expressed disease. At the structural level, a review of longitudinal morphometric studies in manifested SCZ (Olabi et al., 2011) revealed multiple structural alterations in frontal, parietal and temporal regions, as well as reduced whole-brain volume and larger increases of lateral ventricular volumes. In addition, morphological changes were positively associated with the duration of illness. Furthermore, a large-scale cross-sectional study of the ENIGMA consortium (van Erp et al., 2016) pointed to abnormally low subcortical volumes, particularly in the hippocampus, amygdala, thalamus, and the NAcc. Of particular interest for our research question on the reward system, volume increases of the putamen and the pallidum were positively correlated with illness duration. Additionally, the severity of hippocampal volume deficits were associated with a higher proportion of drug-naive patients. In addition, structural

alterations were also found in populations at increased risk for SCZ. For example, Meisenzahl and colleagues (2008) reported GM volume reductions in several areas across the entire brain, including frontal, lateral and medial temporal regions. Together, these findings conveyed a picture of a progressive developmental brain disorder of high complexity.

At the fMRI level, both RS and task-based fMRI studies point to converging alterations in frontotemporal regions, including the dorsolateral prefrontal cortex, orbitofrontal cortex and superior temporal cortex (Mwansisya et al., 2017). In addition to these cortical areas, studies in SCZ also focussed on subcortical regions, including the NAcc. As detailed above (chapter 1), in light of the dopamine hypothesis, the NAcc is of particular importance for SCZ due to its key role within the mesolimbic pathway as the main projection site of dopaminergic neurons in VTA (Grace, 2000). Moreover, it also receives inputs from other brain regions, including amygdala, PFC, hippocampus and thalamus (Groenewegen & Trimble, 2007). Given that these regions are involved in the pathophysiology of SCZ (Harrison, 2004; Mahon et al., 2012; Pergola et al., 2015; Wible et al., 2001), a central role of NAcc in SCZ is further suggested. Furthermore, Knutson et al. (2007) reviewed pharmacological MRI evidence that dopamine release in the NAcc increases indeed local BOLD signals. For example, findings of disturbed NAcc BOLD responses in fMRI provide insight into dopamine functioning of this key node of the reward system. Generally, RS fMRI evidence suggests increased NAcc FC during rest in patients with SCZ (Kiparizoska & Ikuta, 2017; Lee et al., 2019; Liu et al., 2017; Zhuo et al., 2014). Consistency of the direction of this FC effect is mentionable and supports the confidence in this type of RS fMRI marker. The aforementioned relation of hallucinations in SCZ and increased FC between the NAcc and association cortices further supports the importance of this striatal region (Rolland et al., 2015). Preclinical studies also emphasize the role of NAcc in the context of psychotic experience, as animal studies showed that antipsychotic injections into the NAcc suppressed amphetamine-induced behaviours (Pijnenburg et al., 1975), which in turn resemble psychotic symptoms (Shoptaw et al., 2009). Concordant with this, Mikell et al. (2009) even suggested that the NAcc, together with the hippocampus, could be a potential target for high-frequency electrical stimulation in the treatment of positive symptoms in SCZ.

### **Polygenic risk for SCZ and brain development**

So far, several studies in the field of imaging genetics have combined PGRS of SCZ and fMRI measurements, revealing associations of polygenic risk with task-related recruitment of several brain regions (Dezhina et al., 2019). Among these regions and of particular interest for this study, several studies found an association between VS functioning and PGRS of SCZ, for example during choice behaviour (Lancaster et al., 2016) and processing of rewards (Lancaster et al., 2018; Lancaster, Linden, et al., 2016). Besides task-based studies, RS fMRI investigations discovered PGRS effects on FC of multiple brain regions, including the insula (Wang et al., 2017) and the VS (Dandash et al., 2014; Hua et al., 2019). This is interesting as besides striatal areas, the bilateral insula (as part of the salience network) are also involved in reward processing (Fauth-Bühler et al., 2014). Furthermore, findings from

two childhood samples suggested that the FC of the VS is heritable (Achterberg et al., 2018). Of additional interest for this work, Grimm et al. (2014) reported similar functional VS alterations during RA in healthy first-degree relatives of patients with SCZ compared to SCZ patients. Interestingly, one study investigated the relationship between specific dopaminergic risk allele load and volumes of putamen and detected an interaction with childhood adversities (CA) (Hoffmann et al., 2018).

### **Effects of cannabis abuse and CA on brain development**

Increasing research effort also focused on neuroimaging correlates of several environmental factors for SCZ. As already pointed out, reasonable evidence suggests a link between psychotic disorders and cannabis use (Hall & Degenhardt, 2008; Hamilton, 2017; Rolland et al., 2015). Furthermore, cannabis use has not only been linked to the symptoms of SCZ, but also to physiological alterations similar to the actual disease: At the structural level, Yücel et al. (2008) reported volume reductions in both the hippocampus and the amygdala in heavy cannabis users. Moreover, THC-dependent changes in GM density, volume, and surface morphometry were detected in the left NAcc (Gilman et al., 2014). At the functional level, occasional cannabis users exhibited increased striatal glutamate concentrations as well as reduced FC between the NAcc and cortical areas (Mason et al., 2019). Furthermore, Manza et al. (2018) detected increased FCD in several subcortical dopamine-dependent, including the VS (where the NAcc is located) and midbrain areas (covering VTA and substantia nigra). Additionally, reduced connectivity was observed in both the DMN, particularly the PCC, and the anterior insula (Wall et al., 2019). Interestingly, PCC effects were also associated with the subjective experience of the THC intoxication.

While effects of cannabis in the human brain are well-explored through experiments with similar processes compared to the pathophysiology of psychosis, examinations of CA in SCZ are rather complex, not least because of its conceptualization and quantification. Nevertheless, a growing body of findings suggests connections between CA and brain development: According to a recent meta-analysis on CA in SCZ, a history of childhood trauma was associated with reduced GM volume in the PFC and decreased WM integrity in specific traits as well as disturbed FC in network which includes the amygdala, the precuneus/posterior cingulate cortex region, ACC and the temporo-parietal junction (Cancel et al., 2019). In healthy subjects, early life stress was shown to be related to connectivity between amygdala and dorsolateral PFC and between amygdala and the rostral ACC (Kaiser et al., 2018). Moreover, both associations were linked to stress responses in adult life. Another study found that effects of early life stress were reflected in age-related attenuations in VTA-hippocampal circuitry, indicating exacerbations of the effect in trauma-exposed youth (Marusak et al., 2017). Notably, male cocaine users with a history of early life stress were shown to have an aberrant amygdala-striatal connectivity (Kaag et al., 2018), indicating an interaction of the two different environmental risk factors on mesocortical dopaminergic pathways. In addition, animal studies provided consonant findings of impairments in GABA signalling of the NAcc in a mouse model of early life adversity (Mitchell et al., 2018).

Taken together, neuroimaging research suggests effects of CA on multiple regions of the human brain, including striatal regions, particularly the NAcc, a key region in the pathophysiology of SCZ. In addition,



effects of THC exposure have also been observed on several brain regions, including the VS. Furthermore, the study on cocaine users provides a good example that certain risk factors may only become significant when other co-occurring environmental risk factors are present, indicating interaction effects of risk factors for SCZ.

#### **2.1.4 Do childhood trauma and polygenic risk for schizophrenia interact?**

In favour of early detection of SCZ, this chapter focusses on related risk factors and their effects on brain function. Literature so far suggests that the VS, typically involved in established SCZ, was found to be relevant both in the context of SCZ-PGRS studies and in the context of neuroimaging studies on environmental risk factors of the disease, including CA. Against the background of the dopamine hypothesis, in which the NAcc plays a central role, and the heredity of the FC of the VS, which includes the NAcc, the question arises whether RS-FC of the NAcc represents a potential endophenotype that captures a physiological process jointly influenced by genetic and environmental factors.

To pursue this question, we examined whether CA and polygenic risk for SCZ influences NAcc activity, and if these factors interact. Methodologically, we used two different analysis techniques of FCD: Firstly, we calculated FCD maps of the whole brain and extracted regional values from the NAcc. However, while FCD is sensitive to anatomically diffuse or multi-regional FC effects, its averaging principle does not allow the localization of anatomical sources of its effects. Therefore, an additional NAcc seed analysis was performed in order to backtrack FC changes with the NAcc on an anatomical level. These two complementary approaches were employed in a sample of 253 healthy volunteers to evaluate whether genetic risk for SCZ and the interaction between genetic risk and CA influences FC of the NAcc at rest. In addition to these analyses, comparisons between symptomatic SCZ patients and healthy controls were performed in an endophenotype framework, allowing replication of FCD findings in SCZ, and comparison of these effect sizes with effect sizes of the genetic risk or CA.

## 2.2 Methods

### 2.2.1 Sample

The sample examined for this research question originates from four separate imaging genetic studies that were conducted at the Max Planck Institute of Psychiatry between 2014 and 2018. All study protocols were in line with the Declaration of Helsinki and the local ethical review committee of the Ludwig Maximilians University of Munich. First, TMEM was an imaging genetics study investigating effects of genes associated with anxiety and recruited 160 healthy individuals of which 136 were included in this study after ten general exclusions (study abortion, incidental findings), 13 exclusions related to genetics (ethnic outliers, relatedness with other individuals) and one fMRI-related exclusion. Second, from the Imaging Stress Test ('IST') study had 59 healthy individuals of which six were excluded due to quality control (QC) failures regarding genotyping. Third, the PsyCourse ('PSC') study represents a multicentered biopsychological study funded by the German Research Foundation. With the aim of investigating the longitudinal effects of psychotic and affective disorders, the study sample includes patients with unipolar and bipolar depression and SCZ as well as healthy control subjects. In the scope of the present study, 26 healthy subjects and 26 patients of the psychotic spectrum, in particular SCZ (N=15) and schizoaffective disorder (N=11) have been included. Of patients with SCZ, 3 were excluded due to motion artifacts. Finally, the Biological Classification of Mental Disorders ('BeCOME') study is an ongoing project with the ultimate goal of deep phenotyping of psychiatric disorders mainly ranging from depression to anxiety.

### 2.2.2 RS fMRI and T1-weighted image acquisition

Together with anatomical images, functional whole-brain echo-planar imaging data were acquired on a 3 Tesla scanner (Discovery MR750, General Electric, Milwaukee, U.S.A.) using a 32 channel head coil (MR Instruments Inc., Minneapolis, MN, USA) for each subject. Images were recorded with an AC-PC orientation of all slices. In addition, three of the four studies also included single high-contrast echo-planar images (EPI) for the purpose of spatial normalisation. During the RS measurement, participants were instructed to lie still and to gaze on a white fixation cross. The projection was presented on a screen behind the scanner that could be seen by the participant through a mirror. Slight variations of parameters and length of measurement between the four studies were unified for our analysis. In order to allow for a general habituation phase to the environment in the scanner, RS measurements were always conducted after the acquisition of anatomical images. In all studies, anatomical high-resolution images were uniformly acquired with the following settings: T1-weighted, TR = 6.2 ms, TE = 2.3 ms, slice thickness = 1 mm, sagittal FSPGR BRAVO, number of slices = 196, field of view = 25.6 × 25.6 cm<sup>2</sup>, effective resolution = 1 × 1 × 1 mm<sup>3</sup>.

### 2.2.3 Childhood trauma assessment

In all studies, the participants filled out a self-rating questionnaire that included demographic and childhood traumas. Severe childhood experiences were quantified uniformly using the German version of the 34-item Childhood Trauma Questionnaire (CTQ) (Bernstein et al., 2003; Wingenfeld et al., 2010). In this measure, five different types of adverse childhood and adolescence experiences are determined, namely physical, emotional and sexual abuse as well as emotional and physical neglect. Each subscale consists of five Likert-scaled items. Severity classification was then based on validated ranges (Bernstein et al., 2003; Bernstein & Fink, 1998; Häuser et al., 2011). In order to detect downplaying of maltreatment, an additional minimization/denial validity scale is included in the CTQ. Besides that, patients with SCZ were rated using the PANSS (Kay et al., 1987) to quantify present psychotic and negative symptom severity as well as general psychopathology.

### 2.2.4 Genotyping, imputation and polygenic risk score calculation

The genotyping was carried out using Illumina GSA arrays (all BeCOME and all PSC participants in one run) and OmniExpress (all TMEM subjects and all IST subjects in two separate runs). The next step was as strict quality control (QC) in which all SNPs that met one of the following criteria were excluded: a  $p$ -value for deviation from Hardy-Weinberg-Equilibrium below  $1 \times 10^{-5}$ , a minor allele frequency below 1%, or a call rate lower than 98%. A multidimensional scaling analysis (MDS) was performed within each of the cohorts on the LD-pruned genotypes in PLINK (Purcell et al., 2007). Next, missing genotypes were imputed using impute2 (Howie et al., 2009) and shapeit2 (Delaneau et al., 2011). The 1000 Genomes Phase II dataset was selected as the reference sample. The last step of SNP preparation involved the selection of those SNPs that had an info-score above a set threshold of 0.8. In the final dataset, 8847825, 8256847 and 7734296 SNPs were available for batches (1)–(3).

The calculation of PGRS for SCZ was based on a genome-wide association analysis for SCZ (Schizophrenia Working Group of the Psychiatric Genomics Consortium, 2014). In a first step, the best-guessed genotypes (using a probability threshold of 0.9) were LD-clumped according to genome-wide summary statistics. Subsequently, dose information from the clumped SNPs was isolated and applied to the calculation of risk scores. The PGRS was calculated by adding up the risk alleles of those SNPs that had genome-wide significance in the mentioned GWAS and subsequently weighted them with the respective log (OR). Eventually, the resulting PGRS were scaled to the number of SNPs that were used for the PGRS calculation (BeCOME/PSC: 195; TMEM/IST: 193) and Z-transformed (PGRS<sub>z</sub>) separately to control for batch specific shifts. Due to differences of PGRS distributions after scaling, we regarded more lenient  $p^T$  like 0.05 as not reliable enough.

### 2.2.5 RS fMRI preprocessing

Based on Matlab 2017a (MathsWorks Inc., Natick, Massachusetts, USA), scripts for preprocessing fMRI data combined both SPM (version SPM 12) (<https://www.fil.ion.ucl.ac.uk/spm/soft->

ware/spm12) as well as FSL functions (<https://fsl.fmrib.ox.ac.uk/fsl/fslwiki>) and were uniformly applied to each of the four sub-samples under the use of a Linux cluster. The preprocessing of per subject included the following consecutive steps: (1) The first four EPI volumes were removed from the time series to prevent T1-equilibration influencing the slice timing correction process. (2) Realignment was conducted using rigid body motion correction, whereby the first image was selected as a reference image, and images were interpolated (5th spline interpolation). In order to define outliers, voxel-wise root-mean-squared (RMS) intensity differences of the volume N and volume N+1 (DVARs measure) were calculated based on rigid body motion conducted on a copy of time series. Default thresholds (values larger than 75<sup>th</sup> percentile plus 1.5 times the interquartile range) were applied. The dummy regressor matrix resulting from this step marked critical images of the time series and was out aside for later denoising of the data. (3) Subsequently, slice timing correction was performed with regard to study specific number of slices, slice ordering scheme and TR. (4) The spatial normalisation was based on a specifically acquired strongly T2-weighted single EPI (for BeCOME, IST and TMEM) and, In the case of PsyCourse, a segmented average of the first four T1-unequilibrated images. Unified Segmentation (Ashburner, 2007) in SPM12 with default settings was applied. In all studies, a good separation between grey matter (GM), white matter (WM) and cerebrospinal fluid (CSF) was observed. The resulting GM and WM probability maps were then fed into DARTEL's iterative normalization algorithm as a dual input (six generation of Ixi templates, DARTEL default settings) (Ashburner, 2007) in order to create a flowfield (warping information) that connects the MNI and native space. Thereafter, time series were spatially transformed using this transformation matrix and interpolated to a resolution of  $3 \times 3 \times 3 \text{ mm}^3$  for later FCD analysis as well as  $2 \times 2 \times 2 \text{ mm}^3$  for later seed analysis. Additionally, spatially normalised versions of GM, WM and CSF probability maps were created at both resolutions. (5) Using the FSL brain extraction tool, a brain extraction mask was generated and applied to the time series. (6) Within a multiple linear regression, denoising was carried out according to the CompCor method (Behzadi et al., 2007) and included the five PCA components of WM and CSF, which declared ~45% and ~50% of the variance respectively, in addition to six motion coefficients and their temporal derivatives, and the DVARs-based binary matrix. Spatial smoothing ( $6 \times 6 \times 6 \text{ mm}^3$ ) was performed on the resulting residuals and subsequently added to the intercept for following analysis. (7) Afterwards, a temporal bandpass filtering with a range of 0.008-0.100 Hz was applied. (8) In the final step of fMRI preprocessing, all time series were temporally interpolated to a uniform TR of 2.25 ms with a standard Matlab function (*interp1*, piecewise cubic spline). Furthermore, the first five images and a varying number of right-end images, dependent on the substudy, were excluded from these time series to achieve 136 images in each subsample as a common inter-study duration of 5 minutes and 10 seconds. (9) Finally, a quality control included (a) the visualization of an exemplary preprocessing image of the time series overlaid with the normalized GM and WM segment, as well as (b) the exclusion of subjects with more than 10 abrupt motions between two directly consecutive volumes exceeding 2 mm in terms of translation or 0.02 rad in terms of rotation. This criterion defined a cut-off line between the majority of subjects and three SCZ patients that were excluded due to severe outlier features.

### 2.2.6 Anatomical segmentation and NAcc definition

The processing of high-resolution T1-weighted images (T1WI) was carried out in two different manners in order to be used in MNI space along with the EPI BOLD time series: On the one hand, the volumetric segmentation and the reconstruction of cortical areas was conducted with Freesurfer image analysis suite (<http://surfer.nmr.mgh.harvard.edu>, version 6.0). On the other hand, a transformation matrix to the MNI space was generated using DARTEL. Next, a discretized segmentation image of FreeSurfer was spatially transformed to MNI space and interpolated to  $3 \times 3 \times 3 \text{ mm}^3$  for later FCD maps and  $2 \times 2 \times 2 \text{ mm}^3$  for later seed analysis. In either option, we employed an intensity cutoff of  $>0.6$  to return to a binarized version of the mask again. **Figure 6** shows such thresholded ( $>0.6$ ) group average of all study subjects at  $2 \times 2 \times 2 \text{ mm}^3$  in MNI space.

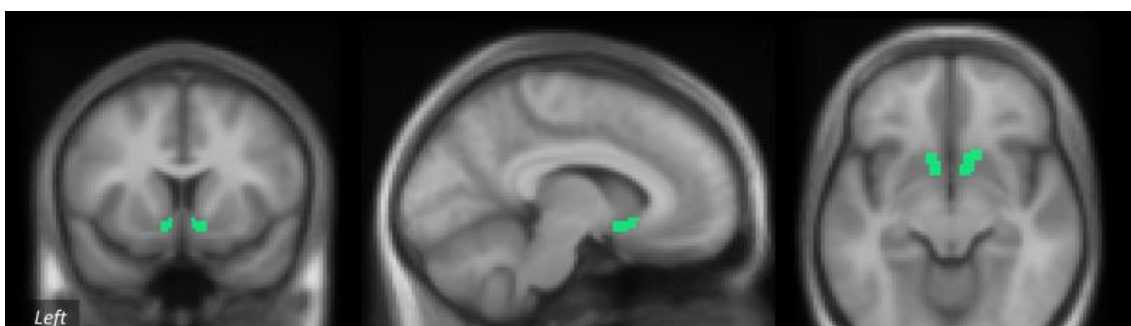


**Figure 6. NAcc mask.** MNI space customized T1 whole-head average on which a binarized ( $>0.6$ ) MNI-normalized and NAcc mask interpolated to  $2 \times 2 \times 2 \text{ mm}^2$  (as employed in the seed analyses) is displayed. Adapted from Eberle et al. (2019).

### 2.2.7 FCD Mapping

The calculation of FCD was based on the preprocessed time series with the resolution of  $3 \times 3 \times 3 \text{ mm}^3$ . A canonical GM probability masked containing 47351 voxels which was multiplied with the individual analysis mask of the residualisation GLM resulted in an average of 43199 (SD 1590) voxels that served as the analysis space. As a next step, we Z-transformed and calculated the mean of FC values using intermediate storage of  $500 \times 500$  cross correlation submatrices to generate an FCD map for each participant. To enhance both sensitivity and distribution proper of the residuals, we smoothed the FCD maps with a  $3 \times 3 \times 3 \text{ mm}^3$  (FWHM) Gaussian filter. **Figure 7** shows proof-of concept averages of both HC and SCZ. In addition, a global FCD value ( $\text{FCD}_{\text{global}}$ ) reflecting the mean of all voxels  $>0.001$  was generated to be applied later as a covariate. Moreover, we recalculated average FCDs of the left and right NAcc ( $\text{FCD}_{\text{NAcc}}$ ) from each binarized  $3 \times 3 \times 3 \text{ mm}^3$  NAcc mask.

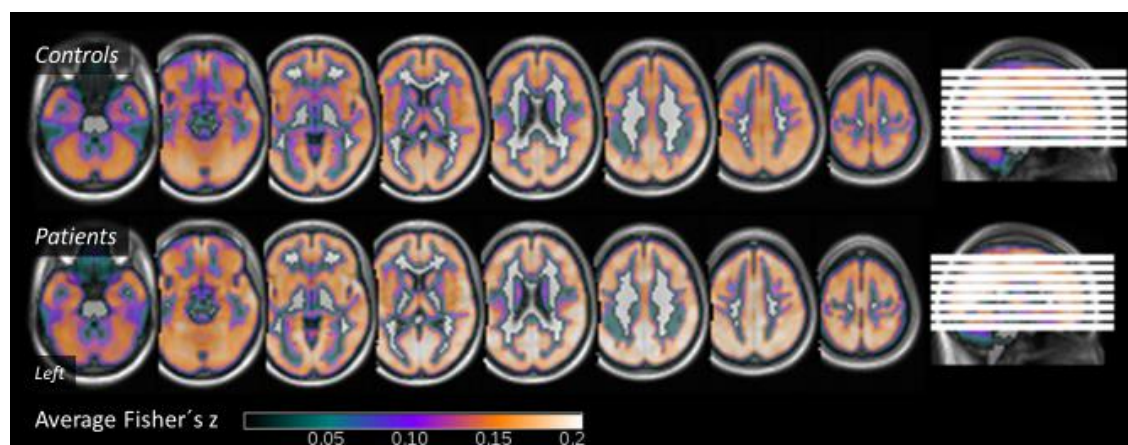


**Figure 7. Proof-of-concept group averages.** Group averages for HC (N=253) (upper panel) and SCZ (N=25) (lower panel). Note typical range of Fisher's Z values around 0.15 and posterior midline hub. Maps shown are not corrected for sex, age and sub-sample. Adapted from Eberle et al. (2019).

### 2.2.8 Proof-of-concept default mode seed analysis and NAcc seed analysis

In order to achieve a higher accuracy of the seed placements and recruited networks, we conducted seed-to-brain analyses on the isometric 2 mm version. Prior to the NAcc analysis, we conducted a seed analysis with anterior and posterior midline nodes of the DMN taken from an independent sample of 25 subjects with EEG-validated wakefulness (Sämann et al., 2011) to confirm the anticipated FC patterns. Together with beta coefficients, the 1<sup>st</sup> level models containing an intercept and time series of the seed region as a regressor of interest were forwarded to a 2<sup>nd</sup> level model that contained age, sex and three source sample dummy variables as covariates. The DMN map revealed both positively and negatively correlated areas, including bilateral insular cortex and inferior parietal regions, indicating the efficiency of the global signal correction as well as mild, yet not overly exaggerated anticorrelations. Interrogations of 2<sup>nd</sup> level NAcc seed patterns yielded the most pronounced FC in the (orbito-) medial PFC, which aligns with previous work (Rolland et al., 2015).

### 2.2.9 FCD and NAcc functional connectivity group effects

Comparing patient and control groups for FCD maps as well as seed-based connectivity of the left, right and bilateral NAcc revealed the following results: First, additionally to our three sample source dummy covariates, we inserted sex, age and  $FCD_{global}$  as nuisance covariates. While no difference of the gender distribution was observed (Pearson Chi-Square 0.190,  $p = 0.663$ ), patients and HC differed in their age ( $T = -5.654$ ,  $p < 0.001$ ). Following the correction for sample source, age and sex,  $FCD_{global}$  showed no group differences (ANCOVA,  $F = 0.746$ ,  $p = 0.388$ ). Furthermore, HC and SCZ differed regarding the relation between  $FCD_{global}$  and bilateral NAcc (partial correlation 0.532 for controls and 0.735 for patients, respectively; group-by- $FCD_{global}$  effect [multiple linear regression]  $t = 6.966$ ,  $p < 0.001$ ). Consequently, for the voxel-wise analyses, age, sex and  $FCD_{global}$  were modelled and centered as separate covariates. The analyses comprised group comparisons of main effects, and, based on conjunction analysis (Friston et al., 2005), combined the group and group-by-covariate effects. The

same procedure was followed for NAcc seed analyses, except for that no global correction variable was available here.

### 2.2.10 Effects of PGRS, CA and PGRS-by-CA-interaction

The effects of PGRS or CA or the interaction of the two factors were analysed in the sample of healthy participants (N=253). Log and z-transformation of the CA scores from the CTQ (CTQ<sub>LOG-Z</sub>), an interaction term (INTER<sub>Z</sub>) was generated by multiplying the CTQ<sub>LOG-Z</sub> with the PGRS<sub>Z</sub>. For examinations of effects of CA, the PGRS and their interaction, a multiple linear regression was performed with age, sex, sample source, CTQ<sub>LOG-Z</sub>, PGRS<sub>Z</sub> and INTER<sub>Z</sub> as predictors. In the following text the effects will be abbreviated as CA, PGRS and INTER for easier reading.

In a first step, this model was used on extracted FCD<sub>global</sub> and FCD<sub>NAcc</sub> (with FCD<sub>global</sub> as covariate). In addition, we analysed FCD effects of the three regressors of interest at the voxel level ( $3 \times 3 \times 3 \text{ mm}^3$ ) within a multiple linear regression model. Furthermore, we conducted multiple test correction of clusters collected at  $p_{\text{voxel}} < 0.001$  for a whole-brain mask (51395 voxels), a study specific mask (collected at  $\text{FWE}_{\text{voxel}} < 0.05$ ,  $k = 10$ ) derived from the SCZ/controls conjunction analysis (182 voxels), and for a bilateral NAcc mask (70 voxels). Lastly, seed analyses of the NAcc were investigated using the same 2nd level setup to evaluate the impact of CA, PGRS and INTER on connections of the NAcc.

### 2.2.11 Post-hoc analysis: comparing clinically established disease with combined high-risk CA/PGRS profile

To examine whether FCD of the NAcc holds potential as a risk indicator for SCZ on which genetic and environmental risks project, HC were subdivided into the following three risk level groups on the basis of a 75<sup>th</sup> percentile split point: (i) low risk, with low levels of PGRS and CA, (ii) medium risk, with low values of either PGRS or CA, (iii) high risk, with high values of both PGRS and CA. Using an ANCOVA (4-level factor risk, adjusted for sample source, age, sex, risk-by-age, risk-b-FCD<sub>global</sub>), we tested differences between each of the three groups and SCZ patients.

### 2.2.12 Significance criteria

In anatomical space analyses performed in the SPM general linear model (GLM) framework, the set significance criteria were clusters sampled at  $p < 0.001$ , supplemented by whole-brain FWE of  $p$ -values of the clusters. Labelling of significant clusters ( $p_{\text{cluster.FWE}} < 0.05$ ) was based on the Automated Anatomical Labelling (AAL) toolbox (Tzourio-Mazoyer et al, 2002). To investigate FCD<sub>global</sub> and regional FCD values of NAcc, respective models were tested using SPSS (Release 18.01, SPSS Inc., Chicago, Illinois) as described, whereas  $p < 0.05$  was set as a significance criterion.

## 2.3 Results

### 2.3.1 Demographic characteristics of study sample

Demographic details of healthy controls (N=253) and patients (N=23) that participated in the fMRI and genetic analyses are shown in **Table 5**. Missing or incomplete CTQ information, lack of genetic data, or failure in passing the fMRI quality control were handled as exclusion criteria.

The diagnoses were made by the patient's psychiatrist during hospitalization and represented the clinical diagnosis at the patient's discharge. The average age of patients and HC differed by about 8.9 years ( $p < 0.001$ ); there was no difference in gender distribution. Regarding CTQ, most of the HC (N=253) exhibited no to minimal severe values (63.6-94.1%), followed by low to moderate (2.4-26.5%) and moderate to severe CTQ values (2.0-7.1%), while only a small number of subjects had severe to extreme CTQ scores (0.4-3.6%). **Table 6** shows the categorization of HC into CTQ severity classes (Bernstein & Fink, 1998; Häuser et al., 2011). Our sample was similar to a large sample in terms of the distribution of CTQ scores, whereby around half of the subjects scored in the low to moderate severity class or higher in at least one of five categories (Häuser et al., 2011). Compared to the patients' CTQ scores, HC were about 9 points lower ( $p < 0.001$ ). Another difference between HC and SCZ was found in the distribution of subjects over the number of CTQs in the range of low to moderate severity (range 0 to 5 categories) (Pearson Chi Square 19.77,  $p < 0.001$ ), which supports the link between CA and SCZ (Read et al., 2005). Among HC, 120 subjects showed elevated CTQ values in one or more categories. Patients had an average duration of disease of about 12.4 years, ranging from first exacerbation to 43 years. At the time of the measurement, around 96% of the patients were undergoing antipsychotic treatment (including typical and atypical antipsychotics). Patients exhibited moderate positive and negative symptoms which seemed to be reasonable considering their current treatment.



**Table 5. Clinical and demographic characteristics of study participants.**

	SCZ	HC			
Study	PSC <sup>1</sup>	PSC <sup>1</sup>	BeCOME <sup>1</sup>	IST <sup>1</sup>	TMEM <sup>1</sup>
N	23	26	38	53	136
Age (years, mean ± SD)	34.6 (± 12.6)	31.9 (± 9.3)	31.3 (± 11.3)	25.0 (± 2.9)	24.0 (± 3.8)
Sex (men/women)	11/12	10/16	17/21	27/26	66/70
CTQ <sup>2</sup>	43.2 (± 14.9)	38.8 (± 12.0)	34.1 (± 10.1)	33.3 (± 9.1)	32.1 (± 6.9)
Diagnosis (F20/F25)	12/11	n/a	n/a	n/a	n/a
Duration of illness (years, mean ± SD)	12.9 (± 15.3)	n/a	n/a	n/a	n/a
PANSS, positive	13.4 (± 5.5)	n/a	n/a	n/a	n/a
PANSS, negative	13.5 (± 5.9)	n/a	n/a	n/a	n/a
PANSS, total	28.8 (± 8.6)	n/a	n/a	n/a	n/a

<sup>1</sup>Acronyms of original imaging genetics study samples (BeCOME: Biological Classification of Mental Disorders, IST: Imaging Stress Test, PSC: PsyCourse, TMEM: Transmembrane Protein).

<sup>2</sup>CTQ: Childhood Trauma Questionnaire; sum of all five clinical subscales (physical abuse, physical neglect, sexual abuse, emotional abuse and emotional neglect).

**Table 6. CTQ severity classes\* of healthy subjects.**

	None to low	Slight to moderate	Moderate to severe	Severe to extreme
Emotional abuse	186 (73.5%)	49 (19.0%)	11 (4.3%)	7 (2.8%)
Physical abuse	234 (92.5%)	10 (4.0%)	5 (2.0%)	4 (1.6%)
Sexual abuse	238 (94.1%)	6 (2.4%)	8 (3.2%)	1 (0.4%)
Emotional neglect	161 (63.6%)	67 (26.5%)	18 (7.1%)	7 (2.8%)
Physical neglect	195 (77.1%)	38 (15.0%)	11 (4.3%)	9 (3.6%)

\*According to Bernstein & Fink (1998) and Häusler et al. (2011).

### 2.3.2 Voxel-wise FCD and NAcc connectivity differences between patients and healthy subjects

The proof-of-concept interrogation of group average FCD maps showed patterns similar to reports from earlier studies (Tomasi & Volkow, 2010) (**Figure 7**). At the whole-brain level, five clusters revealed significantly increased FCD (collection threshold  $p_{\text{voxel}} < 0.001$ ; **Table 7**) in the right posterior thalamus, right caudate, mid-posterior cingulate cortex and precuneus. Regarding group-by-FCD<sub>global</sub> effects, five significant clusters were revealed clusters localizing to the NAcc and bilateral thalamus reaching to the ACC. **Figure 8** visualizes both the group main effects (**A**) and the group-by-FCD<sub>global</sub> effects (**B**) in SCZ

relative to HC. The global conjunction of both contrasts emphasized the bilateral subcortical nuclei including the NAcc, posterior cingulate cortex/precuneus, right temporal cortex and mesencephalon.

**Table 7. Comparison von FCD<sub>voxel</sub> between HC and patients.**

Result cluster #	Anatomical cluster location	Cluster size in voxels	FWE corrected cluster p-value	Peak voxel coordinates
<i>Main effect of group (SCZ &gt; controls)</i>				
1	R thalamus	88	0.005	12 -27 6
2	R olfactory cortex, caudate	54	0.040	12 3 0
3	L/R precuneus R paracentral lobule, postcentral gyrus	61	0.025	9 -39 54
4	R midcingulate cortex, precuneus	55	0.037	9 -60 45
5	L precuneus R superior occipital gyrus, cuneus, precuneus	67	0.017	3 -72 30
<i>Group-by-FCDglobal effect (SCZ &gt; HC)</i>				
1	L/R caudate, thalamus, pallidum, putamen, superior temporal gyrus, insula, superior temporal pole, olfactory cortex, middle temporal gyrus, gyrus rectus L IFG (pars orbitalis), superior temporal gyrus, ACC R lingual gyrus, parahippocampal gyrus, amygdala, middle temporal gyrus, IFG (pars orbitalis) precuneus, hippocampus	1559	< 0.001	12 9 -3
2	L/R ACC, midcingulate cortex L superior frontal gyrus (medial)	362	< 0.001	-12 15 27
3	R middle temporal gyrus, superior temporal gyrus	53	0.043	66 -42 6
4	L/R cuneus, precuneus	127	0.001	21 -57 30
5	L paracentral lobule, precentral, midcingulate cortex, supplemental motor area	56	0.035	-12 -6 48

<sup>a</sup>Result clusters were mapped with the AAL toolbox.

<sup>b</sup>Peak voxel coordinates are given in MNI space.

L and R denote left and right hemispheric location; L/R denotes bilateral location. IFG, inferior frontal gyrus; ACC, anterior cingulate cortex.

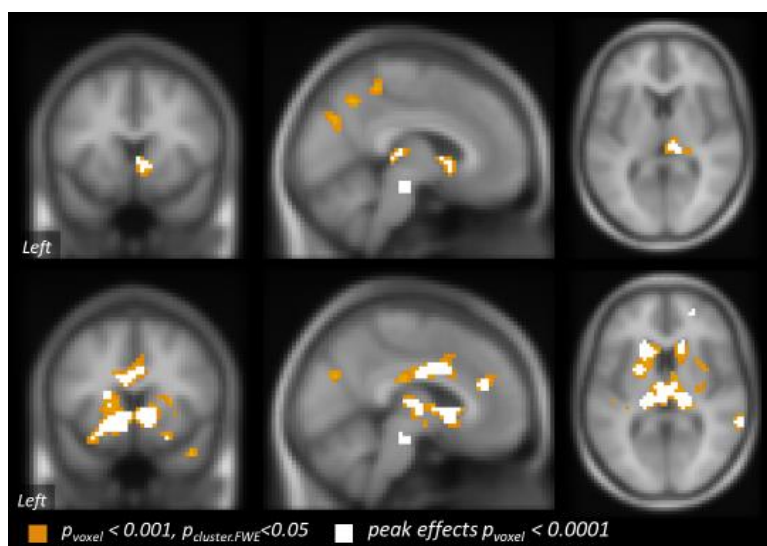


**Figure 8. Comparison of FCD between HC and SCZ. (A)** Group main effect (SCZ > HC). **(B)** Group-by-FCD<sub>global</sub> effect (SCZ > HC). The figure only displays clusters that survived whole-brain correction of  $p_{\text{cluster.FWE}} < 0.05$ . Clusters thresholded at  $p_{\text{voxel}} < 0.001$  are shown in orange; voxels collected at  $p_{\text{voxel}} < 0.001$  are shown in white. Adapted from Eberle et al. (2019).

### 2.3.3 PGRS effects and interaction with childhood adversity on FCD and NAcc seed connectivity

The analysis of FCD<sub>global</sub> as a dependent variable yielded sample original effects, while no effects of CA, PGRS or PGRS-by-CA were observed. Multiple regression analyses on FCD<sub>NAcc</sub> and corrected for FCD<sub>global</sub> showed significant effects for the following variables: (1) sample source (IST,  $T = 2.025$ , standardized beta ( $\beta_s$ ) = 0.114,  $p = 0.046$ ); (2) PGRS ( $T = 2.351$ ,  $\beta_s = 0.119$ ,  $p = 0.020$ ); (3) PGRS-by-CA interaction ( $T = 2.453$ ,  $\beta_s = 0.126$ ,  $p = 0.015$ ). CA did not show any effects on FCD<sub>NAcc</sub> ( $p < 0.215$ ). Neither did age, sex, other sample source or further components of the multidimensional scaling analysis reveal significant effects. Stepwise linear regression yielded the same four significant predictors. Thereby PGRS and the interaction term explained 1.5% and 1.1%, respectively, of the variance. The interaction effect can be further illustrated by an alternative analysis: By limiting the subjects to those who scored on at least one CTQ scale ( $N=120$ ), the PGRS explained even 4.36% of the FCD<sub>NAcc</sub> variance, compared with only 1.1% in the complementary group.

An exploratory whole-brain FCD study of PGRS effects resulted in one positive cluster ( $k > 10$ ) mapped to the right NAcc and caudate ( $k = 24$ ,  $p_{\text{cluster}} = 0.036$ ; at the whole-brain level:  $p_{\text{cluster.FWE}} = 0.349$ ; within the striatal mask:  $p_{\text{cluster.FWE}} = 0.015$ ). CA and PGRS-by-CA did not show any significant clusters. The global conjunction of the positive contrast of PGRS and the interaction yielded one cluster in the left NAcc ( $k = 31$ , whole brain:  $p_{\text{cluster.FWE}} = 0.076$ ; striatal mask:  $p_{\text{cluster.FWE}} = 0.003$ ).

With seed analysis of the NAcc we investigated whether the PGRS and CA-by-PGRS effects on FCD originate from specific brain regions. Bilateral NAcc was shown to be positively associated with PGRS in the middle/superior occipital gyrus, middle temporal gyrus, and parahippocampal gyrus (see **Table 8**). The interaction of CA and PGRS revealed a significant cluster in the occipital cortex

( $p_{\text{cluster.FWE}} = 0.024$ ) which overlapped with the PGRS effect. Conjunction analyses of both PGRS and interaction effects revealed six clusters in occipital parietal regions. Moreover, these conjunction patterns did not overlap with the normative positive or negative NAcc connectivity network (see **Figure 9**).

**Table 8. Seed analysis of the NAcc: Effects of PGRS and PGRS-by-CA.**

Result cluster #	Anatomical cluster locations	Cluster size in voxels	FWE corrected cluster p-value	Peak voxel coordinates <sup>b</sup>
<i>Positive correlation with PGRS</i>				
1	R superior occipital gyrus, middle occipital gyrus	221	0.002	36 -78 24
2	R fusiform gyrus, parahippocampal gyrus, inferior temporal gyrus	236	0.001	42 -42 -14
3	R superior occipital gyrus, superior parietal lobule, precuneus, angular gyrus	128	0.032	24 -64 34
<i>Positive correlation with PGRS-by-CA</i>				
1	R middle occipital gyrus, superior occipital gyrus	137	0.024	32 -82 24
<i>Conjunction of both positive T contrasts (global null)</i>				
1	R angular gyrus, middle/superior occipital gyrus	634	< 0.001	32 -80 24
2	R cerebellum, inferior occipital gyrus, lingual gyrus, fusiform gyrus	417	< 0.001	26 -72 -6
3	L superior/inferior parietal lobule, superior/middle occipital gyrus, middle temporal gyrus	351	< 0.001	-43 -74 12
4	L fusiform gyrus, cerebellum	176	0.001	-28 -60 20
5	R lingual gyrus, precuneus, calcarine	90	0.027	20 -54 8

<sup>a</sup>Result clusters were mapped with the AAL toolbox.

<sup>b</sup>Peak voxel coordinates are given in MNI space.

L and R denote left and right hemispheric location.

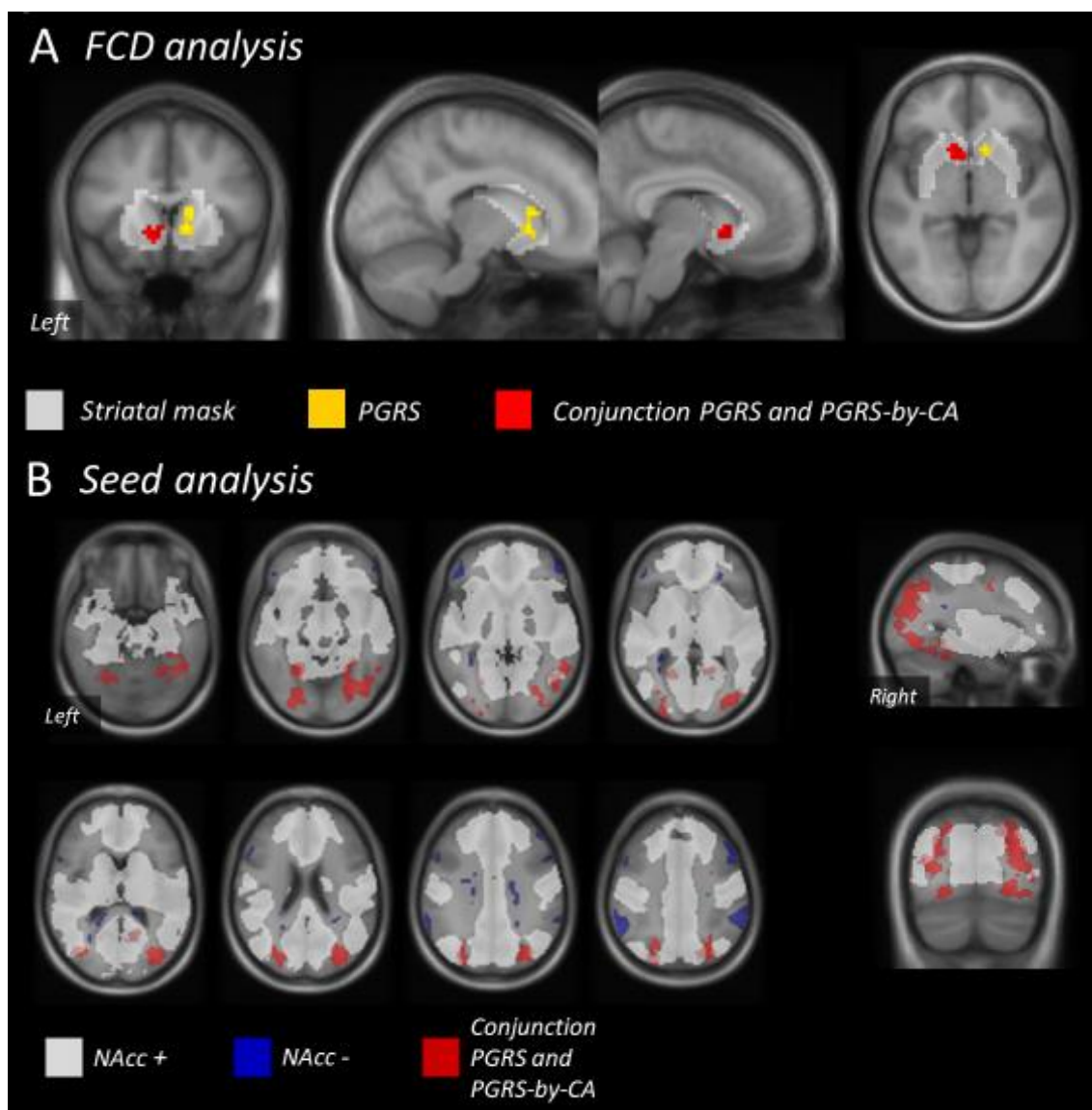


**Figure 9. PGRS effects at the level of FCD and NAcc seed analyses. (A)** FCD analysis: Yellow displays the positive correlation of the right striatal region with the PGRS for SCZ; red shows the positive correlation of the left striatal region with the conjunction effect (PGRS and PGRS-by-CA). Both effects were significant within the volume-of-interest mask. **(B)** NAcc seed analysis: Positive and negative NAcc seed correlations are shown in white and blue, respectively ( $p_{\text{voxel}} < 0.05$ ); red depicts the conjunction effect. Both analyses showed no CA main effect. Adapted from Eberle et al. (2019).

In FCD and NAcc seed analyses, HC were again divided into two groups, namely no trauma (N=133) and at least one trauma (N=120) and tested for PGRS effects. FCD analyses of the latter group revealed a PGRS effect in the striatal region ( $k = 120$ ; whole brain:  $p_{\text{cluster.FWE}} = 0.460$ ; striatal mask:  $p_{\text{cluster.FWE}}=0.030$ ). No effects were seen in the group with no trauma (**Figure 10**, upper part). **Figure 10 (lower part)** depicts PGRS effects on the NAcc seed analysis, again revealing effects only the trauma group.

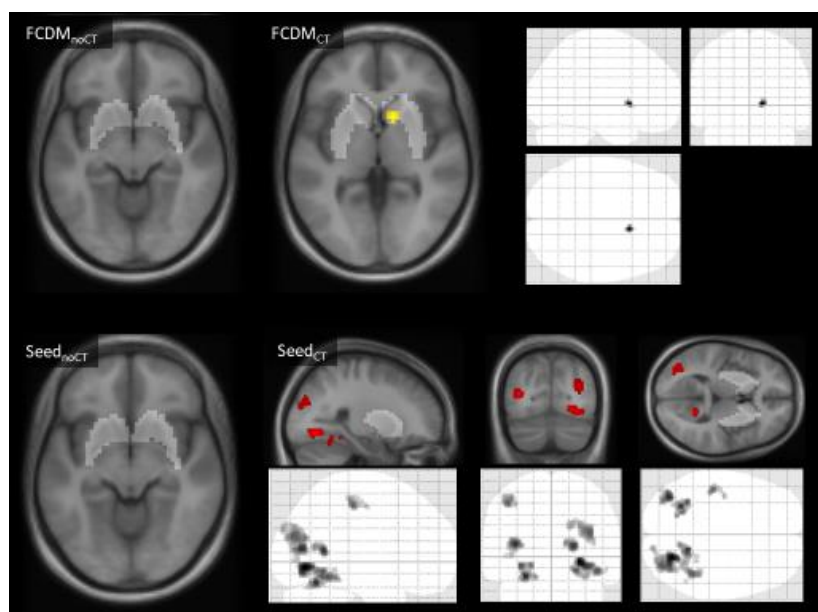


**Figure 10. Effects of PGRS.** Effects of PGRS in HC without trauma (N=133; left) and with at least one trauma (N=120; right). Collection threshold of clusters at  $p_{\text{voxel}} < 0.001$ . FWE-robust clusters (within the striatal mask and whole-brain) were found only in the CA group. Effects of the global conjunction of PGRS and PGRS-by-CA are displayed in red. Striatal masks were applied post-hoc for small volume corrections of the FCD examinations. Adapted from Eberle et al. (2019).

### 2.3.4 Comparing clinically established disease with combined high-risk CA/PGRS profile

Relative to HC, patients with SCZ showed increased  $FCD_{NAcc}$  values ( $F = 6.769$ ,  $p = 0.010$ , partial  $\eta^2 = 0.025$ ) (ANCOVA with covariates age, sex,  $FCD_{\text{global}}$  and sample sources). In addition, using a 4-level factor risk (low (N=145), medium (N=91) and high risk (N=17) in HC, and patients (N=25)) the same model identified a significant main effect of risk ( $F = 2.746$ ,  $p = 0.043$ ). Post-hoc comparisons revealed differences between SCZ and HC at low ( $p = 0.009$ ) and medium ( $p = 0.010$ ) risk. Comparison between SCZ and subjects at high risk did not show any significant difference ( $p = 0.169$ ). An alternative statistical strategy using the ratio between  $FCD_{NAcc}/FCD_{\text{global}}$  instead of the covariate approach affirmed this pattern. Separating the ambiguously defined medium risk group into a group with a high CTQ or high PGRS did not change this pattern in either model.

## 2.4 Discussion

In the present study, we compared effects of established SCZ with effects of PGRS for SCZ and its interaction with CA in HC on RS fMRI measures. The combination of patient/control comparisons and imaging genetic analyses in the scope of the same study has the major advantage of reducing methodological sources of noise which are a common issue using RS fMRI. The starting analyses of this study confirmed earlier reports of higher FCD in subcortical nuclei, such as NAcc, in patients with SCZ. The central analyses revealed that higher values of PGRS for SCZ correlate with FCD of the bilateral NAcc. In addition, we found that higher PGRS was associated with stronger connections of the NAcc with the secondary visual association cortices. Interestingly, PGRS effects were more pronounced in participants with experiences of CA.

### 2.4.1 Replicating associations between SCZ/schizoaffective disorder and subcortical FCD

RS fMRI is not only easy to collect, but also holds a broad potential for the analysis of spontaneously functional activity across the whole brain. This results in a high-dimensional space for analyses (e. g.  $\sim 25,000$  native space voxels with grey matter BOLD signal over  $\sim 150$  time points, resulting in about  $4.5 \times 10^6$  raw data points) that can be analysed in multiple, mostly complementary ways (Lee et al., 2012). Analyses of this study focussed on FCD as an 'entry technique'. FCD gathers information about the connectivity of one voxel to all other voxels in a single measure and can be regarded as a sensitive screening technique that, however, is anatomically unspecific in terms of the origins of the FC effects (Cole et al., 2010; Tomasi & Volkow, 2010, 2011). In this study, patients that have been diagnosed with either SCZ or schizoaffective disorder, showed moderately severe psychotic symptoms at the time of their participation and were under current antipsychotic treatment (96%), exhibited elevated FCD in posterior midline areas and subcortical nuclei. In addition, we observed higher values of voxel/whole-brain FCD correlations in the VS and mesencephalon compared to healthy subjects. This latter result can be interpreted in the way that in patients the VS/mesencephalon total FC is more strongly coupled to whole-brain FCD, in the sense of the loss of local FCD specificity. The conjunctions analysis corroborated that the NAcc in particular shows increased FCD. These findings are in good accordance with previous reports on patients with SCZ regarding directionality and anatomical location (C. Liu et al., 2017; Zhuo et al., 2014). This even remained when taking technical differences into account: While the global FCD (as used here) refers to the connectivity of an index voxel with all other voxels, local FCD focusses on connections between the index voxel and its adjacently connected voxels (Tomasi and Volkow 2010). In their analysis, Zhou et al. (2014, 2017) compared 95 patients to 93 healthy subjects on the basis of unweighted global FCD. After gathering only those voxels which revealed a correlation coefficient above 0.6, they scaled them to the average count in GM. When we adopted this counting approach post-hoc (for better comparability with Zhou et al., 2014, 2017), we found increased counts in subcortical nuclei. Methodologically, this finding shows that our results are not specific to the decision between weighted and unweighted FCD (Cole et al., 2010). In another study on local FCD, Liu et al. (2017) mapped local FCD to (para-)hippocampal areas, bilateral subcortical nuclei,

and to frontotemporal areas to a lesser degree. Interestingly, elevated values of long-range FCD (derived from subtracting local from global FCD) was found in bilateral thalami and pallidum, underlining that both short- and long-range hyperconnectivity of the basal ganglia is present in psychotic patients. Since our sample as well as the sample examined by Zhuo et al. (2014, 2017) and Liu et al. (2017) included patients under neuroleptic treatment, we cannot fully isolate disease from medication effects. Although Lin et al. (2018) conducted a study on drug-naive SCZ patients during their first clinical manifestation, reporting lower FC between the NAcc and the ACC, the study was not a FCD but a cross correlation analysis on a specific frequency band. In another study on unmedicated SCZ patients, FCD effects of distinct frequency bands are described, but not the full frequency range which again impairs the comparability (Wang et al., 2017).

#### 2.4.2 Polygenic risk and its effect on FCD in healthy controls

Following this replication of FCD elevations in subcortical regions in SCZ, the key question - the endophenotype potential of FCD, particularly of the NAcc, in healthy subjects - was approached. To avoid effects of clinical variability on imaging genetic results, including disease duration, acuteness of the disease, or medication, patients were excluded from the respective analyses. The PGRS for SCZ, which was generated based on a meta-GWAS set of SNPs, was positively associated with  $FCD_{NAcc}$  and explained around 1.1.% of its variance in healthy subjects of this study. This finding can be considered as a first hint of specific genetic effects on NAcc connectivity during rest and may mirror an intermediate pathophysiological system susceptible to an inherited risk. This aligns with previous reports from two childhood samples (Achterberg et al., 2018) suggesting the inherent nature of VS seed connectivity. However, we believe that no reports exist for the heritability of NAcc FCD. Even though the PGRS association was rather weak, it is worth noting that PGRS (when collected at  $p^T < 0.05$ ) accounted for around 7% of schizophrenia liability, whereby half the variance was attributed to the small group of genome-wide significant SNPs. This evidence of strong effect of the most strongly associated SNPs prompted us to generate the PGRS in this manner, whilst other techniques of stratification and collection thresholds have been applied when focussing on imaging phenotypes. Despite the collection threshold, both genetic and RS fMRI markers are highly complex involving over a 100 genetic loci as well as NAcc FC throughout the entire brain. Bearing their complexity in mind, it is likely that the focussing on associations between specific SCZ-related genes and specific connections of the NAcc might harbour stronger effects. Therefore, limiting the genetic space to certain functions which are linked to the NAcc, such as dopamine-related genes, might be a potential next step of the research in this respect. Another promising approach would be to further explore bivariate NAcc connectivity and the VTA to improve the network specificity. A recently published negative finding of the connection between whole-genome SCZ PGRS and RS fMRI underlined the influence of the selection of fMRI markers (Barnes, 2001; Chen et al., 2018). In their study, the authors employed the Euclidian distance of a subject from the sample's centroid regarding the network FC in 50-dimensional space reflecting the (temporal) relationship between the time courses of RS networks. On the one hand, this marker captures brain dysfunction at a highly abstract level, whereas it has been proven to be sensitive to SCZ.



On the other hand, it might be that the actual pathological specificity is less than estimated, or that variations in the calculation of the PGRS ( $P^T < 0.0001$ ) had an impact on the result.

### 2.4.3 Dissecting NAcc functional connectivity correlations with polygenic risk

In addition, we were able to identify a correlated cluster with the size of 24 voxels in the right NAcc/caudate when examining the entire FCD voxel space. Although this cluster did not reach significance at the whole-brain level, its detection was beyond chance within the striatal mask, and was more pronounced in those subjects with scores in at least one childhood trauma domain. Regarding the anatomical location, our findings align well with previous work on the influence of genetic risk on striatal activity during the anticipation of reward (Lancaster et al., 2018; Lancaster, Linden, et al., 2016). Moreover, since the conjunction of both genome-wide associations with SCZ at the D2 receptor (Schizophrenia Working Group of the Psychiatric Genomics Consortium, 2014) and pathway analysis indirectly indicated the influence of internalization of the dopamine transporter during brain development (Crisafulli et al., 2015; Schizophrenia Working Group of the Psychiatric Genomics Consortium, 2014), we suggest a sensitivity of fMRI to VS functions is indirectly mirrored in the SCZ PGRS. In turn, seed analysis of the NAcc showed a positive association between the NAcc FC and the visual association cortex, in a spatial pattern overlapping with the dorsal and ventral visual stream (Milner, 2017). This matches intriguingly with reported enhanced connectivity of the NAcc with the visual association cortex in SCZ patients with visuoauditory hallucinations (Rolland et al., 2015). This indicates that RS fMRI correlates of the PGRS not only converge with elevated FCD in SCZ, but also with more specific connectivity of the NAcc as related to positive symptoms of psychosis.

### 2.4.4 Childhood Adversity as a potentiating factor of the polygenic risk for SCZ

Regarding environmental factors, our data suggests that CA interacts with PGRS effects in the same direction. Thereby, the interaction term led to an increase by 1.1% of the explained variance of the  $FCD_{NAcc}$  (on top of the variance already explained by the PGRS). Furthermore, the interaction term revealed a cluster in our NAcc seed analysis. Interestingly, the location of this pattern closely resembled the main effect genetic regressor which is of note as both regressors are by definition orthogonal to each other. The extent of PGRS explained variance varied strongly between the HC without trauma ( $N=133$ ) and HC with at least one trauma according to the CTQ ( $N=120$ ), and this pattern was revealed similarly at the level of both NAcc seed analysis and FCD mapping (see **Figure 8**). We did not find any main effect of CA on either FCD or NAcc seed connectivity. Accordingly, a high genetic risk might be a prerequisite for mediating environmental risk factors for SCZ. Moreover, we also see a potential association between our findings and epidemiological data reporting the disproportionately high occurrence of different types of hallucinations in SCZ patients with a history of child abuse (Read et al., 2005). This link does not only exist in patients with SCZ, but also across diagnostic boundaries, such as BD, and in healthy people: Morrison & Peterson (2003) provided evidence suggestive of a relation between bullying and visual hallucinations in the healthy children. Furthermore, CA interacted with

dopaminergic risk alleles on the putamen volume in the left hemisphere in a SCZ/control sample (Hoffmann et al., 2018). To the best of our knowledge, no other authors have reported interactions of CA and PGRS for SCZ for functional striatal measures. In a recent study, direct effects of CA on RS measures of the mesolimbic dopaminergic circuitry have been a sample of 43 children and adolescents with previous trauma experiences (Marusak et al., 2017). In addition, FC alterations between the amygdala and striatal regions have been found in male cocaine users with previous severe childhood experiences (Kaag et al., 2018). A corresponding animal study (Mitchell et al., 2018) revealed that GABAergic functions of the NAcc are influenced by early life stress. Stronger polygenic effects found in subjects with higher degree of CA may point to epigenetic mechanisms whereby CA causes long-term changes in the expression of genes and subsequent functional adaptations.

#### **2.4.5 Could subcortical FCD be useful as a cumulative risk marker?**

Strikingly, comparison of HC at 'double risk' (i.e. high PGRS (> 75<sup>th</sup> percentile) and high CA) and SCZ revealed similar FCD<sub>NAcc</sub> profiles, while both healthy people with one risk and those with no risk differed significantly from patients with SCZ. Taking together our PGRS and CTQ directed analyses and the existing literature, our findings suggest that RS fMRI measures of NAcc or VTA activity may provide a useful source of biomarkers to identify individuals with altered activity within the dopaminergic and therefore altered SCZ related circuits. These findings could point towards a predictive nature of FCD<sub>NAcc</sub> and should be validated by serial studies in adolescents and young adults, or in high-risk probands.

#### **2.4.6 Limitations**

One important limitation may be seen in the heterogenous definition of healthy status in the four different sample sources. It was therefore not possible to draw on a uniform pool of scales reflecting, for example, the continuum between schizotypy, schizotypic personality and SCZ (Lenzenweger, 2018), cognitive tests, personality scores or other psychometric variables. We thus focussed on the CTQ as clinical variable spanning all samples. Consequently, this made it difficult to explore whether the detected fMRI risk pattern or the combination of CA and PGRS could transfer to such liability traits as it would be typical for an endophenotypic model. Another limitation related to the sample lies in the heterogeneity within the patient sample that comprised both SCZ and schizoaffective order. As pointed out in the first chapter, the overall clinical presentations of these two diagnostic groups may vary widely despite their psychotic commonalities. This, and the heterogenous disease stage of the patients, hampered the identification of more specific symptom correlates of NAcc connectivity. In addition, the patient's higher average age hindered the examination of group vs group-by-age effects, especially in the light of earlier findings stating that age has an impact on certain VS responses, such as loss aversion (Samanez-Larkin et al., 2007; Viswanathan et al., 2015). As statistically no correlation between age and global or voxel-wise FCD was observed in 253 healthy volunteers and since group comparisons were primarily intended to verify a previously reported SCZ-related FCD pattern, this limitation regarding our findings should be small, though. Thirdly, the statistical power in imaging genetic analyses may have been weakened by the different gene batches as well as the minorly different

fMRI acquisition setup. Nevertheless, the  $FCD_{NAcc}$  effects of a meta-analysis were highly similar with the here performed mega-analysis. Fourthly, although motion correction was performed following the usual standards, SCZ required more correction efforts regarding their motion compared to HC, which may have influenced group comparisons of fMRI data. Lastly, and more generally, the quantification of adverse childhood experiences was based on a self-rating instrument which is naturally subject to memory bias in SCZ patients. This bias, due to its omnipresence, should not have affected the four healthy samples in a different way. However, reports of group differences of CTQ scores between HC and SCZ have only been provided for completeness and proof-of-concept and did not affect our main analyses on HC.

## 2.5 Conclusion

This study has shown that a significant amount of FC density variance of the NAcc in healthy people can be explained by polygenic risk for SCZ. In addition, we observed that this association was amplified by higher levels of self-reported CA. More specifically, our data suggested an enhanced connectivity of the NAcc with the visual association cortices as one underlying local neural pattern (Eberle et al. 2019). The similarity of FCD between SCZ and those subjects presenting an increased genetic and environmental risk (as measured by CTQ) underlines the potential role of NAcc FCD as an endophenotype for SCZ and potentially schizoaffective disorder. Overall, self-reported adverse childhood experiences turned out to be a significant modifier of the association between genetic risk for SCZ and RS fMRI markers, suggesting that a better consideration of environmental factors in imaging genetics could help to understand the result heterogeneity in this field.



### **3. Using fMRI activation during reward anticipation to characterize the reward system across diagnostic boundaries**

#### **3.1 Reward anticipation as a source of biomarkers in multiple networks**

Multiple mental disorders, including MDD, BD and SCZ, are characterized by disturbed reward processing (see chapter 1.2.5), suggesting that the underlying neurobiological mechanisms may hold an endophenotype potential to improve the current nosology regarding disorders of the psychotic-affective spectrum. As mentioned before, impairments within the reward system fit the understanding of affective and psychotic disorders both at the conceptual and neuronal level.

'Reward processing' is an umbrella term for distinct components (see chapter 1.2.2), which in turn differ regarding their cognitive and behavioural correlates. Given that the RA involves a number of important, interlinked subprocesses (e.g. recognition of a possible reward, shifting the focus of attention and preparation of goal-oriented behavior), it has a great potential to capture different reward-related impairments across multiple disorders. Therefore, this task-dependent fMRI study seeks to address the question, whether neural underpinnings of RA could serve as an endophenotype in order to improve the current classification of mental diseases of the psychotic-affective spectrum.

Over the past two decades, neuroimaging and a growing body of studies on RA on a multitude of psychiatric disorders was to be witnessed, including psychotic and affective disorders (see chapter 1.2.5). However, one major problem is that paradigms suitable for examining RA often vary substantially in their complexity, type of stimuli and duration of the anticipation phase. Therefore, findings may be confounded and lack clear comparability. In general, current reward paradigms address different cognitive abilities, which in turn demand a multitude of neuronal activities not only within the dopaminergic reward circuitry, but also in other reward-related subsystems (Oldham et al., 2018). With this in mind it is obvious that a uniform examination of RA deficiencies in MDD, BD and SCZ holds the advantage of better methodological comparability. For this reason, the literature review in this paper focuses on the MID task, which was also employed in this sample.

#### **Overlapping and distinct pathomechanisms underlying RA in affective and psychotic disorders**

Since Knutson and colleagues (2001) introduced the MID task, there has been a rapid rise of fMRI studies using this paradigm to investigate neural correlates of RA in the general population and clinical subjects, including MDD (Knutson et al., 2008), BD (Johnson et al., 2019), and SCZ (Subramaniam et al., 2015). The first fMRI studies based on the MID task performed on patients with MDD revealed contradictory results: On the one hand, Knutson et al. (2008) identified *increased* neural activation in unmedicated MDD patients during the anticipation of possible rewards, which became associated with internal affective conflicts. On the other hand, other studies reported *blunted* striatal responses

in MDD during RA, particularly in the left NAcc and bilateral caudate (Pizzagalli et al., 2009). In line with the latter study, Gotlib et al. (2010) reported that girls with maternal depression exhibited weaker putamen responses compared to girls at low risk during RA. Given that a weakened experience of reward and pleasure is a central aspect of MDD, findings of reduced striatal responses would agree better with theoretical considerations. However, there is no consensus on whether patients with MDD show such a pattern during the MID task.

In BD, multiple studies reported decreased VS activity relative to HC during RA (Johnson et al., 2019; Schreier et al., 2016). Interestingly, blunted NAcc responses during gain was shown to be correlated with individual differences in self-reported impulsiveness towards positive emotions in patients with BD (Johnson et al., 2019). In SCZ, results are clearer: A multitude of studies using the MID task found blunted striatal responses during the anticipation of monetary rewards (Juckel et al., 2006; Kirsch et al., 2007; Schlagenhauf et al., 2008). Importantly, evidence suggests that this abnormality is present in unmedicated patients, drug-naive patients, patients on first-generation psychotics, unaffected siblings of patients with SCZ and even healthy subjects with psychotic-like symptoms (Maia & Frank, 2017). These studies on the risk spectrum strongly suggest an endophenotype potential. Moreover, this striatal impairment was correlated with self-reported negative symptoms in unmedicated SCZ patients (Juckel, Schlagenhauf, Koslowski, Wüstenberg, et al., 2006), confirming that anhedonia is an important element of the negative symptom spectrum.

Together, prior work has identified reduced reward-related VS activation across MDD, BD and SCZ, however, the consistency of the results varies depending on the disease group. Therefore, the first goal of this study was to prove whether fMRI measures of RA hold the potential to provide sources of markers to biologically characterize disorders of the psychotic and affective spectrum. Using the MID task, we directly compared RA disturbances of MDD, BD and SCZ relative to healthy subjects. Although there have been several studies on each of these mental conditions, none of the previous studies directly applied the same task to all three clinical subgroups. Another shortcoming of previous work is that conventional SPM analysis lacks regarding the accuracy of the allocation of the effects in brain structures which are difficult to differentiate because of their small size, including subregions of the VS. For this reason, in addition to conventional SPM analyses, we focussed added analyses on predefined hubs of networks that have been shown to be associated with reward processing or general task performance. Given that the VS is a main target of the reward task and comprises multiple subregions with distinct functions (see **chapter 2**), we investigated RA effects in precise segmentation-based subregions. Lastly, we examined whether reward-related pathomechanisms are related to transdiagnostically common features. Given that the literature underlines the importance of anhedonia in multiple mental illnesses, including MDD, BD and SCZ (Trøstheim et al., 2020) and its relatedness to reward processing, anhedonia-related items of the BDI were chosen for a continuous characterization of this psychotic-affective spectrum sample.

## 3.2 Methods

### 3.2.1 Sample

Patient inclusions were based on a consecutive scheme in the time period 10/2016 to 08/2018 during which all newly admitted in-patients of the MPIP were screened for eligibility by contacting the responsible ward doctor about three days after admission. Only if the clinical condition of the patient allowed to interrogate him or her regarding the study, contact was established.

The initial sample consisted of 25 healthy subjects, 39 patients suffering from a major depressive disorder, 13 patients with bipolar disorder and 29 patients with schizophrenia or schizoaffective disorder. Exclusion criteria were any past or present comorbid psychiatric disorder, current, current substance abuse disorder, illegal drug use within the past 2 weeks or concurrent neurological illnesses or an affective or cognitive status too severely impaired to comprehend the study purpose and follow the protocol. All patients were recruited at the hospital of the Max Planck Institute of Psychiatry, and at the Department of Psychiatry of the Ludwig Maximilians University, Munich. 25 HC subjects were recruited through local advertisement and screened for current or past psychiatric disease or substance abuse. Short-sighted participants were given contact lenses for optimal vision during the fMRI scan. One healthy subject and 6 patients were excluded from data analysis due to missing imaging data, excessive head movement, markedly low behavioural task performance during the RA task (reaction times > 1.5 s) or comorbidities diagnosed at the end of their hospitalization. The study protocol was in line with the Declaration of Helsinki and approved by the ethics committee of the Ludwig Maximilians University, Munich.

### 3.2.2 Reward Anticipation Task

The RA task used for our investigations was largely adapted from the monetary incentive delay task developed Knutson et al. (B. Knutson et al., 2001). The general effectiveness of the adapted design in eliciting expected basic fMRI response patterns has been validated during a pilot project before this study. At the beginning, a fixation cross is presented on the screen. Next, one of three squares featuring different stripe orientations (equiluminiscent due to parallel pupillometry) that indicate one of three trial conditions are presented for 6 s (see **Figure 11**). Task trials are composed of a monetary condition with the possibility to gain €1, a non-monetary condition with a verbal feedback, and a trial without a response requirement. In both reward conditions, the respective visual cue is followed by a brief flash of light (white screen) to which participants had to react with a button press with their right hand. Finally, participants were notified by a symbol ('€' in monetary trials; '✓' in verbal trials) that indicates whether their response to the flash has been fast enough and about their cumulative total win sum at that point. All participants were instructed by the same person.

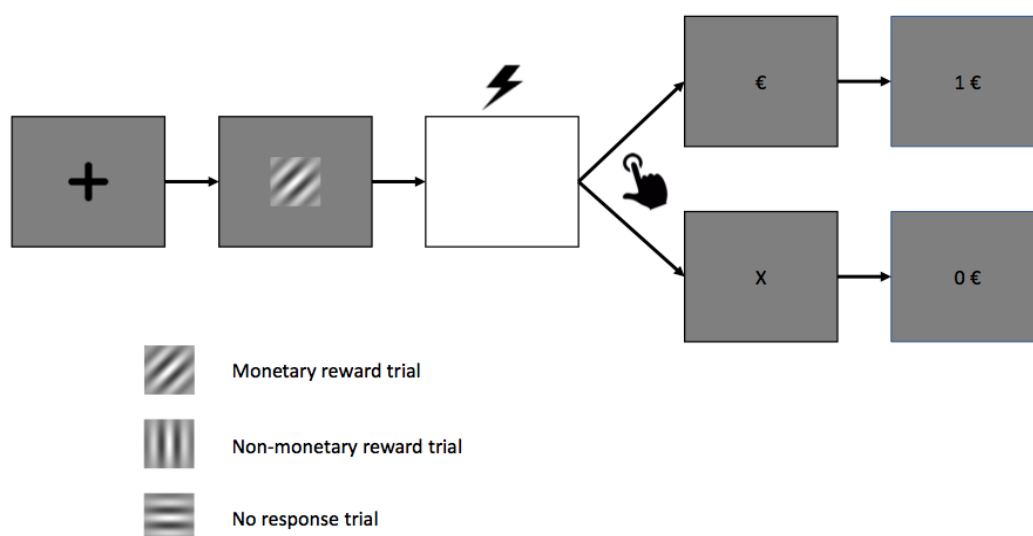


**Figure 11. Trial sequence of the reward anticipation task.** Participants had to respond to a flash of light with a button press as fast as possible. Visual cues indicated potentially monetary rewarded responses (tilted stripes), verbally rewarded responses (vertical stripes) or control trials (horizontal stripes) in which no response was required.

### 3.2.3 Procedure

After the study protocol had been handed out in written form and fully explained, participants provided their written consent or denied to participate. In the case of consent, prior to their performance inside the scanner, participants received an introduction into the RA task and performed a practice version at a computer in order to make sure they had fully understood the task. Once inside the scanner, each subject underwent an anatomical scan before the fMRI acquisition started. During the measurement, tasks were projected on a monitor behind the scanner and could be watched by participants through a mirror attached to the head coil. The fMRI acquisition also included other paradigms as part of a multisite DFG project.

### 3.2.4 Behavioural Data

As reaction time (RT) we defined the time between the presentation of the white screen flash and the button press. For all subjects, average reaction times across all trials were calculated in order to assess whether subjects participated actively, but also in order to test for differences between monetary reward trials and non-monetary trials. After exploring the RT distribution, trials with a response delay no longer than 1.5 seconds (i.e. trials with not outlier properties) were counted for RT group comparisons. However, we decided to leave these trials with delayed response or non-response in the fMRI analysis as they still reflect fundamental disease-related deficits of reward processing.



### 3.2.5 fMRI Acquisition

MRI measurements were acquired using a 3 Tesla scanner (Discovery MR750, General Electric, Milwaukee, U.S.A.) with a 32 channel head coil (MR Instruments Inc., Minneapolis, MN, USA). Along with high resolution T1-weighted anatomical images, whole-brain EPIs covering 40 slices were measured using a T2-weighted gradient echo sequence with a repetition time (TR) of 2500 ms, echo time (TE) = 30 ms, 96 x 96 matrix, 2.5 mm slice thickness, 0.5mm slice gap, and a resulting effective voxel size of  $2 \times 2 \times 3 \text{ mm}^3$ . For the RA task, a total of 182 volumes were collected representing about 7 minutes and 40 seconds.

### 3.2.6 fMRI Preprocessing

Collected fMRI time series of the RA task underwent a multistep preprocessing procedure implemented in MATLAB 2017a (MathsWorks Inc., Natick, Massachusetts, USA) using standard SPM functionalities (version SPM 12, <https://www.fil.ion.ucl.ac.uk/spm/software/spm12>) and in-house scripts. In order to avoid non steady-state effects, the first four volumes were discarded before the preprocessing procedure. The preprocessing scheme included motion correction through rigid-body realignment of images, slice timing correction (interleaved bottom-up acquisition scheme), segmentation into three tissue types (GM, WM, CSF) of the first image, iterative non-linear normalisation and generation of flowfield (DARTEL (Ashburner, 2007)) using the GM and WM probability maps that resulted from segmentation, application of tis flowfield to all EPI images of the time series, resampling to a voxel resolution of  $2 \times 2 \times 2 \text{ mm}^3$  using 5th degree spine interpolation, and eventually spatial smoothing using a Gaussian kernel with full width of half maximum of  $6 \times 6 \times 6 \text{ mm}^3$ .

### 3.2.7 1<sup>st</sup> level GLM

At the 1<sup>st</sup> level, three different models were estimated using the general linear model (GLM) framework of SPM. The difference between the three different 1<sup>st</sup> level GLMs lies in the time frame of RA phases: Initially, we modelled a GLM following the most common approach to the MID task by using the entire 6 s of the RA phase. Due to the versatile mechanisms underlying RA and in order to better explore and highlight brain networks involved dynamically in processing rewarding stimuli, we added two analyses by focussing on different phases of RA. To this end, we dissected the 6 s periods of the anticipation phase into in three 2 s segments: early (0-2 s), middle (2-4 s) and late (4-6 s) RA. In addition to our first GLM, our second 1<sup>st</sup> level variant used the early segment of the RA phase, covering the first 2 s of stimulus presentation, whereas our third 1<sup>st</sup> level variant covered the last 2 s. **Figure 12** visualizes this dissection of the RA phase. In addition to the separate analyses of each of these three (whole, early, late) time windows, we also contrasted early against the late RA phase in order to identify brain areas with the most pronounced dynamical differences.

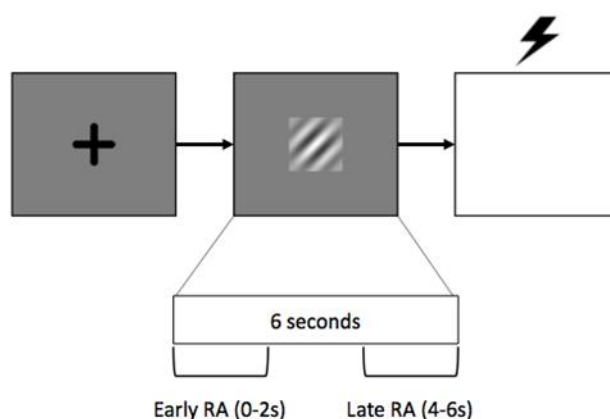


**Figure 12. Temporal dissection of the stimulus presentation in three 2 s segments.** In addition to the GLM using the entire 6 s of the RA phase, two additional models focussing on either early RA (0-2 s of stimulus presentation) or late RA (4-6 s of stimulus presentation) were designed.

Each design matrix included three regressors representing the experimental conditions (one per condition, i.e. monetary reward ['money'], verbal reward ['verbal'], control stimulus ['csm']), that were modelled by convolving the stimulus presentation time with the canonical hemodynamic response function. Differential T-contrasts including 'csm < money', 'csm < verbal' as well as 'verbal < money' were calculated automatically for each of the three GLM variants.

### 3.2.8 2<sup>nd</sup> level GLM

After proof-of-concept interrogations of RA task effects in all groups, we focussed on the following question: How do activation profiles differ between diagnostic groups? Therefore, contrast images of the 1<sup>st</sup> level analysis of all participants were forwarded into a 2<sup>nd</sup> level GLM that was defined as full factorial analysis of covariance with a 4-level group factor (representing HC, MDD, BD and SCZ) and covariates age and sex. An F-test to extract main group effects was performed, followed by pairwise T-tests between the groups. These T-tests were not confined to areas of significant effects of the F-test, but again whole-brain explorations, and a focus was put on comparisons between the respective patient group and HC rather than between patient groups. At the 2<sup>nd</sup> level, clusters were collected at uncorrected  $p_{\text{voxel}} < 0.001$  and assessed at the cluster level regarding their multiple testing robustness. Family-wise error corrected cluster  $p$ -values < 0.05 were considered significant and labelled using the AAL toolbox.

### 3.2.9 Testing dynamic RA effects in network hubs

The analysis of dynamic aspects that might be different in patients compared with HC was also conceptualized also outside the SPM full brain approach: Following the SPM analyses, peak and cluster values of 14 regions that were defined from the early and late RA 1st level GLM were extracted and

entered into a two-factorial repeated-measures ANCOVA (within-subject factor *time* (two levels); between-subjects factor *group*; covariates *age*, *gender*). This allowed to evaluate main effects of group, time and the interaction between group and time. Considering the importance of the basal ganglia for reward processing, we also examined atlas-based regions of interest for a more detailed anatomical information. For this we used 8 pre-defined VS regions in the same manner as cluster analyses of our 14 ROIs. Particularly, the NAcc that is located at the lower tip of the putamen was separated from the rest of the putamen. For all ROI analyses, F-values and *p*-values corrected for heteroscedasticity by the Greenhouse-Geisser method are reported.

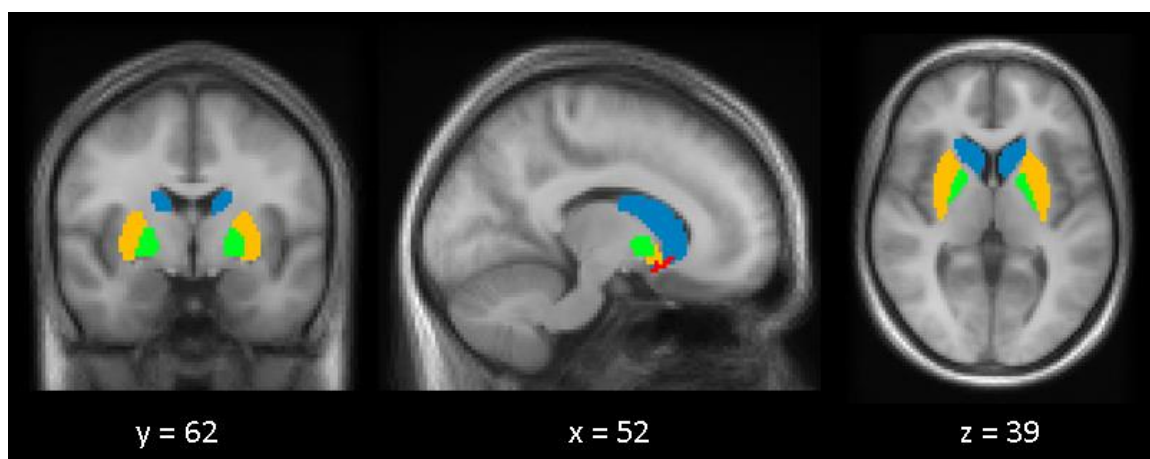


**Figure 13. Atlas-based segmentation of basal ganglia.** The four colours depict the following regions: NAcc (red), globus pallidus (orange), putamen (green), caudate (blue). The AAL single subject atlas was the main basis for these regions (Tzourio-Mazoyer et al. 2002), yet, the left and right NAcc was derived from FreeSurfer segmentation, followed by DARTEL MNI normalization and thresholding and separated from the rest of the putamen.

### 3.3 Results

#### 3.3.1 Demographic characteristics, response times and anhedonia scores of study sample

##### *Demographics*

The final sample of subjects passing the different exclusion criteria consisted of 24 healthy subjects and 75 patients, of which 37 were suffering from major depression, 12 had bipolar disorder and 26 being diagnosed with schizophrenia or schizoaffective disorder. The initial sample consisted of Participants of the initial sample that lacked either incomplete data or failed to pass the fMRI quality control are not listed. In addition, patients whose clinical diagnosis at discharge was not among the ICD-10 codes investigated here (F20, F25, F31-F33) or contained severe comorbidities were excluded. No differences of the male/female distribution or the average age were detected between the four groups. SCZ patients revealed moderate positive and negative. **Table 9** summarizes demographic details of the healthy subjects and the patient sample included in the fMRI analyses.

**Table 9. Demographic and clinical characteristics participants.**

Group	HC	MDD	BD	SCZ
<i>N</i>	24	36	13	27
Age (years, mean±SD)	32.1 (±9.6)	39.2 (±12.9)	40.5 (±9.8)	34.0 (±13.0)
Sex (men/women)	7/17	15/21	5/7	13/15
PANSS*, positive (mean±SD)	N/A	7.2 (± 0.7)	8.7 (±2.4)	14.1 (±4.4)
PANSS*, negative (mean±SD)	N/A	8.8 (± 2.3)	8.9 (±2.3)	14.7 (±6.6)
PANSS*, general (mean±SD)	N/A	22.7 (± 4.1)	20.22 (±3.0)	30.2 (±6.3)

\*PANSS = Positive And Negative Syndrome Scale (Kay et al., 1987).

*Anhedonia Scores*

The anhedonia score was derived from the BDI single items and defined as the sum of items ‘Loss of pleasure’, ‘Loss of interest’, ‘Loss of energy’ and ‘Loss of interest in sex’. Analysis of anhedonia scores revealed significant differences between the investigated groups ( $p < 0.001$ ). Post-hoc analyses showed that healthy subjects exhibited significantly lower anhedonia scores than MDD ( $p < 0.001$ ) and SCZ ( $p = 0.005$ ). **Table 10** displays the group means of BDI scores and anhedonia.

**Table 10. Anhedonia and total score of the BDI.**

Group	HC	MDD	BD	SCZ
Anhedonia* (mean±SD)	0.7 (±1.1)	6.4 (±2.9)	2.4 (±3.0)	3.4 (±2.9)
BDI total	3.1 (±3.8)	29.0 (±11.4)	10.8 (±9.4)	16.9 (±10.7)

\*Anhedonia = Sum score of ‘Loss of pleasure’, ‘Loss of interest’, ‘Loss of energy’ and ‘Loss of interest in sex’ of the BDI.

*Reaction times*

Patients with MDD or BD did not differ from the healthy subjects regarding their RTs. SCZ patients, however, showed slower responses compared to healthy subjects across all trials ( $p = 0.004$ , corrected for *age* and *gender*), with the difference in ‘money’ trials being slightly more pronounced than in ‘verbal’ trials ( $p = 0.005$ ,  $p = 0.011$ , respectively; corrected for *age* and *gender*). Furthermore, the SCZ group revealed a significantly higher mean of missed out responses relative to HC ( $p = 0.041$ ; corrected for *age* and *gender*). With regard to RT difference between ‘verbal’ and ‘money’ trials, no significant group differences were detected.

**Table 11. Overall RTs and RTs by trial type (‘money’, ‘verbal’).**

	HC	MDD	BD	SCZ
Overall RT (mean±SD)	0.254 (± 0.029)	0.259 (± 0.054)	0.262 (± 0.049)	0.304 (± 0.096)
‘verbal’ trials (mean±SD)	0.264 (± 0.041)	0.266 (± 0.067)	0.268 (± 0.051)	0.319 (± .104)
‘money’ trials (mean±SD)	0.243 (± 0.023)	0.253 (± 0.053)	0.258 (± 0.049)	0.290 (± .104)

### 3.3.2 RA task BOLD fMRI effects

As a proof-of-concept interrogation, RA task effects of each group were viewed separately. As indicated above, the entire 6 s of stimulus presentation were examined first before sensitizing the analyses by focussing on the early and late RA phase separately. The same procedure applies to the reports of main effects in diagnostic groups and the investigation of pairwise differences between HC and the patient groups.

#### Main effects of the RA task in healthy controls

##### *Classical approach using 6 s of stimulus presentation*

In healthy subjects, the 2<sup>nd</sup> level positive T-contrast (i.e., task-positive effects) ‘money > csm’ yielded 15 clusters at  $p_{\text{voxel.FWE}} < 0.05$  ( $k > 10$ ), localizing to the bilateral striate area, insular cortex, inferior frontal gyrus, left supplemental motor area (SMA), right cerebellum, right thalamus and right occipital gyrus. Clusters are detailed in **Table 12** and visualized in **Figure 14** below.

**Table 12. Task-positive effects of RA (full 6 s) in healthy controls ( $p_{\text{voxel.FWE}} < 0.05$ ;  $k > 10$ ).**

Result cluster #	Anatomical cluster location <sup>a</sup>	Cluster size in voxels	Peak voxel coordinates <sup>b</sup>
1	<i>R</i> rectus, putamen, pallidum	324	12 6 2
2	<i>R</i> SMA <i>L/R</i> middle cingulate gyrus	380	-4 -8 54
3	<i>L</i> inferior parietal lobule, postcentral gyrus, supramarginal gyrus	723	-42 -22 46
4	<i>R</i> cerebellum	352	30 -52 -26
5	<i>L</i> pallidum, olfactory cortex, putamen	320	-10 4 -2
6	<i>L</i> triangular/orbital part of IFG	118	-30 18 8
7	<i>L</i> rolandic operculum	22	-52 4 10
8	<i>R</i> thalamus	78	8 -28 -6
9	<i>R</i> rolandic operculum	27	52 8 4
10	<i>R</i> opercular/triangular part of IFG	118	32 22 8
11	<i>R</i> SMA	17	6 -10 72
12	<i>R</i> middle frontal gyrus, precentral gyrus	16	40 -8 52
13	<i>R</i> middle cingulate cortex	30	12 6 38
14	<i>L</i> cerebellum	21	-32 -58 -32
15	<i>R</i> middle/superior occipital cortex	19	24 -90 6

<sup>a</sup>Result clusters were mapped with the AAL toolbox.

<sup>b</sup>Peak voxel coordinates are given in MNI space.

*L* and *R* denote left and right hemispheric location; *L/R* denotes bilateral location. SMA, supplemental motor area; IFG, inferior frontal gyrus.

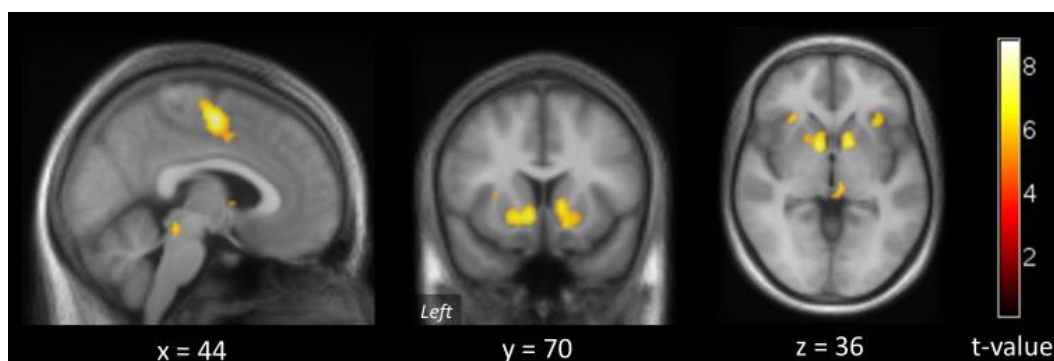


**Figure 14. Task-positive BOLD amplitude effects of RA (full 6 s) in HC.** Hot colours display regions with higher BOLD activity during monetary trials compared with control trials. Statistical maps were sampled at  $p_{\text{voxel.FWE}} < 0.05$  ( $k > 10$ ). Coordinates refer to MNI coordinates of the respective slices. The specific intersection shown here highlights the VS clusters (#1 and #5 in **Table 12**) and the SMA (#2).

The analyses of task-negative effects ('money < csm') identified 11 clusters at  $p_{\text{voxel.FWE}} < 0.05$  ( $k > 10$ ), mainly localizing to the bilateral precuneus, insula, operculum and lateral parietal regions. Details of task-negative effects are listed in **Table 13** and a representative statistical map is shown in **Figure 15**.

**Table 13. Task-negative effects of RA (full 6 s) in healthy controls ( $p_{\text{voxel.FWE}} < 0.05$ ;  $k > 10$ ).**

Result cluster #	Anatomical cluster location <sup>a</sup>	Cluster size in voxels	Peak voxel coordinates <sup>b</sup>
1	<i>R</i> precuneus, lingual gyrus, PCC, calcarine fissure <i>L</i> cuneus, precuneus, calcarine fissure	746	10 -56 10
2	<i>R</i> angular gyrus, middle temporal gyrus	162	46 -72 32
3	<i>L</i> precentral gyrus	120	-48 -12 26
4	<i>R</i> postcentral gyrus	49	60 -8 18
6	<i>R</i> precentral gyrus	38	44 -8 26
7	<i>R</i> insula	34	40 -14 16
8	<i>R</i> parahippocampal gyrus	12	26 -22 -20
9	<i>R</i> middle frontal gyrus	40	24 16 42
10	<i>R</i> middle frontal gyrus	24	30 14 54
11	<i>R</i> superior temporal gyrus	24	66 -10 0

<sup>a</sup>Result clusters were mapped with the AAL toolbox.

<sup>b</sup>Peak voxel coordinates are given in MNI space.

*L* and *R* denote left and right hemispheric location; *L/R* denotes bilateral location. PCC, posterior cingulate cortex.

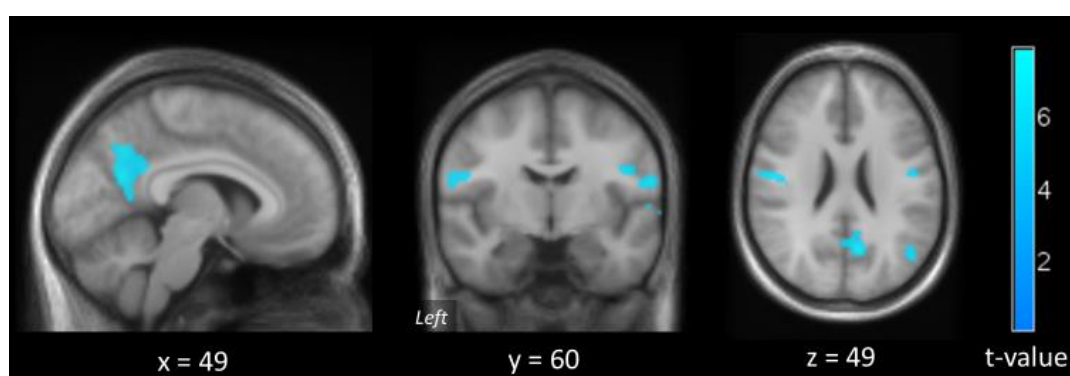


**Figure 15. Task-negative BOLD amplitude effects of RA (full 6 s) in HC.** Clusters displayed in cool colours represent regions with reduced BOLD activity during monetary trials compared with control trials. Statistical maps were sampled at  $p_{\text{voxel.FWE}} < 0.05$  ( $k < 10$ ). Coordinates refer to MNI coordinates of the respective slices. Note the largest cluster locating to the precuneus/PCC area which represents the posterior midline hub.



### Dissection of the BOLD response to RA into an early and a late phase

Following the analysis of the full 6 s of the RA phase, we also analysed BOLD effects of the early and late RA phase, using the same statistical criteria for comparability.

#### Early phase of RA

The early phase analyses of task-positive effects ('money<sub>early</sub> > csm<sub>early</sub>') identified 4 clusters collected at  $p_{\text{voxel.FWE}} < 0.05$  ( $k > 10$ ) (see **Table 14**). These were located to the bilateral pallidum/striate area, left inferior parietal lobule, pre- and postcentral gyri, as well as a centrally located cluster partially covering the cingulate gyrus and extending to the left SMA. A representative intersection of the early RA activation profile is visualized in **Figure 16**.

**Table 14. Task-positive effects of early RA in healthy controls ( $p_{\text{voxel.FWE}} < 0.05$ ;  $k > 10$ ).**

Result cluster #	Anatomical cluster location <sup>a</sup>	Cluster size in voxels	Peak voxel coordinates <sup>b</sup>
1	<i>L</i> pallidum, putamen, olfactory	291	-10 14 -8
2	<i>R</i> pallidum, olfactory, putamen	477	12 6 2
3	<i>L</i> parietal inferior lobule, postcentral gyrus, supra-marginal gyrus	140	-40 -22 46
4	<i>L</i> cingulate	123	-4 -6 52

<sup>a</sup>Result clusters were mapped with the AAL toolbox.

<sup>b</sup>Peak voxel coordinates are given in MNI space.

*L* and *R* denote left and right hemispheric location.

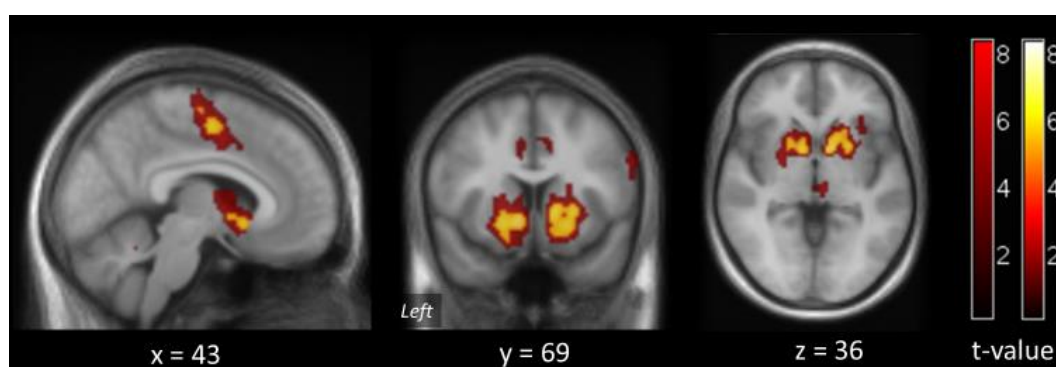


**Figure 16. Task-positive BOLD amplitude effects during early RA in healthy controls.** Red coloured clusters represent effects sampled at an uncorrected  $p_{\text{voxel}} < 0.001$  and thresholded at  $p_{\text{cluster.FWE}} < 0.05$ . Voxels robust to family-wise error correction ( $p_{\text{voxel.FWE}} < 0.05$ ,  $k > 10$ ) are shown in yellow. Coordinates refer to MNI coordinates of the respective slices.

The reverse contrast ‘money<sub>early</sub> < csm<sub>early</sub>’ revealed 7 clusters of task-negative effects at  $p_{\text{voxel.FWE}} < 0.05$  ( $k > 10$ ) (see **Table 15**). Deactivation during the money<sub>early</sub> condition was found in the bilateral cuneus, right precuneus reaching to the medial occipitotemporal gyrus (lingual gyrus) and bilateral calcarine sulci. The deactivation profile is visualized in **Figure 17**.

**Table 15. Task-negative effects of early RA in healthy controls ( $p_{\text{voxel.FWE}} < 0.05$ ;  $k > 10$ ).**

Result cluster #	Anatomical cluster location <sup>a</sup>	Cluster size in voxels	Peak voxel coordinates <sup>b</sup>
1	<i>L</i> cuneus <i>R</i> cuneus	58	6 -88 34
2	<i>R</i> precuneus, cerebellum, lingual gyrus	69	12 -54 6
3	<i>L</i> postcentral gyrus	15	-60 -8 -18
4	<i>R</i> precuneus, cuneus, calcarine fissure	12	6 -62 20
5	<i>L</i> postcentral gyrus	21	-50 -12 26
6	<i>L</i> calcarine fissure	12	-6 -90 2
7	<i>L</i> calcarine fissure	12	0 -90 8

<sup>a</sup>Result clusters were mapped with the AAL toolbox.

<sup>b</sup>Peak voxel coordinates are given in MNI space.

*L* and *R* denote left and right hemispheric location.

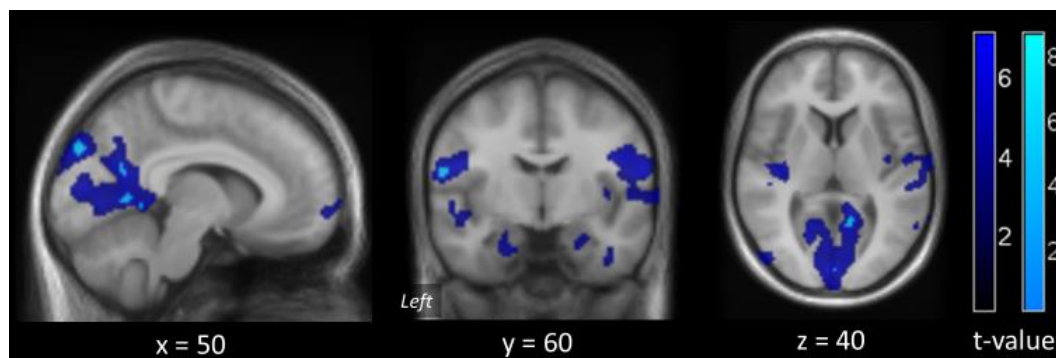


**Figure 17. Task-negative BOLD amplitude effects of early RA in HC.** Dark blue clusters reflect effects sampled at an uncorrected  $p_{\text{voxel}} < 0.001$  and thresholded at  $p_{\text{cluster.FWE}} < 0.05$ . Voxels robust to family-wise error correction ( $p_{\text{voxel.FWE}} < 0.05$ ,  $k > 10$ ) are depicted in bright blue. Coordinates refer to MNI coordinates of the respective slices.

### Late phase of RA

In the analyses of the last two seconds of the stimulus presentation, the contrast ‘money<sub>late</sub> > csm<sub>late</sub>’ revealed 20 clusters at  $p_{\text{voxel.FWE}} < 0.05$  ( $k > 10$ ) (see **Table 16**). Besides a wide-spread activation of the right cerebellum (likely capturing motor response elements or the preparation of it), the clusters localized to brain areas representing the salience network (left superior temporal gyrus and the inferior frontal gyrus, extending to the left insula; right inferior frontal gyrus; the right insula,

dorsal ACC), the left inferior-/lateral parietal lobule (extending to the postcentral and supramarginal gyrus) and the bilateral thalamus. Moreover, similar as in the early RA phase, ventral striatal activation was also identified during the monetary trial, although this effect was less pronounced in the late RA phase. A visualisation of all task-positive effects during late RA can be found in **Figure 18**.

**Table 16. Task-positive effects of late RA in healthy controls ( $p_{\text{voxel.FWE}} < 0.05$ ;  $k > 10$ ).**

Result cluster #	Anatomical cluster location <sup>a</sup>	Cluster size in voxels	Peak voxel coordinates <sup>b</sup>
1	<i>R</i> cerebellum	576	30 -52 -26
2	<i>L</i> STG, rolandic operculum, IFG (pars triangularis/opercularis), insula	457	-28 24 2
3	<i>L</i> inferior parietal lobule, postcentral gyrus, supramarginal gyrus	939	-42 -26 50
4	<i>R</i> thalamus	176	6 -30 -8
5	<i>R</i> caudate, pallidum	233	10 4 2
6	<i>R</i> SMA, middle cingulate gyrus <i>L</i> middle cingulate gyrus, paracentral lobule	388	-4 -8 54
7	<i>R</i> rolandic operculum, IFG (pars opercularis), insula	284	52 8 6
8	<i>R</i> IFG (pars opercularis/triangularis), insula	384	34 36 -4
9	<i>L</i> cerebellum	210	-26 -68 -26
10	<i>R</i> cerebellum	61	4 -66 -18
11	<i>L</i> caudate	79	-8 2 2
12	<i>R</i> cerebellum	26	4 -68 -34
13	<i>R</i> middle frontal gyrus	26	42 -8 52
14	<i>R</i> inferior occipital gyrus, fusiform gyrus	101	34 -86 -2
15	<i>R</i> frontal middle gyrus, precentral gyrus	15	50 2 54
16	<i>R</i> supramarginal gyrus	24	60 -28 48
17	<i>L</i> SMA	14	-8 -10 76
18	<i>R</i> fusiform gyrus	28	30 -76 -12
19	<i>L</i> middle occipital gyrus	14	-26 -86 6
20	<i>L</i> IFG (pars opercularis), precentral gyrus	11	-52 6 22

<sup>a</sup>Result clusters were mapped with the AAL toolbox.

<sup>b</sup>Peak voxel coordinates are given in MNI space.

*L* and *R* denote left and right hemispheric location. STG, superior temporal gyrus; IFG, Inferior frontal gyrus; SMA, supplemental motor area.

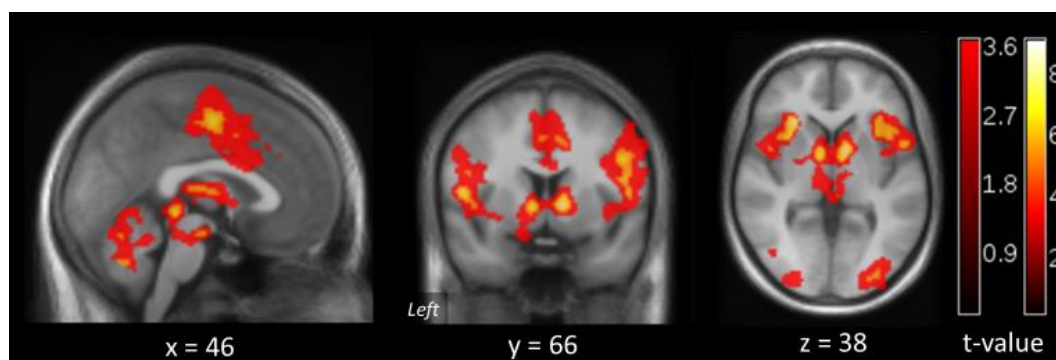


**Figure 18. Task-positive BOLD amplitude effects of late RA in HC.** Red coloured clusters represent effects sampled at an uncorrected  $p < 0.001$  and thresholded at  $p_{\text{cluster.FWE}} < 0.05$ . Voxels robust to family-wise error correction ( $p_{\text{voxel.FWE}} < 0.05$ ,  $k > 10$ ) are shown in yellow. Coordinates refer to MNI coordinates of the respective slices.

As shown in **Table 17**, the reverse contrast ‘money<sub>late</sub> < csm<sub>late</sub>’ yielded 11 clusters of BOLD deactivation at  $p_{\text{voxel.FWE}} < 0.05$  ( $k > 10$ ), mainly localizing to brain areas representing the DMN (posterior cingulate gyrus and precuneus, medial prefrontal and inferior parietal as well as temporolateral regions). In addition, deactivation was also found in a small cluster in the parahippocampal gyrus ( $k = 3$ ; [x y z]: 24 -22 -22) that is also considered to be a part of the DMN (Ward et al., 2014). **Figure 19** displays task-negative effects during late RA phase.

**Table 17. Task-negative effects of late RA in HC ( $p_{\text{voxel.FWE}} < 0.05$ ;  $k > 10$ ).**

Result cluster #	Anatomical cluster location <sup>a</sup>	Cluster size in voxels	Peak voxel coordinates <sup>b</sup>
1	R middle temporal gyrus, superior parietal gyrus	246	46 -72 32
2	R precuneus, posterior cingulate gyrus, middle cingulate gyrus L calcarine fissure	1066	0 -58 38
3	L angular, middle occipital gyrus	75	-44 -76 32
4	R lower mPFC	54	0 58 -8
5	L middle frontal gyrus, precentral gyrus	40	-32 12 54
6	L middle frontal gyrus	22	-22 16 50
7	R superior temporal gyrus	46	60 -10 2
9	R middle frontal gyrus, superior frontal gyrus	14	28 16 56
10	R insula, rolandic operculum	11	38 -12 16
11	L middle temporal gyrus	21	-52 -24 2

<sup>a</sup>Result clusters were mapped with the AAL toolbox.

<sup>b</sup>Peak voxel coordinates are given in MNI space.

L and R denote left and right hemispheric location. mPFC, medial prefrontal cortex.

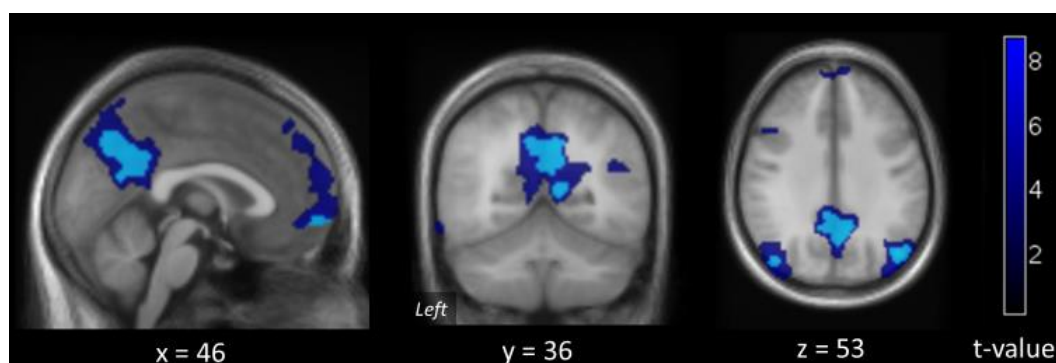


**Figure 19. Task-negative BOLD amplitude effects of late RA in HC.** Dark blue clusters represent effects sampled at an uncorrected  $p < 0.001$  and thresholded at  $p_{\text{cluster.FWE}} < 0.05$ . Voxels that were robust to family-wise error correction ( $p_{\text{voxel.FWE}} < 0.05$ ,  $k > 10$ ) are displayed in light blue. Coordinates refer to MNI coordinates of the respective slices.

### Differences between fMRI patterns of early and late RA

In order to statistically test the dynamics within activation profiles during RA throughout the whole 6 s of stimulus presentation, we mapped the differences of BOLD activation between early (0-2 s) and late (4-6 s) RA phases. Our first approach to contrast the early and late phase of RA was to model this difference within the individual 1<sup>st</sup> level GLM. The double contrast used for this purpose was calculated as follows:  $(\text{money}_{\text{early}} > \text{csm}_{\text{early}}) > / < (\text{money}_{\text{late}} > \text{csm}_{\text{late}})$ . These maps were forwarded to the 2<sup>nd</sup> level for all four groups, with a focus on an in-depth analysis in the healthy controls. Results hereof are reported below. Due to imperfect orthogonality (see **Figure 20**) between the early and late task regressors (after convolution), it was decided to also perform an analysis that makes use of both the early and late RA phase, yet modelled separately at the 1<sup>st</sup> level and conjoined at the 2<sup>nd</sup> level after subtraction from each other (late RA minus early RA). These additional results were in line with the results reported in the following passages on the within-1<sup>st</sup> level subtraction.

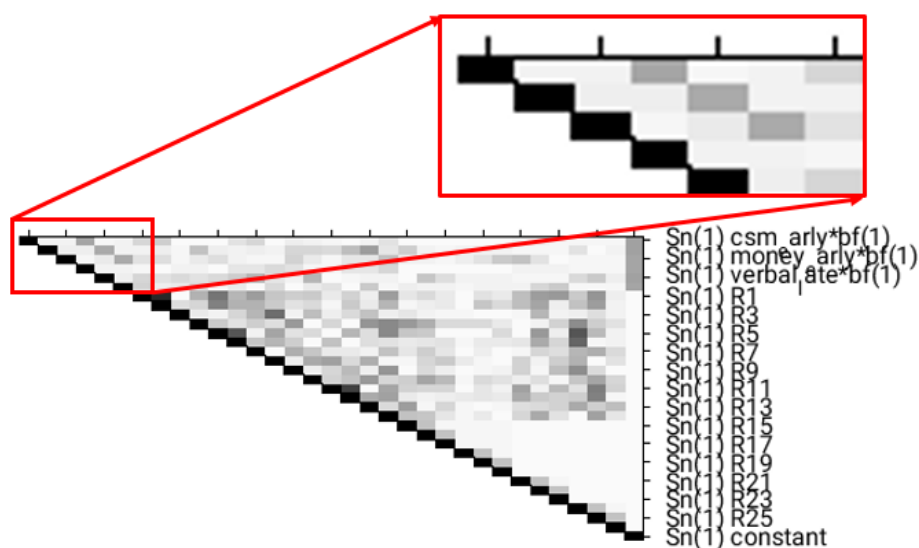


**Figure 20. Violation of regressor orthogonality in combined early/late RA 1<sup>st</sup> level models.** As visualized in the magnified view, after HRF convolution, early and late task regressors overlapped (imperfect orthogonality, three grey steps) and thus competed against each other, possibly not allowing an unambiguous attribution of variance. Therefore, effects were expected to be less strong (i.e. conservative) in this type of approach compared with modelling the early and late RA phase in separate 1<sup>st</sup> level models.

In the control group, contrasting ‘RA<sub>early</sub> > RA<sub>late</sub>’ revealed 7 clusters collected at strict  $p_{\text{voxel.FWE}} < 0.05$ , localizing to the bilateral parietal lobules, precuneus and the medial prefrontal cortex. Details of areas being more strongly activated during the early phase of RA compared with the late phase are listed **Table 18** and visualized in red/yellow in **Figure 21**.

**Table 18. Contrasting ‘RA<sub>early</sub> > RA<sub>late</sub>’ in HC ( $p_{\text{voxel.FWE}} < 0.05$ ).**

Result cluster #	Anatomical cluster location <sup>a</sup>	Cluster size in voxels	Peak voxel coordinates <sup>b</sup>
1	R angular gyrus, middle occipital gyrus	8	46 -72 32
2	R precuneus	5	8 -58 38
3	L lower mPFC	6	-2 54 -8
4	L middle occipital gyrus	11	-42 -78 34
5	R/L precuneus	4	2 -70 42
6	R precuneus	2	12 -52 28
7	L middle frontal gyrus	1	-32 12 58

<sup>a</sup>Result clusters were mapped with the AAL toolbox.

<sup>b</sup>Peak voxel coordinates are given in MNI space.

L and R denote left and right hemispheric location; L/R denotes bilateral location. mPFC, medial prefrontal cortex.

The analyses of the reverse contrast (' $RA_{\text{early}} < RA_{\text{late}}$ ') identified 15 clusters collected at  $p_{\text{voxel.FWE}} < 0.05$  in healthy subjects. The main clusters of this contrast were localized to the bilateral insula reaching to the inferior frontal gyrus and superior temporal pole in both hemispheres, and a cluster comprising the cuneus, calcarine fissure and the lingual gyrus. Moreover, several smaller clusters were found in the occipital cortex and the cerebellum. Cluster details of areas with higher activation profiles during  $RA_{\text{late}}$  compared with  $RA_{\text{early}}$  in HC subjects are listed in **Table 19** and visualized in dark/light blue in **Figure 21**.

**Table 19. Contrasting  $RA_{\text{early}} < RA_{\text{late}}$  in HC ( $p_{\text{voxel.FWE}} < 0.05$ ;  $k > 10$ ).**

Result cluster #	Anatomical cluster location <sup>a</sup>	Cluster size in voxels	FWE corrected cluster p-value	Peak voxel coordinates <sup>b</sup>
1	<i>L</i> calcarine	66	< 0.001	-6 -90 2
2	<i>L</i> superior temporal pole, insula, opercular part of the IFG	301	< 0.001	-48 14 -8
3	<i>R</i> cerebellum	76	< 0.001	40 -46 -22
4	<i>L/R</i> cuneus <i>R</i> calcarine fissure <i>L</i> lingual gyrus	393	< 0.001	10 -60 0
5	<i>R</i> cerebellum, fusiform gyrus, inferior occipital gyrus	182	< 0.001	28 -74 -18
6	<i>R</i> IFG (pars triangularis), middle frontal gyrus, precentral gyrus	127	< 0.001	42 10 22
7	<i>L</i> cerebellum	83	< 0.001	-32 -48 -26
8	<i>R</i> superior temporal pole, IFG (pars orbitalis/triangularis), middle frontal gyrus, rolandic operculum	323	< 0.001	48 14 -4
9	<i>L</i> lingual gyrus	12	0.001	-18 -54 -6
10	<i>L</i> cerebellum	88	< 0.001	-34 -68 -16
11	<i>L</i> fusiform gyrus, lingual gyrus	101	< 0.001	-42 -86 -10
12	<i>R</i> fusiform gyrus, lingual gyrus	15	< 0.001	20 -46 -12
13	<i>R</i> inferior occipital gyrus	24	< 0.001	40 -74 -10
14	<i>L</i> lingual gyrus	46	< 0.001	-12 -64 -4
15	<i>L</i> cerebellum	16	< 0.001	-32 -84 -24

<sup>a</sup>Result clusters were mapped with the AAL toolbox.

<sup>b</sup>Peak voxel coordinates are given in MNI space.

*L* and *R* denote left and right hemispheric location; *L/R* denotes bilateral location. IFG, inferior frontal gyrus.



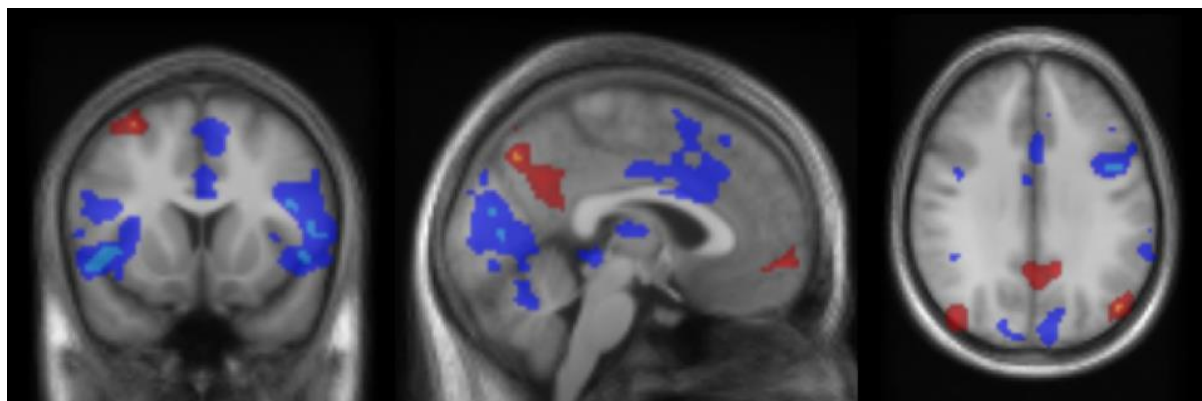


**Figure 21. Differences between task effects in the early and late RA phases.** The positive contrast (hot colours) reflects regions that exhibit more BOLD activity in the early phase of RA. Dark red shows significant clusters at  $p < 0.001$  and FWE-robust voxels are shown in yellow. Blue clusters reflect the reverse pattern, i.e. regions exhibiting stronger activity in the late phase of RA. Dark blue areas represent  $p_{\text{voxel}} < 0.001$  and light value areas show voxel-wise FWE-robust effects ( $p_{\text{voxel.FWE}} < 0.05$ ;  $k > 10$ ).

In comparing the early and late phase of RA against each other, we demonstrated that temporal dynamics of BOLD activation prevails during the 6 s of RA. Due to these dynamics, task effects that are relevant for processing rewarding stimuli could be less pronounced or less specific when the entire phases of stimulus presentation, i.e. the RA phase, is modelled as one homogeneous phase. Therefore, for a comprehensive understanding of group differences, we investigate the usual 6 s of RA phase in addition to the more specific approach of analysing RA<sub>early</sub> and RA<sub>late</sub> separately.

### Identification of three distinct networks participating in RA and definition of ROIs

In addition to the voxel-wise SPM analyses, we thought to analyse key regions in an 'offline' more flexible statistical framework that allowed the application of repeated measure analyses and the flexible model of co-variance. Here, the 'repeated' aspect is the time factor of early and late responses within the same subject. Knowing the above described early/late RA activation maps, in order to not bias our analysis towards dynamic effects (emphasis in the early or late phase), which would filter out more steady activation patterns, we decided to actually base the ROI definition on the conventional approach that uses the full anticipation phase as detailed in **Tables 12** and **13** and **Figures 14** and **15**. In doing so, the analysis approach can be considered conservative in that it also allows temporally *stable* results to enter the 2<sup>nd</sup> level ROI statistics. Expectedly, the positive contrast of the full RA phase thus included both ventral striatal areas (more active in the early phase, see **Figure 16**, depicting the early task-positive response) and salience network areas (more active in the late phase, see **Figure 17**, the task-positive late phase). Taken together, with the deactivation mostly taking place in the late phase (default mode network) we can thus assume that a minimum of three major brain networks are covered by the analyses (see **Figure 21**). From these three networks, a total of 14 ROIs were defined as follows: (1-3) bilateral ventral striate and a mesencephalic region, as representing core regions re-

sponding during reward processing; (4-6) bilateral anterior insula and SMA as representing the salience network; (7-14) posterior and anterior (dorsomedial PFC) midline hubs of the DMN, in addition to its bilateral parietal nodes, its bilateral temporo-lateral nodes, and parts of the bilateral hippocampus. **Figure 22** visualizes the final set of ROIs sorted into three networks coloured respectively.

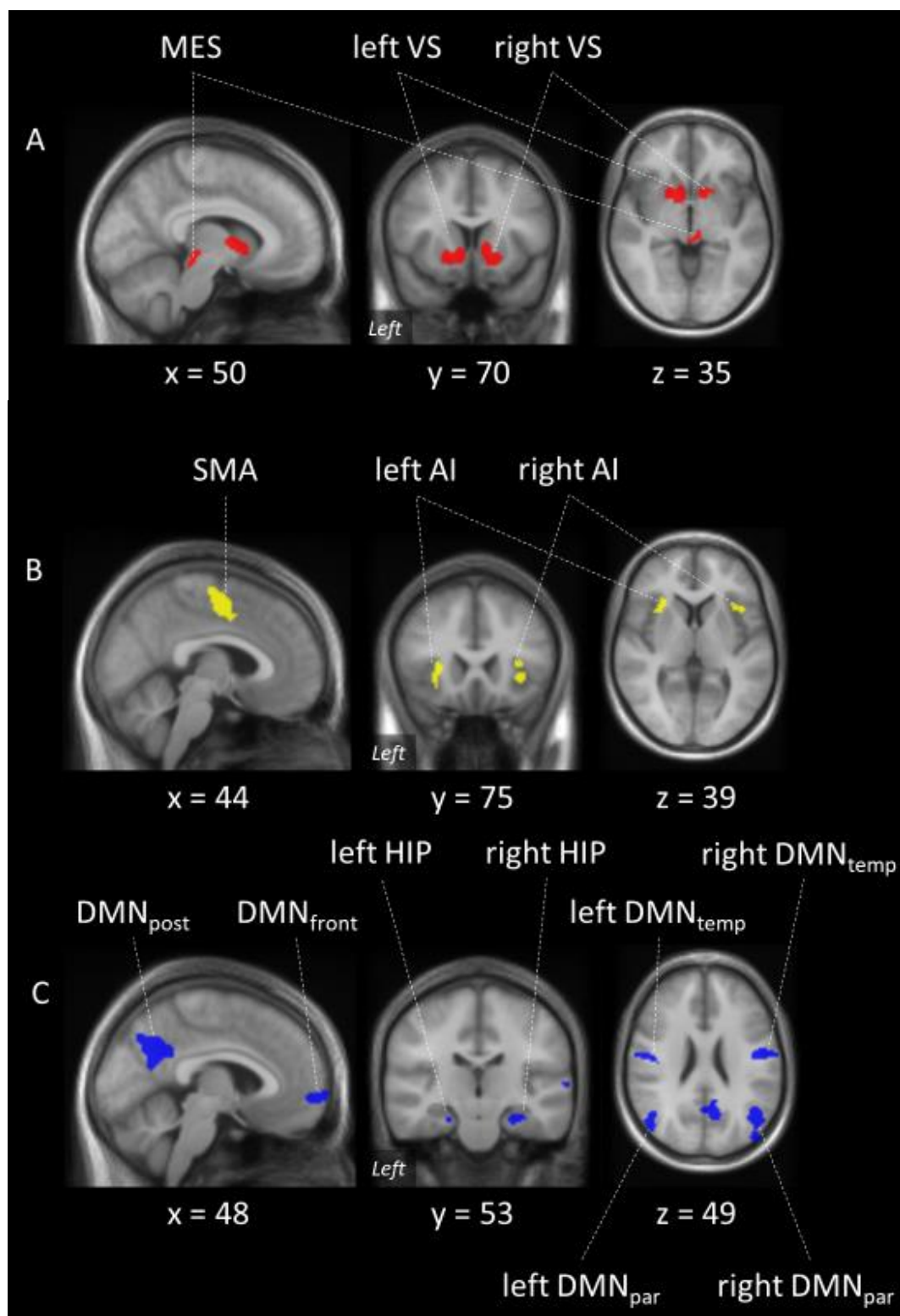


**Figure 22. Final ROI selection based on activation and deactivation during 6 s of RA. (A)** Reward network, comprising the left and right VS and the mesencephalon. **(B)** Salience network consisting of left and right insula and the bilateral (midline) SMA. **(C)** DMN including the precuneus, medial frontal, inferior parietal, lateral temporal regions and (para-)hippocampus. Note that primary motor cortex and cerebellar areas were omitted from the ROI selection due to likely representing more unspecific motor processes that accompany the task. Similarly, also to keep the number of tests limited, we omitted the two frontal eye-field areas of the task-negative response (i.e., the DMN). Abbreviations: DMN, default mode network; VS, ventral striate; SMA, supplementary motor area; HIP, hippocampus; AI, anterior insula, MES, mesencephalon.

### 3.3.3 Comparison of RA between patients and HC

Before addressing the main question, i.e. how different diagnostic groups are reflected in different BOLD activation profiles during reward processing, RA tasks effects for each clinical group were verified in the sense of proof-of-concept analyses. Therefore, the first section of this chapter sets out the main effects for each diagnostic group separately before investigating group differences between the patient groups and HC in RA, as well as the specific network hubs defined in the previous chapter. The presentation of both main effects in each group and differences between groups is done according to the same principle as in HC, whereby the entire 6 s phase of RA is each investigated first before separate reports on early and late RA effects.

#### Main effects of RA in different diagnostic conditions

##### MDD

In patients with MDD (N=36), the contrast ‘money > csm’ revealed 16 clusters of activation at  $p_{\text{voxel.FWE}} < 0.05$  ( $k > 10$ ). Activation was found in the bilateral striate area reaching to the temporal-insular regions, the midcingulate cortex, SMA, parietal lobe and thalamus. The reverse contrast (‘money < csm’) identified 6 clusters of deactivation at  $p_{\text{voxel.FWE}} < 0.05$  ( $k > 10$ ), localizing to the precuneus and medial frontal, inferior parietal cortical regions. Statistical maps can be found in **Figure 23**.

**Table 20. Task-positive and negative effects of RA in MDD ( $p_{\text{voxel.FWE}} < 0.05$ ;  $k > 10$ ).**

Result cluster #	Anatomical cluster location <sup>a</sup>	Cluster size in voxels	Peak voxel coordinates <sup>b</sup>
<i>Task-positive effects</i>			
1	L putamen, insula, IFG (pars opercularis)	1078	-30 18 8
2	L olfactory cortex, putamen R thalamus	1593	8 -26 -4
3	R putamen, IFG(pars triangularis/opercularis), insula	1171	52 8 4
4	L inferior parietal lobule, pre-/postcentral gyrus	1115	-42 -18 46
5	L SFG (pars medialis), paracentral lobule R midcingulate cortex, SMA	2471	10 -2 54
6	R cerebellum	280	28 -52 -28
7	R angular gyrus, supramarginal gyrus	312	60 -46 36
8	R middle frontal gyrus	185	52 2 44
9	R cerebellum	66	4 -66 -20
10	L STG, postcentral gyrus, supramarginal gyrus	58	-54 -24 14

11	<i>R</i> inferior/superior occipital gyrus, fusiform gyrus, calcarine fissure	102	26 -88 2
12	<i>R</i> cerebellum	13	8 -56 -10
13	<i>L</i> STG	106	-48 -42 26
14	<i>R</i> cerebellum	29	4 -68 -34
15	<i>L</i> inferior parietal gyrus, postcentral gyrus	11	-28 -42 48
16	<i>L</i> pallidum	10	-22 -6 -2
<i>Task-negative effects</i>			
1	<i>R</i> angular gyrus, STG	767	48 -68 26
2	<i>R</i> precuneus <i>L</i> cuneus <i>L/R</i> calcarine fissure	1151	6 -58 32
3	<i>L</i> inferior parietal lobule, middle occipital gyrus	402	-40 -74 32
4	<i>L</i> middle frontal gyrus	260	30 18 50
5	<i>L</i> middle frontal gyrus	422	-18 32 40
6	<i>L</i> ACC, medial part of the SFG	20	-2 58 4

<sup>a</sup>Result clusters were mapped with the AAL toolbox.

<sup>b</sup>Peak voxel coordinates are given in MNI space.

*L* and *R* denote left and right hemispheric location; *L/R* denotes bilateral location. IFG, inferior frontal gyrus; SFG, superior frontal gyrus; SMA, supplemental motor area; STG, superior temporal gyrus; ACC, anterior cingulate cortex.

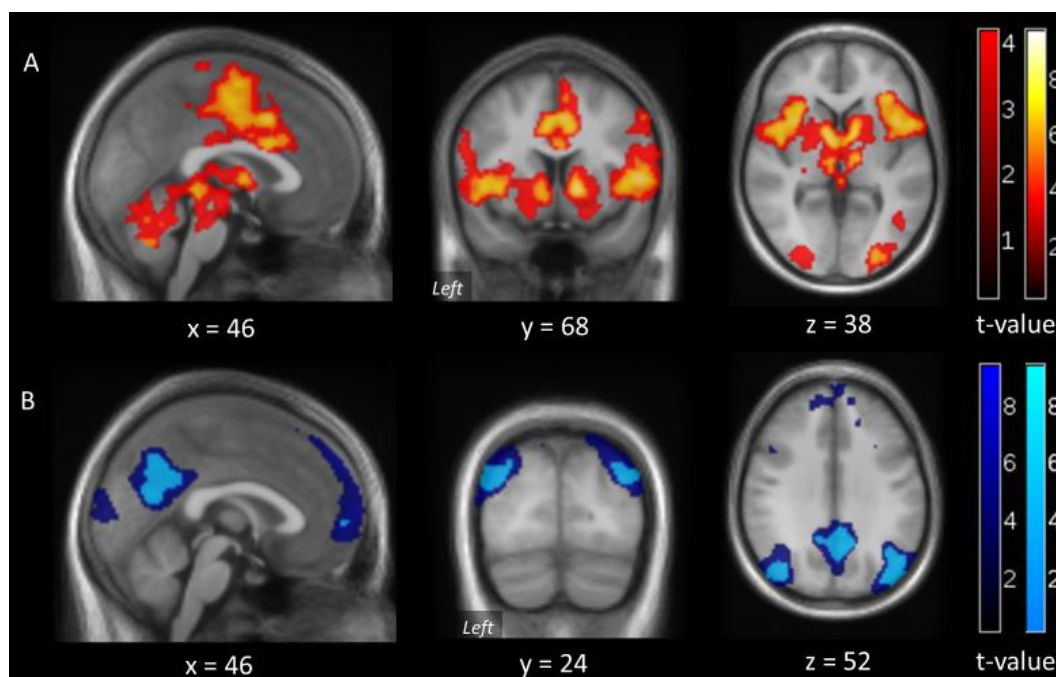


**Figure 23. Task effects of RA in patients with MDD. (A)** Task-positive effects. Statistical maps shown in red were sampled at uncorrected  $p_{\text{voxel}} < 0.001$  and clusters were thresholded at a cluster-wise  $p_{\text{cluster.FWE}} < 0.05$ . Clusters in hot colours show voxel-wise effects robust to family-wise error correction ( $p_{\text{voxel.FWE}} < 0.05$ ,  $k > 10$ ). **(B)** Task-negative effects. Dark blue shows significant clusters sampled at uncorrected  $p < 0.001$ . Voxel-wise FWE-robust ( $p_{\text{voxel.FWE}} < 0.05$ ,  $k > 10$ ) effects are overlaid in brighter blue.

Next, we focussed on the early phase of RA in MDD. Here, the contrast ‘money<sub>early</sub> > csm<sub>early</sub>’ revealed 11 clusters of enhanced activation at  $p_{\text{voxel.FWE}} < 0.05$  ( $k > 10$ ), mainly localizing to the bilateral putamen/striate area, SMA and dACC, bilateral insula area and thalamus. In the analyses of the reverse contrast ‘money<sub>early</sub> < csm<sub>early</sub>’, 6 clusters of BOLD deactivation at  $p_{\text{voxel.FWE}} < 0.05$  ( $k > 10$ ) emerged. Deactivation was found in the parietal lobule, right cuneus, medial prefrontal gyrus and the visual cortex. Statistical details are listed in **Table 21** below. **Figure 24** depicts the distribution of activation and deactivation in MDD during early RA.

**Table 21. Task-positive and negative effects of early RA in MDD ( $p_{\text{voxel.FWE}} < 0.05$ ;  $k > 10$ ).**

Result cluster #	Anatomical cluster location <sup>a</sup>	Cluster size in voxels	Peak voxel coordinates <sup>b</sup>
<i>Task-positive effects</i>			
1	<i>L</i> SFG (pars orbitalis), pallidum, putamen <i>R</i> putamen, caudate	965	12 8 -2
2	<i>L</i> midcingulate cortex, paracentral lobule <i>R</i> SMA, middle cingulate gyrus	969	2 -6 64
3	<i>L</i> STG, insula	214	-30 18 8
4	<i>L</i> postcentral gyrus, precentral gyrus	400	-42 -22 54
5	<i>R</i> thalamus	16	8 -24 -4
6	<i>R</i> putamen, insula, rolandic operculum, IFG	119	46 4 2
7	<i>R</i> ACC	25	-4 18 28
8	<i>R</i> cerebellum	19	36 -52 -34
9	<i>L</i> postcentral gyrus	25	-42 -34 54
10	<i>L</i> middle cingulate gyrus	25	-8 -30 48
11	<i>R</i> precentral gyrus	11	54 -2 46
<i>Task-negative effects</i>			
1	<i>R</i> angular, middle temporal gyrus	187	48 -66 22
2	<i>R</i> cuneus, precuneus	30	6 -64 18
3	<i>R</i> middle frontal gyrus	24	32 16 48
4	<i>R</i> middle occipital gyrus	29	38 -80 28
5	<i>L</i> middle frontal gyrus	11	-38 12 52
6	<i>L</i> triangular/opercular part of the IFG	10	-36 16 22

<sup>a</sup>Result clusters were mapped with the AAL toolbox.

<sup>b</sup>Peak voxel coordinates are given in MNI space.

*L* and *R* denote left and right hemispheric location. STG, superior temporal gyrus; SFG, superior frontal gyrus; ACC, anterior cingulate cortex; IFG inferior frontal gyrus.

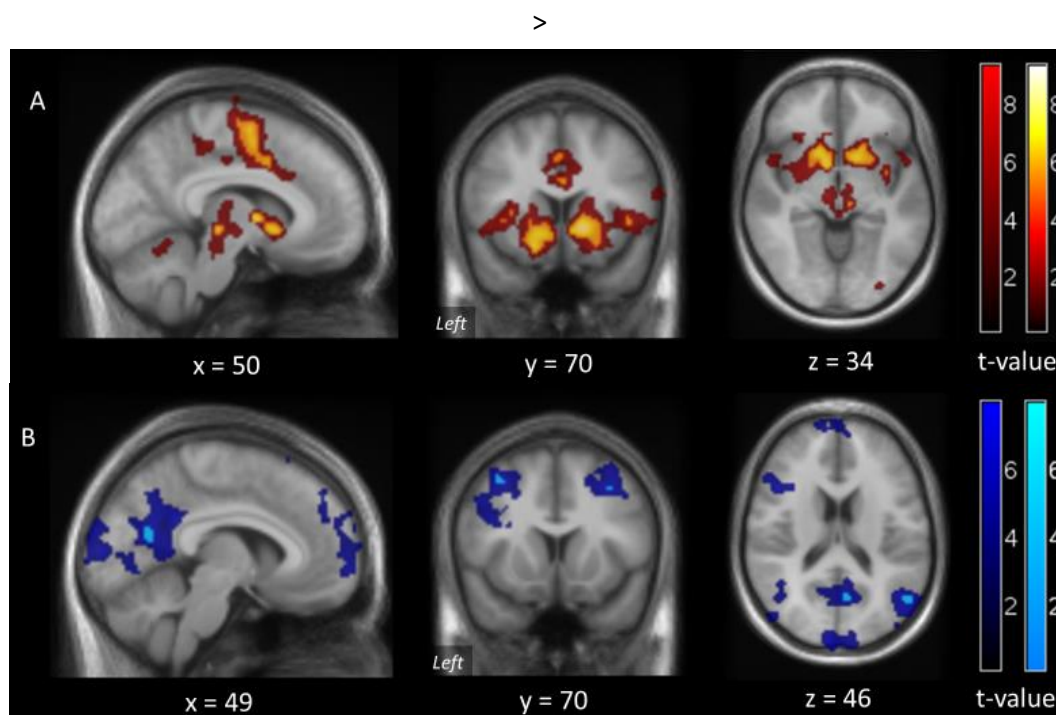


**Figure 24. Task effects of early RA in patients with MDD. (A)** Task-positive effects. Statistical maps shown in red were sampled at uncorrected  $p_{\text{voxel}} < 0.001$ . Yellow clusters show voxel-wise FWE-robust effects ( $p_{\text{voxel.FWE}} < 0.05$ ,  $k > 10$ ). **(B)** Task-negative effects. Blue shows significant clusters sampled at uncorrected  $p_{\text{voxel}} < 0.001$  and thresholded at a  $p_{\text{cluster.FWE}} < 0.05$ . Voxel-wise FWE-robust ( $p_{\text{voxel.FWE}} < 0.05$ ,  $k > 10$ ) effects are overlaid in light blue.

Next, we investigated the late RA phase in MDD: During the late phase of RA, 20 task-positive clusters of BOLD activation were observed at a threshold of  $p_{\text{voxel.FWE}} < 0.05$  ( $k > 10$ ). Increased activation was found in the bilateral anterior insula and rolandic operculum (whereby the right cluster is reached to the STG), dACC, bilateral putamen/striate area, occipital lobe as well as the cerebellum. The reverse contrast ‘ $\text{money}_{\text{late}} < \text{csm}_{\text{late}}$ ’ revealed seven deactivation clusters at  $p_{\text{voxel.FWE}} < 0.05$  ( $k > 10$ ), localizing to the posterior cingulate gyrus and precuneus, inferior parietal as well as temporal regions. The following **Table 22** lists cluster details of task effects in patients with MDD. Statistical maps are displayed in **Figure 25**.



**Table 22. Task-positive and task-negative effects of late RA in MDD ( $p_{\text{voxel.FWE}} < 0.05$ ;  $k > 10$ ).**

Result cluster #	Anatomical cluster location <sup>a</sup>	Cluster size in voxels	Peak voxel coordinates <sup>b</sup>
<i>Task-positive effects</i>			
1	L putamen, rolandic operculum, insula, IFG (pars opercularis)	1281	-30 18 8
2	R putamen, IFG (pars triangularis), middle frontal gyrus, precentral gyrus, insula, rolandic operculum	2301	48 16 -8
3	L medial superior frontal gyrus, paracentral lobule R middle cingulate gyrus, SMA	2782	6 10 44
4	R lingual gyrus, thalamus	1414	8 -28 -6
5	L inferior parietal lobule, postcentral gyrus	992	-40 -24 48
6	R temporal inferior, fusiform gyrus, inferior occipital gyrus, cerebellum	1157	30 -52 -24
7	R STG, middle temporal gyrus, supramarginal gyrus	591	62 -40 24
8	R lingual gyrus	160	4 -76 -16
9	L STG, supramarginal gyrus, postcentral gyrus	114	-54 -20 18
10	L inferior occipital gyrus	94	-34 -90 6
11	L STG	173	-46 -42 24
12	R cerebellum	20	8 -56 -10
13	L inferior parietal lobule	33	-28 -44 48
14	L cerebellum	124	-28 -66 -22
15	L inferior temporal gyrus, fusiform gyrus	47	-42 -62 -12
16	L/R cerebellum	17	4 -68 -34
17	L precentral gyrus	48	-48 2 32
18	R middle temporal gyrus	12	48 -24 -10
19	L IFG (pars opercularis), precentral gyrus	15	-40 2 22
20	L postcentral gyrus	14	-24 -28 76
<i>Task-negative effects</i>			
1	R precuneus, PCC L/R calcarine fissure	1050	6 -58 32

2	<i>R</i> angular gyrus, middle temporal gyrus, middle occipital gyrus	564	48 -68 26
3	<i>L</i> inferior parietal lobule, middle temporal gyrus, middle occipital gyrus	458	-42 -76 32
4	<i>L</i> middle frontal gyrus	479	-20 14 54
5	<i>R</i> middle frontal gyrus	156	28 18 50
6	<i>L</i> middle temporal gyrus, angular gyrus	14	-40 -60 22
7	<i>L</i> superior parietal gyrus, superior occipital gyrus	10	-12 -82 50

<sup>a</sup>Result clusters were mapped with the AAL toolbox.

<sup>b</sup>Peak voxel coordinates are given in MNI space.

*L* and *R* denote left and right hemispheric location; *L/R* denotes bilateral location. IFG, inferior frontal gyrus; SMA, supplemental motor area; STG, superior temporal gyrus; PCC, posterior cingulate cortex.

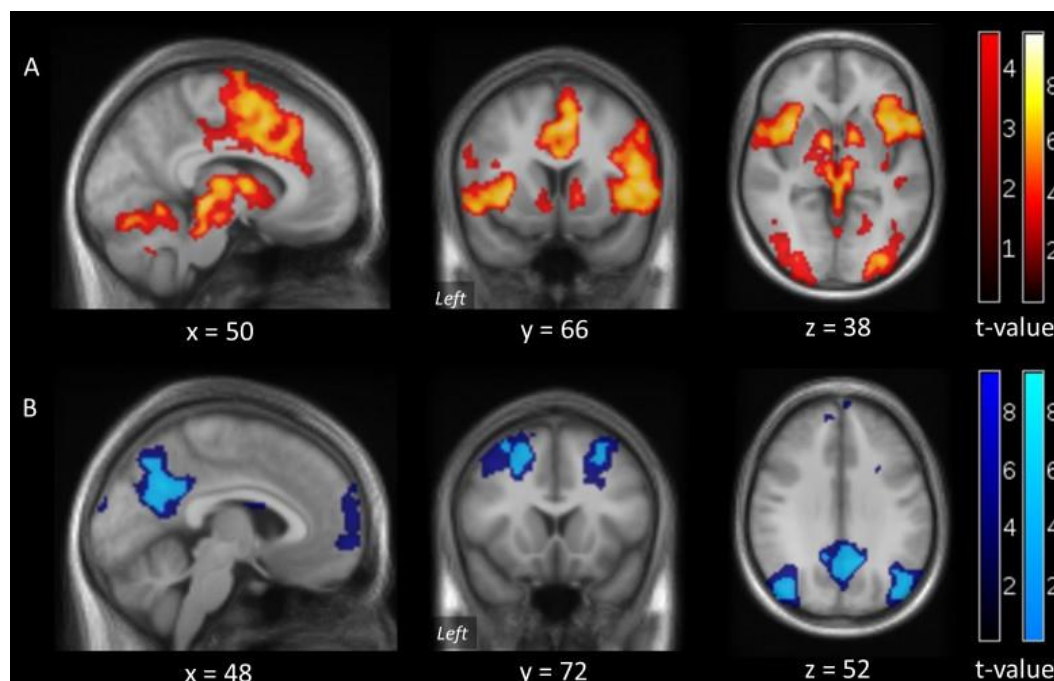


**Figure 25. Task effects of late RA in patients with MDD. (A)** Task-positive effects. Statistical maps shown in red were sampled at uncorrected  $p < 0.001$  and clusters were thresholded at a  $p_{\text{cluster.FWE}} < 0.05$ . Yellow clusters show voxel-wise FWE-robust effects ( $p_{\text{voxel.FWE}} < 0.05$ ,  $k > 10$ ). **(B)** Task-negative effects. Dark blue shows significant clusters collected at  $p < 0.001$  and thresholded at  $p_{\text{cluster.FWE}} < 0.05$  and FWE-robust voxels are overlaid in light blue.

### BD

In patients with BD (N=13), the contrast ‘money > csm’ revealed 11 significant clusters at  $p_{\text{voxel.FWE}} < 0.05$  (see **Table 23**). During monetary reward trials, stronger activation was observed in the insular-temporal area, cingulate cortex and SMA. The reverse contrast yielded two clusters at  $p_{\text{voxel.FWE}} < 0.05$ , located in the precuneus and the right parietal lobe. A visualisation of RA effects in BD is given in **Figure 26**.

**Table 23. Task-positive and negative effects of RA in BD ( $p_{\text{voxel.FWE}} < 0.05$ ;  $k > 10$ ).**

Result cluster #	Anatomical cluster location <sup>a</sup>	Cluster size in voxels	Peak voxel coordinates <sup>b</sup>
<i>Task-positive effects</i>			
1	R rolandic operculum, IFG (pars opercularis)	70	58 10 20
2	R IFG (pars triangularis/opercularis)	147	58 10 4
3	L insula	70	-28 22 4
4	L/R midcingulate cortex, SMA	22	4 10 44
5	R midcingulate cortex	24	8 20 34
6	L insula	17	-40 0 6
7	R insula	46	32 22 0
8	L ACC	30	-8 22 30
9	L insula	11	-38 12 -6
11	R insula	23	40 4 0
<i>Task-negative effects</i>			
1	L/R precuneus	32	6 -62 28
2	R angular gyrus	11	40 -60 24

<sup>a</sup>Result clusters were mapped with the AAL toolbox.

<sup>b</sup>Peak voxel coordinates are given in MNI space.

L and R denote left and right hemispheric location; L/R denotes bilateral location. IFG, inferior frontal gyrus; SMA, supplemental motor area; ACC, anterior cingulate cortex.

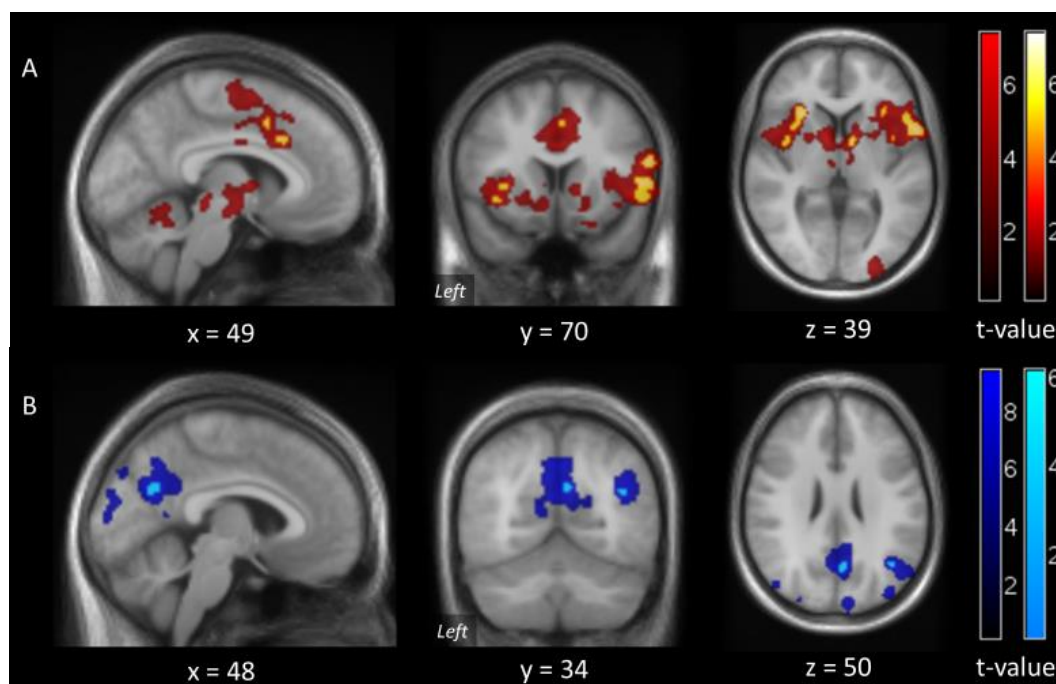


**Figure 26. Task effects of RA in patients with BD. (A)** Task-positive effects. Red clusters were sampled at uncorrected  $p < 0.001$  and thresholded at a cluster-wise  $p_{\text{cluster.FWE}} < 0.05$ . Yellow clusters represent voxel-wise FWE-robust effects ( $p_{\text{voxel.FWE}} < 0.05$ ,  $k > 10$ ). **(B)** Task-negative effects. Dark blue shows significant clusters sampled at uncorrected  $p < 0.001$  and thresholded at a cluster-wise  $p_{\text{cluster.FWE}} < 0.05$ . Voxel-wise FWE-robust ( $p_{\text{voxel.FWE}} < 0.05$ ,  $k > 10$ ) effects are shown in light blue.

In early RA, neither the contrast ‘ $\text{money}_{\text{early}} > \text{csm}_{\text{early}}$ ’ nor the reverse contrast yielded any significant voxels at  $p_{\text{voxel.FWE}} < 0.05$  in patients diagnosed with BD. Nevertheless, typical task-positive striatal and dACC activation patterns could be retrieved at a more lenient threshold ( $p_{\text{voxel.FWE}} < 0.001$ ) still correcting for multiple testing at the cluster level ( $p_{\text{cluster.FWE}} < 0.05$ ). In parallel, the reverse contrast ‘ $\text{money}_{\text{early}} < \text{csm}_{\text{early}}$ ’ also revealed deactivation in regions similar to those of healthy subjects. Statistical maps for task-positive and task-negative effects in BD are visualized in **Figure 27** below.

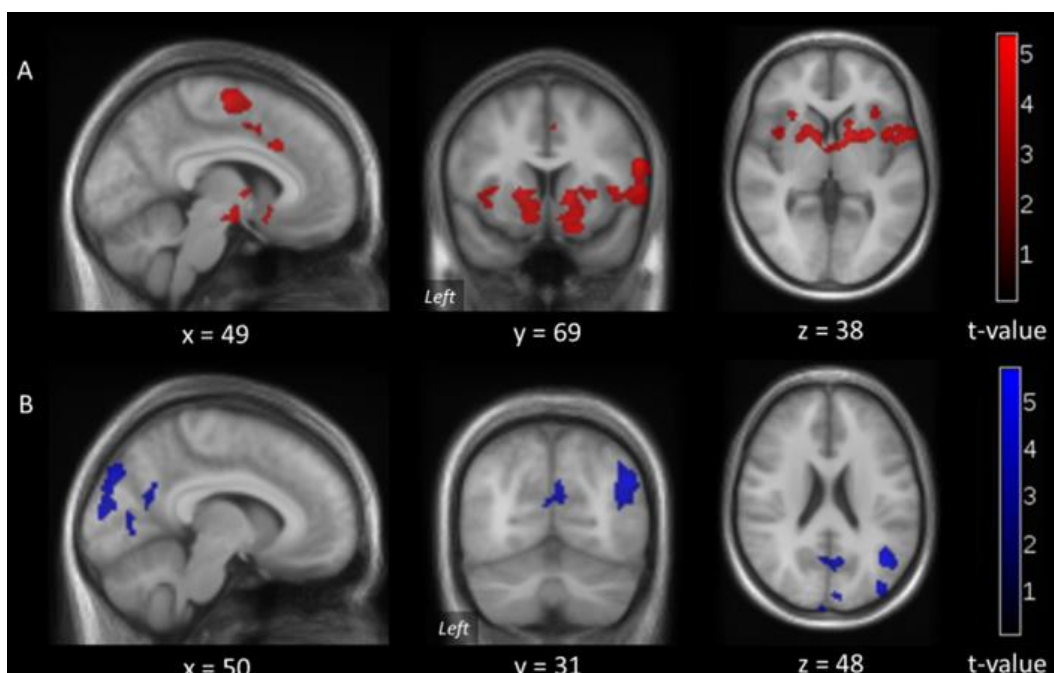


**Figure 27. Task effects of early RA in patients with BD.** Both statistical maps were sampled at uncorrected  $p < 0.001$  and thresholded at a cluster-wise  $p_{\text{cluster.FWE}} < 0.05$  ( $k > 10$ ). **(A)** Task-positive effects. **(B)** Task-negative effects. Effects are likely weaker due to the lower N of patients in the BD group.

The late phase analyses identified 11 task-positive clusters at  $p_{\text{voxel.FWE}} < 0.05$  ( $k > 10$ ) in patients with BD, localizing to bilateral fronto-insular regions, dACC and right cerebellum. The reverse contrast ‘money<sub>late</sub> < csm<sub>late</sub>’ yielded one cluster in the precuneus. Cluster details of both contrasts are listed in **Table 24** and statistical maps are visualized in **Figure 28** below.

**Table 24. Task-positive and negative effects of late RA in BD ( $p_{\text{voxel.FWE}} < 0.05$ ;  $k > 10$ ).**

Result cluster #	Anatomical cluster location <sup>a</sup>	Cluster size in voxels	Peak voxel coordinates <sup>b</sup>
<i>Task-positive effects</i>			
1	R IFG (pars triangularis), insula, superior temporal pole	317	56 12 6
2	L insula	172	-28 22 4
3	L medial superior frontal gyrus R SMA	100	4 10 44
4	L cerebellum	57	30 -54 -22
5	R IFG (pars triangularis/orbitalis)	94	32 20 -4
6	L insula	12	-40 -2 6
7	R supramarginal gyrus	19	58 -22 24
8	R insula	16	38 2 2
9	R midcingulate cortex	20	8 20 34
10	R cerebellum	17	16 -54 -18
11	L/R midcingulate cortex	18	2 -8 -40
<i>Task-negative effects</i>			
1	R/L precuneus	19	6 -62 28

<sup>a</sup>Result clusters were mapped with the AAL toolbox.

<sup>b</sup>Peak voxel coordinates are given in MNI space.

L and R denote left and right hemispheric location; L/R denotes bilateral location. IFG, inferior frontal gyrus; SMA, supplemental motor area.

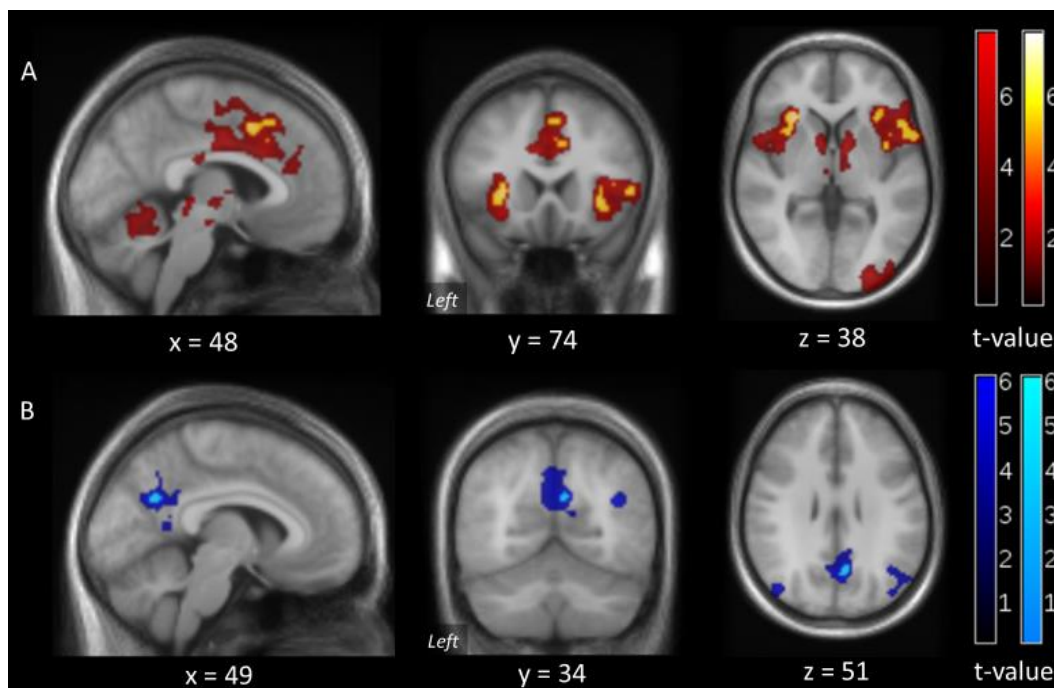


**Figure 28. Task effects of late RA in patients with BD. (A)** Task-positive effects. Statistical maps shown in red were sampled at uncorrected  $p < 0.001$  and clusters were thresholded at a cluster-wise  $p_{\text{cluster.FWE}} < 0.05$ . Yellow clusters show voxel-wise FWE-robust effects ( $p_{\text{voxel.FWE}} < 0.05$ ,  $k > 10$ ). **(B)** Task-negative effects. Dark blue clusters were sampled at uncorrected  $p < 0.001$  and thresholded at a cluster-wise  $p_{\text{cluster.FWE}} < 0.05$ . Bright blue clusters show voxel-wise FWE-robust effects ( $p_{\text{voxel.FWE}} < 0.05$ ,  $k > 10$ ).

### SCZ

In patients diagnosed with SCZ (N=27), the contrast ‘money > csm’ yielded six clusters at  $p_{\text{voxel.FWE}} < 0.05$ , localizing to bilateral midcingulate cortex/SMA, cerebellum and both central gyri. The reverse contrast ‘money < csm’ revealed a right-sided pattern of decreased activation in the parahippocampus. Statistical maps of both contrasts are detailed and visualized below.

**Table 25. Task-positive and -negative effects of RA in SCZ ( $p_{\text{voxel.FWE}} < 0.05$ ;  $k > 10$ ).**

Result cluster #	Anatomical cluster location <sup>a</sup>	Cluster size in voxels	Peak voxel coordinates <sup>b</sup>
<i>Task-positive effects</i>			
1	R midcingulate cortex	116	8 2 52
2	L midcingulate cortex	119	-4 -6 50
3	R cerebellum	29	38 -48 -36
4	L inferior parietal lobe, supramarginal gyrus	93	-48 -28 42
5	L precentral gyrus	19	-30 -10 54
6	L pre-/postcentral gyrus	14	-42 -12 50
<i>Task-negative effects</i>			
1	R parahippocampus	10	22 -18 -24

<sup>a</sup>Result clusters were mapped with the AAL toolbox.

<sup>b</sup>Peak voxel coordinates are given in MNI space.

L and R denote left and right hemispheric location.

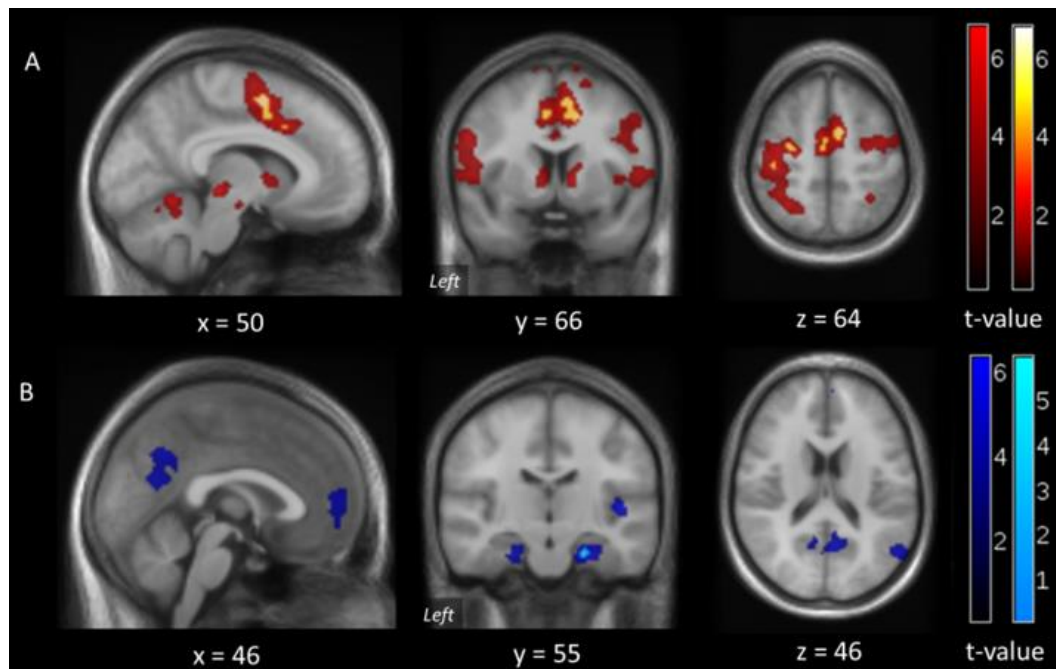


**Figure 29. Task effects of RA in patients with SCZ. (A) Task-positive effects.** Statistical maps shown in red were sampled at uncorrected  $p_{\text{voxel}} < 0.001$  and clusters were thresholded at a cluster-wise  $p_{\text{cluster.FWE}} < 0.05$ . Clusters in hot colours show voxel-wise FWE-robust effects ( $p_{\text{voxel.FWE}} < 0.05$ ,  $k > 10$ ). Note comparatively weak VS effects. **(B) Task-negative effects.** Blue shows significant clusters sampled at uncorrected  $p_{\text{voxel}} < 0.001$  and thresholded at a cluster-wise  $p_{\text{cluster.FWE}} < 0.05$ . Voxel-wise FWE-robust ( $p_{\text{voxel.FWE}} < 0.05$ ,  $k > 10$ ) effects are shown in light blue.



During the early phase of RA, three clusters of increased BOLD activity were observed in patients with SCZ. Activation was localized to the left precentral gyrus, dACC and bilateral SMA as well as the right cerebellum. The complete lack of the VS response was noted. The reverse contrast ('money<sub>early</sub> < csm<sub>early</sub>') revealed one cluster in the precuneus at the threshold of  $p_{\text{voxel.FWE}} < 0.05$ . **Table 26** displays cluster details of task effects during early RA in SCZ, whereas statistical maps are shown in **Figures 30**.

**Table 26. Task-positive and -negative effects of early RA in SCZ ( $p_{\text{voxel.FWE}} < 0.05$ ;  $k > 10$ ).**

Result cluster #	Anatomical cluster location <sup>a</sup>	Cluster size in voxels	Peak voxel coordinates <sup>b</sup>
<i>Task-positive effects</i>			
1	<i>L</i> precentral gyrus	40	-28 -12 54
2	<i>L</i> SMA, midcingulate cortex	199	-12 -10 64
3	<i>R</i> cerebellum	11	38 -50 -36
<i>Task-negative effects</i>			
1	<i>R</i> precuneus, lingual gyrus, calcarine fissure	15	14 -52 8

<sup>a</sup>Result clusters were mapped with the AAL toolbox.

<sup>b</sup>Peak voxel coordinates are given in MNI space.

*L* and *R* denote left and right hemispheric location. SMA, supplemental motor area.

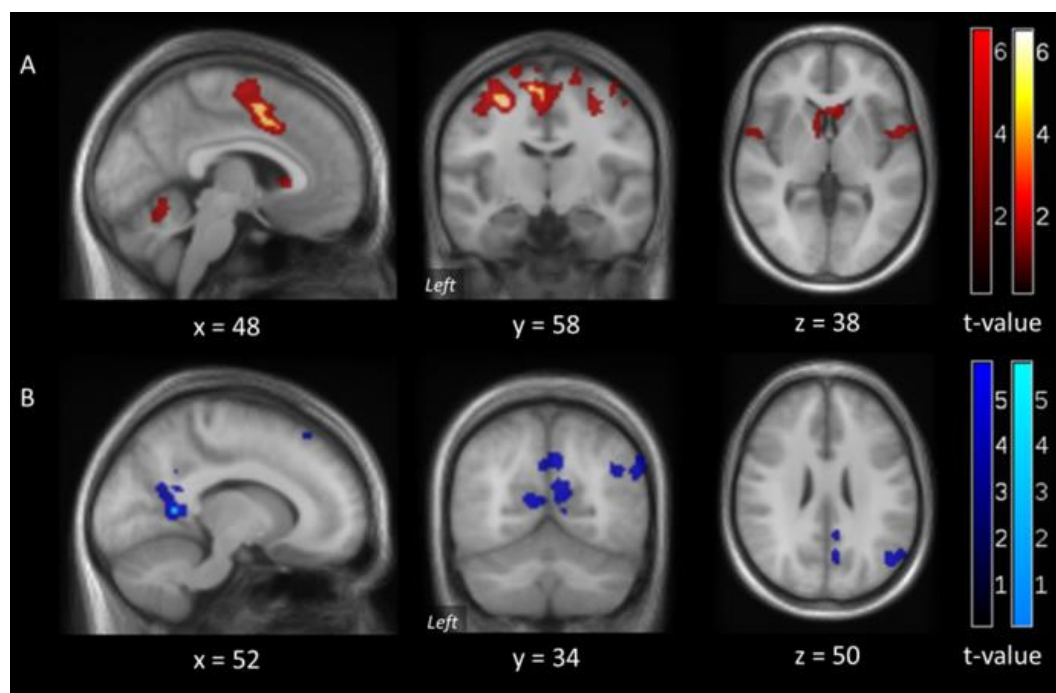


**Figure 30. Task effects of early RA in patients with SCZ. (A)** Task-positive effects. Statistical maps shown in red were sampled at uncorrected  $p_{\text{voxel}} < 0.001$  and clusters were thresholded at a cluster-wise  $p_{\text{cluster.FWE}} < 0.05$ . Voxel-wise FWE-robust clusters are shown in yellow. **(B)** Task-negative effects. Statistical maps shown in darker blue were sampled at uncorrected  $p_{\text{voxel}} < 0.001$  and clusters were thresholded at a cluster-wise  $p_{\text{cluster.FWE}} < 0.05$ . The cluster displayed in brighter blue shows voxel-wise FWE-robust effects.

In the late RA phase analysis, task effects were found in 18 clusters  $p_{\text{voxel.FWE}} < 0.05$  ( $k > 10$ ). Activation during the late RA phase was observed in the occipital lobe, cerebellum, dACC and the posterior frontal lobe. The reverse contrast revealed no significant clusters surviving a threshold of  $p_{\text{voxel.FWE}} < 0.05$ . Cluster details and visualization can be found in **Table 27** and **Figure 31** below. VS activation was only found at the more lenient threshold (**Figure 31**, red), but not at the voxel-wise FWE threshold that underlies the cluster in **Table 27**.

**Table 27. Task-positive effects of late RA in SCZ ( $p_{\text{voxel.FWE}} < 0.05$ ;  $k > 10$ ).**

Result cluster #	Anatomical cluster location <sup>a</sup>	Cluster size in voxels	Peak voxel coordinates <sup>b</sup>
<i>Task-positive effects</i>			
1	<i>L</i> middle/superior occipital gyrus	146	-24 -76 22
2	<i>R</i> fusiform gyrus	143	30 -74 -10
3	<i>R</i> cerebellum	143	34 -46 -22
4	<i>R</i> rolandic operculum	31	56 10 6
5	<i>L</i> inferior parietal lobule, supramarginal gyrus	152	-48 -28 42
6	<i>R</i> IFG (pars opercularis)	38	44 4 30
7	<i>L</i> cerebellum	50	-32 -68 -18
8	<i>L</i> inferior parietal lobule	86	-26 -56 44
9	<i>L</i> insula, rolandic operculum	12	-40 -4 16
10	<i>L</i> postcentral gyrus	24	-40 -12 46
11	<i>R</i> precentral gyrus	26	40 0 42
12	<i>L</i> insula	20	-28 20 4
13	<i>L</i> middle cingulate gyrus, SMA	14	-4 -6 50
14	<i>L</i> superior temporal gyrus, supramarginal gyrus, rolandic operculum	17	-52 -26 16
15	<i>R</i> SMA	37	8 2 52
16	<i>R</i> superior/middle occipital gyrus	21	30 -76 14
17	<i>R</i> fusiform gyrus, inferior/middle occipital gyrus	10	24 -82 -2
18	<i>R</i> inferior parietal lobule	14	32 -48 52
<i>Task-negative effects</i>			
*		-	-

<sup>a</sup>Result clusters were mapped with the AAL toolbox.

<sup>b</sup>Peak voxel coordinates are given in MNI space.

*L* and *R* denote left and right hemispheric location. IFG, inferior temporal gyrus; SMA, supplemental motor area.

\*No deactivation clusters at the strict voxel-wise threshold; clusters at a more lenient  $p_{\text{voxel}} < 0.001$  are shown in Figure 31.

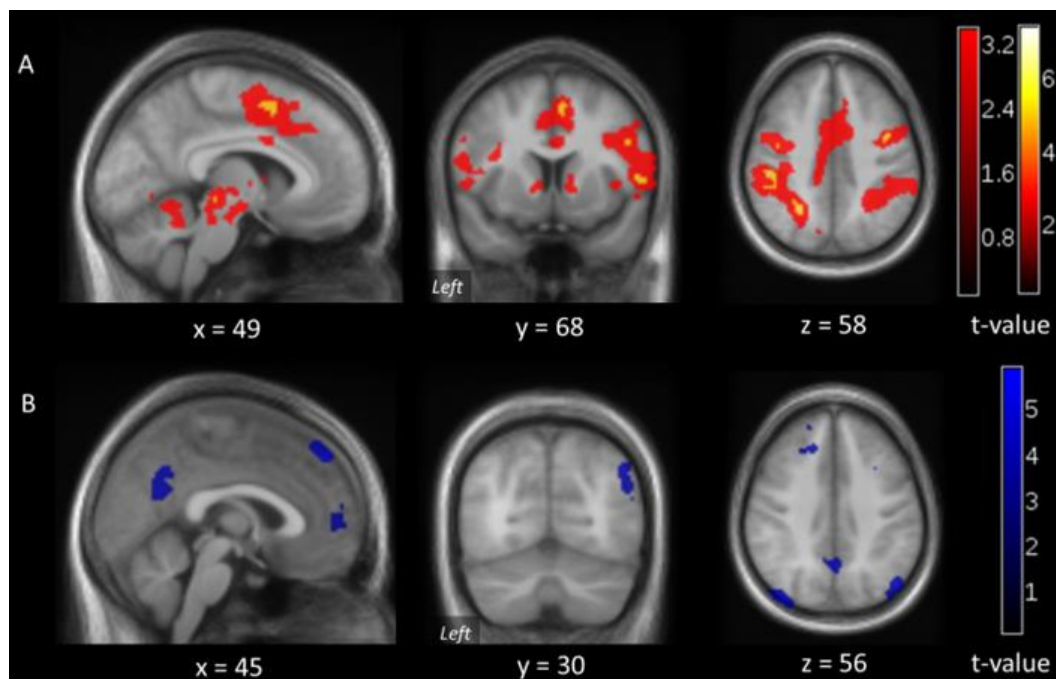


**Figure 31. Task effects of late RA in SCZ. (A)** Task-positive effects. Red shows significant clusters at  $p_{\text{voxel}} < 0.001$  and thresholded at a cluster-wise  $p_{\text{cluster.FWE}} < 0.05$  ( $k > 10$ ), whereas FWE-robust voxels are shown in yellow. **(B)** Task-negative effects. Statistical maps shown in dark blue were sampled at uncorrected  $p_{\text{voxel}} < 0.001$  and clusters were thresholded at a cluster-wise  $p_{\text{cluster.FWE}} < 0.05$ .

*Panoramic overview of main effects of RA in different groups*

For an overview, the following **Figure 32** aims to provide a brief depiction of main RA effects in all diagnostic groups. While the slices in the previous figures (Chapter 3.3.1) were selected based on the effects of the respective group, here they are all in the same slice in order to enhance visual comparability.

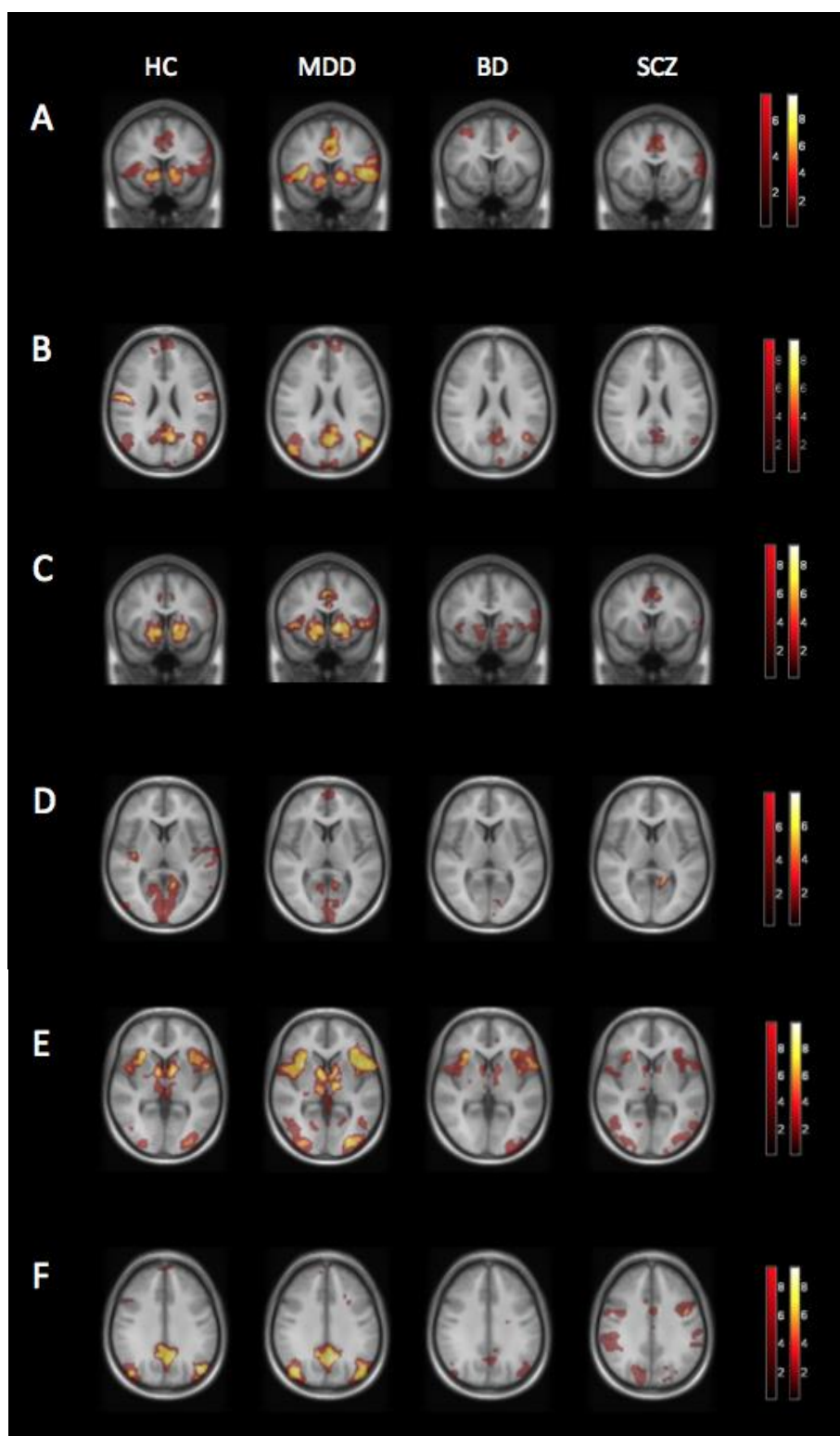


**Figure 32. Panoramic overview of RA task effects per diagnostic group.** The slice numbers on the respective axis in MNI space are indicated in brackets. All effects refer to the model not differentiating between early and late RA. **(A)** Task-positive effects ( $y = 70$ ). **(B)** Task-negative effects ( $z = 49$ ). **(C)** Task-positive effects during early RA ( $y = 69$ ). **(D)** Task-negative effects during early RA ( $z = 40$ ). **(E)** Task-positive effects during late RA ( $z = 38$ ). **(F)** Task-negative effects during RA ( $z = 53$ ). As in the figures before, the darker colours refer to significant clusters ( $p_{\text{voxel}} < 0.001$ ,  $p_{\text{cluster.FWE}} < 0.05$ ) and the lighter/hot colour refers to family-wise corrected voxels.

### Pairwise differences between diagnostic groups

After proof-of-concept interrogation of RA task effects in each diagnostic group, the core question of this study – differences in the effects of RA on BOLD activation between diagnostic groups – was approached. Again, we first analysed the GLM with 6 s of stimulus presentation as the RA phase in line with the original studies using the MID task based on Knutson et al. (2001). Subsequently, we investigated group differences separately for the early and late RA phase.

#### *Overall group differences in RA using 6 s of stimulus presentation*

A differential, undirected F-test comparing effects of RA across four diagnostic groups revealed two significant whole-brain-corrected clusters sampled at uncorrected  $p_{\text{voxel}} < 0.005$  and corrected at the cluster level ( $p_{\text{cluster.FWE}} < 0.05$ ), localizing to the left striate area (partly extending to the insula) (cluster #1) as well as left precentral/postcentral gyri and rolandic operculum (cluster #2). The anatomical location of peak voxels and the corresponding  $p$ -values are given in **Table 28**. Additionally, one trend cluster (cluster #3) was found in the right precentral/postcentral gyri area. Contrast plots of peak voxel parameter estimates (**Figure 33B**) allowed further qualitative observations: (i) For the left ventral striatal cluster, patients with SCZ yielded very low to negative values and BP patients showed relatively high values; (ii) in the parietal cluster, all patients groups showed no clear deactivation which was different from HC.

**Table 28. F-contrast of RA between diagnostic groups ( $p_{\text{voxel}} < 0.005$ ,  $p_{\text{cluster.FWE}} < 0.1$ ).**

Result cluster #	Anatomical cluster location <sup>a</sup>	Cluster size in voxels	FWE corrected cluster p-value	Peak voxel coordinates <sup>b</sup>
1	<i>L</i> pallidum, caudate, IFG (pars opercularis), putamen	334	0.001	-32 6 -6
2	<i>L</i> precentral gyrus	187	0.032	-60 -4 20
3	<i>R</i> precentral/postcentral gyrus	159	0.072	42 -10 28

<sup>a</sup>Result clusters were mapped with the AAL toolbox.

<sup>b</sup>Peak voxel coordinates are given in MNI space.

L and R denote left and right hemispheric location. IFG, inferior frontal gyrus.

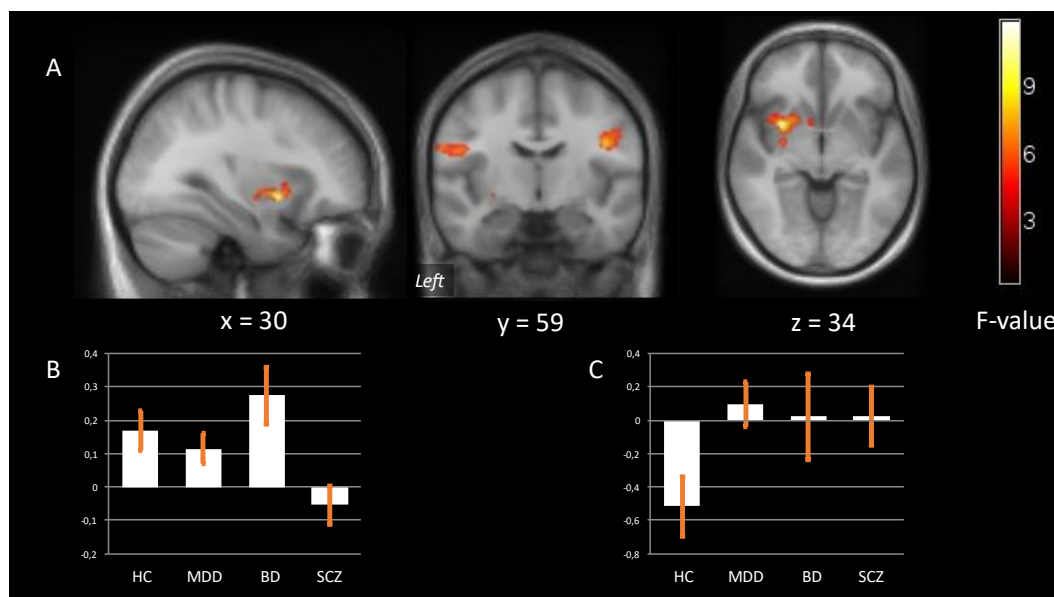


**Figure 33. F-contrast of RA effects. (A)** Sagittal, coronal, and axial projections on the group template illustrating of whole-brain significant and trend clusters in which BOLD-signals differed across all four groups (undirected F-test;  $p_{cluster.FWE} < .10$ ; collection threshold  $p < 0.005$ ). **(B & C)** Graph bars represent contrast estimates for peak voxels of these clusters. **(B)** displays contrast estimates for the cluster in the ventral striate. **(C)** shows contrast estimates for the left-sided parietal cluster.

Next, differences in BOLD activity between the groups were explored through directed T-tests. Overall, 5 (out of 6) individual comparisons of the three patient groups with HC revealed 7 significant results (see **Table 29**): In summary, patients with MDD showed two clusters of more activation (or less deactivation) in bilateral insular-temporal areas (clusters #1 and #2); BD show a blunted BOLD responses in the left posterior parietal cortex (cluster #3) and two clusters of abnormally strong activation in the ACC extending to the mPFC (cluster #4) and the IFG extending to the insula (cluster #5); SCZ showed less activation in the putamen/striate area reaching to the insula/IFG (cluster #6) while the reverse contrast yielded one cluster of higher activation in the occipital gyrus (cluster #8). Additionally, a trend-reduced activation in SCZ was found in the PCC/thalamus/hippocampus (cluster #7). Anatomical locations and corresponding  $p$ -values are listed in **Table 29**. Statistical maps of post-hoc comparisons are visualized in **Figures 34-36**.

**Table 29. Regions showing group differences in RA in directed T-contrasts ( $p_{\text{voxel}} < 0.005$ ;  $p_{\text{cluster.FWE}} < 0.05$ ).**

Result cluster #	Anatomical cluster location <sup>a</sup>	Cluster size in voxels	FWE corrected cluster p-value	Peak voxel coordinates <sup>b</sup>
<i>MDD &gt; HC (see Figure 34)</i>				
1	R supramarginal gyrus, precentral gyrus, insula, superior temporal pole	802	< 0.001	58 -10 18
2	L superior temporal pole, supramarginal gyrus, precentral gyrus, postcentral gyrus, STG, insula	1938	< 0.001	-48 -30 6
<i>BD &lt; HC (see Figure 35)</i>				
3	L precuneus, superior parietal gyrus, postcentral gyrus	291	0.030	-26 -52 66
<i>BD &gt; HC (see Figure 35)</i>				
4	R middle/anterior cingulate gyrus, medial frontal gyrus (pars orbitalis) L olfactory cortex	478	0.001	52 32 -6
5	R IFG (pars orbitalis/triangularis), rolandic operculum, insula	374	0.007	52 32 -6
<i>SCZ &lt; HC (see Figure 36)</i>				
6	L pallidum, SFG (pars orbitalis), putamen	466	0.002	-30 6 -6
7	L posterior cingulum R hippocampus	229	0.090	10 -36 12
<i>SCZ &gt; HC (see Figure 36)</i>				
8	L middle/superior occipital gyrus	389	0.006	-22 -88 28

<sup>a</sup>Result clusters were mapped with the AAL toolbox.

<sup>b</sup>Peak voxel coordinates are given in MNI space.

L and R denote left and right hemispheric location. STG, superior temporal gyrus; IFG, inferior frontal gyrus; SFG, superior frontal gyrus.



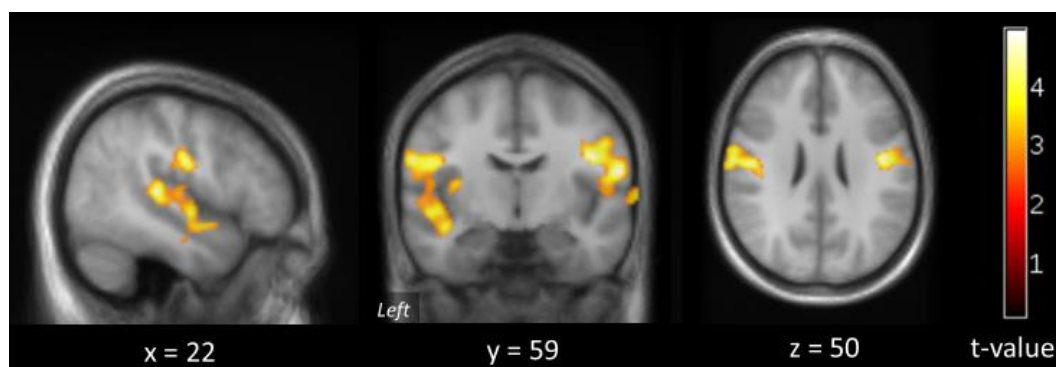


**Figure 34. Group differences in RA (6 s of stimulus presentation) between MDD and HC.** Results for the contrast ‘money > csm’ (thresholded at  $p_{\text{voxel}} < 0.005$ ;  $p_{\text{cluster.FWE}} < 0.05$ ). As noted above, MDD patients showed significantly stronger activation (or less deactivation) in a bilateral insular-temporal region throughout the whole 6 s of stimulus presentation. While both clusters likewise include areas like the rolandic operculum, insula, supra-marginal gyrus, STG, the left-sided cluster extended also to the left thalamus.

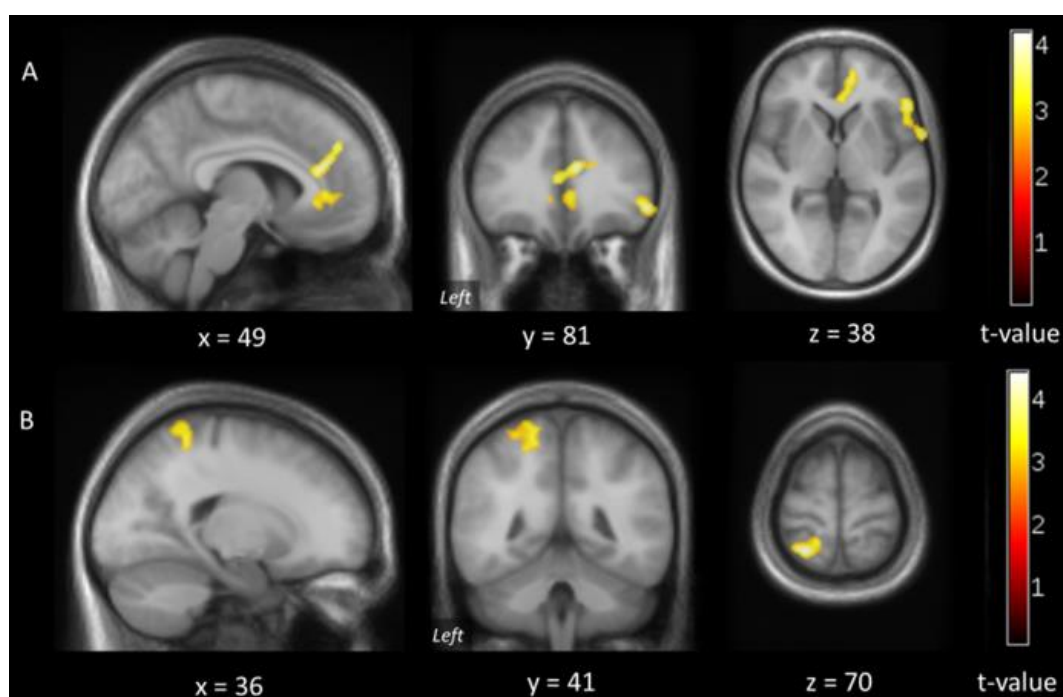


**Figure 35. Group differences in RA (6 s of stimulus presentation) between BD and HC.** Results for the contrast ‘money > csm’ (thresholded at  $p_{\text{voxel}} < 0.005$ ;  $p_{\text{cluster.FWE}} < 0.05$ ). **(A)** Regions in which BD show significantly more activation. Stronger BOLD response was observed in ACC reaching to the mPFC and a second cluster including IFG, insula, rolandic operculum and STG. **(B)** Regions in which BD show significantly less BOLD activation. BD showed one cluster of reduced activation in the left precuneus, superior parietal lobule and postcentral gyrus.

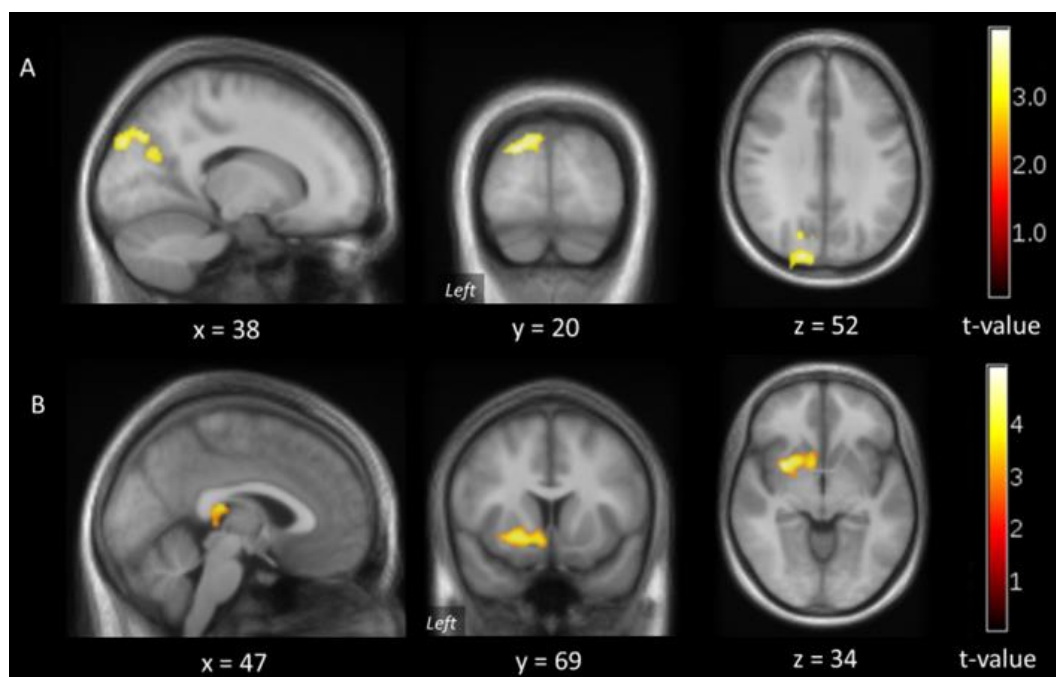


**Figure 36. Group differences in RA (6 s of stimulus presentation) between SCZ and HC.** Results for the contrast ‘money > csm’ (thresholded at  $p_{\text{voxel}} < 0.005$ ;  $p_{\text{cluster.FWE}} < 0.05$ ). **(A)** Regions in which SCZ show significantly more activation. Compared to HC, patients with SCZ showed one cluster of higher activation mainly localizing to the superior occipital gyrus, extending to the cuneus and precuneus. **(B)** Regions in which SCZ show significantly less activation. Here, the larger cluster is localized to the left pallidum and putamen, also reaching to the SFG, caudate, insula and IFG. A smaller trend cluster was localized to the thalamus and right posterior hippocampus.

### Group differences in early RA

When early RA task effects of the four groups were compared using an undirected F-test, one significant whole-brain-corrected cluster ( $p_{\text{voxel}} < 0.005$ ,  $p_{\text{cluster.FWE}} < 0.05$ ) in the left-sided striatal area (pallidum, insula, putamen, caudate) emerged (**Table 30 & Figure 37**).

**Table 30. F-contrast of early RA between diagnostic groups ( $p_{\text{voxel}} < 0.005$ ,  $p_{\text{cluster.FWE}} < 0.05$ ).**

Result cluster #	Anatomical cluster location <sup>a</sup>	Cluster size in voxels	FWE corrected cluster p-value	Peak voxel coordinates <sup>b</sup>
1	L pallidum, insula	437	< 0.001	-24 -4 -4

<sup>a</sup>Result clusters were mapped with the AAL toolbox.

<sup>b</sup>Peak voxel coordinates are given in MNI space.

L denotes left hemispheric location.

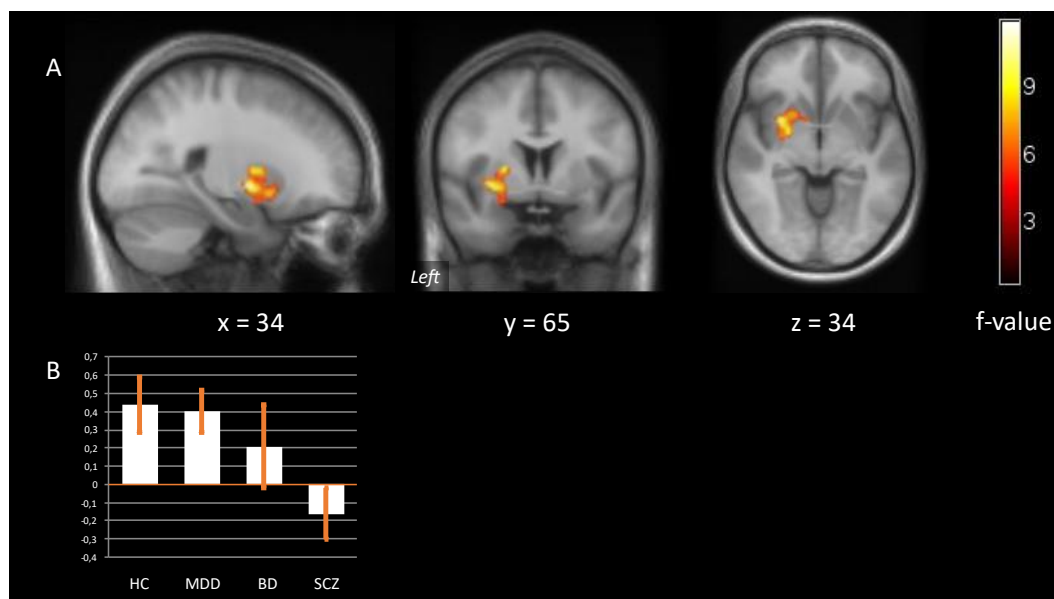


**Figure 37. F-contrast of early RA effects. (A)** One significant cluster with significant group effect during early RA localizing to the left striatal area. **(B)** Contrast bars demonstrate a stepwise pattern of cluster values with highest response in HC, nearly normal position of MDD, intermediate position of BD and weakest response in SCZ.

When exploring specific differences between diagnostic groups and HC during the early RA phase through T-contrasts, only patients with SCZ showed two significant clusters of less activation bilaterally in the striate area (cluster #2 and #3). Cluster details are listed in **Table 31** and visualized in **Figure 38**. One trend-significant cluster of was found in the parietal lobule where patients with BD showed less activation compared to HC.

**Table 31. T-contrasts of early RA effects between patient groups and HC ( $p_{\text{voxel}} < 0.005$ ;  $p_{\text{cluster.FWE}} < 0.05$ ).**

Result cluster #	Anatomical cluster location <sup>a</sup>	Cluster size in voxels	FWE corrected cluster p-value	Peak voxel coordinates <sup>b</sup>
<i>BD &lt; HC</i>				
1	<i>L</i> precuneus, postcentral gyrus, superior parietal gyrus	216	0.091	-24 -50 66
<i>SCZ &lt; HC (Figure 38)</i>				
2	<i>L</i> pallidum, superior frontal gyrus (pars orbitalis), putamen	672	< 0.001	-24 -2 -4
3	<i>R</i> pallidum, SFG (pars orbitalis), putamen	400	0.003	18 12 -6

<sup>a</sup>Result clusters were mapped with the AAL toolbox.

<sup>b</sup>Peak voxel coordinates are given in MNI space.

*L* and *R* denote left and right hemispheric location. SFG, superior frontal gyrus.

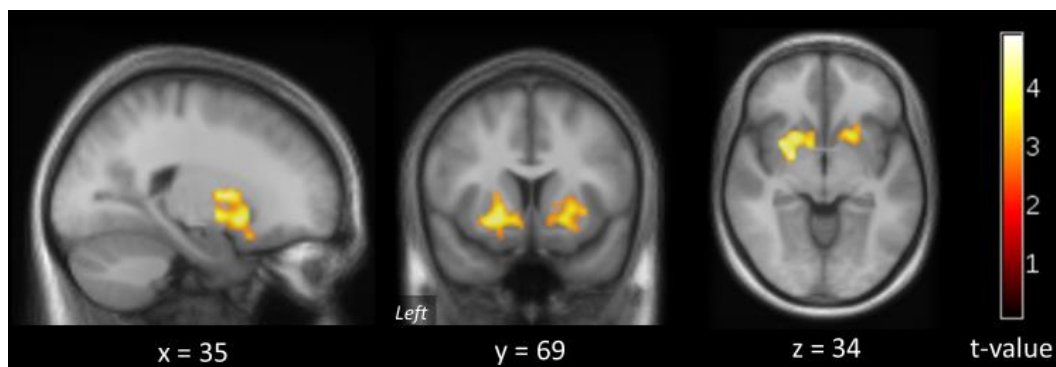


**Figure 38. Group differences in early RA between SCZ and HC.** Results for the contrast ‘money > csm’ (thresholded at  $p_{\text{voxel}} < 0.005$ ;  $p_{\text{cluster.FWE}} < 0.05$ ). Compared to HC, patients with SCZ exhibit less activation in bilateral VS regions, including putamen and pallidum.

### *Group differences in late RA*

Between-group differences in the explorative F-contrast during late RA were found in one cluster in the visual cortex and cuneus. Anatomical details can be found in **Table 32** and results are visualized in **Figure 39**.

**Table 32. F-contrast of late RA between diagnostic groups ( $p_{\text{voxel}} < 0.005$ ,  $p_{\text{cluster.FWE}} < 0.05$ ).**

Result cluster #	Anatomical cluster location <sup>a</sup>	Cluster size in voxels	FWE corrected cluster p-value	Peak voxel coordinates <sup>b</sup>
1	L middle/superior occipital gyrus	238	0.007	-22 -74 32

<sup>a</sup>Result clusters were mapped with the AAL toolbox.

<sup>b</sup>Peak voxel coordinates are given in MNI space.

L and R denote left and right hemispheric location.

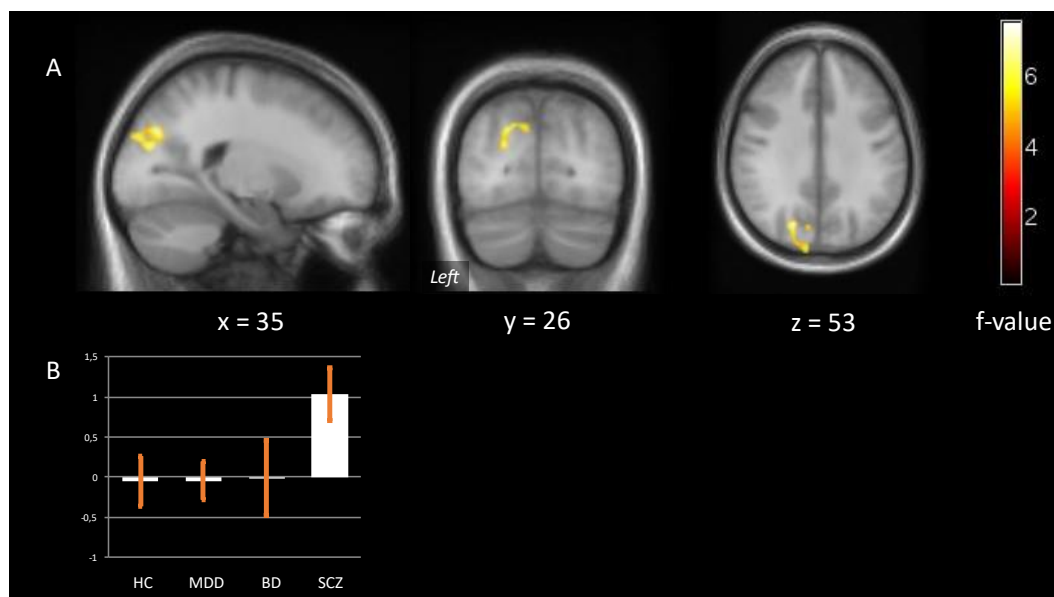


**Figure 39. F-contrast of late RA effects. (A)** One significant cluster with significant group effect during late RA localizing to the visual cortex. **(B)** Graph bars represent contrast estimates for peak voxels of these clusters. Note relatively higher activation (or deactivation) in SCZ patients compared with other groups.

Further explorations of activity changes during late RA by T-tests identified three significant activity changes in patients compared to HC ( $p_{\text{voxel}} < 0.005$ ,  $p_{\text{cluster.FWE}} < 0.05$ ) (**Table 33**). Specifically, two clusters bilaterally in insular-temporal regions showed stronger activation (or less deactivation) in patients with MDD compared with HC (clusters #1 and #2) (**Figure 40**). Additionally, the left STG cluster showed a trend significance (cluster #3). Moreover, in SCZ, activation was significantly stronger compared with HC in the visual cortex reaching to the superior parietal lobule (cluster #4). A trend-effect was found in the occipital lobule (cluster #5) (**Figure 41**).

**Table 33. T-contrasts of the late RA phase between the patient groups and HC ( $p_{\text{voxel}} < 0.005$ ;  $p_{\text{cluster.FWE}} < 0.05$ ).**

Result cluster #	Anatomical cluster location <sup>a</sup>	Cluster size in voxels	FWE corrected cluster p-value	Peak voxel coordinates <sup>b</sup>
<i>MDD &gt; HC (Figure 40)</i>				
1	R precentral gyrus, supramarginal gyrus, postcentral gyrus, superior temporal pole	633	< 0.001	6 -28 34
2	L heschl gyrus, middle temporal gyrus, precentral gyrus	681	< 0.001	-50 -12 26
3	L middle temporal gyrus, heschl gyrus	229	0.086	-52 -26 2
<i>SCZ &gt; HC (Figure 41)</i>				
4	R precuneus L middle/superior occipital gyrus	1272	< 0.001	8 -58 40
5	L inferior/middle occipital gyrus, inferior/middle temporal gyrus	230	0.084	-44 -58 2

<sup>a</sup>Result clusters were mapped with the AAL toolbox.

<sup>b</sup>Peak voxel coordinates are given in MNI space.

L and R denote left and right hemispheric location.

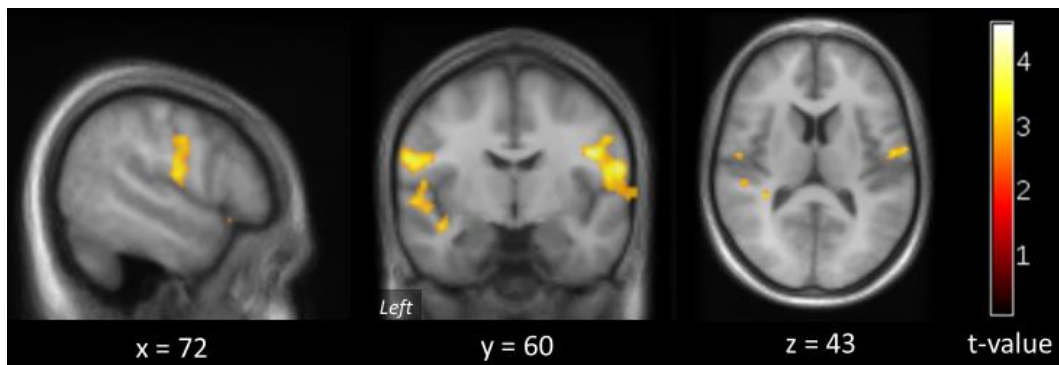


**Figure 40. Group differences in late RA between MDD and HC.** Results for the contrast ‘money > csm’ (thresholded at  $p_{\text{voxel}} < 0.005$ ;  $p_{\text{cluster.FWE}} < 0.05$ ). Compared to HC, patients with MDD showed more activation (or less deactivation) in bilateral insular temporal regions.

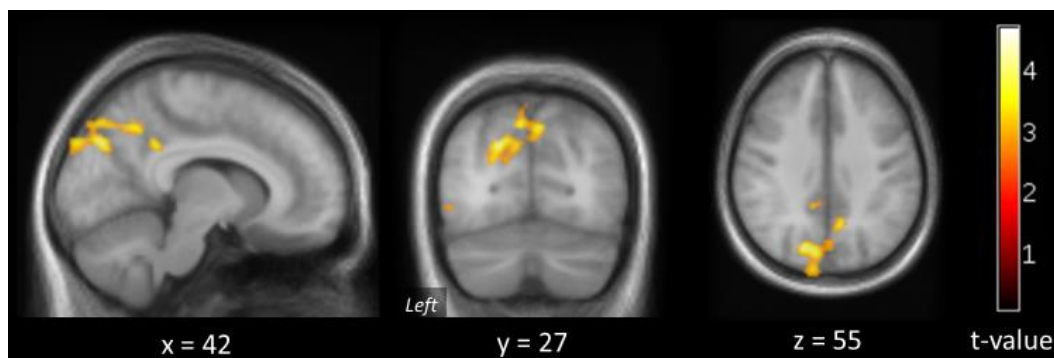


**Figure 41. Group differences in late RA between SCZ and HC.** Results for the contrast ‘money > csm’ (thresholded at  $p_{\text{voxel}} < 0.005$ ;  $p_{\text{cluster.FWE}} < 0.05$ ). Compared to HC, patients with SCZ exhibit more activation in visual cortex reaching to the superior parietal lobule

#### *Summary of voxel-wise SPM comparisons of the RA between disease groups and HC*

The key findings of the groupwise comparisons of RA effects using voxel-wise analyses in SPM can be summarized as follows: Investigating activation group differences using an F-test during 6 s of RA yielded mainly a left-striatal area and a left-precentral area. The more concise effect located in the left striatal region was primarily driven by patients with SCZ that showed markedly less activation compared to healthy subjects. Here, BD patients took an intermediate position. Examinations of RA sub-phases indicated that aberrant VS activation in SCZ was particularly pronounced during the early phase of RA.

As an F-test may not be very sensitive in the case of only one group showing a deviation, we also performed T-tests between the patient groups and HC. Here, robust significant effects emerged in bilateral temporolateral cortex due to stronger activation in MDD. Further analyses showed that this effect was particularly strong during the late phase of RA and located to areas expected to deactivate during this phase. Since these regions represented subregions of the task negative network of this task, this effect can be circumscribed as insufficient deactivation (of the DMN) in MDD. In BD, the pattern was similar in that also the late RA phase produced insufficient deactivation of the DMN, though in regions in the ACC, different from the regions affected in MDD.

Group effects in the occipital lobe occurred more pronounced during the late phase of RA and can be tracked back to abnormally high response in patients with SCZ.

#### **Investigation of network hubs**

In addition to SPM analyses, hubs of the reward network (3 ROIs), salience network (3 ROIs) and the DMN (8 ROIs) were investigated in a statistically more sparse way that explicitly modelled the dynamic (i.e. temporal) factor (early vs. late RA phase). Extracted values from both the peak voxels and the entire cluster value (first eigenvariate) were tested for main effects of group (4 levels, independent), time (2 levels, dependent) and their interaction. Due to the importance of the striatum for the pro-

cession of rewarding stimuli, its complex structure and the different roles of its subdivisions, we further analysed this region using a division based on an atlas/segmentation as a final step. However, to have a full picture of the differences between early and late RA in HC, **Table 34** provides an overview of all 14 ROIs and 6 atlas regions and paired T-tests between both time windows.

**Table 34. Dynamic characteristics (early vs. late RA phase) in all 14 ROIs and 6 atlas regions.**

	T	<i>p</i>
<b><i>ROIs</i></b>		
<i>L VS</i>	1.218	0.236
<i>R VS</i>	-0.194	0.848
SMA	-1.480	0.152
Mesencephalon	-3.962	0.001
<i>L AI</i>	-5.913	< 0.001
<i>R AI</i>	-5.072	< 0.001
DMN <sub>par</sub>	4.377	< 0.001
DMN <sub>front</sub>	3.439	0.002
<i>L DMN<sub>temp</sub></i>	0.565	0.578
<i>R DMN<sub>temp</sub></i>	1.235	0.229
<i>L DMN<sub>par</sub></i>	5.778	< 0.001
<i>R DMN<sub>par</sub></i>	3.694	0.001
<i>L HIP</i>	1.060	0.300
<i>R HIP</i>	1.240	0.227
<b><i>Atlas-/segmentation based regions</i></b>		
<i>L NAcc</i>	2.453	0.022
<i>R NAcc</i>	1.642	0.114
<i>L Putamen</i>	2.132	0.044
<i>R Putamen</i>	3.094	0.005
<i>L Pallidum</i>	0.804	0.104
<i>R Pallidum</i>	1.692	0.104

*L* and *R* denote left and right hemispheric location.



*Effects of group and time in peak voxels of ROIs*

The analyses of BOLD activation in peak voxels revealed significant effects of group, time and group-by-time. Statistical values of each peak voxel in all ROIs can be found in **Table 35**. Values that were robust to Bonferroni correction for the 14 ROIs being explored ( $p < 0.05/14 \sim 0.0036$ ) are displayed in bar plots below in addition. It should be emphasized that the ROIs were identified strictly in the HC groups, and that the entire 6 s of the RA phase were used to prevent regions showing a more stable response over the whole RA phase being excluded.

At the group level, a repeated-measures ANCOVA for all groups (covarying for *age* and *sex*) focusing on peak voxel effects revealed five significant effects: The most pronounced group effect was detected in bilateral temporal hubs of the DMN (*left*:  $x = -48$ ;  $y = -12$ ,  $z = 26$ ; *right*:  $x = 60$ ,  $y = -8$ ,  $z = 18$ ), stable against Bonferroni correction. Post-hoc analyses showed that in the right temporal DMN hub, all patient groups (and not just MDD as in the SPM analysis) showed a lack of deactivation compared to HC. A similar pattern emerged in the left temporal DMN hub, where MDD and SCZ showed significantly less deactivation than HC. In both temporal DMN ROIs, MDD had the least deactivation, matching the SPM results. In the bar plots below, contrast estimates of peak activations of both temporal DMN hubs including nominal  $p$ -values of the post hoc analyses towards the HC group are depicted (**Figure 42**). Apart from these Bonferroni robust results, nominally significant ANCOVA effects were found in the right VS ( $x = 12$ ;  $y = 6$ ;  $z = 2$ ), with SCZ showing reduced BOLD response compared to HC ( $p = 0.002$ ), in the right anterior insula ( $x = -30$ ;  $y = 18$ ;  $z = 8$ ), with SCZ exhibiting less activation than HC ( $p = 0.044$ ), and in the posterior midline area of the DMN ( $x = 8$ ;  $y = -62$ ;  $z = 22$ ), where both MDD and SCZ showed less deactivation than HC (MDD:  $p = 0.021$ ; SCZ:  $p = 0.005$ ).

Two significant main effects of the time factor were found (**Table 35**): The right anterior insula ( $x = -30$ ,  $y = 18$ ,  $z = 8$ ) showed a Bonferroni robust effect with rising activation between early and late RA (**Figure 43**). Additionally, analyses revealed peak voxel time effects in the left hippocampus ( $x = -24$ ;  $y = -22$ ;  $z = -22$ ), with decreasing values over time, i.e. showing a stronger deactivation in the late RA phase. This latter effect did not survive the conservative Bonferroni correction.

The interaction between group and time yielded nominally significant effects in the right parietal DMN area ( $x = 46$ ;  $y = -72$ ;  $z = 32$ ) and the left hippocampus.

**Table 35. Group main effects, time main effects and group-by-time effects in peak voxels.**

Region	Group		Time		Group x Time	
	F	<i>p</i>	F	<i>p</i>	F	<i>p</i>
<i>L</i> VS	3.558	0.017*	2.563	0.113	0.221	0.882
<i>R</i> VS	3.379	0.022*	3.502	0.064	0.318	0.812
SMA	1.641	0.185	0.246	0.621	1.178	0.322
Mesencephalon	2.292	0.083	0.425	0.516	0.325	0.807
<i>L</i> AI	2.355	0.077	3.904	0.051	1.284	0.284
<i>R</i> AI	2,752	0.047*	9.714	0.002**	1.746	0.163
DMN <sub>post</sub>	3.034	0.033*	0.318	0.574	1.639	0.186
DMN <sub>front</sub>	2.433	0.070	0.758	0.386	0.849	0.471
<i>L</i> DMN <sub>temp</sub>	6.173	0.001**	1.637	0.204	1.006	0.394
<i>R</i> DMN <sub>temp</sub>	7.059	< 0.001**	1.546	0.217	0.277	0.842
<i>L</i> DMN <sub>par</sub>	1.742	0.164	1.540	0.218	0.365	0.779
<i>R</i> DMN <sub>par</sub>	2.185	0.095	0.314	0.576	4.132	0.008*
<i>L</i> HIP	1.686	0.175	4.009	0.048*	3.805	0.013*
<i>R</i> HIP	1.177	0.323	0.321	0.573	2.143	0.100

\*Nominal significant at  $p < 0.05$ .

\*\* Robust to Bonferroni correction for 14 regions ( $p < 0.05/14 \sim 0.0036$ ).

*L* and *R* denote left and right hemispheric location.

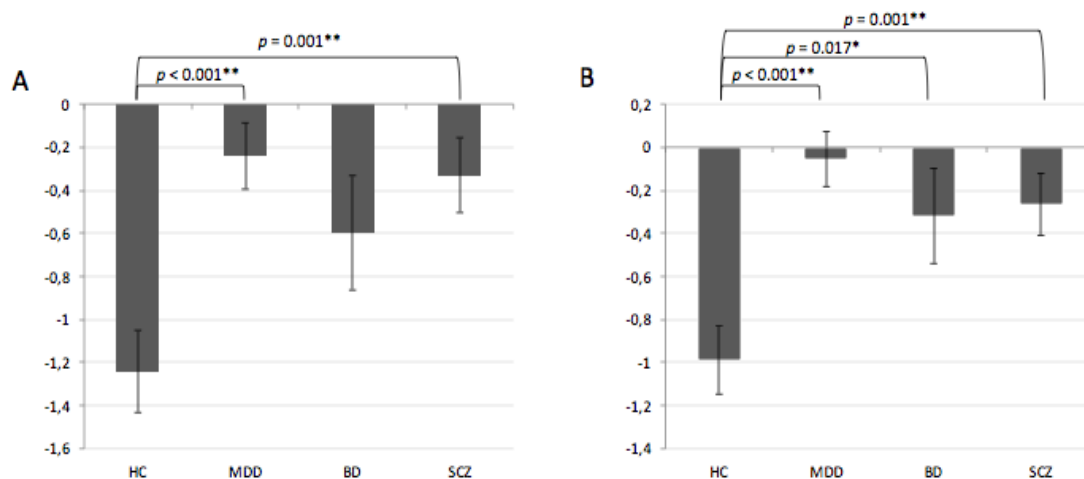


**Figure 42. BOLD activation in peak voxels of temporal DMN hubs.** Bar plots represent contrast estimates of group effects of peak voxels. **(A)** In the left temporal DMN hub, HC revealed the most pronounced deactivation. Significant less deactivation was found for SCZ and MDD. **(B)** In the right temporal DMN hub, each diagnostic group showed significantly less deactivation compared with HC.

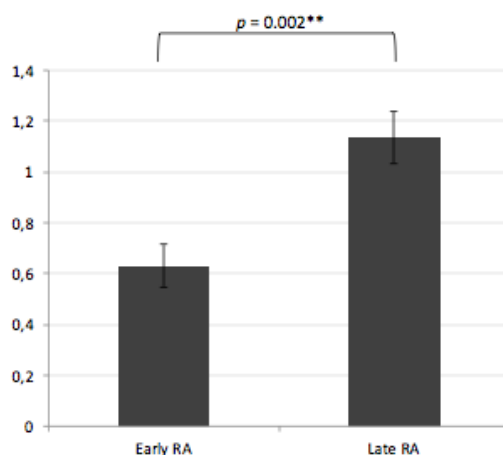


**Figure 43. Significant time main effect in the right anterior insula.** Graph bars represent contrast estimates of time effects of peak voxel of the right anterior insular ROI in early and late RA across all diagnostic groups, showing increasing right anterior insular activation between early and late RA.

A closer look at these time-by-group effects shows that in the right parietal DMN hub, activation decreased moderately in HC with time, whereas a sharp decline was observed in BD, and a contrary (paradox) increase in SCZ. In the left hippocampus, HC showed a steep decline, whereas the course was flattened in all patient groups. This ‘flattening’, however, reached only significance in patients with SCZ. Both examples also show that group-by-time interaction effects can mask a (normative) time effect (as long as all diagnostic groups are analysed), which is why we appended an analysis of the time effect only in the HC group.

**Table 36. Pairwise post hoc T-tests group-by-time interaction effects. The last column of this table shows mean value plots of all four groups in the early and later RA phase to illustrate the dynamics.**

Peak voxel	Overall	MDD/HC	BD/ HC	SCZ/HC	
<i>R</i> DMN <sub>par</sub>	0.008*	0.064	0.038*	0.004*	
<i>L</i> HIP	0.013*	0.869	0.207	0.030*	

■ = HC, ● = MDD, ◆ = BD, ▲ = SCZ

\*Nominal significant at  $p < 0.05$ .

*L* and *R* denote left and right hemispheric location.

### *Effects of group and time in entire ROI clusters*

Contrast estimates of cluster activations of the 14 selected ROIs also showed group, time and group-by-time effects in BOLD activation. Again, statistical values and cluster details of all ROIs are listed in **Table 37**.

Our analyses revealed 7 main effects in the bilateral VS, mesencephalon, left anterior insula as well as bilateral temporal and the posterior midline hubs of the DMN. In line with findings of the peak voxel analysis, the bilateral temporal DMN network hubs showed the strongest effects, robust towards Bonferroni correction ( $p < 0.05/14 \sim 0.0036$ ). Post-hoc T-tests yielded that all patient groups showed significantly less deactivation in these ROIs. The most insufficient deactivation was found in patients with MDD, again matching the SPM result. A visualisation of contrast estimates of the cluster values and nominal  $p$ -values of the pairwise post-hoc tests can be found in **Figure 44**. A weaker DMN effect was found in the posterior DMN hub, only driven by SCZ. Regarding the nominal group effects in the VS, post-hoc analyses confirmed that this result was driven by a weaker activation in SCZ. The group effect in the mesencephalon was also driven by the SCZ group. In the left anterior insula, post-hoc tests showed that activation deficiencies were also a SCZ-specific phenomenon.

Over time, varying activation profiles were found in cluster values of the mesencephalon as well as the bilateral anterior insula. Contrast values in the mesencephalic cluster showed Bonferroni robust time effects with rising values between early and late RA. This was different from the peak voxel results, potentially indicating that here the measurement from the more voxels for higher robustness is needed. Further details are given in **Figure 45** below. Activation in the left and right anterior insula pointed to increases over time, but these effects did not survive the Bonferroni correction.

Analysing group-by-time effects revealed five nominally significant results, localizing to the left anterior insula, the posterior midline hub as well as the parietal hub of the DMN and bilateral hippocampus. Further T-tests to compare diagnostic groups one by one with HC are described and detailed below (**Table 37**).

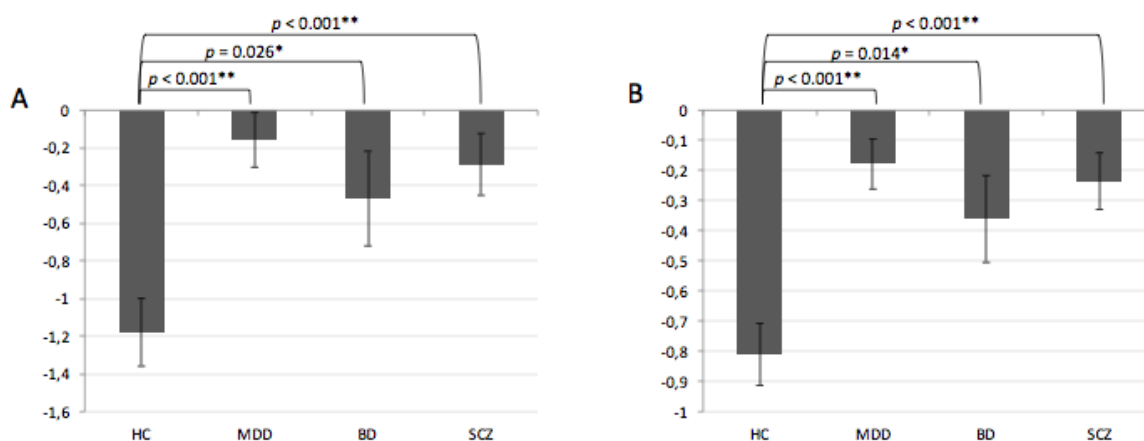
**Table 37. Group main effects, time main effects and group-by-time effects in cluster ROIs.**

Region	Cluster size	Group		Time		Group x Time	
		F	<i>p</i>	F	<i>p</i>	F	<i>p</i>
<i>L</i> VS	320	4.637	0.005*	6.554	0.012	0.321	0.810
<i>R</i> VS	324	4.606	0.005*	3.168	0.078	0.237	0.871
SMA	380	0.771	0.513	0.016	0.899	0.710	0.549
Mesencephalon	131	3.188	0.027*	9.311	0.003**	2.037	0.114
<i>L</i> AI	118	2.748	0.047*	8.405	0.005*	2.942	0.037*
<i>R</i> AI	118	2.431	0.070	8.145	0.005*	1.425	0.240
DMN <sub>post</sub>	746	2.272	0.048*	0.057	0.812	4.132	0.008*
DMN <sub>front</sub>	154	1.750	0.162	0.578	0.449	2.362	0.076
<i>L</i> DMN <sub>temp</sub>	120	6.972	< 0.001**	0.313	0.577	0.679	0.567
<i>R</i> DMN <sub>temp</sub>	818	8.324	< 0.001**	0.081	0.777	0.333	0.802
<i>L</i> DMN <sub>par</sub>	359	1.556	0.205	2.336	0.130	1.558	0.205
<i>R</i> DMN <sub>par</sub>	675	2.090	0.107	1.117	0.733	3.391	0.021*
<i>L</i> HIP	18	1.037	0.380	2.240	0.138	3.773	0.013*
<i>R</i> HIP	102	1.073	0.364	0.000	0.995	2.793	0.045*

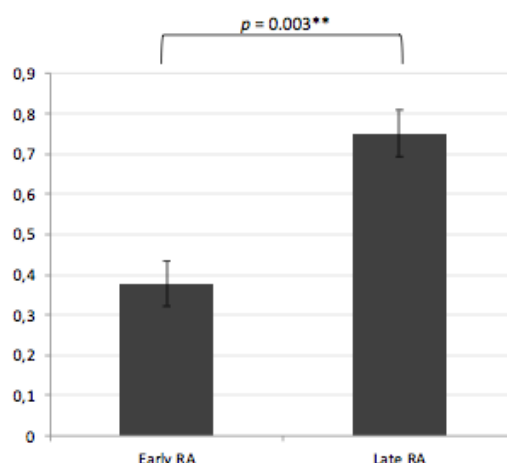
\*Nominal significance,  $p < 0.05$ .

\*\* Robust to Bonferroni correction for 14 regions ( $p < 0.05/14 \sim 0.0036$ ).

*L* and *R* denote left and right hemispheric location.



**Figure 44. BOLD deactivation in temporal DMN hubs.** Bar plots represent the contrast estimates of group effects of cluster values in the left **(A)** and right **(B)** ROI. Relative to HC, all diagnostic groups showed a lack of deactivation in both ROIs, most strongly in MDD.

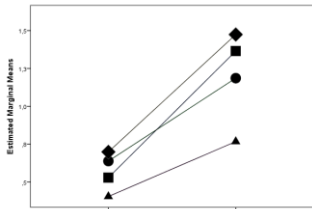
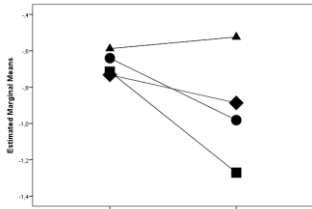
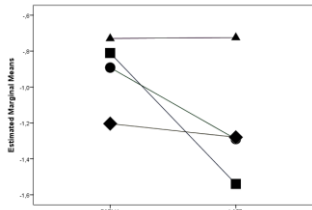
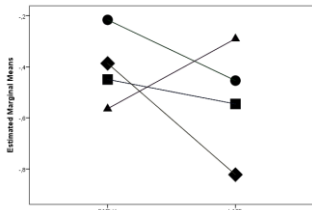
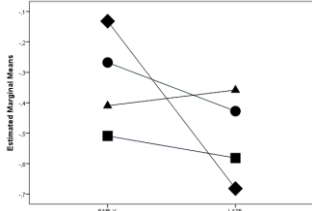


**Figure 45. Significant time effect of the mesencephalic cluster.** Graph bars represent contrast estimates of time effects of cluster values of the mesencephalon in early and late RA. Over all diagnostic groups, activation of the mesencephalon increased between early and late RA.

Further investigations of the five time-by-group effects allowed the following observations (also see **Table 38**, last column, for plots): (i) In the left anterior insula, average activation values increased less strongly in SCZ compared to HC ( $p = 0.011$ ). (ii) In the posterior midline hub of the DMN, the interaction was driven by SCZ that showed practically no deactivation over time ( $p = 0.003$ ). (iii) In the right parietal hub, consistent with results of peak voxel activations, the interaction was driven by BD ( $p = 0.042$ ) and SCZ ( $p = 0.005$ ). BD showed a slight decrease over time while values of HC dropped markedly. Activation profiles of SCZ stayed on a similar level over time. The contradiction between bilateral hippocampal overall time-by-group effects and no significant results in the separate groups is explained

by the ‘spectral’ pattern around HC, with disease groups deviating into different directions, some showing a stronger decline (e.g. BD), some a less strong decline or even increase (e.g. SCZ).

**Table 38. Post hoc time-by-group effects in cluster ROIs investigated separately per patient group.**

Cluster	Overall	MDD/HC	BD/ HC	SCZ/HC	
<i>L</i> AI	0.037*	0.153	0.610	0.011*	
DMN <sub>post</sub>	0.008*	0.164	0.123	0.003**	
<i>R</i> DMN <sub>par</sub>	0.021*	0.202	0.042*	0.005*	
<i>L</i> HIP	0.013*	0.416	0.204	0.064	
<i>R</i> HIP	0.045*	0.825	0.054	0.528	

■ = HC, ● = MDD, ◆ = BD, ▲ = SCZ

\*Nominal significant at  $p < 0.05$ .

*L* and *R* denote left and right hemispheric location.

*The association between early and late RA fMRI response and anhedonia*

Stepwise forward multiple linear regression (in all diagnostic groups, including HC) of both early and late RA cluster values was used to evaluate whether they hold the potential to explain a significant amount of variance of the anhedonia score. The analysis revealed three models with the model showing the highest explained variance containing the early left hippocampal cluster, the early right temporal DMN and the late left temporal DMN cluster. This latter model explained 19.8% of the total variance.

We did not detect any significant group effects in the early left hippocampal cluster (**Figure 46**), in line with ROI results in **Table 37**. In contrast, we confirmed highly significant group effects in both early right and left late temporal DMN clusters, with attenuated deactivation in patients relative to HC. Since anhedonia scores – similarly as the temporal DMN values – were abnormal in all patient groups ( $p < 0.001$ ), the next step was to evaluate whether the predictive value of both temporal DMN clusters merely reflects the step between healthy subjects and patients. Therefore, we repeated the multiple regression analysis under exclusion of the HC. Here, only early RA left hippocampus cluster was identified as significant predictor ( $p = 0.002$ ) explaining 13.8% of the anhedonia variance.

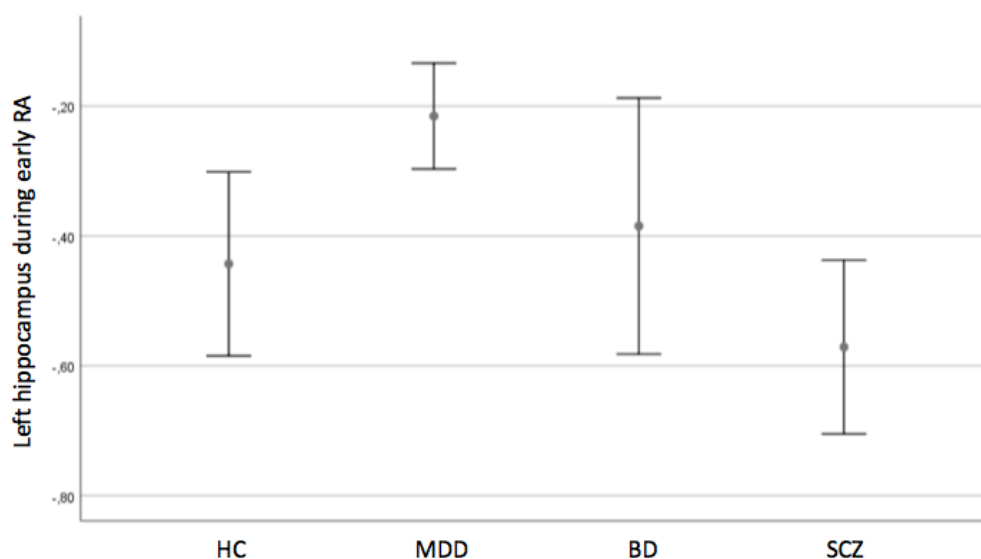


**Figure 46. BOLD activation in the left hippocampal cluster during early RA.** Bar plots represent the contrast estimates of group effects of cluster values. No significant group effects between HC and diagnostic groups were detected.

In addition, we tested the specificity of these results by predicting BDI single items one by one the BDI total score and an 'inverse score' (total score minus anhedonia score) with the physiological data of the predefined clusters. Technically, partial correlations (partial  $r$ ) corrected for *age* and *gender* are reported. Among the 21 BDI items, eight reached nominal significance level, including three out of four anhedonia items. Both total scores and the 'inverse score' were also significantly correlated with the early left hippocampus. However, the correlation with anhedonia in the patient group was one



magnitude stronger ( $p = 0.003$ ) than that with the inverse score ( $p = 0.030$ ), indicating some specificity. Taken together, the early left hippocampal activation can be considered a specific predictor for the anhedonia score. **Table 39** summarizes results of the specificity interrogation with the single items of the anhedonia score printed in bold.

**Table 39. Specificity interrogation of left hippocampal (early RA) predicting single items, the total score of the BDI-II, the anhedonia score and the inverse score (sum of non-anhedonia single items).**

BDI categories	<i>r</i>	<i>p</i>
Sadness	.169	0.175
Pessimism	.245	0.048*
Past failure	.119	0.342
<b>Loss of pleasure</b>	.253	0.041*
Guilty feelings	.108	0.386
Punishment feelings	-.094	0.454
Self-dislike	.241	0.052
Self-criticalness	.201	0.106
Suicidal thoughts or wishes	.164	0.187
Crying	.241	0.051
Agitation	.074	0.554
<b>Loss of interest</b>	.324	0.008*
Indecisiveness	.306	0.012*
Worthlessness	.296	0.016*
<b>Loss of energy</b>	.289	0.019*
Changing in Sleeping pattern	.232	0.061
Irritability	.230	0.064
Changes in Appetite	-.010	0.935
Concentration Difficulty	.186	0.136
Tiredness or Fatigue	.265	0.032*
<b>Loss of Interest in Sex</b>	.349	0.004*
<b>Total scores</b>	.296	0.016*
<b>Anhedonia score</b>	.358	0.003*
<b>Inverse Score</b>	.267	0.030*

\*Nominal significance,  $p < 0.05$ ; corrected for *age* and *gender*.

Correlation between early left hippocampal activation and anhedonia were similarly steep across all patient groups, while higher values of the respective cluster in HC were not linked to higher anhedonia scores (see **Figure 47**).

Next, we tested this more formally: Using a 4-level group factor, no significant group-by-hippocampus interaction was detected ( $p = 0.492$ ) (see **Figure 47A**), whereas both group and the hippocampal marker were significant predictors ( $p < 0.001$  and  $p = 0.009$ , respectively). When we collapsed the patients into one group, a trend group-by-hippocampus effects ( $p = 0.072$ ) emerged (see **Figure 47B**).

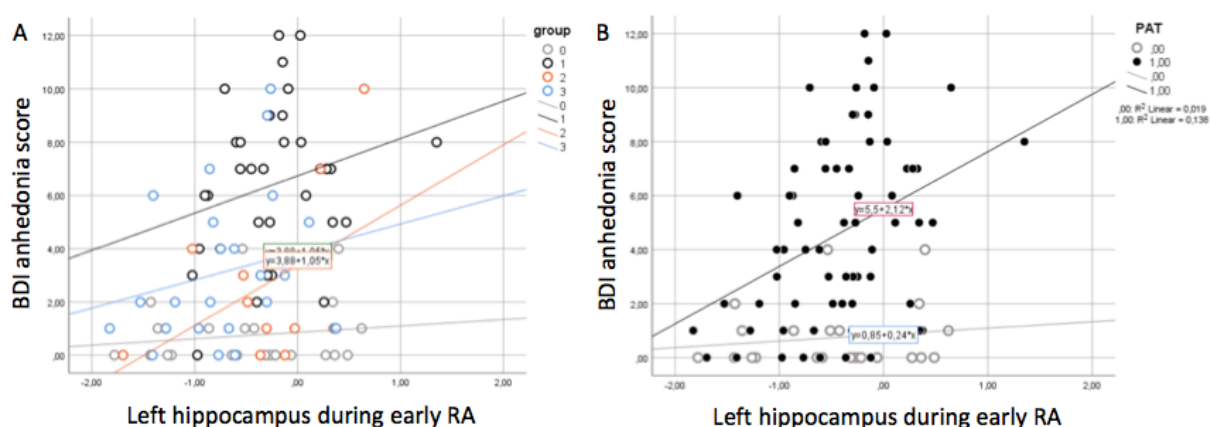


**Figure 47. Correlation between BDI-based anhedonia scores and the left hippocampal cluster contrast value during early RA. (A)** The left scatter plot depicts the correlation for each group separately (0 = HC; 1 = MDD; 2 = BD; 3 = SCZ). **(B)** In the right scatter plot, the three diagnostic groups were pooled (0 = HC, 1 = Patients).

### *Effect of group and time in VS regions based on atlas segmentation*

Analyses of group effects in atlas and segmentation-based basal ganglia regions revealed three significant results, two of them robust to Bonferroni correction for 6 tested regions ( $p < 0.05/6 \sim 0.0083$ ): (i) In the left NAcc, we found a strong group effect that was robust to Bonferroni correction. Post-hoc analyses indicate a weaker BOLD response of the left NAcc in SCZ compared to HC (**Figure 48**). (ii) Similarly, a Bonferroni robust group effect that was mainly driven by lower activation profiles in SCZ compared to HC was found in the left putamen (**Figure 49**). (iii) The group effect in the left pallidum was also driven by significantly reduced activation in SCZ compared to HC (**Figure 50**). In addition to those three highly significant group effects in the left hemisphere, analyses of right NAcc and right putamen revealed trend effects. In line with the Bonferroni robust results, those effects were also driven by weaker activation in SCZ ( $p = 0.008$ ;  $p = 0.025$ , respectively).

Investigation of the time main effect in these regions yielded three significant results, all due to decreasing values in these ROIs. More specifically, the time effect was localizing to the bilateral NAcc (**Figure 51**), with the effect on the left side being robust to Bonferroni correction, and the left putamen (**Figure 52**). Details can be found in **Table 40**.

A group-by-time interaction effect was detected in the left putamen. Similar to cluster results of bilateral hippocampi (see Chapter 3.3.3), this effect was driven by a strongly deviant activation profile in one group, here the SCZ group. The respective plot in **Table 41** demonstrates that BD and MDD, as HC, show clear activation of the left putamen and a consistent decrease over time, whereas SCZ patients show no activation early, and also no change (or even a slight increase) over time.

**Table 40. Group main effects, time main effects and group-by-time effects activation in atlas/segmentation based pre-defined VS regions.**

Region	Group		Time		Group x Time	
	F	<i>p</i>	F	<i>p</i>	F	<i>p</i>
L Nacc	4.713	0.004**	11.441	0.001**	0.457	0.713
R Nacc	2.646	0.054	4.046	0.047*	0.365	0.778
L Putamen	6.427	0.001**	4.764	0.032*	3.577	0.017*
R Putamen	2.578	0.058	1.145	0.287	2.691	0.051
L Pallidum	3.766	0.013*	0.564	0.454	0.838	0.476
R Pallidum	1.788	0.155	0.229	0.633	0.968	0.411

\*Nominal significance,  $p < 0.05$ .

\*\* Robust to Bonferroni correction for 6 regions ( $P < 0.05/6 \sim 0.0083$ ).

L and R denote left and right hemispheric location.

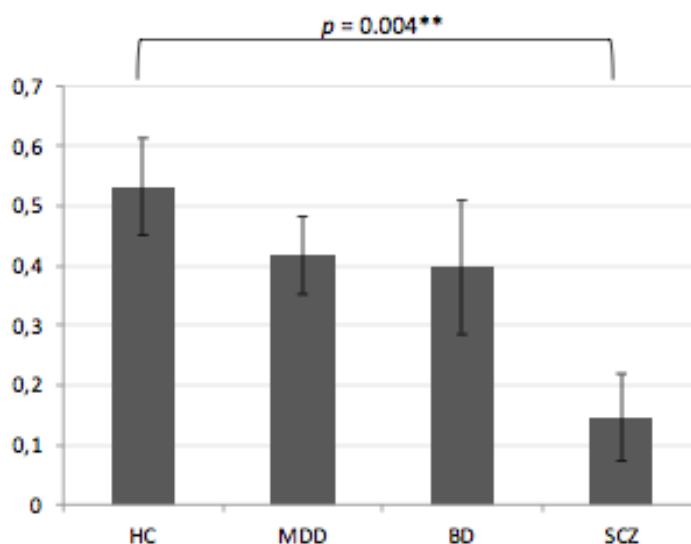


**Figure 48. Group effects of RA in the left NAcc.** Graph bars represent the mean HRF contrast estimate value for each group. Note the significant difference between SCZ and HC.

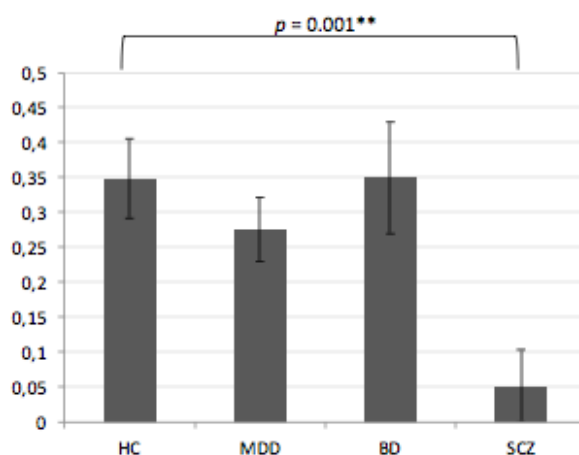


**Figure 49. Group effects of RA in the left putamen.** Graph bars represent mean HRF values of each group. Note the sharply reduced activation in patients with SCZ which was highly significant compared to HC.

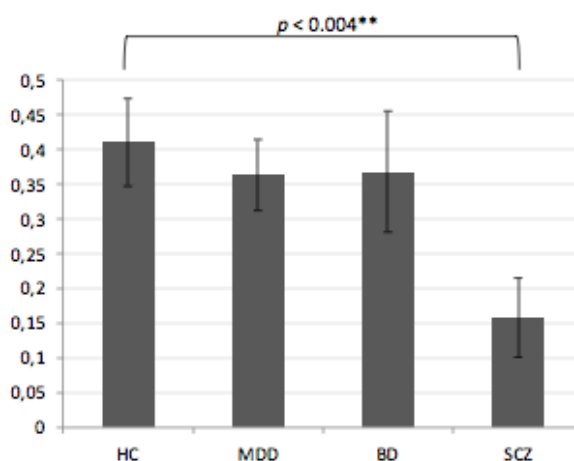


**Figure 50. Group effects in the left pallidum.** Graph bars represent mean HRF values of each group. Note that group effects were driven by patients with SCZ.

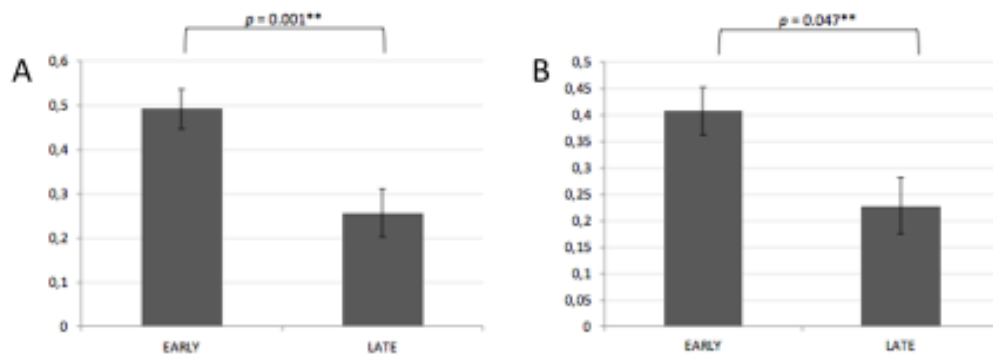


**Figure 51.** Time effect of RA in the left (A) and right NAcc (B). Graph bars represent the mean response in early and late RA across all diagnostic groups. Both activation profiles show a decrease over time.

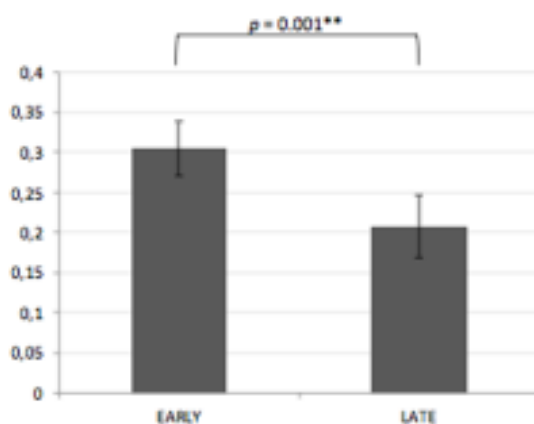
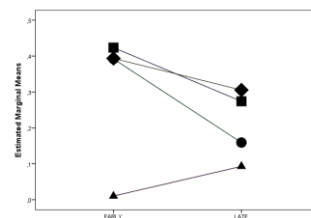


**Figure 53.** Time effects in the left putamen. Over time, values of BOLD signal decreased in all participants.

**Table 41. Group-by-time effects in atlas- and segmentation-based VS regions.**

ROI	Overall	MDD/HC	BD/ HC	SCZ/HC
L Putamen	0.017*	0.536	0.826	0.078



■ = HC, ● = MDD, ◆ = BD, ▲ = SCZ

\*Nominal significant at  $p < 0.05$ .

L denotes left hemispheric location.

### 3.4 Discussion

The study behind chapter 3 sought to elicit neural underpinnings of RA across common affective and psychotic disorders by using fMRI combined with a RA task. Therefore, we utilized a reward paradigm which was composed of the same basic elements as the MID task developed by Knutson et al. (2001). Overall, several distinct approaches of analyses highlighted multiple reward-related alterations in SCZ, BD and MDD. While some of these abnormalities appear to be shared pathophysiological phenomena, we also found disturbances that were specific for the clinical diagnostic classes. Remarkably, our findings suggest that disruptions of RA are not limited to the VS as an expected and highly validated response region, but also affect other large-scale brain networks, namely the salience network and the DMN. In this respect, we were able to extend the fMRI-based characterization of pathological alterations of reward processing and emphasize that the RA task is a compelling tool to study all three networks. In addition, we found a predictive potential of the left hippocampus for anhedonia, a clinical symptom that cuts across diagnostic boundaries of the psychotic-affective spectrum (Horan et al., 2006).

#### 3.4.1 Reduced VS activation in SCZ

In line with a previous meta-analysis on studies using the MID task (Oldham et al., 2018), the interrogation of task effects revealed the expected increase in hemodynamic responses (as measure by BOLD fMRI) of the VS during the anticipation of monetary rewards across all four groups. Furthermore, we found corresponding activation patterns in a mesencephalic cluster that could represent the VTA, the key source of dopaminergic neurons projecting to the VS. Together, elevated activation in both VS and mesencephalon indicated a coherent engagement of the dopaminergic system and met the hypothesized VS task effects.

Although similar task activation was observed across all four groups, patients with SCZ had blunted striatal activity during RA compared with HC. Beyond whole-brain investigations, additional ROI analyses pointed to the same pattern of disturbance, and highlighted the NAcc as site of this effect, rather than dorsal putamen, the caudate or the pallidum that were equally investigated. Both the directionality and localization align well with earlier findings of altered VS responses in drug-naive (Esslinger et al., 2012; Nielsen et al., 2012) and chronic patients (Juckel, Schlagenhauf, Koslowski, Filonov, et al., 2006; Zink et al., 2004). Moreover, striatal abnormalities were more pronounced in the left hemisphere in our experiment. This lateralization is concordant with a study by Juckel et al. (2006) who not only reported a general reduction in striatal activation in unmedicated SCZ patients, but also a negative correlation between left VS activation and the severity of negative symptoms. Given that striatal responses are regarded indicative of dopaminergic activity (Knutson & Gibbs, 2007), these findings are in good agreement with the dopamine hypothesis of SCZ (Howes & Kapur, 2009) as well as reward-related findings in SCZ patients based on other measures (Brunelin et al., 2013). In addition, since dopaminergic projections within mesocorticolimbic pathways originate in mesencephalic neurons, particularly in the VTA (McQuiston, 2011) (see chapter 1.2.4), our finding of reduced activation in the

mesencephalic cluster in SCZ lends further support for the assumption of dopamine disruptions as a physiological core feature of SCZ.

Additional analysis of atlas-based regions (including the segmented bilateral NAcc) allowed a more detailed decoding of striatal deviations: Consistent with whole-brain and ROI-based analysis, the left-sided lateralization was also reflected here. Furthermore, since we observed the most pronounced striatal effects in the left NAcc, our experiment not only correspond to prior fMRI studies particularly highlighting aberrant NAcc functioning in SCZ during RA (Juckel, Schlagenhauf, Koslowski, Filonov, et al., 2006; Kirschner et al., 2016), but also to RS fMRI studies reporting alterations in this limbic node (Kiparizoska & Ikuta, 2017; Lee et al., 2019; Liu et al., 2017; Zhuo et al., 2014). Due to its central role within the reward circuitry as the main projection site of dopaminergic neurons of the VTA (Han et al., 2017), this provides additional support for the dopamine hypothesis (Howes & Kapur, 2009). In addition, bearing in mind that the NAcc also receives input from other SCZ-related brain regions (see **Figure 2**, p. 34), including hippocampus (Lieberman et al., 2018), mPFC (Razafimandimby et al., 2016) and the amygdala (Ho et al., 2019), the key role of the NAcc in SCZ gets further emphasized. In sum, our results concerning the reward system in SCZ patients draw a coherent picture of brain alterations that are likely to be attributable to dopamine dysfunctions. This strengthened the trustworthiness of the results obtained in the other diagnostic groups.

In MDD, the absence of VS alterations while performing the MID task support findings by Knutson et al. (2008). However, as mentioned above, findings on reward-related striatal activation in MDD are not entirely unequivocal: Pizzagalli et al. (2009) employed the same task to a MDD sample to differentiate neural responses to RA and gain of rewards. Although the main VS anomalies were found during the feedback phase, similar, yet slightly weaker VS effects emerged in a small sector of the left putamen during the anticipation phase. As their results point to a primary deficit to reward consumption in MDD patients, our respective findings are not entirely contradicting.

Since we neither observe any abnormal striatal responses in BD, our results align with previous studies employing the same task in bipolar patients in euthymic states (Kollmann et al., 2017; Yip et al., 2015), euthymic to mild depression (Berghorst et al., 2016) and mania (Berpohl et al., 2009). Furthermore, the absence of VS effects in currently depressed BD patients would parallel findings in MDD which speak for the proximity of these two affective disorder groups.

From a transdiagnostic perspective, our data indicates that striatal dysfunctions during RA are a rather SCZ specific phenomenon, while this subprocess of reward processing seems to be preserved in affective disorders.

### 3.4.2 Neural imprints of aberrant salience in SCZ

Interrogations of task effects also revealed a typical pattern of more activation in the bilateral anterior insula and the dACC. This coactivation is a commonly observed phenomenon across multiple cognitive task demands and represents a functional network known as the salience network (Menon, 2015;

Taylor et al., 2009). Since this network generally shifts the attention to salient stimuli that are associated with positive outcomes and therefore triggers and facilitates goal-directed behaviours (Ryali et al., 2016), the salience network is particularly relevant to this reward task. Besides general task effects within the salience network, the temporal dissection RA revealed that this insular activation was particularly pronounced during the late RA phase. In accordance, modelling the dynamic factor in additional ROI analyses consistently suggested rising neural responses throughout the course of RA.

Although each group for itself yielded robust activation of the salience network at the group level, further analyses revealed disease-specific abnormalities among its associated nodes. In patients with SCZ, salience network changes emerged in two different dimensions: On the one hand, we observed attenuated activation of the bilateral anterior insula compared to HC. On the other hand, investigations of the dynamics features revealed that relative to healthy subjects, patients with SCZ exhibited an attenuated increase in the left insula activation over time. In other words, regardless of their lower levels of activation, SCZ patients also fail to boost salience network responses to a similar extent as healthy subjects. In general, the involvement of the insula in the pathophysiology of SCZ is a common observation: Anatomical changes of the insular cortex for example are a well-known feature in SCZ, including decreases in GM and GM fractional anisotropy, and functional impairments have also been reported across various task demands (Honea et al., 2005; Kasai et al., 2003; Manoliu et al., 2013). Furthermore, White et al. (2010) observed reduced functional network connectivity of the insula with the ventromedial frontal cortex, ACC, left central executive network and the posterior cingulate and anterior gyrus. However, our observations of insular decreases not only concur with previous findings on reward processing in SCZ (Murray et al., 2008), but also harmonize with theoretical concepts of psychotic symptoms: According to a Bayesian approach, positive symptoms of SCZ are related to disturbed error-dependent updating of inferences and beliefs about the world (Fletcher & Frith, 2009). Given that the insular cortex is involved in predicting error coding (Gogolla, 2017), this component of the salience network is of particular relevance to this understanding of positive symptoms.

Although our results suggest an SCZ-specific phenomenon at first glance, it should be noted that a partially overlapping effect pattern partly covering the right insula was observed in patients with BD. However, as this effect pattern only encompassed the insular cortex marginally, while it extended more to the IFG, the association between this effect and salience network functioning in BD should be considered with caution.

In sum, our findings suggest that dysfunctions within the salience network are mainly restricted to the pathophysiology of SCZ. Given that this network is associated with the detection and filtering of meaningful environmental stimuli (McCutcheon et al., 2019), our results corroborate with the hypothesis of aberrant salience (see chapter 1.2.5).



### 3.4.3 Common and distinct DMN disruptions

In addition to findings in the task positive networks that were particularly striking in SCZ, we also investigated deactivating regions (i.e., the task negative network) during RA. Here, the typical DMN configuration emerged across all groups, including reductions in precuneus, mPFC, medial temporal (hippocampal) and lateral parietal regions. Given that the DMN is a well-known set of brain regions that deactivate during attention-demanding paradigms (Fox et al., 2005), these observations match our expectations.

Despite this roughly similar deactivation pattern across all groups, we observed significant functional anomalies within the DMN in the disease groups compared to HC. In MDD, the DMN has been the topic of considerable research and ascribed functional impairments by way of neuroimaging studies. A consistent body of literature suggests a failure to down-regulate activation within the DMN in patients with MDD (Sheline et al., 2009; Zhou et al., 2020, Grimm et al., 2009; Rodríguez-Cano et al., 2017; Sheline et al., 2009; Spies et al., 2017) that can be associated with negative rumination as a core symptom of MDD (Papageorgiou & Wells, 2020). In harmony with previous work, we found impaired deactivation in several DMN nodes in patients with MDD, including the posterior midline hub and both bilateral temporolateral clusters. Since the posterior midline DMN component mainly comprises the precuneus and the PCC, Dutta et al. (2019) suggest that this region might be particularly important for self-reflective thinking and autobiographical memory. In turn, both of these regions have been shown to be impaired in MDD (Takano & Tanno, 2009; Williams & Scott, 1988). Interestingly, Spies et al. (2017) recently reported that MDD patients with a stronger deactivation suppression in this region during emotion processing were more likely to benefit from antidepressant treatment after two weeks. Correspondingly, and also in the context of emotion processing, deactivation deficits in the posterior midline DMN hub were shown to normalize after antidepressant treatment (Delaveau et al., 2011). Hence, our findings of insufficient deactivation of the precuneus indicate that disease-related important DMN-deficits also emerge during the anticipation of monetary rewards. However, further investigations are required to test whether the treatment response predictive character of this anomaly also applies in the context of RA. Actually, it is an important research question, to what degree DMN deficiencies are task specific.

Besides posterior DMN deficits, we also observed deactivation suppression in lateral temporal DMN regions (mainly covering the STG) in MDD patients. Generally, this region is associated with episodic memory function (Buckner, 2013). Among all disease groups, depressive patients showed the most pronounced temporal DMN differences compared to HC. Several studies have been performed on alterations of the STG in patients with MDD: At the structural level, Takahashi et al. (2009) reported STG volume reductions in patients with current and past major depression. Interestingly, the volume of the right STG was observed to be reduced in treatment resistant depressive adolescents with a history of suicide attempts relative to healthy subjects (McLellan et al., 2018). At the functional level, Yang et al. (2016) observed diminished STG responses in MDD patients during a decision making task. Furthermore, Renner et al. (2017) found increased PCC - STG and inferior temporal cortex connectivity

in patients with MDD. Additionally, this association was modulated by induced negative mood states. This functional connectivity finding is not in contradiction with our task-based finding, as more intra-network connectivity may also occur during a task and make regional responses in MDD more similar. Taking task-negative findings in MDD together, our data confirms previous reports of impaired DMN deactivation in depressive patients. This impairment might reflect both excessive rumination in MDD and the inability to shift the focus of attention away from internal cognitive and emotional states to the demands of the outside world. It is also important to recapitulate that also in this model-like RA task, the DMN and with this, a substantial cognitive component, is involved.

In schizophrenic patients, we also observed attenuated deactivation at several sites in the DMN, including the posterior midline hub, right lateral parietal DMN, temporolateral regions and the hippocampus. The complex symptomatology of SCZ has been frequently associated with DMN dysfunctions. In contrast to affective disorders, DMN dysfunctions in psychotic disorders are rather associated with overly intensive self-reference, attentional impairments and working memory deficits (Whitfield-Gabrieli & Ford, 2012). Based on fMRI, various methodological approaches have been applied to characterize these dysfunctions in SCZ: On the one hand, a considerable amount of RS studies suggests DMN abnormalities, i.e. FC (Forlim et al., 2020) or regional homogeneity (Liu et al., 2018). On the other hand, task-based fMRI studies based on multiple paradigms, including multi-source interference task, working memory task, selective attention task, auditory oddball task, and semantic repetition priming task, reported aberrant activation in DMN regions in patients with SCZ (Hu et al., 2017). While a number of results point to a deactivation deficit (Guerrero-Pedraza et al., 2012; Metzak et al., 2012; Pomarol-Clotet et al., 2008), however, contradictory results were also found (Hu et al., 2017). Our findings of reduced suppression in the PCC and the precuneus lend support to previous findings of a deactivation deficit in the posterior midline region of the DMN in SCZ (Salgado-Pineda et al., 2011). Two recent fMRI studies further highlighted the role of the precuneus/PCC in SCZ: Firstly, reduced FC within the precuneus was reported to be associated with the severity of negative symptoms, particularly apathy (Forlim et al., 2020). Secondly, Shan et al. (2020) provided evidence that metacognitive training, a widely applied cognitive behavioural treatment approach of positive SCZ symptoms, is linked to the modulation of DMN homogeneity in SCZ, particularly in the precuneus/PCC. Besides the relation between the PCC/precuneus and SCZ, and as mentioned in chapter 2, this DMN region was also found to be associated with cannabis use: According to Wall et al. (2019), the PCC was among other regions showing decreased connectivity in subjects frequently using cannabis, and this effect was associated with the subjective experience of the THC intoxication. Given the close association between cannabis and SCZ, this study corroborates the central role of the posterior midline DMN hub in SCZ and thus supports our respective finding.

In temporal DMN regions, SCZ exhibited a similar, yet not as striking deactivation deficit as MDD. Our experiments thus confirm previous results of deficits in down-regulating temporal DMN nodes covering the middle and superior temporal gyrus during task performance in SCZ (Nygård et al., 2012; Salgado-Pineda et al., 2011). However, the connection between abnormality in the temporal region and psychopathology might be of a different nature compared to MDD. Like the precuneus, this region

also plays an important role in the pathophysiology of SCZ: Previously, it has been evidenced that hyperactivity in the STG is a robust finding in patients with SCZ and auditory verbal hallucinations (Orlov et al., 2018).

In the right parietal node of the DMN, SCZ patients exhibited constant or even increasing levels of activation, while the controls show a continuous deactivation throughout the RA phase. This result particularly underlines the scattered nature of neural functioning in SCZ. Although these alterations in the parietal node are not reflected in group comparisons, abnormal dynamics are another indication of a failure to deactivate this DMN hub and in good agreement with previous reports of deactivation suppression in this region in SCZ (Salgado-Pineda et al., 2011). A similar finding was observed in the left hippocampus: While no group differences were found for the overall level of deactivation, we observed a failure in SCZ to continue the hippocampal deactivation also in the late RA phase. This effect was stronger in the peak voxel than the cluster analysis, pointing out that it possibly affects only hippocampal subregions. Both post-mortem and in vivo neuroimaging studies have highlighted a central role of the hippocampus in SCZ (Lieberman et al., 2018). Mikell et al. (2009) suggested that the hippocampus, together with the NAcc, could even be a potential target for high-frequency electrical stimulation in the treatment of positive symptoms in SCZ. Moreover, findings of hippocampal alterations are not restricted to the disease in general: Heckers and Konradi (2015) summarized that two main characteristics of SCZ, namely reality distortion and cognitive deficits, could root in impaired hippocampal functioning. Of particular interest for our research question, Nenadic et al (2015) compared brain structures of patients with BD and SCZ as well as healthy subjects. Besides common abnormalities in both diagnostic groups, structural deficits of the hippocampus only emerged in SCZ patients, setting apart the two disease groups.

BD patients also exhibited task-negative abnormalities relative to HC. In general, in the literature, DMN disruptions are a reported feature in patients with BD, including functional abnormalities in prefrontal regions, precuneus, PCC and the inferior parietal cortex (Gong et al., 2019; Zovetti et al., 2020). In our data, similar to MDD and SCZ, also BD patients showed a suppression of deactivation in the temporal DMN hub relative to healthy individuals. Since this abnormality occurred in both psychotic and affective patients, our findings of insufficient deactivation of temporal DMN nodes could represent a disease unspecific, transdiagnostic finding in the psychotic-affective syndrome.

The group-by-time effect in the parietal DMN region in BD needs to be interpreted with caution, because the analyses of peak and cluster both revealed aberrant dynamics throughout the anticipation phase, yet the effect direction was not consistent. Despite these inconsistencies, aberrant parietal DMN activation would generally match with previous reports: According to Ongür et al. (2010), recruitment of the parietal cortex is altered in patients with BD. Furthermore, in their work, this anomaly was correlated with mania severity.

In contrast to hypothesized effects in the posterior midline DMN based on the cited literature (Zovetti et al., 2020), we did not observe abnormalities in this region in BD. Besides possible task- or sample related reasons, the symptomatic history of our BD patients might be one cause for this: One of the

two studies referred to in the cited review included only BD patients with a positive history of psychotic symptoms (Khadka et al., 2013). Correspondingly, by comparing psychotic and non-psychotic BD patients, Zhong et al. (2019) suggested that FC alterations in the posterior midline DMN were restricted to psychotic BD patients. This would also be consistent with our results from a transdiagnostic perspective, as the effect was absent in BD.

Given that the direction of alterations reported in BD is mostly mixed across studies and bearing in mind that BD includes mental states ranging from mania to depression, a possible explanation might be that this diagnostic group is too heterogeneous and needs to be further subdivided in favour of a better characterization of DMN impairments.

Taking task-negative findings together, DMN deficits cut across all three clinical groups and align with the previous literature. At the phenomenological level, these results indicate that both affective and psychotic patients struggle to focus on 'cognitive' subsection the task at hand, that is, the phase in which response readiness needs to be kept up. However, as some DMN impairments were regionally different between the diagnostic groups, the suspected failure to successfully shift the focus of attention from the internal world to the external environment in patients could result from distinct neurobiological pathomechanisms, or there exists a spectrum of different degrees of regional susceptibility of DMN pathology that starts focally and, across the affective-psychosis spectrum, generalizes to the entire network in SCZ. Furthermore, considering the multifaceted, partly disease-specific deactivation impairments in patients, the DMN activation during the MID task, particularly with its possibility to specifically study early and late RA, holds a potential as source of biomarkers for larger studies that help to distinguish often highly complex clinical presentations of the psychotic-affective disorders.

#### **3.4.4 Disruptions in the interplay of large-scale brain networks during RA**

Modelling the dynamic factor revealed a certain sequential train of large-scale brain network activation during RA, including a strong pronunciation of VS (particularly the NAcc) responses during the initial phase, rising activation within nodes of the salience network throughout the anticipation phase and, conversely, stepwise DMN deactivation. Fox et al. (2005) were among the first to suggest that the human brain is organized into dynamic and in part anticorrelated functional brain networks. In this interplay, the salience network acts as a mediator, able to switch between a central executive network and the DMN, two networks that are involved in internally and externally oriented processes, respectively (Bressler & Menon, 2010; Menon & Uddin, 2010). The antagonistic relationship between the DMN and the salience network is reflected in their functional anticorrelation, for example in RS fMRI studies.

The characterization of brain-wide dynamics during RA supports the notion of such an intrinsic brain organization: Temporal aspects of bilateral VS activation indicate that it gets triggered immediately after the reward cue gets presented. While the salience network detects the reward-indicating cue, the reward system recognizes the potential win in this trial. Against the background of the association between VS responses to rewards, this finding further indicates that the recognition of the reward

indicating cue is accompanied by an initial rewarding experience. As the salience network also includes subcortical nodes, particularly in the VS and amygdala (Menon, 2015), increasing activation of the bilateral insula following strong early striatal responses not only matches previous reports of salience network responses to task demands, but also draws an image of the VS as an 'ignition' of the neural orchestration of RA. Furthermore, rising salience network activation might mirror efforts to switch from internally orientated processes to the task demands needed to obtain the reward. Additionally, decreases of several DMN nodes that parallel the increases in salience network activity match this image.

Such network-oriented conceptualization is increasingly extending current neurobiological models of psychiatric diseases, and it widens the search field for pathomechanisms underlying impairments in different domains of cognition, including reward processing. Williamson (2007) was among the first to propose disruptions in the coordination of distinct brain networks as a core feature in SCZ. In the light of our results it also emerges that reward-related dysfunctions in SCZ might be related to a causal chain of disruptions originating in initial activation in the reward circuitry: Bearing in mind that the salience network also includes nodes in the VS (Menon, 2015), our findings of blunted striatal responses in the initial phase of RA and a failure to sufficiently co-activate the SN throughout the anticipation phase are likely associated. Furthermore, several lines of evidence suggestive of a reduced FC between the reward circuitry and the salience network in SCZ corroborate the hypothesized causality of network impairments: On the one hand, previous RS investigations revealed decreased FC between the VS and the salience network, including the anterior insular cortex, in SCZ (Han et al., 2020; Karcher et al., 2019). Matching that Karcher et al. (2019) reported particularly decreased connectivity between the salience network and the left VS, we also observed a left-hemispheric dominance of striatal effects in SCZ. Only recently, Han et al. (2020) suggested that the connection between the salience network, including its insular nodes, and the VS could represent a treatment-success marker for antipsychotic treatments. On the other hand, our findings suggest that attenuated activation within the reward circuitry in SCZ also concerns mesencephalic neurons. Given that the FC between the midbrain and the insula during reward processing has been reported to be reduced in SCZ (Gradin et al., 2013), our similar findings of reductions in both the mesencephalic and insular responses substantiate the theory of a disturbed network interplay of these regions. That is, both findings could be related: On top of a reduced mesencephalic activation, reduced FC between the two regions further hinders the involvement of the insula. The extent of FC decrease between midbrain and insular regions was reportedly associated with the severity of psychotic symptoms (Gradin et al., 2013). In line with the literature, an explorative analysis of all network hubs within the pooled patient group demonstrated that early VS activation deficits were correlated with early and late salience network (data not shown in detail). This corroborated that only in SCZ patients, all three networks are affected with the salience network dysfunction possibly explaining specific portions of the DMN failure. With regard to affective disorders, it is of note that not only VS deficits, but also impairments of the salience network were largely absent in BD and MDD in our study.

Besides SCZ-specific dysfunctions in the reward system and the salience network, we also observed DMN disruptions that were restricted to psychotic patients. Against the background of the ‘triple network model’ (Menon, 2011) and at this stage of understanding, striatal and subsequent salience network failures might explain disease-specific suppression of the deactivation also in parietal and posterior DMN hubs. In harmony with this, the explorative analysis in the pooled patient group revealed a correlation between the early VS and early posterior and parietal DMN dysfunction.

Taken together, this shows that other networks involved in reward processing need to be considered in order to capture consequences dopaminergic dysfunctions during reward processing in SCZ holistically. Moreover, according to this hypothetical consideration, transdiagnostically shared impairments of *temporal* DMN regions could represent biomarkers that are not related to dysfunctions in the salience network and the reward circuitry. In other words, the presence of temporal DMN deficits appears to be independent of the occurrence of psychosis-specific DMN abnormalities.

### 3.4.5 Trans-nosological factors of RA dysfunctioning

Inspired by the transdiagnostic approach of the RDoC project (Insel et al., 2010), we show in the RA paradigm that the weaker the left hippocampal deactivation was during early RA, the higher the anhedonia scores were. In our data, anhedonia scores were also correlated with right temporal DMN alterations during early RA and left temporal DMN alterations in the late RA phase. However, as both anhedonia and temporal DMN deactivation were significantly present in all diagnostic groups relative to healthy participants, a large portion of the explained variance of anhedonia by temporal DMN hubs might be related to this step between illness and health. This was confirmed by confining the analysis to patients: Here, the left hippocampus of the early RA remained as a predictor for anhedonia. The slope of the regression lines were not significantly different.

Our finding suggestive of the anhedonia-predictive nature of the hippocampus across diagnostic conditions not only underlines the central role of this region in various psychopathologies, but also raises the question of how this physiological mechanism is actually constituted: Since the hippocampus activation synchronously decreased with the rest of the DMN and against the background of its involvement in the DMN (Menon, 2015), we understood hippocampal task effects as an indicator of efficient DMN deactivation. In this light, the positive correlation of hippocampal responses and anhedonia scores (see **Figure 46**) suggests that the severity of anhedonic symptoms might be reflected in the extent of the failure to deactivate the hippocampus as part of the DMN. Furthermore, given that anhedonia is a core feature of depression, our result also lends support to the plethora of studies highlighting suppressed deactivation of widely distributed elements of the DMN in depression (Grimm et al., 2009; Rodríguez-Cano et al., 2017; Sheline et al., 2009; Spies et al., 2017). Strikingly, our results demonstrate that reduced deactivation of the early left hippocampus was transdiagnostically linked to anhedonia severity regardless of the ICD-10 diagnosis. In contrast, anhedonia scores differed by diagnosis in our sample, with the hippocampal marker following the anhedonia scores rather than the

diagnostic group status. Of note, the left early RA hippocampal marker showed no patient/HC difference. Thus, another, unknown factor seems to come into play to span the correlation between the hippocampal early RA marker and anhedonia.

Taken together, our results provide evidence for a transdiagnostic correlation of the hippocampal deactivation during early RA with (current) anhedonia, a common symptom in both psychotic and affective disorders.

### **3.4.6 Methodological pitfalls and study limitations**

Finally, a number of potential weaknesses need to be considered. The first point is that although our group is of comparable size relative to other fMRI studies, the smaller sample size of BD and SCZ requires caution when considering results of group comparisons. This limitation underlines the difficulty of collecting data of critically ill patients. This limitation was particularly noticeable in the BD group, as this group is anyway quite heterogeneous due to its broad range of symptom states. Despite these conditions, interesting results in favour of our hypotheses of BD bridging psychotic and affective disorders became apparent.

Secondly, the characteristics of the sample also limit the generalizability of the results. Participants were recruited at different stages of their treatment: While some patients were close to the end of their hospitalization, others were willing to participate in the study during acute phases at the beginning of their treatment. Furthermore, inclusion rates were moderate, and many patients asked negated to participate in our study. Therefore, the selection is not completely random and thus not entirely representative. Still, the clinical characterization of the patients was carried out at the time the MR scanning and is thus representative for the current state.

Thirdly, due to the small groups, we could not disentangle effects of medication across all groups. As antipsychotics are targeting the dopamine system, it is important to consider the limitations of medication in psychotic patients when interpreting the results. Still, this does not invalidate our results entirely: The literature shows that the influence of this factor on our results appears to be restricted to typical antipsychotics with their direct D2-antagonistic action only: Multiple studies suggest that atypical antipsychotics are not related to the availability of dopamine transporter (a indirect measure of striatal dopaminergic traffic) in human brain (Kim et al., 2007; Artiges et al., 2017). In addition, Juckel et al. (2007) provided evidence that atypical psychotic medication does not affect VS activation patterns to monetary rewards.

Fourthly, even though we tested group effects of the RA test on a behavioural level (i.e., reaction times and slow-/non-response-rates) we included all trials in our SPM analyses. The dilemma regarding this decision is that although the comparability between successful trials may be considered more adequate, very slow trials or non-response to the actual target are also immanent to disease-related impairment of the reward system as a whole, particularly when the RA phase is studied. As the task is

very simple (button press after the white flash) and as participants with failed trials all showed sufficiently fast trials in the same run, it seems that fluctuating cognitive ability to maintain the focus plays in.

An additional possible source of error is that the control condition of the MID task did not require a pressing of a button by the study participants. As a result, neural underpinnings of motor preparation are not taken into account when contrasting monetary trials against control trials. Ideally, a button press would also be required in the control trials to create uniform conditions across all trials.

### 3.5 Conclusions

Despite its limitations, we believe that the present study could be a springboard for enhancing the understanding of neurobiological underpinnings of reward processing across psychotic and affective diagnostic boundaries. We confirm VS and salience network deficits in SCZ and demonstrate rather preserved VS responses in affective disorders. It is further highlighted that MDD, BD and SCZ are characterized by different disruptions of the DMN in the context of reward processing. The deactivation profiles of specific DMN regions appear to be affected to different degrees in the disorders, suggesting that these brain sites could potentially provide endophenotypes for a better characterization of clinical presentations in the affective-psychosis spectrum. Moreover, in SCZ, our observations suggest specific DMN alterations that originate in a failure of VS activation and propagate towards a failure to activate the salience network. Taken together, our investigations of the reward-related processes in MDD, BD and SCZ revealed involvement of at least three networks in RA, with a stronger role of the DMN than expected, and both shared and diagnosis specific alterations. For a hippocampal marker we demonstrate a transdiagnostic correlation with anhedonia, an example that functional testing may provide better objective markers for dysfunctional states and help to develop more targeted and personalized treatment approaches than current classifications.

Against the background of Zald and Treadway's differentiation of reward subsystems (2017) (see chapter 1.2), the present findings also imply that the RA phase of the MID task is suitable to capture multiple, partly distinct impairments across all disease groups examined here. Furthermore, this indicates that neural underpinnings of reward processing might be a rich source of biomarkers to more precisely characterize clinical presentations of the psychotic-affective spectrum, perhaps even across diagnostic boundaries.



## 4. General Discussion

### 4.1 Overall Summary

The overall goal of this thesis was to evaluate the role of the brain's reward system, particularly the VS, in patients of the psychotic-affective spectrum and healthy individuals for which their polygenetic risk for SCZ was known. Two separate projects provided the basis for this research effort: The first study showed that the connectivity of the NAcc is modulated by severe childhood experiences in that it increased their polygenetic influence further in the direction of a psychosis pattern. This finding not only confirms the key role of the NAcc in the pathophysiology of psychotic diseases, but also shows its potential to represent an endophenotype on which both genetic and environmental factors for SCZ risk converge in healthy people. The second experiment also added to the understanding of reward-related dysfunctions psychopathological conditions of the psychotic-affective spectrum as the results demonstrated that neural impairments exceed the reward system and affects at least two other large-scale brain networks, the salience network and DMN. Counter-intuitively, failure to activate VS and the salience network seemed to be a rather psychosis-specific phenomenon, whereas deactivation suppression of the DMN was common to all diagnostic groups. In general, alterations of the latter network are likely to reflect difficulties in focusing on external demands, albeit the anatomical localization of absent suppression varied between the clinical populations in addition to shared DMN alterations. Given that SCZ patients exhibited disruptions in all three networks studied here, we proposed that VS failures might result in DMN deficits specific to psychosis due to concatenation of neuronal processes during the anticipation of rewards. Apart from that, common DMN changes confirm that endophenotypes cutting across affective and psychotic disorders can be derived from a network-based model. One such transdiagnostic marker was hippocampal deactivation during early RA that correlated with current anhedonia, although it was not generally pathologically altered compared with HC.

Taken together, both studies confirm a key role of ventral striatal function in psychotic disorders. In addition, both studies have in common that they point to a diagnosis-independent phenomenon: The first project indicates that NAcc alterations are present in subjects with higher polygenetic risk, in the absence of clinical symptoms. The second project indicates that striatal changes in RA are a phenomenon rather specific to psychosis, whereas normal functioning of this region tends to prevail in affective disorders. Nevertheless, as other neuronal circuitries seemed to be affected in all patients during the anticipation of rewards, reward processing proved to remain as a potential research target which might provide treatment implications (e.g., network modulation by transcranial magnetic stimulation) in both psychotic and affective disorders.

## 4.2 The potential of reward processing in psychiatry

As mentioned in the introduction, current classification systems that are still anchored in Kraepelin's dichotomy show shortcomings in the context of psychotic and affective disorders, and an affective-psychosis spectrum has long been claimed. On the one hand, echoing Wittgenstein's metaphor of clouds, disorders of the respective spectrum are of a heterogeneous nature which thus implies a certain arbitrariness to diagnostic boundaries. Particularly in view of the substantial progress in psychiatric research since Kraepelin first introduced his *Zweiteilungsprinzip* (two entities principle) (1889), it became more and more apparent that disorders of the psychotic-affective spectrum are characterized by overlaps at the level of both physiology and symptomatology. To disentangle what Kraepelin described as an "amorphous mass" (Brockington & Leff, 1979) of psychotic and affective disorders with biological validity, the translation of neurobiological research findings into clinical practice is essential.

Given that reward processing is a fundamental aspect of a person's well-being, forming the basis of pleasure, but also motivation and goal-seeking as part of our everyday life, our findings conforming to respective impairments across all three disease groups propose that it is a promising research target for a better understanding of psychotic and affective clinical presentations. In this sense, our observations complement this assumption by indicating that RA is not limited to the dopaminergic reward system in the strict sense, but requires the successful recruitment of other large-scale brain networks, particularly the DMN. Particularly, finding that DMN parameters predict clinical reward scores prior to VS parameters is indicative that disturbances of the VS seem not a prerequisite for disturbed RA. This high potential of reward processing provides hope for the establishment of related biologically validated subtypes which would foster the selection of treatment strategies tailored to the individual needs of patients.

## 4.3 The diminution of the phenomenological reduction

As implied in the introduction, the categorization of verbally reported symptoms are an additional factor that complicates psychiatric diagnosis due to their low biological validity. Sigmund Freud, who was among the pioneers in the exploration and treatment of mental disorders, already recognized this weakness and longed for a remedy by unveiling the biological basis of the mental disorders and thus bridging the mind/body problem (Erreich, 2016). However, as techniques to examine the brain were in their infancy in Freud's days, he had to settle for a meaning-based approach by elaborately deciphering the somatic and behavioural symptoms reported by his patients.

Ever since, a century has passed which, as has also been shown in this work, was marked by remarkable technical innovations that not only helped illuminate the human brain, but also allowed to characterize disease-related changes in vivo in great detail. But does this imply that the dream of Freud and many others in the early days of psychiatry has been sufficiently fulfilled? Although the neurobiological examination of psychiatric disorders led to substantial improvements in the understanding of

mental illnesses, clustering of symptoms into a group still entails a strong phenomenological reduction, as the same symptom may root from different biological mechanisms. In our study, for example, network disturbances in RA processing were different between the clinical groups which justifies this order to some degree, but the hierarchy of the network deficiencies needs to be investigated in more detail. In this respect, a new intermediate level of phenomena – that of physiological (e.g., fMRI) data – is likely to dominate the scene. Still, in contrast to traditional symptom classifications, translating neurophysiological findings entails a considerable advancement in biological validity of diagnostic categories that could only have been wished for in the days of Kraepelin and Freud.

#### **4.4 The potential of neurobiological measures to overcome the classification of verbally reported symptoms**

Against the background of these advances, the question arises whether modern neuroimaging techniques allow a further approximation of the subjective experience of mental illness disease thus expanding the capture of acute clinical conditions. A simple thought experiment by the philosopher Thomas Nagel might enhance clarity: In his essay ‘What it’s really like to be a bat?’ (1974), Nagel argues that even if we precisely knew all neural correlates of a bat’s echolocation-based perception, we would still not know what it is like to have such echolocation perceptual experience. Transferred to the neurobiological assessment of psychiatric diseases, this sobering reminder of the mind/body-problem implies that the path to actual inner experiences in mental disorders remains blocked. This may be particularly relevant for psychotic disease more than affective symptoms that at least temporarily lie within typical human experience.

What role is played by research findings like those of the predictive quality of the hippocampus for anhedonia in this debate? Neurobiological correlates of symptom domains within the framework of the RDoC project bring diagnostics one step closer to a more objective view of the actual suffering of patients and, in a sense, bypass both the mind/body-problem and heterogeneity diagnostic categories. Although our DMN results can only be considered as an initial step in this direction, it can still be concluded that establishing transdiagnostic physiological symptom markers is one promising path to develop more biologically targeted treatment approaches.



## References

- 1000 Genomes Project Consortium, Auton, A., Brooks, L. D., Durbin, R. M., Garrison, E. P., Kang, H. M., Korbel, J. O., Marchini, J. L., McCarthy, S., McVean, G. A., & Abecasis, G. R. (2015). A global reference for human genetic variation. *Nature*, *526*(7571), 68–74.
- Abel, K. M., Drake, R., & Goldstein, J. M. (2010). Sex differences in schizophrenia. *International Review of Psychiatry*, *22*(5), 417–428.
- Abler, B., Greenhouse, I., Ongur, D., Walter, H., & Heckers, S. (2008). Abnormal reward system activation in mania. *Neuropsychopharmacology: Official Publication of the American College of Neuropsychopharmacology*, *33*(9), 2217–2227.
- Achterberg, M., Bakermans-Kranenburg, M. J., van Ijzendoorn, M. H., van der Meulen, M., Tottenham, N., & Crone, E. A. (2018). Distinctive heritability patterns of subcortical-prefrontal cortex resting state connectivity in childhood: A twin study. *NeuroImage*, *175*, 138–149.
- Agcaoglu, O., Miller, R., Damaraju, E., Rashid, B., Bustillo, J., Cetin, M. S., Van Erp, T. G. M., McEwen, S., Preda, A., Ford, J. M., Lim, K. O., Manoach, D. S., Mathalon, D. H., Potkin, S. G., & Calhoun, V. D. (2018). Decreased hemispheric connectivity and decreased intra- and inter- hemisphere asymmetry of resting state functional network connectivity in schizophrenia. *Brain Imaging and Behavior*, *12*(3), 615–630.
- Allen, A. J., Griss, M. E., Folley, B. S., Hawkins, K. A., & Pearlson, G. D. (2009). Endophenotypes in schizophrenia: a selective review. *Schizophrenia Research*, *109*(1-3), 24–37.
- Alwi, Z. B. (2005). The Use of SNPs in Pharmacogenomics Studies. *The Malaysian Journal of Medical Sciences: MJMS*, *12*(2), 4–12.
- American Psychiatric Association. (2013). *Diagnostic and Statistical Manual of Mental Disorders (DSM-5®)*. American Psychiatric Pub.
- Andreasen, N. C. (1982). Negative symptoms in schizophrenia. Definition and reliability. *Archives of General Psychiatry*, *39*(7), 784–788.
- Andreasen, N. C. (2007). DSM and the death of phenomenology in america: an example of unintended consequences. *Schizophrenia Bulletin*, *33*(1), 108–112.

- Angst, J. (1980). [Course of unipolar depressive, bipolar manic-depressive, and schizoaffective disorders. Results of a prospective longitudinal study (author's transl)]. *Fortschritte der Neurologie, Psychiatrie, und ihrer Grenzgebiete*, 48(1), 3–30.
- Apicella, P., Ljungberg, T., Scarnati, E., & Schultz, W. (1991). Responses to reward in monkey dorsal and ventral striatum. In *Experimental Brain Research* (Vol. 85, Issue 3). <https://doi.org/10.1007/bf00231732>
- Arbabshirani, M. R., Castro, E., & Calhoun, V. D. (2014). Accurate classification of schizophrenia patients based on novel resting-state fMRI features. *Conference Proceedings: ... Annual International Conference of the IEEE Engineering in Medicine and Biology Society. IEEE Engineering in Medicine and Biology Society. Conference, 2014*, 6691–6694.
- Arias-Carrión, O., & Pöppel, E. (2007). Dopamine, learning, and reward-seeking behavior. *Acta Neurobiologiae Experimentalis*, 67(4), 481–488.
- Artiges, E., Leroy, C., Dubol, M., Prat, M., Pepin, A., Mabondo, A., de Beaupaire, R., Beaufils, B., Korwin, J.-P., Galinowski, A., D'Albis, M.-A., Santiago-Ribeiro, M.-J., Granger, B., Tzavara, E. T., Martinot, J.-L., & Trichard, C. (2017). Striatal and Extrastriatal Dopamine Transporter Availability in Schizophrenia and Its Clinical Correlates: A Voxel-Based and High-Resolution PET Study. *Schizophrenia Bulletin*, 43(5), 1134–1142.
- Ashburner, J. (2007). A fast diffeomorphic image registration algorithm. In *NeuroImage* (Vol. 38, Issue 1, pp. 95–113). <https://doi.org/10.1016/j.neuroimage.2007.07.007>
- Aston-Jones, G., & Waterhouse, B. (2016). Locus coeruleus: From global projection system to adaptive regulation of behavior. *Brain Research*, 1645, 75–78.
- Azorin, J.-M., Kaladjian, A., & Fakra, E. (2005). Aspects actuels du trouble schizo-affectif. *L'Encéphale*, 31(3), 359–365.
- Baliki, M. N., Mansour, A., Baria, A. T., Huang, L., Berger, S. E., Fields, H. L., & Apkarian, A. V. (2013). Parceling human accumbens into putative core and shell dissociates encoding of values for reward and pain. *The Journal of Neuroscience: The Official Journal of the Society for Neuroscience*, 33(41), 16383–16393.
- Barch, D. M., Bustillo, J., Gaebel, W., Gur, R., Heckers, S., Malaspina, D., Owen, M. J., Schultz, S., Tandon, R., Tsuang, M., Van Os, J., & Carpenter, W. (2013). Logic and justification for dimensional assessment of symptoms and related clinical phenomena in psychosis: Relevance to DSM-5. In *Schizophrenia Research* (Vol. 150, Issue 1, pp. 15–20). <https://doi.org/10.1016/j.schres.2013.04.027>

- Barch, D. M., Treadway, M. T., & Schoen, N. (2014). Effort, anhedonia, and function in schizophrenia: reduced effort allocation predicts amotivation and functional impairment. *Journal of Abnormal Psychology, 123*(2), 387–397.
- Barkhuizen, W., Pain, O., Dudbridge, F., & Ronald, A. (2020). Genetic overlap between psychotic experiences in the community across age and with psychiatric disorders. *Translational Psychiatry, 10*(1), 86.
- Barnes, J. (2001). Visual hallucinations in Parkinson's disease: a review and phenomenological survey. *Journal of Neurology, Neurosurgery, and Psychiatry, 70*(6), 727–733.
- Barnes, T. R. E., Leeson, V. C., Mutsatsa, S. H., Watt, H. C., Hutton, S. B., & Joyce, E. M. (2008). Duration of untreated psychosis and social function: 1-year follow-up study of first-episode schizophrenia. *The British Journal of Psychiatry: The Journal of Mental Science, 193*(3), 203–209.
- Barnett, J. H., & Smoller, J. W. (2009). The genetics of bipolar disorder. *Neuroscience, 164*(1), 331–343.
- Bas-Hoogendam, J. M., Blackford, J. U., Brühl, A. B., Blair, K. S., van der Wee, N. J. A., & Westenberg, P. M. (2016). Neurobiological candidate endophenotypes of social anxiety disorder. *Neuroscience and Biobehavioural Reviews, 71*, 362–378.
- Beauchaine, T. P., & Constantino, J. N. (2017). Redefining the endophenotype concept to accommodate transdiagnostic vulnerabilities and etiological complexity. *Biomarkers in Medicine, 11*(9), 769–780.
- Bebbington, P., & Ramana, R. (1995). The epidemiology of bipolar affective disorder. *Social Psychiatry and Psychiatric Epidemiology, 30*(6), 279–292.
- Bechara, A., Damasio, A. R., Damasio, H., & Anderson, S. W. (1994). Insensitivity to future consequences following damage to human prefrontal cortex. *Cognition, 50*(1-3), 7–15.
- Beckmann, C. F., DeLuca, M., Devlin, J. T., & Smith, S. M. (2005). Investigations into resting-state connectivity using independent component analysis. In *Philosophical Transactions of the Royal Society B: Biological Sciences* (Vol. 360, Issue 1457, pp. 1001–1013). <https://doi.org/10.1098/rstb.2005.1634>
- Behzadi, Y., Restom, K., Liu, J., & Liu, T. T. (2007). A component based noise correction method (CompCor) for BOLD and perfusion based fMRI. *NeuroImage, 37*(1), 90–101.
- Belmaker, R. H. (2004). Bipolar disorder. *The New England Journal of Medicine, 351*(5), 476–486.
- Bentall, R. P., & Fernyhough, C. (2008). Social predictors of psychotic experiences: specificity and psychological mechanisms. *Schizophrenia Bulletin, 34*(6), 1012–1020.

- Bentall, R. P., Wickham, S., Shevlin, M., & Varese, F. (2012). Do specific early-life adversities lead to specific symptoms of psychosis? A study from the 2007 the Adult Psychiatric Morbidity Survey. *Schizophrenia Bulletin*, *38*(4), 734–740.
- Berghorst, L. H., Kumar, P., Greve, D. N., Deckersbach, T., Ongur, D., Dutra, S. J., & Pizzagalli, D. A. (2016). Stress and reward processing in bipolar disorder: a functional magnetic resonance imaging study. *Bipolar Disorders*, *18*(7), 602–611.
- Bermpohl, F., Dalanay, U., Kahnt, T., Sajonz, B., Heimann, H., Ricken, R., Stoy, M., Hägele, C., Schlagenhaut, F., Adli, M., Wrase, J., Ströhle, A., Heinz, A., & Bauer, M. (2009). A preliminary study of increased amygdala activation to positive affective stimuli in mania. *Bipolar Disorders*, *11*(1), 70–75.
- Bernstein, D. P., & Fink, L. (1998). *Childhood Trauma Questionnaire: A Retrospective Self-report : Manual*.
- Bernstein, D. P., Stein, J. A., Newcomb, M. D., Walker, E., Pogge, D., Ahluvalia, T., Stokes, J., Handelsman, L., Medrano, M., Desmond, D., & Zule, W. (2003). Development and validation of a brief screening version of the Childhood Trauma Questionnaire. *Child Abuse & Neglect*, *27*(2), 169–190.
- Berridge, K. C., & Robinson, T. E. (1998). What is the role of dopamine in reward: hedonic impact, reward learning, or incentive salience? In *Brain Research Reviews* (Vol. 28, Issue 3, pp. 309–369).  
[https://doi.org/10.1016/s0165-0173\(98\)00019-8](https://doi.org/10.1016/s0165-0173(98)00019-8)
- Bersani, G., Orlandi, V., Kotzalidis, G. D., & Pancheri, P. (2002). Cannabis and schizophrenia: impact on onset, course, psychopathology and outcomes. *European Archives of Psychiatry and Clinical Neuroscience*, *252*(2), 86–92.
- Bigos, K. L., & Weinberger, D. R. (2010). Imaging genetics—days of future past. *NeuroImage*, *53*(3), 804–809.
- Bipolar Disorder and Schizophrenia Working Group of the Psychiatric Genomics Consortium. Electronic address: douglas.ruderfer@vanderbilt.edu, & Bipolar Disorder and Schizophrenia Working Group of the Psychiatric Genomics Consortium. (2018). Genomic Dissection of Bipolar Disorder and Schizophrenia, Including 28 Subphenotypes. *Cell*, *173*(7), 1705–1715.e16.
- Biswal, B., Yetkin, F. Z., Haughton, V. M., & Hyde, J. S. (1995). Functional connectivity in the motor cortex of resting human brain using echo-planar MRI. *Magnetic Resonance in Medicine: Official Journal of the Society of Magnetic Resonance in Medicine / Society of Magnetic Resonance in Medicine*, *34*(4), 537–541.



- Björklund, A., & Dunnett, S. B. (2007). Dopamine neuron systems in the brain: an update. In *Trends in Neurosciences* (Vol. 30, Issue 5, pp. 194–202). <https://doi.org/10.1016/j.tins.2007.03.006>
- Brandl, F., Avram, M., Weise, B., Shang, J., Simões, B., Bertram, T., Hoffmann Ayala, D., Penzel, N., Gürsel, D. A., Bäuml, J., Wohlschläger, A. M., Vukadinovic, Z., Koutsouleris, N., Leucht, S., & Sorg, C. (2019). Specific Substantial Dysconnectivity in Schizophrenia: A Transdiagnostic Multimodal Meta-analysis of Resting-State Functional and Structural Magnetic Resonance Imaging Studies. *Biological Psychiatry*, *85*(7), 573–583.
- Bressler, S. L., & Menon, V. (2010). Large-scale brain networks in cognition: emerging methods and principles. In *Trends in Cognitive Sciences* (Vol. 14, Issue 6, pp. 277–290). <https://doi.org/10.1016/j.tics.2010.04.004>
- Brockington, I. F., & Leff, J. P. (1979). Schizo-affective psychosis: definitions and incidence. In *Psychological Medicine* (Vol. 9, Issue 1, pp. 91–99). <https://doi.org/10.1017/s0033291700021590>
- Brunelin, J., Fecteau, S., & Suaud-Chagny, M.-F. (2013). Abnormal striatal dopamine transmission in schizophrenia. *Current Medicinal Chemistry*, *20*(3), 397–404.
- Buckley, P. F., Miller, B. J., Lehrer, D. S., & Castle, D. J. (2009). Psychiatric Comorbidities and Schizophrenia. In *Schizophrenia Bulletin* (Vol. 35, Issue 2, pp. 383–402). <https://doi.org/10.1093/schbul/sbn135>
- Buckner, R. L. (2013). The brain's default network: origins and implications for the study of psychosis. *Dialogues in Clinical Neuroscience*, *15*(3), 351–358.
- Buckner, R. L., Andrews-Hanna, J. R., & Schacter, D. L. (2008). The Brain's Default Network. In *Annals of the New York Academy of Sciences* (Vol. 1124, Issue 1, pp. 1–38). <https://doi.org/10.1196/annals.1440.011>
- Bumgarner, R. (2013). Overview of DNA microarrays: types, applications, and their future. *Current Protocols in Molecular Biology / Edited by Frederick M. Ausubel ... [et Al.], Chapter 22, Unit 22.1.*
- Burgess, N., Maguire, E. A., & O'Keefe, J. (2002). The Human Hippocampus and Spatial and Episodic Memory. In *Neuron* (Vol. 35, Issue 4, pp. 625–641). [https://doi.org/10.1016/s0896-6273\(02\)00830-9](https://doi.org/10.1016/s0896-6273(02)00830-9)
- Bush, G., Vogt, B. A., Holmes, J., Dale, A. M., Greve, D., Jenike, M. A., & Rosen, B. R. (2002). Dorsal anterior cingulate cortex: a role in reward-based decision making. *Proceedings of the National Academy of Sciences of the United States of America*, *99*(1), 523–528.
- Caetano, S. C., Fonseca, M., Hatch, J. P., Olvera, R. L., Nicoletti, M., Hunter, K., Lafer, B., Pliszka, S. R., & Soares, J. C. (2007). Medial temporal lobe abnormalities in pediatric unipolar depression. *Neuroscience Letters*, *427*(3), 142–147.

- Cancel, A., Dallel, S., Zine, A., El-Hage, W., & Fakra, E. (2019). Understanding the link between childhood trauma and schizophrenia: A systematic review of neuroimaging studies. *Neuroscience and Biobehavioural Reviews*, *107*, 492–504.
- Cardno, A. G., & Owen, M. J. (2014). Genetic relationships between schizophrenia, bipolar disorder, and schizoaffective disorder. *Schizophrenia Bulletin*, *40*(3), 504–515.
- Carver, C. S., & White, T. L. (1994). Behavioural inhibition, behavioural activation, and affective responses to impending reward and punishment: The BIS/BAS Scales. In *Journal of Personality and Social Psychology* (Vol. 67, Issue 2, pp. 319–333). <https://doi.org/10.1037/0022-3514.67.2.319>
- Caseras, X., Lawrence, N. S., Murphy, K., Wise, R. G., & Phillips, M. L. (2013). Ventral Striatum Activity in Response to Reward: Differences Between Bipolar I and II Disorders. In *American Journal of Psychiatry* (Vol. 170, Issue 5, pp. 533–541). <https://doi.org/10.1176/appi.ajp.2012.12020169>
- Cerimele, J. M., Chwastiak, L. A., Chan, Y.-F., Harrison, D. A., & Unützer, J. (2013). The presentation, recognition and management of bipolar depression in primary care. *Journal of General Internal Medicine*, *28*(12), 1648–1656.
- Chao-Gan, Y., & Yu-Feng, Z. (2010). DPARSF: A MATLAB Toolbox for “Pipeline” Data Analysis of Resting-State fMRI. *Frontiers in Systems Neuroscience*, *4*, 13.
- Chase, H. W., Nusslock, R., Almeida, J. R., Forbes, E. E., LaBarbara, E. J., & Phillips, M. L. (2013). Dissociable patterns of abnormal frontal cortical activation during anticipation of an uncertain reward or loss in bipolar versus major depression. *Bipolar Disorders*, *15*(8), 839–854.
- Chen, J., Rashid, B., Yu, Q., Liu, J., Lin, D., Du, Y., Sui, J., & Calhoun, V. D. (2018). Variability in Resting State Network and Functional Network Connectivity Associated With Schizophrenia Genetic Risk: A Pilot Study. *Frontiers in Neuroscience*, *12*, 114.
- Chesney, E., Goodwin, G. M., & Fazel, S. (2014). Risks of all-cause and suicide mortality in mental disorders: a meta-review. *World Psychiatry: Official Journal of the World Psychiatric Association*, *13*(2), 153–160.
- Chung, Y. S., & Barch, D. M. (2016). Frontal-striatum dysfunction during reward processing: Relationships to amotivation in schizophrenia. *Journal of Abnormal Psychology*, *125*(3), 453–469.
- Cloninger, C. R. (1991). THE TRIDIMENSIONAL PERSONALITY QUESTIONNAIRE: U.S. NORMATIVE DATA. *Pharmacological Reports: PR*, *69*(7), 1047.

- Cole, M. W., Pathak, S., & Schneider, W. (2010). Identifying the brain's most globally connected regions. *NeuroImage*, 49(4), 3132–3148.
- Cooper, J. A., Arulpragasam, A. R., & Treadway, M. T. (2018). Anhedonia in depression: biological mechanisms and computational models. *Current Opinion in Behavioural Sciences*, 22, 128–135.
- Coulter, C., Baker, K. K., & Margolis, R. L. (2019). Specialized Consultation for Suspected Recent-onset Schizophrenia: Diagnostic Clarity and the Distorting Impact of Anxiety and Reported Auditory Hallucinations. *Journal of Psychiatric Practice*, 25(2), 76–81.
- Craddock, N., O'Donovan, M. C., & Owen, M. J. (2005). The genetics of schizophrenia and bipolar disorder: dissecting psychosis. *Journal of Medical Genetics*, 42(3), 193–204.
- Craddock, N., & Owen, M. J. (2005). The beginning of the end for the Kraepelinian dichotomy. In *British Journal of Psychiatry* (Vol. 186, Issue 5, pp. 364–366). <https://doi.org/10.1192/bjp.186.5.364>
- Crisafulli, C., Drago, A., Calabrò, M., Spina, E., & Serretti, A. (2015). A molecular pathway analysis informs the genetic background at risk for schizophrenia. *Progress in Neuro-Psychopharmacology & Biological Psychiatry*, 59, 21–30.
- Cross-Disorder Group of the Psychiatric Genomics Consortium, Lee, S. H., Ripke, S., Neale, B. M., Faraone, S. V., Purcell, S. M., Perlis, R. H., Mowry, B. J., Thapar, A., Goddard, M. E., Witte, J. S., Absher, D., Agartz, I., Akil, H., Amin, F., Andreassen, O. A., Anjorin, A., Anney, R., Anttila, V., ... International Inflammatory Bowel Disease Genetics Consortium (IBDGC). (2013). Genetic relationship between five psychiatric disorders estimated from genome-wide SNPs. *Nature Genetics*, 45(9), 984–994.
- Crump, C., Sundquist, K., Winkleby, M. A., & Sundquist, J. (2013). Comorbidities and Mortality in Bipolar Disorder. In *JAMA Psychiatry* (Vol. 70, Issue 9, p. 931). <https://doi.org/10.1001/jamapsychiatry.2013.1394>
- Cuijpers, P., Stringaris, A., & Wolpert, M. (2020). Treatment outcomes for depression: challenges and opportunities. *The Lancet. Psychiatry*, 7(11), 925–927.
- Cuijpers, P., Vogelzangs, N., Twisk, J., Kleiboer, A., Li, J., & Penninx, B. W. (2014). Comprehensive meta-analysis of excess mortality in depression in the general community versus patients with specific illnesses. *The American Journal of Psychiatry*, 171(4), 453–462.
- Daalman, K., Diederik, K. M. J., Derks, E. M., van Lutterveld, R., Kahn, R. S., & Sommer, I. E. C. (2012). Childhood trauma and auditory verbal hallucinations. *Psychological Medicine*, 42(12), 2475–2484.

- Damoiseaux, J. S., Beckmann, C. F., Arigita, E. J. S., Barkhof, F., Scheltens, P., Stam, C. J., Smith, S. M., & Rombouts, S. A. R. B. (2008). Reduced resting-state brain activity in the “default network” in normal aging. *Cerebral Cortex*, 18(8), 1856–1864.
- Dandash, O., Fornito, A., Lee, J., Keefe, R. S. E., Chee, M. W. L., Adcock, R. A., Pantelis, C., Wood, S. J., & Harrison, B. J. (2014). Altered striatal functional connectivity in subjects with an at-risk mental state for psychosis. *Schizophrenia Bulletin*, 40(4), 904–913.
- Daniel, R., & Pollmann, S. (2014). A universal role of the ventral striatum in reward-based learning: evidence from human studies. *Neurobiology of Learning and Memory*, 114, 90–100.
- D’Argembeau, A. (2013). On the role of the ventromedial prefrontal cortex in self-processing: the valuation hypothesis. *Frontiers in Human Neuroscience*, 7, 372.
- Deister, A., & Marneros, A. (1993). Subtypes in schizophrenic disorders: frequencies in long-term course and premorbid features. In *Social Psychiatry and Psychiatric Epidemiology* (Vol. 28, Issue 4, pp. 164–171). <https://doi.org/10.1007/bf00797318>
- Delaneau, O., Marchini, J., & Zagury, J.-F. (2011). A linear complexity phasing method for thousands of genomes. *Nature Methods*, 9(2), 179–181.
- Delaveau, P., Jabourian, M., Lemogne, C., Guionnet, S., Bergouignan, L., & Fossati, P. (2011). Brain effects of antidepressants in major depression: a meta-analysis of emotional processing studies. *Journal of Affective Disorders*, 130(1-2), 66–74.
- DelBello, M. P., Hanseman, D., Adler, C. M., Fleck, D. E., & Strakowski, S. M. (2007). Twelve-Month Outcome of Adolescents With Bipolar Disorder Following First Hospitalization for a Manic or Mixed Episode. In *American Journal of Psychiatry* (Vol. 164, Issue 4, pp. 582–590). <https://doi.org/10.1176/ajp.2007.164.4.582>
- Der-Avakian, A., & Markou, A. (2012). The neurobiology of anhedonia and other reward-related deficits. *Trends in Neurosciences*, 35(1), 68–77.
- Desai, P. R., Lawson, K. A., Barner, J. C., & Rascati, K. L. (2013). Estimating the direct and indirect costs for community-dwelling patients with schizophrenia: Schizophrenia-related costs for community-dwellers. *Journal of Pharmaceutical Health Services Research: An Official Journal of the Royal Pharmaceutical Society of Great Britain*, 4(4), 187–194.

- de Vos, F., Koini, M., Schouten, T. M., Seiler, S., van der Grond, J., Lechner, A., Schmidt, R., de Rooij, M., & Rombouts, S. A. R. B. (2018). A comprehensive analysis of resting state fMRI measures to classify individual patients with Alzheimer's disease. *NeuroImage*, *167*, 62–72.
- Dezhina, Z., Ranlund, S., Kyriakopoulos, M., Williams, S. C. R., & Dima, D. (2019). A systematic review of associations between functional MRI activity and polygenic risk for schizophrenia and bipolar disorder. *Brain Imaging and Behavior*, *13*(3), 862–877.
- Dichter, G. S., Damiano, C. A., & Allen, J. A. (2012). Reward circuitry dysfunction in psychiatric and neurodevelopmental disorders and genetic syndromes: animal models and clinical findings. *Journal of Neurodevelopmental Disorders*, *4*(1), 19.
- Dichter, G. S., Kozink, R. V., McClernon, F. J., & Smoski, M. J. (2012). Remitted major depression is characterized by reward network hyperactivation during reward anticipation and hypoactivation during reward outcomes. *Journal of Affective Disorders*, *136*(3), 1126–1134.
- Diekhof, E. K., Kaps, L., Falkai, P., & Gruber, O. (2012). The role of the human ventral striatum and the medial orbitofrontal cortex in the representation of reward magnitude - an activation likelihood estimation meta-analysis of neuroimaging studies of passive reward expectancy and outcome processing. *Neuropsychologia*, *50*(7), 1252–1266.
- Dolcos, F., LaBar, K. S., & Cabeza, R. (2004). Dissociable effects of arousal and valence on prefrontal activity indexing emotional evaluation and subsequent memory: an event-related fMRI study. *NeuroImage*, *23*(1), 64–74.
- Drysdale, A. T., Grosenick, L., Downar, J., Dunlop, K., Mansouri, F., Meng, Y., Fetcho, R. N., Zebley, B., Oathes, D. J., Etkin, A., Schatzberg, A. F., Sudheimer, K., Keller, J., Mayberg, H. S., Gunning, F. M., Alexopoulos, G. S., Fox, M. D., Pascual-Leone, A., Voss, H. U., ... Liston, C. (2017). Resting-state connectivity biomarkers define neurophysiological subtypes of depression. *Nature Medicine*, *23*(1), 28–38.
- Dutta, A., McKie, S., Downey, D., Thomas, E., Juhasz, G., Arnone, D., Elliott, R., Williams, S., Deakin, J. F. W., & Anderson, I. M. (2019). Regional default mode network connectivity in major depressive disorder: modulation by acute intravenous citalopram. *Translational Psychiatry*, *9*(1), 116.
- Ebdrup, B. H., Glenthøj, B., Rasmussen, H., Aggernaes, B., Langkilde, A. R., Paulson, O. B., Lublin, H., Skimminge, A., & Baaré, W. (2010). Hippocampal and caudate volume reductions in antipsychotic-naïve first-episode schizophrenia. *Journal of Psychiatry & Neuroscience: JPN*, *35*(2), 95–104.

- Ebert, A., & Bär, K.-J. (2010). Emil Kraepelin: A pioneer of scientific understanding of psychiatry and psychopharmacology. *Indian Journal of Psychiatry, 52*(2), 191–192.
- Eberle C, Peterse Y, Jukic F, Müller-Myhsok B, Czamara D, Martins J, et al. Endophenotype Potential of Nucleus Accumbens Functional Connectivity: Effects of Polygenic Risk for Schizophrenia Interacting with Childhood Adversity. *J Psychiatry Brain Sci.* 2019;4:e190011. <https://doi.org/10.20900/jpbs.20190011>
- Erreich, A. (2016). An Exchange with Thomas Nagel: The Mind-Body Problem and Psychoanalysis. *Journal of the American Psychoanalytic Association, 64*(2), 389–403.
- Esslinger, C., Englisch, S., Inta, D., Rausch, F., Schirmbeck, F., Mier, D., Kirsch, P., Meyer-Lindenberg, A., & Zink, M. (2012). Ventral striatal activation during attribution of stimulus saliency and reward anticipation is correlated in unmedicated first episode schizophrenia patients. *Schizophrenia Research, 140*(1-3), 114–121.
- Esteller, M. (2008). Epigenetics in evolution and disease. In *The Lancet* (Vol. 372, pp. S90–S96). [https://doi.org/10.1016/s0140-6736\(08\)61887-5](https://doi.org/10.1016/s0140-6736(08)61887-5)
- Faden, J., & Citrome, L. (2019). Resistance is not futile: treatment-refractory schizophrenia – overview, evaluation and treatment. In *Expert Opinion on Pharmacotherapy* (Vol. 20, Issue 1, pp. 11–24). <https://doi.org/10.1080/14656566.2018.1543409>
- Fagiolini, A., Coluccia, A., Maina, G., Forgiione, R. N., Goracci, A., Cuomo, A., & Young, A. H. (2015). Diagnosis, Epidemiology and Management of Mixed States in Bipolar Disorder. *CNS Drugs, 29*(9), 725–740.
- Fischer, A. S., Whitfield-Gabrieli, S., Roth, R. M., Brunette, M. F., & Green, A. I. (2014). Impaired functional connectivity of brain reward circuitry in patients with schizophrenia and cannabis use disorder: Effects of cannabis and THC. *Schizophrenia Research, 158*(1-3), 176–182.
- Fletcher, P. C., & Frith, C. D. (2009). Perceiving is believing: a Bayesian approach to explaining the positive symptoms of schizophrenia. *Nature Reviews. Neuroscience, 10*(1), 48–58.
- Forlim, C. G., Klock, L., Bächle, J., Stoll, L., Giemsa, P., Fuchs, M., Schoofs, N., Montag, C., Gallinat, J., & Kühn, S. (2020). Reduced Resting-State Connectivity in the Precuneus is correlated with Apathy in Patients with Schizophrenia. *Scientific Reports, 10*(1), 2616.
- Fox, M. D., Snyder, A. Z., Vincent, J. L., Corbetta, M., Van Essen, D. C., & Raichle, M. E. (2005). The human brain is intrinsically organized into dynamic, anticorrelated functional networks. *Proceedings of the National Academy of Sciences of the United States of America, 102*(27), 9673–9678.

- Freedman, R., Leonard, S., Olincy, A., Kaufmann, C. A., Malaspina, D., Robert Cloninger, C., Svrakic, D., Faraone, S. V., & Tsuang, M. T. (2001). Evidence for the multigenic inheritance of schizophrenia. In *American Journal of Medical Genetics* (Vol. 105, Issue 8, pp. 794–800). <https://doi.org/10.1002/ajmg.10100>
- Frey, B. N., Andreatza, A. C., Nery, F. G., Martins, M. R., Quevedo, J., Soares, J. C., & Kapczinski, F. (2007). The role of hippocampus in the pathophysiology of bipolar disorder. In *Behavioural Pharmacology* (Vol. 18, Issues 5-6, pp. 419–430). <https://doi.org/10.1097/fbp.0b013e3282df3cde>
- Friston, K. J., Frith, C. D., Liddle, P. F., & Frackowiak, R. S. (1993). Functional connectivity: the principal-component analysis of large (PET) data sets. *Journal of Cerebral Blood Flow and Metabolism: Official Journal of the International Society of Cerebral Blood Flow and Metabolism*, 13(1), 5–14.
- Friston, K. J., Harrison, L., & Penny, W. (2003). Dynamic causal modelling. *NeuroImage*, 19(4), 1273–1302.
- Friston, K. J., Penny, W. D., & Glaser, D. E. (2005). Conjunction revisited. *NeuroImage*, 25(3), 661–667.
- Frye, M. A., Watzl, J., Banakar, S., O'Neill, J., Mintz, J., Davanzo, P., Fischer, J., Chirichigno, J. W., Ventura, J., Elman, S., Tsuang, J., Walot, I., & Thomas, M. A. (2007). Increased anterior cingulate/medial prefrontal cortical glutamate and creatine in bipolar depression. *Neuropsychopharmacology: Official Publication of the American College of Neuropsychopharmacology*, 32(12), 2490–2499.
- Fusar-Poli, P., & Meyer-Lindenberg, A. (2013). Striatal presynaptic dopamine in schizophrenia, part II: meta-analysis of [(18)F]/[(11)C]-DOPA PET studies. *Schizophrenia Bulletin*, 39(1), 33–42.
- Gage, S. H., Zammit, S., & Hickman, M. (2013). Stronger evidence is needed before accepting that cannabis plays an important role in the aetiology of schizophrenia in the population. *F1000 Medicine Reports*, 5, 2.
- Galvan, A., Hare, T. A., Parra, C. E., Penn, J., Voss, H., Glover, G., & Casey, B. J. (2006). Earlier development of the accumbens relative to orbitofrontal cortex might underlie risk-taking behavior in adolescents. *The Journal of Neuroscience: The Official Journal of the Society for Neuroscience*, 26(25), 6885–6892.
- Gelenberg, A. J. (2010). Depression Symptomatology and Neurobiology. In *The Journal of Clinical Psychiatry* (Vol. 71, Issue 01, p. e02). <https://doi.org/10.4088/jcp.8001tx16c>
- Gigante, A. D., Bond, D. J., Lafer, B., Lam, R. W., Young, L. T., & Yatham, L. N. (2012). Brain glutamate levels measured by magnetic resonance spectroscopy in patients with bipolar disorder: a meta-analysis. *Bipolar Disorders*, 14(5), 478–487.

- Gilman, S. E., Sucha, E., Kingsbury, M., Horton, N. J., Murphy, J. M., & Colman, I. (2017). Depression and mortality in a longitudinal study: 1952–2011. In *Canadian Medical Association Journal* (Vol. 189, Issue 42, pp. E1304–E1310). <https://doi.org/10.1503/cmaj.170125>
- Glahn, D. C., & Burdick, K. E. (2011). Clinical endophenotypes for bipolar disorder. *Current Topics in Behavioural Neurosciences*, 5, 51–67.
- Gogolla, N. (2017). The insular cortex. *Current Biology: CB*, 27(12), R580–R586.
- Gogtay, N., Vyas, N. S., Testa, R., Wood, S. J., & Pantelis, C. (2011). Age of onset of schizophrenia: perspectives from structural neuroimaging studies. *Schizophrenia Bulletin*, 37(3), 504–513.
- Goldberg, D. (2011). The heterogeneity of “major depression.” *World Psychiatry: Official Journal of the World Psychiatric Association*, 10(3), 226–228.
- Gold, J. M., Strauss, G. P., Waltz, J. A., Robinson, B. M., Brown, J. K., & Frank, M. J. (2013). Negative symptoms of schizophrenia are associated with abnormal effort-cost computations. *Biological Psychiatry*, 74(2), 130–136.
- Goldstein, B. L., & Klein, D. N. (2014). A review of selected candidate endophenotypes for depression. *Clinical Psychology Review*, 34(5), 417–427.
- Gong, J., Chen, G., Jia, Y., Zhong, S., Zhao, L., Luo, X., Qiu, S., Lai, S., Qi, Z., Huang, L., & Wang, Y. (2019). Disrupted functional connectivity within the default mode network and salience network in unmedicated bipolar II disorder. *Progress in Neuro-Psychopharmacology & Biological Psychiatry*, 88, 11–18.
- Goodwin, F. K., & Jamison, K. R. (2007). *Manic-Depressive Illness: Bipolar Disorders and Recurrent Depression*. Oxford University Press.
- Gotlib, I. H., Hamilton, J. P., Cooney, R. E., Singh, M. K., Henry, M. L., & Joormann, J. (2010). Neural processing of reward and loss in girls at risk for major depression. *Archives of General Psychiatry*, 67(4), 380–387.
- Gottesman, I. I., & Gould, T. D. (2003). The Endophenotype Concept in Psychiatry: Etymology and Strategic Intentions. In *American Journal of Psychiatry* (Vol. 160, Issue 4, pp. 636–645). <https://doi.org/10.1176/appi.ajp.160.4.636>
- Grace, A. A. (2000). Gating of information flow within the limbic system and the pathophysiology of schizophrenia. *Brain Research. Brain Research Reviews*, 31(2-3), 330–341.



- Gradin, V. B., Waiter, G., O'Connor, A., Romaniuk, L., Stickle, C., Matthews, K., Hall, J., & Douglas Steele, J. (2013). Salience network-midbrain dysconnectivity and blunted reward signals in schizophrenia. *Psychiatry Research, 211*(2), 104–111.
- Grasby, K. L., Jahanshad, N., Painter, J. N., Colodro-Conde, L., Bralten, J., Hibar, D. P., Lind, P. A., Pizzagalli, F., Ching, C. R. K., McMahon, M. A. B., Shatokhina, N., Zsembik, L. C. P., Thomopoulos, S. I., Zhu, A. H., Strike, L. T., Agartz, I., Alhusaini, S., Almeida, M. A. A., Alnæs, D., ... Enhancing NeuroImaging Genetics through Meta-Analysis Consortium (ENIGMA)—Genetics working group. (2020). The genetic architecture of the human cerebral cortex. *Science, 367*(6484). <https://doi.org/10.1126/science.aay6690>
- Gray, J. A. (1990). Brain Systems that Mediate both Emotion and Cognition. *Cognition & Emotion, 4*(3), 269–288.
- Gray, P. (2010). *Psychology*.
- Greene, D. J., Lessov-Schlaggar, C. N., & Schlaggar, B. L. (2016). Development of the Brain's Functional Network Architecture. In *Neurobiology of Language* (pp. 399–406). Elsevier.
- Green, E. K., Grozeva, D., Jones, I., Jones, L., Kirov, G., Caesar, S., Gordon-Smith, K., Fraser, C., Forty, L., Russell, E., Hamshere, M. L., Moskvina, V., Nikolov, I., Farmer, A., McGuffin, P., Wellcome Trust Case Control Consortium, Holmans, P. A., Owen, M. J., O'Donovan, M. C., & Craddock, N. (2010). The bipolar disorder risk allele at CACNA1C also confers risk of recurrent major depression and of schizophrenia. *Molecular Psychiatry, 15*(10), 1016–1022.
- Grimm, O., Heinz, A., Walter, H., Kirsch, P., Erk, S., Haddad, L., Plichta, M. M., Romanczuk-Seiferth, N., Pöhland, L., Mohnke, S., Mühleisen, T. W., Mattheisen, M., Witt, S. H., Schäfer, A., Cichon, S., Nöthen, M., Rietschel, M., Tost, H., & Meyer-Lindenberg, A. (2014). Striatal response to reward anticipation: evidence for a systems-level intermediate phenotype for schizophrenia. *JAMA Psychiatry, 71*(5), 531–539.
- Grimm, S., Boesiger, P., Beck, J., Schuepbach, D., Bermpohl, F., Walter, M., Ernst, J., Hell, D., Boeker, H., & Northoff, G. (2009). Altered negative BOLD responses in the default-mode network during emotion processing in depressed subjects. *Neuropsychopharmacology: Official Publication of the American College of Neuropsychopharmacology, 34*(4), 932–943.
- Groenewegen, H. J., & Trimble, M. (2007). The ventral striatum as an interface between the limbic and motor systems. *CNS Spectrums, 12*(12), 887–892.

- Grof, P., Alda, M., & Ahrens, B. (1995). Clinical course of affective disorders: were Emil Kraepelin and Jules Angst wrong? *Psychopathology*, *28 Suppl 1*, 73–80.
- Guerrero-Pedraza, A., McKenna, P. J., Gomar, J. J., Sarró, S., Salvador, R., Amann, B., Carrión, M. I., Landin-Romero, R., Blanch, J., & Pomarol-Clotet, E. (2012). First-episode psychosis is characterized by failure of deactivation but not by hypo- or hyperfrontality. *Psychological Medicine*, *42*(1), 73–84.
- Gustavsson, A., Svensson, M., Jacobi, F., Allgulander, C., Alonso, J., Beghi, E., Dodel, R., Ekman, M., Faravelli, C., Fratiglioni, L., Gannon, B., Jones, D. H., Jennum, P., Jordanova, A., Jönsson, L., Karampampa, K., Knapp, M., Kobelt, G., Kurth, T., ... CDBE2010Study Group. (2011). Cost of disorders of the brain in Europe 2010. *European Neuropsychopharmacology: The Journal of the European College of Neuropsychopharmacology*, *21*(10), 718–779.
- Haber, S. N., & Knutson, B. (2010). The reward circuit: linking primate anatomy and human imaging. *Neuropsychopharmacology: Official Publication of the American College of Neuropsychopharmacology*, *35*(1), 4–26.
- Häfner, H., Maurer, K., Löffler, W., Fätkenheuer, B., an der Heiden, W., Riecher-Rössler, A., Behrens, S., & Gattaz, W. F. (1994). The epidemiology of early schizophrenia. Influence of age and gender on onset and early course. *The British Journal of Psychiatry. Supplement*, *23*, 29–38.
- Häfner, H., Maurer, K., Trendler, G., an der Heiden, W., Schmidt, M., & Könncke, R. (2005). Schizophrenia and depression: challenging the paradigm of two separate diseases—a controlled study of schizophrenia, depression and healthy controls. *Schizophrenia Research*, *77*(1), 11–24.
- Hall, G. B. C., Milne, A. M. B., & MacQueen, G. M. (2014). An fMRI study of reward circuitry in patients with minimal or extensive history of major depression. In *European Archives of Psychiatry and Clinical Neuroscience* (Vol. 264, Issue 3, pp. 187–198). <https://doi.org/10.1007/s00406-013-0437-9>
- Hall, W., & Degenhardt, L. (2008). Cannabis use and the risk of developing a psychotic disorder. *World Psychiatry: Official Journal of the World Psychiatric Association*, *7*(2), 68–71.
- Hamilton, I. (2017). Cannabis, psychosis and schizophrenia: unravelling a complex interaction. In *Addiction* (Vol. 112, Issue 9, pp. 1653–1657). <https://doi.org/10.1111/add.13826>
- Hamilton, M. (1986). The Hamilton Rating Scale for Depression. In *Assessment of Depression* (pp. 143–152). [https://doi.org/10.1007/978-3-642-70486-4\\_14](https://doi.org/10.1007/978-3-642-70486-4_14)

- Han, S., Becker, B., Duan, X., Cui, Q., Xin, F., Zong, X., Hu, M., Yang, M., Li, R., Yu, Y., Liao, W., Chen, X., & Chen, H. (2020). Distinct striatum pathways connected to salience network predict symptoms improvement and resilient functioning in schizophrenia following risperidone monotherapy. *Schizophrenia Research*, *215*, 89–96.
- Han, X., Jing, M.-Y., Zhao, T.-Y., Wu, N., Song, R., & Li, J. (2017). Role of dopamine projections from ventral tegmental area to nucleus accumbens and medial prefrontal cortex in reinforcement behaviors assessed using optogenetic manipulation. *Metabolic Brain Disease*, *32*(5), 1491–1502.
- Hariri, A. R., Drabant, E. M., & Weinberger, D. R. (2006). Imaging Genetics: Perspectives from Studies of Genetically Driven Variation in Serotonin Function and Corticolimbic Affective Processing. In *Biological Psychiatry* (Vol. 59, Issue 10, pp. 888–897). <https://doi.org/10.1016/j.biopsych.2005.11.005>
- Harrison, P. J. (2004). The hippocampus in schizophrenia: a review of the neuropathological evidence and its pathophysiological implications. *Psychopharmacology*, *174*(1), 151–162.
- Hauser, T. U., Eldar, E., & Dolan, R. J. (2017). Separate mesocortical and mesolimbic pathways encode effort and reward learning signals. *Proceedings of the National Academy of Sciences of the United States of America*, *114*(35), E7395–E7404.
- Häuser, W., Schmutzer, G., Brähler, E., & Glaesmer, H. (2011). Maltreatment in childhood and adolescence: results from a survey of a representative sample of the German population. *Deutsches Arzteblatt International*, *108*(17), 287–294.
- Hawton, K., Casañas I Comabella, C., Haw, C., & Saunders, K. (2013). Risk factors for suicide in individuals with depression: a systematic review. *Journal of Affective Disorders*, *147*(1-3), 17–28.
- Heckers, S., & Konradi, C. (2002). Hippocampal neurons in schizophrenia. *Journal of Neural Transmission*, *109*(5-6), 891–905.
- Heckers, S., & Konradi, C. (2015). GABAergic mechanisms of hippocampal hyperactivity in schizophrenia. *Schizophrenia Research*, *167*(1-3), 4–11.
- Hernandez, G., Hamdani, S., Rajabi, H., Conover, K., Stewart, J., Arvanitogiannis, A., & Shizgal, P. (2006). Prolonged rewarding stimulation of the rat medial forebrain bundle: neurochemical and behavioural consequences. *Behavioural Neuroscience*, *120*(4), 888–904.

- Hibar, D. P., Stein, J. L., Renteria, M. E., Arias-Vasquez, A., Desrivieres, S., Jahanshad, N., Toro, R., Wittfeld, K., Abramovic, L., Andersson, M., Aribisala, B. S., Armstrong, N. J., Bernard, M., Bohlken, M. M., Boks, M. P., Bralten, J., Brown, A. A., Chakravarty, M. M., Chen, Q., ... Medland, S. E. (2015). Common genetic variants influence human subcortical brain structures. *Nature*, *520*(7546), 224–229.
- Hilker, R., Helenius, D., Fagerlund, B., Skytthe, A., Christensen, K., Werge, T. M., Nordentoft, M., & Glenthøj, B. (2018). Heritability of Schizophrenia and Schizophrenia Spectrum Based on the Nationwide Danish Twin Register. *Biological Psychiatry*, *83*(6), 492–498.
- Hoffmann, C., Van Rheenen, T. E., Mancuso, S. G., Zalesky, A., Bruggemann, J., Lenroot, R. K., Sundram, S., Weickert, C. S., Weickert, T. W., Pantelis, C., Cropley, V., & Bousman, C. A. (2018). Exploring the moderating effects of dopaminergic polymorphisms and childhood adversity on brain morphology in schizophrenia-spectrum disorders. *Psychiatry Research. Neuroimaging*, *281*, 61–68.
- Honea, R., Crow, T. J., Passingham, D., & Mackay, C. E. (2005). Regional deficits in brain volume in schizophrenia: a meta-analysis of voxel-based morphometry studies. *The American Journal of Psychiatry*, *162*(12), 2233–2245.
- Ho, N. F., Li Hui Chong, P., Lee, D. R., Chew, Q. H., Chen, G., & Sim, K. (2019). The Amygdala in Schizophrenia and Bipolar Disorder: A Synthesis of Structural MRI, Diffusion Tensor Imaging, and Resting-State Functional Connectivity Findings. *Harvard Review of Psychiatry*, *27*(3), 150–164.
- Horan, W. P., Kring, A. M., & Blanchard, J. J. (2006). Anhedonia in schizophrenia: a review of assessment strategies. *Schizophrenia Bulletin*, *32*(2), 259–273.
- Hor, K., & Taylor, M. (2010). Suicide and schizophrenia: a systematic review of rates and risk factors. *Journal of Psychopharmacology*, *24*(4 Suppl), 81–90.
- Howes, O. D., & Kapur, S. (2009). The Dopamine Hypothesis of Schizophrenia: Version III--The Final Common Pathway. In *Schizophrenia Bulletin* (Vol. 35, Issue 3, pp. 549–562). <https://doi.org/10.1093/schbul/sbp006>
- Howes, O. D., Montgomery, A. J., Asselin, M.-C., Murray, R. M., Valli, I., Tabraham, P., Bramon-Bosch, E., Valmaggia, L., Johns, L., Broome, M., McGuire, P. K., & Grasby, P. M. (2009). Elevated striatal dopamine function linked to prodromal signs of schizophrenia. *Archives of General Psychiatry*, *66*(1), 13–20.
- Howie, B. N., Donnelly, P., & Marchini, J. (2009). A Flexible and Accurate Genotype Imputation Method for the Next Generation of Genome-Wide Association Studies. *PLoS Genetics*, *5*(6), e1000529.

- Hua, J. P. Y., Karcher, N. R., Merrill, A. M., O'Brien, K. J., Straub, K. T., Trull, T. J., & Kerns, J. G. (2019). Psychosis risk is associated with decreased resting-state functional connectivity between the striatum and the default mode network. *Cognitive, Affective & Behavioural Neuroscience*, *19*(4), 998–1011.
- Hu, M.-L., Zong, X.-F., Mann, J. J., Zheng, J.-J., Liao, Y.-H., Li, Z.-C., He, Y., Chen, X.-G., & Tang, J.-S. (2017). A Review of the Functional and Anatomical Default Mode Network in Schizophrenia. *Neuroscience Bulletin*, *33*(1), 73–84.
- Hwang, J., Lyoo, I. K., Dager, S. R., Friedman, S. D., Oh, J. S., Lee, J. Y., Kim, S. J., Dunner, D. L., & Renshaw, P. F. (2006). Basal ganglia shape alterations in bipolar disorder. *The American Journal of Psychiatry*, *163*(2), 276–285.
- Insel, T., Cuthbert, B., Garvey, M., Heinssen, R., Pine, D. S., Quinn, K., Sanislow, C., & Wang, P. (2010). Research domain criteria (RDoC): toward a new classification framework for research on mental disorders. *The American Journal of Psychiatry*, *167*(7), 748–751.
- Insel, T. R. (2008). Assessing the economic costs of serious mental illness [Review of *Assessing the economic costs of serious mental illness*]. *The American Journal of Psychiatry*, *165*(6), 663–665.
- Jablensky, A. (2011). Diagnosis and Revision of the Classification Systems. In *Schizophrenia* (pp. 1–30). <https://doi.org/10.1002/9780470978672.ch1>
- Jablensky, A. (2012). Course and outcome of schizophrenia and their prediction. In A. Jablensky (Ed.), *New Oxford Textbook of Psychiatry* (pp. 568–578). Oxford University Press.
- Jablensky, A. (2016). Psychiatric classifications: validity and utility. In *World Psychiatry* (Vol. 15, Issue 1, pp. 26–31). <https://doi.org/10.1002/wps.20284>
- Jacobs, D., & Silverstone, T. (1986). Dextroamphetamine-induced arousal in human subjects as a model for mania. *Psychological Medicine*, *16*(2), 323–329.
- John, B., & Lewis, K. R. (1966). Chromosome variability and geographic distribution in insects. *Science*, *152*(3723), 711–721.
- Johnson, S. L., Mehta, H., Ketter, T. A., Gotlib, I. H., & Knutson, B. (2019). Neural responses to monetary incentives in bipolar disorder. *NeuroImage. Clinical*, *24*, 102018.
- Jonas, K. G., Lencz, T., Li, K., Malhotra, A. K., Perlman, G., Fochtmann, L. J., Bromet, E. J., & Kotov, R. (2019). *Schizophrenia Polygenic Risk Score and 20-Year Course of Illness in Psychotic Disorders*. <https://doi.org/10.1101/581579>

- Joyce, P. R. (1984). Age of onset in bipolar affective disorder and misdiagnosis as schizophrenia. *Psychological Medicine*, *14*(1), 145–149.
- Juckel, G., Schlagenhauf, F., Koslowski, M., Filonov, D., Wüstenberg, T., Villringer, A., Knutson, B., Kienast, T., Gallinat, J., Wrase, J., & Heinz, A. (2006). Dysfunction of ventral striatal reward prediction in schizophrenic patients treated with typical, not atypical, neuroleptics. In *Psychopharmacology* (Vol. 187, Issue 2, pp. 222–228). <https://doi.org/10.1007/s00213-006-0405-4>
- Juckel, G., Schlagenhauf, F., Koslowski, M., Wüstenberg, T., Villringer, A., Knutson, B., Wrase, J., & Heinz, A. (2006). Dysfunction of ventral striatal reward prediction in schizophrenia. *NeuroImage*, *29*(2), 409–416.
- Kaag, A. M., Reneman, L., Homberg, J., van den Brink, W., & van Wingen, G. A. (2018). Enhanced Amygdala-Striatal Functional Connectivity during the Processing of Cocaine Cues in Male Cocaine Users with a History of Childhood Trauma. *Frontiers in Psychiatry / Frontiers Research Foundation*, *9*, 70.
- Kable, J. W., & Glimcher, P. W. (2009). The Neurobiology of Decision: Consensus and Controversy. In *Neuron* (Vol. 63, Issue 6, pp. 733–745). <https://doi.org/10.1016/j.neuron.2009.09.003>
- Kaiser, R. H., Clegg, R., Goer, F., Pechtel, P., Beltzer, M., Vitaliano, G., Olson, D. P., Teicher, M. H., & Pizzagalli, D. A. (2018). Childhood stress, grown-up brain networks: corticolimbic correlates of threat-related early life stress and adult stress response. *Psychological Medicine*, *48*(7), 1157–1166.
- Kalivas, P. W., Volkow, N., & Seamans, J. (2005). Unmanageable motivation in addiction: a pathology in prefrontal-accumbens glutamate transmission. *Neuron*, *45*(5), 647–650.
- Karcher, N. R., Rogers, B. P., & Woodward, N. D. (2019). Functional Connectivity of the Striatum in Schizophrenia and Psychotic Bipolar Disorder. *Biological Psychiatry. Cognitive Neuroscience and Neuroimaging*, *4*(11), 956–965.
- Kasai, K., Shenton, M. E., Salisbury, D. F., Onitsuka, T., Toner, S. K., Yurgelun-Todd, D., Kikinis, R., Jolesz, F. A., & McCarley, R. W. (2003). Differences and similarities in insular and temporal pole MRI gray matter volume abnormalities in first-episode schizophrenia and affective psychosis. *Archives of General Psychiatry*, *60*(11), 1069–1077.
- Kasanin, J. (1933). THE ACUTE SCHIZOAFFECTIVE PSYCHOSES. In *American Journal of Psychiatry* (Vol. 90, Issue 1, pp. 97–126). <https://doi.org/10.1176/ajp.90.1.97>

- Kavanagh, D. J., McGrath, J., Saunders, J. B., Dore, G., & Clark, D. (2002). Substance misuse in patients with schizophrenia: epidemiology and management. *Drugs*, *62*(5), 743–755.
- Kay, S. R., Fiszbein, A., & Opler, L. A. (1987). The positive and negative syndrome scale (PANSS) for schizophrenia. *Schizophrenia Bulletin*, *13*(2), 261–276.
- Kay, S. R., Opler, L. A., Spitzer, R. L., Williams, J. B. W., Fiszbein, A., & Gorelick, A. (1991). SCID-PANSS: Two-tier diagnostic system for psychotic disorders. In *Comprehensive Psychiatry* (Vol. 32, Issue 4, pp. 355–361).  
[https://doi.org/10.1016/0010-440x\(91\)90085-q](https://doi.org/10.1016/0010-440x(91)90085-q)
- Keck, P. E., Jr, McElroy, S. L., Havens, J. R., Altshuler, L. L., Nolen, W. A., Frye, M. A., Suppes, T., Denicoff, K. D., Kupka, R., Leverich, G. S., Rush, A. J., & Post, R. M. (2003). Psychosis in bipolar disorder: phenomenology and impact on morbidity and course of illness. *Comprehensive Psychiatry*, *44*(4), 263–269.
- Keller, M. C. (2018). Evolutionary Perspectives on Genetic and Environmental Risk Factors for Psychiatric Disorders. *Annual Review of Clinical Psychology*, *14*, 471–493.
- Kendler, K. S., & Eaves, L. J. (2007). *Psychiatric Genetics*. American Psychiatric Pub.
- Kendler, K. S., & Gardner, C. O. (2014). Sex differences in the pathways to major depression: a study of opposite-sex twin pairs. *The American Journal of Psychiatry*, *171*(4), 426–435.
- Kendler, K. S., Karkowski, L. M., & Walsh, D. (1998). The structure of psychosis: latent class analysis of probands from the Roscommon Family Study. *Archives of General Psychiatry*, *55*(6), 492–499.
- Keren, H., O’Callaghan, G., Vidal-Ribas, P., Buzzell, G. A., Brotman, M. A., Leibenluft, E., Pan, P. M., Meffert, L., Kaiser, A., Wolke, S., Pine, D. S., & Stringaris, A. (2018). Reward Processing in Depression: A Conceptual and Meta-Analytic Review Across fMRI and EEG Studies. *The American Journal of Psychiatry*, *175*(11), 1111–1120.
- Kessler, R. C., Angermeyer, M., Anthony, J. C., DE Graaf, R., Demyttenaere, K., Gasquet, I., DE Girolamo, G., Gluzman, S., Gureje, O., Haro, J. M., Kawakami, N., Karam, A., Levinson, D., Medina Mora, M. E., Oakley Browne, M. A., Posada-Villa, J., Stein, D. J., Adley Tsang, C. H., Aguilar-Gaxiola, S., ... Ustün, T. B. (2007). Lifetime prevalence and age-of-onset distributions of mental disorders in the World Health Organization’s World Mental Health Survey Initiative. *World Psychiatry: Official Journal of the World Psychiatric Association*, *6*(3), 168–176.
- Kessler, R. C., Chiu, W. T., Demler, O., Merikangas, K. R., & Walters, E. E. (2005). Prevalence, severity, and comorbidity of 12-month DSM-IV disorders in the National Comorbidity Survey Replication. *Archives of General Psychiatry*, *62*(6), 617–627.

- Khadka, S., Meda, S. A., Stevens, M. C., Glahn, D. C., Calhoun, V. D., Sweeney, J. A., Tamminga, C. A., Keshavan, M. S., O'Neil, K., Schretlen, D., & Pearlson, G. D. (2013). Is aberrant functional connectivity a psychosis endophenotype? A resting state functional magnetic resonance imaging study. *Biological Psychiatry*, *74*(6), 458–466.
- Kim, S. M., Park, S. Y., Kim, Y. I., Son, Y. D., Chung, U.-S., Min, K. J., & Han, D. H. (2016). Affective network and default mode network in depressive adolescents with disruptive behaviors. *Neuropsychiatric Disease and Treatment*, *12*, 49–56.
- Kiparizoska, S., & Ikuta, T. (2017). Disrupted Olfactory Integration in Schizophrenia: Functional Connectivity Study. *The International Journal of Neuropsychopharmacology / Official Scientific Journal of the Collegium Internationale Neuropsychopharmacologicum*, *20*(9), 740–746.
- Kirkbride, J. B., Fearon, P., Morgan, C., Dazzan, P., Morgan, K., Tarrant, J., Lloyd, T., Holloway, J., Hutchinson, G., Leff, J. P., Mallett, R. M., Harrison, G. L., Murray, R. M., & Jones, P. B. (2006). Heterogeneity in incidence rates of schizophrenia and other psychotic syndromes: findings from the 3-center AeSOP study. *Archives of General Psychiatry*, *63*(3), 250–258.
- Kirschner, M., Hager, O. M., Bischof, M., Hartmann, M. N., Kluge, A., Seifritz, E., Tobler, P. N., & Kaiser, S. (2016). Ventral striatal hypoactivation is associated with apathy but not diminished expression in patients with schizophrenia. In *Journal of Psychiatry & Neuroscience* (Vol. 41, Issue 2, pp. 152–161).  
<https://doi.org/10.1503/jpn.140383>
- Kirsch, P., Ronshausen, S., Mier, D., & Gallhofer, B. (2007). The influence of antipsychotic treatment on brain reward system reactivity in schizophrenia patients. *Pharmacopsychiatry*, *40*(5), 196–198.
- Knutson, B., Bhanji, J. P., Cooney, R. E., Atlas, L. Y., & Gotlib, I. H. (2008). Neural responses to monetary incentives in major depression. *Biological Psychiatry*, *63*(7), 686–692.
- Knutson, B., Fong, G. W., Adams, C. M., Varner, J. L., & Hommer, D. (2001). Dissociation of reward anticipation and outcome with event-related fMRI. *Neuroreport*, *12*(17), 3683–3687.
- Knutson, B., Fong, G. W., Bennett, S. M., Adams, C. M., & Hommer, D. (2003). A region of mesial prefrontal cortex tracks monetarily rewarding outcomes: characterization with rapid event-related fMRI. *NeuroImage*, *18*(2), 263–272.
- Knutson, B., & Gibbs, S. E. B. (2007). Linking nucleus accumbens dopamine and blood oxygenation. *Psychopharmacology*, *191*(3), 813–822.



- Kollmann, B., Scholz, V., Linke, J., Kirsch, P., & Wessa, M. (2017). Reward anticipation revisited- evidence from an fMRI study in euthymic bipolar I patients and healthy first-degree relatives. *Journal of Affective Disorders, 219*, 178–186.
- Kraepelin, E. (1889). *Psychiatrie: ein kurzes Lehrbuch für Studierende und Aerzte*.
- Krishnan, K. R., McDonald, W. M., Escalona, P. R., Doraiswamy, P. M., Na, C., Husain, M. M., Figiel, G. S., Boyko, O. B., Ellinwood, E. H., & Nemeroff, C. B. (1992). Magnetic resonance imaging of the caudate nuclei in depression. Preliminary observations. *Archives of General Psychiatry, 49*(7), 553–557.
- Kühn, S., & Gallinat, J. (2013). Resting-state brain activity in schizophrenia and major depression: a quantitative meta-analysis. *Schizophrenia Bulletin, 39*(2), 358–365.
- Lancaster, T. M., Dimitriadis, S. L., Tansey, K. E., Perry, G., Ihssen, N., Jones, D. K., Singh, K. D., Holmans, P., Pocklington, A., Smith, G. D., Zammit, S., Hall, J., O'Donovan, M. C., Owen, M. J., & Linden, D. E. (2018). Structural and Functional Neuroimaging of Polygenic Risk for Schizophrenia: A Recall-by-Genotype-Based Approach. In *Schizophrenia Bulletin*. <https://doi.org/10.1093/schbul/sby037>
- Lancaster, T. M., Ihssen, N., Brindley, L. M., Tansey, K. E., Mantripragada, K., O'Donovan, M. C., Owen, M. J., & Linden, D. E. J. (2016). Associations between polygenic risk for schizophrenia and brain function during probabilistic learning in healthy individuals. *Human Brain Mapping, 37*(2), 491–500.
- Lancaster, T. M., Linden, D. E., Tansey, K. E., Banaschewski, T., Bokde, A. L. W., Bromberg, U., Büchel, C., Cattrell, A., Conrod, P. J., Flor, H., Frouin, V., Gallinat, J., Garavan, H., Gowland, P., Heinz, A., Ittermann, B., Martinot, J.-L., Paillère Martinot, M.-L., Artiges, E., ... IMAGEN Consortium. (2016). Polygenic Risk of Psychosis and Ventral Striatal Activation During Reward Processing in Healthy Adolescents. *JAMA Psychiatry, 73*(8), 852–861.
- Larsen, T. K., Melle, I., Auestad, B., Haahr, U., Joa, I., Johannessen, J. O., Opjordsmoen, S., Rund, B. R., Rossberg, J. I., Simonsen, E., Vaglum, P., Friis, S., & McGlashan, T. (2011). Early detection of psychosis: positive effects on 5-year outcome. *Psychological Medicine, 41*(7), 1461–1469.
- Larson, M. K., Walker, E. F., & Compton, M. T. (2010). Early signs, diagnosis and therapeutics of the prodromal phase of schizophrenia and related psychotic disorders. *Expert Review of Neurotherapeutics, 10*(8), 1347–1359.
- Laursen, T. M., Agerbo, E., & Pedersen, C. B. (2009). Bipolar disorder, schizoaffective disorder, and schizophrenia overlap: a new comorbidity index. *The Journal of Clinical Psychiatry, 70*(10), 1432–1438.

- Leboyer, M., Henry, C., Paillere-Martinot, M.-L., & Bellivier, F. (2005). Age at onset in bipolar affective disorders: a review. In *Bipolar Disorders* (Vol. 7, Issue 2, pp. 111–118). <https://doi.org/10.1111/j.1399-5618.2005.00181.x>
- Ledonne, A., & Mercuri, N. B. (2017). Current Concepts on the Physiopathological Relevance of Dopaminergic Receptors. *Frontiers in Cellular Neuroscience*, *11*, 27.
- Lee, J., Choi, S., Kang, J., Won, E., Tae, W.-S., Lee, M.-S., & Ham, B.-J. (2017). Structural characteristics of the brain reward circuit regions in patients with bipolar I disorder: A voxel-based morphometric study. *Psychiatry Research: Neuroimaging*, *269*, 82–89.
- Lee, K.-H., Oh, H., Suh, J.-H. S., Cho, K. I. K., Yoon, Y. B., Shin, W.-G., Lee, T. Y., & Kwon, J. S. (2019). Functional and Structural Connectivity of the Cerebellar Nuclei With the Striatum and Cerebral Cortex in First-Episode Psychosis. *The Journal of Neuropsychiatry and Clinical Neurosciences*, *31*(2), 143–151.
- Lee, M. H., Smyser, C. D., & Shimony, J. S. (2012). Resting-State fMRI: A Review of Methods and Clinical Applications. *AJNR. American Journal of Neuroradiology*, *34*(10), 1866–1872.
- LeGates, T. A., Kvarta, M. D., Tooley, J. R., Chase Francis, T., Lobo, M. K., Creed, M. C., & Thompson, S. M. (2018). Reward behaviour is regulated by the strength of hippocampus–nucleus accumbens synapses. In *Nature* (Vol. 564, Issue 7735, pp. 258–262). <https://doi.org/10.1038/s41586-018-0740-8>
- Lemieux, B., Aharoni, A., & Schena, M. (1998). 10.1023/A:1009654300686. In *Molecular Breeding* (Vol. 4, Issue 4, pp. 277–289). <https://doi.org/10.1023/A:1009654300686>
- Lenzenweger, M. F. (2018). Schizotypy, schizotypic psychopathology and schizophrenia. *World Psychiatry: Official Journal of the World Psychiatric Association*, *17*(1), 25–26.
- Leroy, A., Amad, A., D'Hondt, F., Pins, D., Jaafari, N., Thomas, P., & Jardri, R. (2020). Reward anticipation in schizophrenia: A coordinate-based meta-analysis. *Schizophrenia Research*, *218*, 2–6.
- Levey, D. F., Stein, M. B., Wendt, F. R., Pathak, G. A., Zhou, H., Aslan, M., Quaden, R., Harrington, K. M., Sanacora, G., McIntosh, A. M., Concato, J., Polimanti, R., Gelernter, J., & on behalf of the Million Veteran Program. (2020). GWAS of Depression Phenotypes in the Million Veteran Program and Meta-analysis in More than 1.2 Million Participants Yields 178 Independent Risk Loci. <https://doi.org/10.1101/2020.05.18.20100685>
- Leykin, Y., Roberts, C. S., & DeRubeis, R. J. (2011). Decision-Making and Depressive Symptomatology. In *Cognitive Therapy and Research* (Vol. 35, Issue 4, pp. 333–341). <https://doi.org/10.1007/s10608-010-9308-0>

- Lichtenstein, P., Björk, C., Hultman, C. M., Scolnick, E., Sklar, P., & Sullivan, P. F. (2006). Recurrence risks for schizophrenia in a Swedish national cohort. *Psychological Medicine, 36*(10), 1417–1425.
- Lieberman, J. A., Girgis, R. R., Brucato, G., Moore, H., Provenzano, F., Kegeles, L., Javitt, D., Kantrowitz, J., Wall, M. M., Corcoran, C. M., Schobel, S. A., & Small, S. A. (2018). Hippocampal dysfunction in the pathophysiology of schizophrenia: a selective review and hypothesis for early detection and intervention. *Molecular Psychiatry, 23*(8), 1764–1772.
- Liu, C., Zhang, W., Chen, G., Tian, H., Li, J., Qu, H., Cheng, L., Zhu, J., & Zhuo, C. (2017). Aberrant patterns of local and long-range functional connectivity densities in schizophrenia. *Oncotarget, 8*(29), 48196–48203.
- Liu, Y., Zhang, Y., Lv, L., Wu, R., Zhao, J., & Guo, W. (2018). Abnormal neural activity as a potential biomarker for drug-naïve first-episode adolescent-onset schizophrenia with coherence regional homogeneity and support vector machine analyses. *Schizophrenia Research, 192*, 408–415.
- Li, W., Mai, X., & Liu, C. (2014). The default mode network and social understanding of others: what do brain connectivity studies tell us. *Frontiers in Human Neuroscience, 8*, 74.
- Li, X., Lu, Z.-L., D'Argembeau, A., Ng, M., & Bechara, A. (2010). The Iowa Gambling Task in fMRI images. *Human Brain Mapping, 31*(3), 410–423.
- Lin P, Wang X, Zhang B, Kirkpatrick B, Öngür D, Levitt JJ, Jovicich J, Yao S, Wang X. Functional dysconnectivity of the limbic loop of frontostriatal circuits in first-episode, treatment-naïve schizophrenia. *Hum Brain Mapp.* 2018 Feb;39(2):747-757. doi: 10.1002/hbm.23879.
- Loebel, A. D., Lieberman, J. A., Alvir, J. M., Mayerhoff, D. I., Geisler, S. H., & Szymanski, S. R. (1992). Duration of psychosis and outcome in first-episode schizophrenia. *The American Journal of Psychiatry, 149*(9), 1183–1188.
- London, E. D. (2020). Human Brain Imaging Links Dopaminergic Systems to Impulsivity. *Current Topics in Behavioural Neurosciences*. [https://doi.org/10.1007/7854\\_2019\\_125](https://doi.org/10.1007/7854_2019_125)
- Luo, X., Mao, Q., Shi, J., Wang, X., & Li, C.-S. R. (2019). Putamen gray matter volumes in neuropsychiatric and neurodegenerative disorders. *World Journal of Psychiatry and Mental Health Research, 3*(1). <https://www.ncbi.nlm.nih.gov/pubmed/31328186>
- Luykx, J. J., Laban, K. G., van den Heuvel, M. P., Boks, M. P. M., Mandl, R. C. W., Kahn, R. S., & Bakker, S. C. (2012). Region and state specific glutamate downregulation in major depressive disorder: a meta-analysis of (1)H-MRS findings. *Neuroscience and Biobehavioural Reviews, 36*(1), 198–205.

- MacMaster, F. P., Mirza, Y., Szeszko, P. R., Kmiecik, L. E., Easter, P. C., Taormina, S. P., Lynch, M., Rose, M., Moore, G. J., & Rosenberg, D. R. (2008). Amygdala and hippocampal volumes in familial early onset major depressive disorder. *Biological Psychiatry*, *63*(4), 385–390.
- Macoveanu, J., Kjaerstad, H. L., Chase, H. W., Frangou, S., Knudsen, G. M., Vinberg, M., Kessing, L. V., & Miskowiak, K. W. (2020). Abnormal prefrontal cortex processing of reward prediction errors in recently diagnosed patients with bipolar disorder and their unaffected relatives. *Bipolar Disorders*. <https://doi.org/10.1111/bdi.12915>
- Maguire, E. A., Gadian, D. G., Johnsrude, I. S., Good, C. D., Ashburner, J., Frackowiak, R. S., & Frith, C. D. (2000). Navigation-related structural change in the hippocampi of taxi drivers. *Proceedings of the National Academy of Sciences of the United States of America*, *97*(8), 4398–4403.
- Mahajan, R., & Mostofsky, S. H. (2015). Neuroimaging endophenotypes in autism spectrum disorder. *CNS Spectrums*, *20*(4), 412–426.
- Mahon, P. B., Eldridge, H., Crocker, B., Notes, L., Gindes, H., Postell, E., King, S., Potash, J. B., Ratnanather, J. T., & Barta, P. E. (2012). An MRI study of amygdala in schizophrenia and psychotic bipolar disorder. *Schizophrenia Research*, *138*(2-3), 188–191.
- Maia, T. V., & Frank, M. J. (2017). An Integrative Perspective on the Role of Dopamine in Schizophrenia. *Biological Psychiatry*, *81*(1), 52–66.
- Manoliu, A., Riedl, V., Zherdin, A., Mühlau, M., Schwerthöffer, D., Scherr, M., Peters, H., Zimmer, C., Förstl, H., Bäuml, J., Wohlschläger, A. M., & Sorg, C. (2013). Aberrant Dependence of Default Mode/Central Executive Network Interactions on Anterior Insular Salience Network Activity in Schizophrenia. *Schizophrenia Bulletin*, *40*(2), 428–437.
- Manza, P., Tomasi, D., & Volkow, N. D. (2018). Subcortical Local Functional Hyperconnectivity in Cannabis Dependence. *Biological Psychiatry. Cognitive Neuroscience and Neuroimaging*, *3*(3), 285–293.
- Marchetti, I., Koster, E. H. W., Sonuga-Barke, E. J., & De Raedt, R. (2012). The Default Mode Network and Recurrent Depression: A Neurobiological Model of Cognitive Risk Factors. In *Neuropsychology Review* (Vol. 22, Issue 3, pp. 229–251). <https://doi.org/10.1007/s11065-012-9199-9>
- Marcus, M., Taghi Yasamy, M., van van Ommeren, M., Chisholm, D., & Saxena, S. (2012). Depression: A Global Public Health Concern. In *PsycEXTRA Dataset*. <https://doi.org/10.1037/e517532013-004>

- Marshall, M., Lewis, S., Lockwood, A., Drake, R., Jones, P., & Croudace, T. (2005). Association between duration of untreated psychosis and outcome in cohorts of first-episode patients: a systematic review. *Archives of General Psychiatry*, *62*(9), 975–983.
- Marusak, H. A., Hatfield, J. R. B., Thomason, M. E., & Rabinak, C. A. (2017). Reduced Ventral Tegmental Area-Hippocampal Connectivity in Children and Adolescents Exposed to Early Threat. *Biological Psychiatry. Cognitive Neuroscience and Neuroimaging*, *2*(2), 130–137.
- Mason, N. L., Theunissen, E. L., Hutten, N. R. P. W., Tse, D. H. Y., Toennes, S. W., Stiers, P., & Ramaekers, J. G. (2019). Cannabis induced increase in striatal glutamate associated with loss of functional corticostriatal connectivity. *European Neuropsychopharmacology: The Journal of the European College of Neuropsychopharmacology*, *29*(2), 247–256.
- Matheson, S. L., Shepherd, A. M., Pinchbeck, R. M., Laurens, K. R., & Carr, V. J. (2013). Childhood adversity in schizophrenia: a systematic meta-analysis. *Psychological Medicine*, *43*(2), 225–238.
- Ma, X., Liu, J., Liu, T., Ma, L., Wang, W., Shi, S., Wang, Y., Gong, Q., & Wang, M. (2019). Altered Resting-State Functional Activity in Medication-Naive Patients With First-Episode Major Depression Disorder vs. Healthy Control: A Quantitative Meta-Analysis. *Frontiers in Behavioural Neuroscience*, *13*, 89.
- McCutcheon, R. A., Nour, M. M., Dahoun, T., Jauhar, S., Pepper, F., Expert, P., Veronese, M., Adams, R. A., TMcLellan, Q., Wilkes, T. C., Swansburg, R., Jaworska, N., Langevin, L. M., & MacMaster, F. P. (2018). History of suicide attempt and right superior temporal gyrus volume in youth with treatment-resistant major depressive disorder. *Journal of Affective Disorders*, *239*, 291–294.
- urkheimer, F., Mehta, M. A., & Howes, O. D. (2019). Mesolimbic Dopamine Function Is Related to Salience Network Connectivity: An Integrative Positron Emission Tomography and Magnetic Resonance Study. In *Biological Psychiatry* (Vol. 85, Issue 5, pp. 368–378). <https://doi.org/10.1016/j.biopsych.2018.09.010>
- McGrath, J., Saha, S., Chant, D., & Welham, J. (2008). Schizophrenia: A Concise Overview of Incidence, Prevalence, and Mortality. In *Epidemiologic Reviews* (Vol. 30, Issue 1, pp. 67–76). <https://doi.org/10.1093/epirev/mxn001>
- McQuiston, R. (2011). Mesolimbic Dopaminergic Projections. In *Encyclopedia of Clinical Neuropsychology* (pp. 1577–1577). Springer, New York, NY.

- Meda, S. A., Gill, A., Stevens, M. C., Lorenzoni, R. P., Glahn, D. C., Calhoun, V. D., Sweeney, J. A., Tamminga, C. A., Keshavan, M. S., Thaker, G., & Pearlson, G. D. (2012). Differences in resting-state functional magnetic resonance imaging functional network connectivity between schizophrenia and psychotic bipolar probands and their unaffected first-degree relatives. *Biological Psychiatry*, *71*(10), 881–889.
- Meer, L. van der, van der Meer, L., Costafreda, S., Aleman, A., & David, A. S. (2010). Self-reflection and the brain: A theoretical review and meta-analysis of neuroimaging studies with implications for schizophrenia. In *Neuroscience & Biobehavioural Reviews* (Vol. 34, Issue 6, pp. 935–946). <https://doi.org/10.1016/j.neubio-rev.2009.12.004>
- Menon, V. (2011). Large-scale brain networks and psychopathology: a unifying triple network model. *Trends in Cognitive Sciences*, *15*(10), 483–506.
- Menon, V. (2015). Salience Network. In *Brain Mapping* (pp. 597–611). <https://doi.org/10.1016/b978-0-12-397025-1.00052-x>
- Menon, V., & Uddin, L. Q. (2010). Saliency, switching, attention and control: a network model of insula function. *Brain Structure & Function*, *214*(5-6), 655–667.
- Merikangas, K. R., Jin, R., He, J.-P., Kessler, R. C., Lee, S., Sampson, N. A., Viana, M. C., Andrade, L. H., Hu, C., Karam, E. G., Ladea, M., Medina-Mora, M. E., Ono, Y., Posada-Villa, J., Sagar, R., Wells, J. E., & Zarkov, Z. (2011). Prevalence and correlates of bipolar spectrum disorder in the world mental health survey initiative. *Archives of General Psychiatry*, *68*(3), 241–251.
- Metzak, P. D., Riley, J. D., Wang, L., Whitman, J. C., Ngan, E. T. C., & Woodward, T. S. (2012). Decreased efficiency of task-positive and task-negative networks during working memory in schizophrenia. *Schizophrenia Bulletin*, *38*(4), 803–813.
- Mikell, C. B., McKhann, G. M., Segal, S., McGovern, R. A., Wallenstein, M. B., & Moore, H. (2009). The hippocampus and nucleus accumbens as potential therapeutic targets for neurosurgical intervention in schizophrenia. *Stereotactic and Functional Neurosurgery*, *87*(4), 256–265.
- Miller, R., Wickens, J. R., & Beninger, R. J. (1990). Dopamine D-1 and D-2 receptors in relation to reward and performance: a case for the D-1 receptor as a primary site of therapeutic action of neuroleptic drugs. *Progress in Neurobiology*, *34*(2), 143–183.

- Milner, A. D. (2017). How do the two visual streams interact with each other? *Experimental Brain Research. Experimentelle Hirnforschung. Experimentation Cerebrale*, 235(5), 1297–1308.
- Missale, C., Russel Nash, S., Robinson, S. W., Jaber, M., & Caron, M. G. (1998). Dopamine Receptors: From Structure to Function. In *Physiological Reviews* (Vol. 78, Issue 1, pp. 189–225).  
<https://doi.org/10.1152/physrev.1998.78.1.189>
- Mitchell, S. J., Maguire, E. P., Cunningham, L., Gunn, B. G., Linke, M., Zechner, U., Dixon, C. I., King, S. L., Stephens, D. N., Swinny, J. D., Belelli, D., & Lambert, J. J. (2018). Early-life adversity selectively impairs  $\alpha 2$ -GABAA receptor expression in the mouse nucleus accumbens and influences the behavioural effects of cocaine. In *Neuropharmacology* (Vol. 141, pp. 98–112). <https://doi.org/10.1016/j.neuropharm.2018.08.021>
- Möller, H. J. (1995). The psychopathology of schizophrenia: an integrated view on positive symptoms and negative symptoms. *International Clinical Psychopharmacology*, 10 Suppl 3, 57–64.
- Moore, T. H. M., Zammit, S., Lingford-Hughes, A., Barnes, T. R. E., Jones, P. B., Burke, M., & Lewis, G. (2007). Cannabis use and risk of psychotic or affective mental health outcomes: a systematic review. In *The Lancet* (Vol. 370, Issue 9584, pp. 319–328). [https://doi.org/10.1016/s0140-6736\(07\)61162-3](https://doi.org/10.1016/s0140-6736(07)61162-3)
- Morgan, J. K., Olino, T. M., McMakin, D. L., Ryan, N. D., & Forbes, E. E. (2013). Neural response to reward as a predictor of increases in depressive symptoms in adolescence. *Neurobiology of Disease*, 52, 66–74.
- Morrison, A. P., & Petersen, T. (2003). Trauma, Metacognition And Predisposition To Hallucinations In Non-Patients. *Behavioural and Cognitive Psychotherapy*, 31(3), 235–246.
- Morris, R., Griffiths, O., Le Pelley, M. E., & Weickert, T. W. (2013). Attention to Irrelevant Cues Is Related to Positive Symptoms in Schizophrenia. In *Schizophrenia Bulletin* (Vol. 39, Issue 3, pp. 575–582).  
<https://doi.org/10.1093/schbul/sbr192>
- Morris, R. W., Vercammen, A., Lenroot, R., Moore, L., Langton, J. M., Short, B., Kulkarni, J., Curtis, J., O'Donnell, M., Weickert, C. S., & Weickert, T. W. (2012). Disambiguating ventral striatum fMRI-related BOLD signal during reward prediction in schizophrenia. *Molecular Psychiatry*, 17(3), 235, 280–289.
- Morris, S. E., & Cuthbert, B. N. (2012). Research Domain Criteria: cognitive systems, neural circuits, and dimensions of behavior. *Dialogues in Clinical Neuroscience*, 14(1), 29–37.
- Mukherjee, S., Shukla, S., Woodle, J., Rosen, A. M., & Olarte, S. (1983). Misdiagnosis of schizophrenia in bipolar patients: a multiethnic comparison. *The American Journal of Psychiatry*, 140(12), 1571–1574.

- Muneer, A. (2017). Mixed States in Bipolar Disorder: Etiology, Pathogenesis and Treatment. *Chonnam Medical Journal*, 53(1), 1–13.
- Murray, C. J. L., Vos, T., Lozano, R., Naghavi, M., Flaxman, A. D., Michaud, C., Ezzati, M., Shibuya, K., Salomon, J. A., Abdalla, S., Aboyans, V., Abraham, J., Ackerman, I., Aggarwal, R., Ahn, S. Y., Ali, M. K., AlMazroa, M. A., Alvarado, M., Anderson, H. R., ... Lopez, A. D. (2012). Disability-adjusted life years (DALYs) for 291 diseases and injuries in 21 regions, 1990–2010: a systematic analysis for the Global Burden of Disease Study 2010. *The Lancet*, 380(9859), 2197–2223.
- Murray, G. K., Corlett, P. R., Clark, L., Pessiglione, M., Blackwell, A. D., Honey, G., Jones, P. B., Bullmore, E. T., Robbins, T. W., & Fletcher, P. C. (2008). Substantia nigra/ventral tegmental reward prediction error disruption in psychosis. *Molecular Psychiatry*, 13(3), 239, 267–276.
- Mwansisywa, T. E., Hu, A., Li, Y., Chen, X., Wu, G., Huang, X., Lv, D., Li, Z., Liu, C., Xue, Z., Feng, J., & Liu, Z. (2017). Task and resting-state fMRI studies in first-episode schizophrenia: A systematic review. *Schizophrenia Research*, 189, 9–18.
- Myers, N. L. (2010). Culture, stress and recovery from schizophrenia: lessons from the field for global mental health. *Culture, Medicine and Psychiatry*, 34(3), 500–528.
- Nagel, T. (1974). What Is It Like to Be a Bat? In *The Philosophical Review* (Vol. 83, Issue 4, p. 435).  
<https://doi.org/10.2307/2183914>
- Nenadic, I., Maitra, R., Langbein, K., Dietzek, M., Lorenz, C., Smesny, S., Reichenbach, J. R., Sauer, H., & Gaser, C. (2015). Brain structure in schizophrenia vs. psychotic bipolar I disorder: A VBM study. *Schizophrenia Research*, 165(2-3), 212–219.
- Nesse, R. M., & Stein, D. J. (2012). Towards a genuinely medical model for psychiatric nosology. *BMC Medicine*, 10, 5.
- Ng, T. H., Alloy, L. B., & Smith, D. V. (2019). Meta-analysis of reward processing in major depressive disorder reveals distinct abnormalities within the reward circuit. *Translational Psychiatry*, 9(1), 293.
- Nielsen, M. Ø., Rostrup, E., Broberg, B. V., Wulff, S., & Glenthøj, B. (2018). Negative Symptoms and Reward Disturbances in Schizophrenia Before and After Antipsychotic Monotherapy. *Clinical EEG and Neuroscience: Official Journal of the EEG and Clinical Neuroscience Society*, 49(1), 36–45.



- Nielsen, M. O., Rostrup, E., Wulff, S., Bak, N., Broberg, B. V., Lublin, H., Kapur, S., & Glenthøj, B. (2012). Improvement of brain reward abnormalities by antipsychotic monotherapy in schizophrenia. *Archives of General Psychiatry*, *69*(12), 1195–1204.
- Nurnberger, J. I., Jr, Blehar, M. C., Kaufmann, C. A., York-Cooler, C., Simpson, S. G., Harkavy-Friedman, J., Severe, J. B., Malaspina, D., & Reich, T. (1994). Diagnostic interview for genetic studies. Rationale, unique features, and training. NIMH Genetics Initiative. *Archives of General Psychiatry*, *51*(11), 849–859; discussion 863–864.
- Nusslock, R., & Alloy, L. B. (2017). Reward processing and mood-related symptoms: An RDoC and translational neuroscience perspective. In *Journal of Affective Disorders* (Vol. 216, pp. 3–16).  
<https://doi.org/10.1016/j.jad.2017.02.001>
- Nygård, M., Eichele, T., Løberg, E.-M., Jørgensen, H. A., Johnsen, E., Kroken, R. A., Berle, J. Ø., & Hugdahl, K. (2012). Patients with Schizophrenia Fail to Up-Regulate Task-Positive and Down-Regulate Task-Negative Brain Networks: An fMRI Study Using an ICA Analysis Approach. *Frontiers in Human Neuroscience*, *6*, 149.
- Ogawa, S., Lee, T. M., Kay, A. R., & Tank, D. W. (1990). Brain magnetic resonance imaging with contrast dependent on blood oxygenation. *Proceedings of the National Academy of Sciences of the United States of America*, *87*(24), 9868–9872.
- Olabi, B., Ellison-Wright, I., McIntosh, A. M., Wood, S. J., Bullmore, E., & Lawrie, S. M. (2011). Are there progressive brain changes in schizophrenia? A meta-analysis of structural magnetic resonance imaging studies. *Biological Psychiatry*, *70*(1), 88–96.
- Oldham, S., Murawski, C., Fornito, A., Youssef, G., Yücel, M., & Lorenzetti, V. (2018). The anticipation and outcome phases of reward and loss processing: A neuroimaging meta-analysis of the monetary incentive delay task. In *Human Brain Mapping* (Vol. 39, Issue 8, pp. 3398–3418). <https://doi.org/10.1002/hbm.24184>
- Olds, J., & Milner, P. (1954). Positive reinforcement produced by electrical stimulation of septal area and other regions of rat brain. *Journal of Comparative and Physiological Psychology*, *47*(6), 419–427.
- Ongür, D., Lundy, M., Greenhouse, I., Shinn, A. K., Menon, V., Cohen, B. M., & Renshaw, P. F. (2010). Default mode network abnormalities in bipolar disorder and schizophrenia. *Psychiatry Research*, *183*(1), 59–68.
- Orlov, N. D., Giampietro, V., O'Daly, O., Lam, S.-L., Barker, G. J., Rubia, K., McGuire, P., Shergill, S. S., & Allen, P. (2018). Real-time fMRI neurofeedback to down-regulate superior temporal gyrus activity in patients with schizophrenia and auditory hallucinations: a proof-of-concept study. *Translational Psychiatry*, *8*(1), 46.

- O'Sullivan, N., Szczepanowski, R., El-Deredy, W., Mason, L., & Bentall, R. P. (2011). fMRI evidence of a relationship between hypomania and both increased goal-sensitivity and positive outcome-expectancy bias. *Neuropsychologia*, *49*(10), 2825–2835.
- Ozomaro, U., Wahlestedt, C., & Nemeroff, C. B. (2013). Personalized medicine in psychiatry: problems and promises. *BMC Medicine*, *11*, 132.
- Pan, P. M., Sato, J. R., Salum, G. A., Rohde, L. A., Gadelha, A., Zugman, A., Mari, J., Jackowski, A., Picon, F., Miguel, E. C., Pine, D. S., Leibenluft, E., Bressan, R. A., & Stringaris, A. (2017). Ventral Striatum Functional Connectivity as a Predictor of Adolescent Depressive Disorder in a Longitudinal Community-Based Sample. In *American Journal of Psychiatry* (Vol. 174, Issue 11, pp. 1112–1119). <https://doi.org/10.1176/appi.ajp.2017.17040430>
- Papageorgiou, C., & Wells, A. (2020). Nature, Functions, and Beliefs about Depressive Rumination. In *Depressive Rumination* (pp. 1–20). <https://doi.org/10.1002/9780470713853.ch1>
- Parker, D. B., & Razlighi, Q. R. (2019). Task-evoked Negative BOLD Response and Functional Connectivity in the Default Mode Network are Representative of Two Overlapping but Separate Neurophysiological Processes. *Scientific Reports*, *9*(1), 14473.
- Park, S.-C. (2019). Karl Jaspers' General Psychopathology (Allgemeine Psychopathologie) and Its Implication for the Current Psychiatry. *Psychiatry Investigation*, *16*(2), 99–108.
- Patel, V., & Saxena, S. (2014). Transforming Lives, Enhancing Communities — Innovations in Global Mental Health. In *New England Journal of Medicine* (Vol. 370, Issue 6, pp. 498–501). <https://doi.org/10.1056/nejmp1315214>
- Pergola, G., Selvaggi, P., Trizio, S., Bertolino, A., & Blasi, G. (2015). The role of the thalamus in schizophrenia from a neuroimaging perspective. *Neuroscience and Biobehavioural Reviews*, *54*, 57–75.
- Perkins, D. O., Gu, H., Boteva, K., & Lieberman, J. A. (2005). Relationship between duration of untreated psychosis and outcome in first-episode schizophrenia: a critical review and meta-analysis. *The American Journal of Psychiatry*, *162*(10), 1785–1804.
- Pessiglione, M., Seymour, B., Flandin, G., Dolan, R. J., & Frith, C. D. (2006). Dopamine-dependent prediction errors underpin reward-seeking behaviour in humans. *Nature*, *442*(7106), 1042–1045.
- Pierce, R. C., & Kumaresan, V. (2006). The mesolimbic dopamine system: the final common pathway for the reinforcing effect of drugs of abuse? *Neuroscience and Biobehavioural Reviews*, *30*(2), 215–238.

- Pijnenburg, A. J., Honig, W. M., & Van Rossum, J. M. (1975). Inhibition of d-amphetamine-induced locomotor activity by injection of haloperidol into the nucleus accumbens of the rat. *Psychopharmacologia*, *41*(2), 87–95.
- Pincus, H. A., Tew, J. D., & First, M. B. (2004). Psychiatric comorbidity: is more less? *World Psychiatry: Official Journal of the World Psychiatric Association*, *3*(1), 18–23.
- Pineda, D. A., Lopera, F., Puerta, I. C., Trujillo-Orrego, N., Aguirre-Acevedo, D. C., Hincapié-Henao, L., Arango, C. P., Acosta, M. T., Holzinger, S. I., Palacio, J. D., Pineda-Alvarez, D. E., Velez, J. I., Martinez, A. F., Lewis, J. E., Muenke, M., & Arcos-Burgos, M. (2011). Potential cognitive endophenotypes in multigenerational families: segregating ADHD from a genetic isolate. *Attention Deficit and Hyperactivity Disorders*, *3*(3), 291–299.
- Pizzagalli, D. A., Holmes, A. J., Dillon, D. G., Goetz, E. L., Birk, J. L., Bogdan, R., Dougherty, D. D., Iosifescu, D. V., Rauch, S. L., & Fava, M. (2009). Reduced Caudate and Nucleus Accumbens Response to Rewards in Unmedicated Individuals With Major Depressive Disorder. In *American Journal of Psychiatry* (Vol. 166, Issue 6, pp. 702–710). <https://doi.org/10.1176/appi.ajp.2008.08081201>
- Plichta, M. M., Vasic, N., Wolf, R. C., Lesch, K.-P., Brummer, D., Jacob, C., Fallgatter, A. J., & Grön, G. (2009). Neural hyporesponsiveness and hyperresponsiveness during immediate and delayed reward processing in adult attention-deficit/hyperactivity disorder. *Biological Psychiatry*, *65*(1), 7–14.
- Pomarol-Clotet, E., Salvador, R., Sarró, S., Gomar, J., Vila, F., Martínez, A., Guerrero, A., Ortiz-Gil, J., Sans-Sansa, B., Capdevila, A., Cebamano, J. M., & McKenna, P. J. (2008). Failure to deactivate in the prefrontal cortex in schizophrenia: dysfunction of the default mode network? *Psychological Medicine*, *38*(8), 1185–1193.
- Portela, A., & Esteller, M. (2010). Epigenetic modifications and human disease. In *Nature Biotechnology* (Vol. 28, Issue 10, pp. 1057–1068). <https://doi.org/10.1038/nbt.1685>.
- Pourhassan Shamchi, S., Khosravi, M., Taghvaei, R., Zirkachian Zadeh, M., Paydary, K., Emamzadehfard, S., Werner, T. J., Høilund-Carlsen, P. F., & Alavi, A. (2018). Normal patterns of regional brain F-FDG uptake in normal aging. *Hellenic Journal of Nuclear Medicine*, *21*(3), 175–180.
- Prochaska, J. J., Das, S., & Young-Wolff, K. C. (2017). Smoking, Mental Illness, and Public Health. *Annual Review of Public Health*, *38*, 165–185.
- Prossin, A. R., McInnis, M. G., Anand, A., Heitzeg, M. M., & Zubieta, J.-K. (2010). Tackling the Kraepelinian Dichotomy: a Neuroimaging Review. *Psychiatric Annals*, *40*(3), 154–159.

- Province, M. A., Shannon, W. D., & Rao, D. C. (2001). Classification methods for confronting heterogeneity. *Advances in Genetics*, *42*, 273–286.
- Psychiatrie. Ein Lehrbuch für Studierende und Aerzte von Dr. Emil Kraepelin, Professor an der Universität Heidelberg. Sechste, vollständig umgearbeitete Auflage. (Leipzig, Verlag von Johann Ambrosius Barth. 1899.) (Psychiatry. By Dr. EMIL KRAEPELIN. Sixth completely revised edition.). (1900). In *American Journal of Psychiatry* (Vol. 57, Issue 1, pp. 191–194). <https://doi.org/10.1176/ajp.57.1.191>
- Purcell, S., Neale, B., Todd-Brown, K., Thomas, L., Ferreira, M. A. R., Bender, D., Maller, J., Sklar, P., de Bakker, P. I. W., Daly, M. J., & Sham, P. C. (2007). PLINK: a tool set for whole-genome association and population-based linkage analyses. *American Journal of Human Genetics*, *81*(3), 559–575.
- Quevedo, K., Ng, R., Scott, H., Kodavaganti, S., Smyda, G., Diwadkar, V., & Phillips, M. (2017). Ventral Striatum Functional Connectivity during Rewards and Losses and Symptomatology in Depressed Patients. *Biological Psychology*, *123*, 62–73.
- Raichle, M. E., MacLeod, A. M., Snyder, A. Z., Powers, W. J., Gusnard, D. A., & Shulman, G. L. (2001). A default mode of brain function. *Proceedings of the National Academy of Sciences of the United States of America*, *98*(2), 676–682.
- Rangel, A., Camerer, C., & Montague, P. R. (2008). A framework for studying the neurobiology of value-based decision making. *Nature Reviews. Neuroscience*, *9*(7), 545–556.
- Razafimandimby, A., Hervé, P.-Y., Marzloff, V., Brazo, P., Tzourio-Mazoyer, N., & Dollfus, S. (2016). Functional deficit of the medial prefrontal cortex during emotional sentence attribution in schizophrenia. *Schizophrenia Research*, *178*(1-3), 86–93.
- Read, J., van Os, J., Morrison, A. P., & Ross, C. A. (2005). Childhood trauma, psychosis and schizophrenia: a literature review with theoretical and clinical implications. *Acta Psychiatrica Scandinavica*, *112*(5), 330–350.
- Regier, D. A. (1990). Comorbidity of mental disorders with alcohol and other drug abuse. Results from the Epidemiologic Catchment Area (ECA) Study. In *JAMA: The Journal of the American Medical Association* (Vol. 264, Issue 19, pp. 2511–2518). <https://doi.org/10.1001/jama.264.19.2511>
- Rehm, J., & Shield, K. D. (2019). Global Burden of Disease and the Impact of Mental and Addictive Disorders. *Current Psychiatry Reports*, *21*(2), 10.

- Reitz, C., & Mayeux, R. (2009). Endophenotypes in normal brain morphology and Alzheimer's disease: a review. *Neuroscience*, *164*(1), 174–190.
- Renner, F., Siep, N., Arntz, A., van de Ven, V., Peeters, F. P. M. L., Quaedflieg, C. W. E. M., & Huibers, M. J. H. (2017). Negative mood-induction modulates default mode network resting-state functional connectivity in chronic depression. *Journal of Affective Disorders*, *208*, 590–596.
- Richards, J. M., Plate, R. C., & Ernst, M. (2013). A systematic review of fMRI reward paradigms used in studies of adolescents vs. adults: the impact of task design and implications for understanding neurodevelopment. *Neuroscience and Biobehavioural Reviews*, *37*(5), 976–991.
- Robert Cloninger, C., & Svrakic, D. M. (1994). *The Temperament and Character Inventory (TCI): A Guide to Its Development and Use*.
- Rodríguez-Cano, E., Alonso-Lana, S., Sarró, S., Fernández-Corcuera, P., Goikolea, J. M., Vieta, E., Maristany, T., Salvador, R., McKenna, P. J., & Pomarol-Clotet, E. (2017). Differential failure to deactivate the default mode network in unipolar and bipolar depression. *Bipolar Disorders*, *19*(5), 386–395.
- Roehrig, C. (2016). Mental Disorders Top The List Of The Most Costly Conditions In The United States: \$201 Billion. *Health Affairs*, *35*(6), 1130–1135.
- Rolland, B., Amad, A., Poulet, E., Bordet, R., Vignaud, A., Bation, R., Delmaire, C., Thomas, P., Cottencin, O., & Jardri, R. (2015). Resting-state functional connectivity of the nucleus accumbens in auditory and visual hallucinations in schizophrenia. *Schizophrenia Bulletin*, *41*(1), 291–299.
- Ross, C. A., & Margolis, R. L. (2019). Research Domain Criteria: Strengths, Weaknesses, and Potential Alternatives for Future Psychiatric Research. *Molecular Neuropsychiatry*, *5*(4), 218–236.
- Rost, K., Zhang, M., Fortney, J., Smith, J., Coyne, J., & Smith, G. R., Jr. (1998). Persistently poor outcomes of undetected major depression in primary care. *General Hospital Psychiatry*, *20*(1), 12–20.
- Russo, G., Zegar, C., & Giordano, A. (2003). Advantages and limitations of microarray technology in human cancer. In *Oncogene* (Vol. 22, Issue 42, pp. 6497–6507). <https://doi.org/10.1038/sj.onc.1206865>
- Ryali, S., Supekar, K., Chen, T., Kochalka, J., Cai, W., Nicholas, J., Padmanabhan, A., & Menon, V. (2016). Temporal Dynamics and Developmental Maturation of Salience, Default and Central-Executive Network Interactions Revealed by Variational Bayes Hidden Markov Modeling. In *PLOS Computational Biology* (Vol. 12, Issue 12, p. e1005138). <https://doi.org/10.1371/journal.pcbi.1005138>

- Sacchet, M. D., Livermore, E. E., Iglesias, J. E., Glover, G. H., & Gotlib, I. H. (2015). Subcortical volumes differentiate Major Depressive Disorder, Bipolar Disorder, and remitted Major Depressive Disorder. *Journal of Psychiatric Research, 68*, 91–98.
- Saha, S., Chant, D., & McGrath, J. (2007). A Systematic Review of Mortality in Schizophrenia. In *Archives of General Psychiatry* (Vol. 64, Issue 10, p. 1123). <https://doi.org/10.1001/archpsyc.64.10.1123>
- Salgado-Pineda, P., Fakra, E., Delaveau, P., McKenna, P. J., Pomarol-Clotet, E., & Blin, O. (2011). Correlated structural and functional brain abnormalities in the default mode network in schizophrenia patients. *Schizophrenia Research, 125*(2-3), 101–109.
- Salvatore, J. E., Gottesman, I. I., & Dick, D. M. (2015). Endophenotypes for Alcohol Use Disorder: An Update on the Field. *Current Addiction Reports, 2*(1), 76–90.
- Samanez-Larkin, G. R., Gibbs, S. E. B., Khanna, K., Nielsen, L., Carstensen, L. L., & Knutson, B. (2007). Anticipation of monetary gain but not loss in healthy older adults. *Nature Neuroscience, 10*(6), 787–791.
- Sämman, P. G., Wehrle, R., Hoehn, D., Spoormaker, V. I., Peters, H., Tully, C., Holsboer, F., & Czisch, M. (2011). Development of the brain's default mode network from wakefulness to slow wave sleep. *Cerebral Cortex, 21*(9), 2082–2093.
- Sartorius, N., Shapiro, R., Kimura, M., & Barrett, K. (1972). WHO International Pilot Study of Schizophrenia. In *Psychological Medicine* (Vol. 2, Issue 4, pp. 422–425). <https://doi.org/10.1017/s0033291700045244>
- Satterthwaite, T. D., Kable, J. W., Vandekar, L., Katchmar, N., Bassett, D. S., Baldassano, C. F., Ruparel, K., Elliott, M. A., Sheline, Y. I., Gur, R. C., Gur, R. E., Davatzikos, C., Leibenluft, E., Thase, M. E., & Wolf, D. H. (2015). Common and Dissociable Dysfunction of the Reward System in Bipolar and Unipolar Depression. *Neuropsychopharmacology: Official Publication of the American College of Neuropsychopharmacology, 40*(9), 2258–2268.
- Saunders, K. E. A., & Goodwin, G. M. (2010). The course of bipolar disorder. In *Advances in Psychiatric Treatment* (Vol. 16, Issue 5, pp. 318–328). <https://doi.org/10.1192/apt.bp.107.004903>
- Schacter, D., Gilbert, D., Wegner, D., & Hood, B. (2015). *Psychology: Second European Edition*. Macmillan International Higher Education.
- Schizoaffective Disorder in the DSM-5. (2013). *Schizophrenia Research, 150*(1), 21–25.
- Schizophrenia Working Group of the Psychiatric Genomics Consortium. (2014). Biological insights from 108 schizophrenia-associated genetic loci. *Nature, 511*(7510), 421–427.

- Schlagenhauf, F., Juckel, G., Koslowski, M., Kahnt, T., Knutson, B., Dembler, T., Kienast, T., Gallinat, J., Wrase, J., & Heinz, A. (2008). Reward system activation in schizophrenic patients switched from typical neuroleptics to olanzapine. *Psychopharmacology*, *196*(4), 673–684.
- Schneider, M., Leuchs, L., Czisch, M., Sämann, P. G., & Spoormaker, V. I. (2018). Disentangling reward anticipation with simultaneous pupillometry / fMRI. *NeuroImage*, *178*, 11–22.
- Schöpf, V., Windischberger, C., Kasess, C. H., Lanzenberger, R., & Moser, E. (2010). Group ICA of resting-state data: a comparison. *Magma*, *23*(5-6), 317–325.
- Schreiter, S., Spengler, S., Willert, A., Mohnke, S., Herold, D., Erk, S., Romanczuk-Seiferth, N., Quinlivan, E., Hindi-Attar, C., Banzhaf, C., Wackerhagen, C., Romund, L., Garbusow, M., Stamm, T., Heinz, A., Walter, H., & Bermanpohl, F. (2016). Neural alterations of fronto-striatal circuitry during reward anticipation in euthymic bipolar disorder. In *Psychological Medicine* (Vol. 46, Issue 15, pp. 3187–3198).  
<https://doi.org/10.1017/s0033291716001963>
- Schultze-Lutter, F., Ruhrmann, S., Pickler, H., von Reventlow, H. G., Brockhaus-Dumke, A., & Klosterkötter, J. (2007). Basic symptoms in early psychotic and depressive disorders. *The British Journal of Psychiatry. Supplement*, *51*, s31–s37.
- Schultz, W. (1998). Predictive Reward Signal of Dopamine Neurons. In *Journal of Neurophysiology* (Vol. 80, Issue 1, pp. 1–27). <https://doi.org/10.1152/jn.1998.80.1.1>
- Schultz, W. (2016). Dopamine reward prediction-error signalling: a two-component response. *Nature Reviews. Neuroscience*, *17*(3), 183–195.
- Schultz, W., Apicella, P., Scarnati, E., & Ljungberg, T. (1992). Neuronal activity in monkey ventral striatum related to the expectation of reward. *The Journal of Neuroscience: The Official Journal of the Society for Neuroscience*, *12*(12), 4595–4610.
- Schulze, T. G., Akula, N., Breuer, R., Steele, J., Nalls, M. A., Singleton, A. B., Degenhardt, F. A., Nöthen, M. M., Cichon, S., Rietschel, M., Bipolar Genome Study, & McMahon, F. J. (2014). Molecular genetic overlap in bipolar disorder, schizophrenia, and major depressive disorder. *The World Journal of Biological Psychiatry: The Official Journal of the World Federation of Societies of Biological Psychiatry*, *15*(3), 200–208.

- Shan, X., Liao, R., Ou, Y., Ding, Y., Liu, F., Chen, J., Zhao, J., Guo, W., & He, Y. (2020). Metacognitive Training Modulates Default-Mode Network Homogeneity During 8-Week Olanzapine Treatment in Patients With Schizophrenia. *Frontiers in Psychiatry / Frontiers Research Foundation*, *11*, 234.
- Sheline, Y. I., Barch, D. M., Price, J. L., Rundle, M. M., Vaishnavi, S. N., Snyder, A. Z., Mintun, M. A., Wang, S., Coalson, R. S., & Raichle, M. E. (2009). The default mode network and self-referential processes in depression. *Proceedings of the National Academy of Sciences of the United States of America*, *106*(6), 1942–1947.
- Shoptaw, S. J., Kao, U., & Ling, W. (2009). Treatment for amphetamine psychosis. In *Cochrane Database of Systematic Reviews*. <https://doi.org/10.1002/14651858.cd003026.pub3>
- Smitha, K. A., Akhil Raja, K., Arun, K. M., Rajesh, P. G., Thomas, B., Kapilamoorthy, T. R., & Kesavadas, C. (2017). Resting state fMRI: A review on methods in resting state connectivity analysis and resting state networks. *The Neuroradiology Journal*, *30*(4), 305–317.
- Smoller, J. W., Andreassen, O. A., Edenberg, H. J., Faraone, S. V., Glatt, S. J., & Kendler, K. S. (2019). Psychiatric genetics and the structure of psychopathology. In *Molecular Psychiatry* (Vol. 24, Issue 3, pp. 409–420). <https://doi.org/10.1038/s41380-017-0010-4>
- Smoller, J. W., & Finn, C. T. (2003). Family, twin, and adoption studies of bipolar disorder. In *American Journal of Medical Genetics Part C: Seminars in Medical Genetics* (Vol. 123C, Issue 1, pp. 48–58). <https://doi.org/10.1002/ajmg.c.20013>
- Snyder, J. S., Soumier, A., Brewer, M., Pickel, J., & Cameron, H. A. (2011). Adult hippocampal neurogenesis buffers stress responses and depressive behaviour. *Nature*, *476*(7361), 458–461.
- Spies, M., Kraus, C., Geissberger, N., Auer, B., Klöbl, M., Tik, M., Stürkat, I.-L., Hahn, A., Woletz, M., Pfabigan, D. M., Kasper, S., Lamm, C., Windischberger, C., & Lanzenberger, R. (2017). Default mode network deactivation during emotion processing predicts early antidepressant response. *Translational Psychiatry*, *7*(1), e1008.
- Stahl, E. A., Breen, G., Forstner, A. J., McQuillin, A., Ripke, S., Trubetskoy, V., Mattheisen, M., Wang, Y., Coleman, J. R. I., Gaspar, H. A., de Leeuw, C. A., Steinberg, S., Pavlides, J. M. W., Trzaskowski, M., Byrne, E. M., Pers, T. H., Holmans, P. A., Richards, A. L., Abbott, L., ... Bipolar Disorder Working Group of the Psychiatric Genomics Consortium. (2019). Genome-wide association study identifies 30 loci associated with bipolar disorder. *Nature Genetics*, *51*(5), 793–803.



- Stein, D. J., Szatmari, P., Gaebel, W., Berk, M., Vieta, E., Maj, M., de Vries, Y. A., Roest, A. M., de Jonge, P., Maercker, A., Brewin, C. R., Pike, K. M., Grilo, C. M., Fineberg, N. A., Briken, P., Cohen-Kettenis, P. T., & Reed, G. M. (2020). Mental, behavioural and neurodevelopmental disorders in the ICD-11: an international perspective on key changes and controversies. *BMC Medicine*, *18*(1), 21.
- Stein, J. L., Medland, S. E., Vasquez, A. A., Hibar, D. P., Senstad, R. E., Winkler, A. M., Toro, R., Appel, K., Bartecek, R., Bergmann, Ø., Bernard, M., Brown, A. A., Cannon, D. M., Chakravarty, M. M., Christoforou, A., Domin, M., Grimm, O., Hollinshead, M., Holmes, A. J., ... Enhancing Neuro Imaging Genetics through Meta-Analysis Consortium. (2012). Identification of common variants associated with human hippocampal and intracranial volumes. *Nature Genetics*, *44*(5), 552–561.
- Stevens, L., & Rodin, I. (2011). Depressive disorder – clinical presentation. In *Psychiatry* (pp. 52–53). Elsevier.
- Stott, S. R. W., & Ang, S.-L. (2013). The Generation of Midbrain Dopaminergic Neurons. In *Patterning and Cell Type Specification in the Developing CNS and PNS* (pp. 435–453). <https://doi.org/10.1016/b978-0-12-397265-1.00099-x>
- Strauss, G. P., & Gold, J. M. (2012). A new perspective on anhedonia in schizophrenia. *The American Journal of Psychiatry*, *169*(4), 364–373.
- Stringaris, A., Belil, P. V.-R., Artiges, E., Lemaitre, H., Gollier-Briant, F., Wolke, S., Vulser, H., Miranda, R., Penttilä, J., Struve, M., Fadai, T., Kappel, V., Grimmer, Y., Goodman, R., Poustka, L., Conrod, P., Cattrell, A., Banaschewski, T., Bokde, A. L. W., ... IMAGEN Consortium. (2015). The Brain's Response to Reward Anticipation and Depression in Adolescence: Dimensionality, Specificity, and Longitudinal Predictions in a Community-Based Sample. In *American Journal of Psychiatry* (Vol. 172, Issue 12, pp. 1215–1223). <https://doi.org/10.1176/appi.ajp.2015.14101298>
- Subramaniam, K., Hooker, C. I., Biagiante, B., Fisher, M., Nagarajan, S., & Vinogradov, S. (2015). Neural signal during immediate reward anticipation in schizophrenia: Relationship to real-world motivation and function. *NeuroImage. Clinical*, *9*, 153–163.
- Sullivan, P. F., Kendler, K. S., & Neale, M. C. (2003). Schizophrenia as a complex trait: evidence from a meta-analysis of twin studies. *Archives of General Psychiatry*, *60*(12), 1187–1192.

- Sullivan, P. F., Neale, M. C., & Kendler, K. S. (2000). Genetic Epidemiology of Major Depression: Review and Meta-Analysis. In *American Journal of Psychiatry* (Vol. 157, Issue 10, pp. 1552–1562).  
<https://doi.org/10.1176/appi.ajp.157.10.1552>
- Swann, A. C., Pazzaglia, P., Nicholls, A., Dougherty, D. M., & Moeller, F. G. (2003). Impulsivity and phase of illness in bipolar disorder. *Journal of Affective Disorders*, 73(1-2), 105–111.
- Syan, S. K., Smith, M., Frey, B. N., Remtulla, R., Kapczynski, F., Hall, G. B. C., & Minuzzi, L. (2018). Resting-state functional connectivity in individuals with bipolar disorder during clinical remission: a systematic review. *Journal of Pediatric Neurology: JPN*, 43(5), 298–316.
- Takahashi, T., Yücel, M., Lorenzetti, V., Walterfang, M., Kawasaki, Y., Whittle, S., Suzuki, M., Pantelis, C., & Allen, N. B. (2010). An MRI study of the superior temporal subregions in patients with current and past major depression. *Progress in Neuro-Psychopharmacology & Biological Psychiatry*, 34(1), 98–103.
- Takano, K., & Tanno, Y. (2009). Self-rumination, self-reflection, and depression: self-rumination counteracts the adaptive effect of self-reflection. *Behaviour Research and Therapy*, 47(3), 260–264.
- Tandon, R., Gaebel, W., Barch, D. M., Bustillo, J., Gur, R. E., Heckers, S., Malaspina, D., Owen, M. J., Schultz, S., Tsuang, M., Van Os, J., & Carpenter, W. (2013). Definition and description of schizophrenia in the DSM-5. *Schizophrenia Research*, 150(1), 3–10.
- Tandon, R., & Maj, M. (2008). Nosological status and definition of schizophrenia: Some considerations for DSM-V and ICD-11. *Asian Journal of Psychiatry*, 1(2), 22–27.
- Taylor, K. S., Seminowicz, D. A., & Davis, K. D. (2009). Two systems of resting state connectivity between the insula and cingulate cortex. *Human Brain Mapping*, 30(9), 2731–2745.
- The limbic (emotional) system. (2009). In *Auricular Acupuncture & Addiction* (pp. 57–67). Elsevier.
- Thomas, P. E., Klinger, R., Furlong, L. I., Hofmann-Apitius, M., & Friedrich, C. M. (2011). Challenges in the association of human single nucleotide polymorphism mentions with unique database identifiers. *BMC Bioinformatics*, 12 Suppl 4, S4.
- Thompson, P. M., Stein, J. L., Medland, S. E., Hibar, D. P., Vasquez, A. A., Renteria, M. E., Toro, R., Jahanshad, N., Schumann, G., Franke, B., Wright, M. J., Martin, N. G., Agartz, I., Alda, M., Alhusaini, S., Almasry, L., Almeida, J.,

- Alpert, K., Andreasen, N. C., ... Alzheimer's Disease Neuroimaging Initiative, EPIGEN Consortium, IMAGEN Consortium, Saguenay Youth Study (SYS) Group. (2014). The ENIGMA Consortium: large-scale collaborative analyses of neuroimaging and genetic data. *Brain Imaging and Behavior*, *8*(2), 153–182.
- Tomasi, D., & Volkow, N. D. (2010). Functional connectivity density mapping. *Proceedings of the National Academy of Sciences of the United States of America*, *107*(21), 9885–9890.
- Tomasi, D., & Volkow, N. D. (2011). Functional connectivity hubs in the human brain. In *NeuroImage* (Vol. 57, Issue 3, pp. 908–917). <https://doi.org/10.1016/j.neuroimage.2011.05.024>
- Torrubia, R., Ávila, C., Moltó, J., & Caseras, X. (2001). The Sensitivity to Punishment and Sensitivity to Reward Questionnaire (SPSRQ) as a measure of Gray's anxiety and impulsivity dimensions. *Personality and Individual Differences*, *31*(6), 837–862.
- Trautmann, S., Rehm, J., & Wittchen, H.-U. (2016). The economic costs of mental disorders: Do our societies react appropriately to the burden of mental disorders? *EMBO Reports*, *17*(9), 1245–1249.
- Travis, A. (2003). Mood Disorders, Biology. In *Encyclopedia of the Neurological Sciences* (pp. 202–208). <https://doi.org/10.1016/b0-12-226870-9/01184-9>
- Tripp, G., & Wickens, J. R. (2008). Research review: dopamine transfer deficit: a neurobiological theory of altered reinforcement mechanisms in ADHD. *Journal of Child Psychology and Psychiatry, and Allied Disciplines*, *49*(7), 691–704.
- Trøstheim, M., Eikemo, M., Meir, R., Hansen, I., Paul, E., Kroll, S. L., Garland, E. L., & Leknes, S. (2020). Assessment of Anhedonia in Adults With and Without Mental Illness: A Systematic Review and Meta-analysis. *JAMA Network Open*, *3*(8), e2013233.
- Trost, S., Diekhof, E. K., Zvonik, K., Lewandowski, M., Usher, J., Keil, M., Zilles, D., Falkai, P., Dechent, P., & Gruber, O. (2014). Disturbed anterior prefrontal control of the mesolimbic reward system and increased impulsivity in bipolar disorder. *Neuropsychopharmacology: Official Publication of the American College of Neuropsychopharmacology*, *39*(8), 1914–1923.
- Trudeau, L.-E. (2004). Glutamate co-transmission as an emerging concept in monoamine neuron function. *Journal of Psychiatry & Neuroscience: JPN*, *29*(4), 296–310.

- Tzourio-Mazoyer, N., Landeau, B., Papathanassiou, D., Crivello, F., Etard, O., Delcroix, N., Mazoyer, B., & Joliot, M. (2002). Automated anatomical labeling of activations in SPM using a macroscopic anatomical parcellation of the MNI MRI single-subject brain. *NeuroImage*, *15*(1), 273–289.
- Urošević, S., Luciana, M., Jensen, J. B., Youngstrom, E. A., & Thomas, K. M. (2016). Age associations with neural processing of reward anticipation in adolescents with bipolar disorders. *NeuroImage. Clinical*, *11*, 476–485.
- van Dam, D. S., van der Ven, E., Velthorst, E., Selten, J. P., Morgan, C., & de Haan, L. (2012). Childhood bullying and the association with psychosis in non-clinical and clinical samples: a review and meta-analysis. *Psychological Medicine*, *42*(12), 2463–2474.
- van den Heuvel, M. P., & Hulshoff Pol, H. E. (2010). Exploring the brain network: a review on resting-state fMRI functional connectivity. *European Neuropsychopharmacology: The Journal of the European College of Neuropsychopharmacology*, *20*(8), 519–534.
- van Erp, T. G. M., Hibar, D. P., Rasmussen, J. M., Glahn, D. C., Pearlson, G. D., Andreassen, O. A., Agartz, I., Westlye, L. T., Haukvik, U. K., Dale, A. M., Melle, I., Hartberg, C. B., Gruber, O., Kraemer, B., Zilles, D., Donohoe, G., Kelly, S., McDonald, C., Morris, D. W., ... Turner, J. A. (2016). Subcortical brain volume abnormalities in 2028 individuals with schizophrenia and 2540 healthy controls via the ENIGMA consortium. *Molecular Psychiatry*, *21*(4), 585.
- Vanes, L. D., Mouchlianitis, E., Collier, T., Averbach, B. B., & Shergill, S. S. (2018). Differential neural reward mechanisms in treatment-responsive and treatment-resistant schizophrenia. *Psychological Medicine*, *48*(14), 2418–2427.
- van Leijenhorst, L., Crone, E. A., & Bunge, S. A. (2006). Neural correlates of developmental differences in risk estimation and feedback processing. *Neuropsychologia*, *44*(11), 2158–2170.
- Van Leijenhorst, L., Zanolie, K., Van Meel, C. S., Westenberg, P. M., Rombouts, S. A. R. B., & Crone, E. A. (2010). What motivates the adolescent? Brain regions mediating reward sensitivity across adolescence. *Cerebral Cortex*, *20*(1), 61–69.
- van Os, J., Kenis, G., & Rutten, B. P. F. (2010). The environment and schizophrenia. *Nature*, *468*(7321), 203–212.
- Varese, F., Barkus, E., & Bentall, R. P. (2012). Dissociation mediates the relationship between childhood trauma and hallucination-proneness. *Psychological Medicine*, *42*(5), 1025–1036.

- Verhaak, P. F. M., Schellevis, F. G., Nuijen, J., & Volkers, A. C. (2006). Patients with a psychiatric disorder in general practice: determinants of general practitioners' psychological diagnosis. *General Hospital Psychiatry, 28*(2), 125–132.
- Vermani, M., Marcus, M., & Katzman, M. A. (2011). Rates of detection of mood and anxiety disorders in primary care: a descriptive, cross-sectional study. *The Primary Care Companion to CNS Disorders, 13*(2).  
<https://doi.org/10.4088/PCC.10m01013>
- Visscher, P. M., Wray, N. R., Zhang, Q., Sklar, P., McCarthy, M. I., Brown, M. A., & Yang, J. (2017). 10 Years of GWAS Discovery: Biology, Function, and Translation. *American Journal of Human Genetics, 101*(1), 5–22.
- Viswanathan, V., Lee, S., Gilman, J. M., Kim, B. W., Lee, N., Chamberlain, L., Livengood, S. L., Raman, K., Lee, M. J., Kuster, J., Stern, D. B., Calder, B., Mulhern, F. J., Blood, A. J., & Breiter, H. C. (2015). Age-related striatal BOLD changes without changes in behavioural loss aversion. *Frontiers in Human Neuroscience, 9*, 176.
- Walker, E. R., McGee, R. E., & Druss, B. G. (2015). Mortality in Mental Disorders and Global Disease Burden Implications. In *JAMA Psychiatry* (Vol. 72, Issue 4, p. 334). <https://doi.org/10.1001/jamapsychiatry.2014.2502>
- Wang, T., Zhang, X., Li, A., Zhu, M., Liu, S., Qin, W., Li, J., Yu, C., Jiang, T., & Liu, B. (2017). Polygenic risk for five psychiatric disorders and cross-disorder and disorder-specific neural connectivity in two independent populations. *NeuroImage. Clinical, 14*, 441–449.
- Wang, X., Zhang, Y., Long, Z., Zheng, J., Zhang, Y., Han, S., Wang, Y., Duan, X., Yang, M., Zhao, J., & Chen, H. (2017). Frequency-specific alteration of functional connectivity density in antipsychotic-naïve adolescents with early-onset schizophrenia. *Journal of Psychiatric Research, 95*, 68–75.
- Wang, Y., Gao, Y., Tang, S., Lu, L., Zhang, L., Bu, X., Li, H., Hu, X., Hu, X., Jiang, P., Jia, Z., Gong, Q., Sweeney, J. A., & Huang, X. (2020). Large-scale network dysfunction in the acute state compared to the remitted state of bipolar disorder: A meta-analysis of resting-state functional connectivity. *EBioMedicine, 54*, 102742.
- Ward, A. M., Schultz, A. P., Huijbers, W., Van Dijk, K. R. A., Hedden, T., & Sperling, R. A. (2014). The parahippocampal gyrus links the default-mode cortical network with the medial temporal lobe memory system. *Human Brain Mapping, 35*(3), 1061–1073.
- Weickert, T. W., Goldberg, T. E., Gold, J. M., Bigelow, L. B., Egan, M. F., & Weinberger, D. R. (2000). Cognitive impairments in patients with schizophrenia displaying preserved and compromised intellect. *Archives of General Psychiatry, 57*(9), 907–913.

- White, T. P., Gilleen, J., & Shergill, S. S. (2013). Dysregulated but not decreased salience network activity in schizophrenia. In *Frontiers in Human Neuroscience* (Vol. 7). <https://doi.org/10.3389/fnhum.2013.00065>
- White, T. P., Joseph, V., Francis, S. T., & Liddle, P. F. (2010). Aberrant salience network (bilateral insula and anterior cingulate cortex) connectivity during information processing in schizophrenia. *Schizophrenia Research*, *123*(2-3), 105–115.
- Whitfield-Gabrieli, S., & Ford, J. M. (2012). Default mode network activity and connectivity in psychopathology. *Annual Review of Clinical Psychology*, *8*, 49–76.
- Whitton, A. E., Treadway, M. T., & Pizzagalli, D. A. (2015). Reward processing dysfunction in major depression, bipolar disorder and schizophrenia. *Current Opinion in Psychiatry*, *28*(1), 7–12.
- Wible, C. G., Anderson, J., Shenton, M. E., Kricun, A., Hirayasu, Y., Tanaka, S., Levitt, J. J., O'Donnell, B. F., Kikinis, R., Jolesz, F. A., & McCarley, R. W. (2001). Prefrontal cortex, negative symptoms, and schizophrenia: an MRI study. In *Psychiatry Research: Neuroimaging* (Vol. 108, Issue 2, pp. 65–78). [https://doi.org/10.1016/s0925-4927\(01\)00109-3](https://doi.org/10.1016/s0925-4927(01)00109-3)
- Williams, J. M., & Scott, J. (1988). Autobiographical memory in depression. *Psychological Medicine*, *18*(3), 689–695.
- Williamson, P. (2007). Are anticorrelated networks in the brain relevant to schizophrenia? *Schizophrenia Bulletin*, *33*(4), 994–1003.
- Willis, M. A., & Haines, D. E. (2018). The Limbic System. In *Fundamental Neuroscience for Basic and Clinical Applications* (pp. 457–467.e1). <https://doi.org/10.1016/b978-0-323-39632-5.00031-1>
- Wilson, R. P., Colizzi, M., Bossong, M. G., Allen, P., Kempton, M., MTAC, & Bhattacharyya, S. (2018). The Neural Substrate of Reward Anticipation in Health: A Meta-Analysis of fMRI Findings in the Monetary Incentive Delay Task. *Neuropsychology Review*, *28*(4), 496–506.
- Wingenfeld, K., Spitzer, C., Mensebach, C., Grabe, H., Hill, A., Gast, U., Schlosser, N., Höpp, H., Beblo, T., & Driessen, M. (2010). Die deutsche Version des Childhood Trauma Questionnaire (CTQ): Erste Befunde zu den psychometrischen Kennwerten. In *PPmP - Psychotherapie · Psychosomatik · Medizinische Psychologie* (Vol. 60, Issue 11, pp. 442–450). <https://doi.org/10.1055/s-0030-1247564>
- Wise, R. A., & Rompre, P. P. (1989). Brain Dopamine and Reward. In *Annual Review of Psychology* (Vol. 40, Issue 1, pp. 191–225). <https://doi.org/10.1146/annurev.ps.40.020189.001203>

- Wittchen, H. U., Jacobi, F., Rehm, J., Gustavsson, A., Svensson, M., Jönsson, B., Olesen, J., Allgulander, C., Alonso, J., Faravelli, C., Fratiglioni, L., Jennum, P., Lieb, R., Maercker, A., van Os, J., Preisig, M., Salvador-Carulla, L., Simon, R., & Steinhausen, H.-C. (2011). The size and burden of mental disorders and other disorders of the brain in Europe 2010. *European Neuropsychopharmacology: The Journal of the European College of Neuropsychopharmacology*, *21*(9), 655–679.
- Wittgenstein, L. (1996). *Philosophische Bemerkungen*.
- World Health Organization, WHO Staff, & WHO. (1992). *The ICD-10 Classification of Mental and Behavioural Disorders: Clinical Descriptions and Diagnostic Guidelines*. World Health Organization.
- Wulsin, L. R., Vaillant, G. E., & Wells, V. E. (1999). A Systematic Review of the Mortality of Depression. In *Psychosomatic Medicine* (Vol. 61, Issue 1, pp. 6–17). <https://doi.org/10.1097/00006842-199901000-00003>
- Yang, X.-H., Huang, J., Lan, Y., Zhu, C.-Y., Liu, X.-Q., Wang, Y.-F., Cheung, E. F. C., Xie, G.-R., & Chan, R. C. K. (2016). Diminished caudate and superior temporal gyrus responses to effort-based decision making in patients with first-episode major depressive disorder. *Progress in Neuro-Psychopharmacology & Biological Psychiatry*, *64*, 52–59.
- Yip, S. W., Worhunsky, P. D., Rogers, R. D., & Goodwin, G. M. (2015). Hypoactivation of the ventral and dorsal striatum during reward and loss anticipation in antipsychotic and mood stabilizer-naïve bipolar disorder. *Neuropsychopharmacology: Official Publication of the American College of Neuropsychopharmacology*, *40*(3), 658–666.
- Zald, D. H., & Treadway, M. T. (2017). Reward Processing, Neuroeconomics, and Psychopathology. *Annual Review of Clinical Psychology*, *13*, 471–495.
- Zeng, L.-L., Shen, H., Liu, L., Wang, L., Li, B., Fang, P., Zhou, Z., Li, Y., & Hu, D. (2012). Identifying major depression using whole-brain functional connectivity: a multivariate pattern analysis. *Brain: A Journal of Neurology*, *135*(Pt 5), 1498–1507.
- Zhong, Y., Wang, C., Gao, W., Xiao, Q., Lu, D., Jiao, Q., Su, L., & Lu, G. (2019). Aberrant Resting-State Functional Connectivity in the Default Mode Network in Pediatric Bipolar Disorder Patients with and without Psychotic Symptoms. *Neuroscience Bulletin*, *35*(4), 581–590.
- Zhou, H.-X., Chen, X., Shen, Y.-Q., Li, L., Chen, N.-X., Zhu, Z.-C., Castellanos, F. X., & Yan, C.-G. (2020). Rumination and the default mode network: Meta-analysis of brain imaging studies and implications for depression. *NeuroImage*, *206*, 116287.

- Zhuo, C., Zhu, J., Qin, W., Qu, H., Ma, X., Tian, H., Xu, Q., & Yu, C. (2014). Functional connectivity density alterations in schizophrenia. *Frontiers in Behavioural Neuroscience, 8*. <https://doi.org/10.3389/fnbeh.2014.00404>
- Zhuo, C., Zhu, J., Wang, C., Qu, H., Ma, X., Tian, H., Liu, M., & Qin, W. (2017). Brain structural and functional dissociated patterns in schizophrenia. *BMC Psychiatry, 17*(1), 45.
- Zink, C. F., Pagnoni, G., Martin-Skurski, M. E., Chappelow, J. C., & Berns, G. S. (2004). Human striatal responses to monetary reward depend on saliency. *Neuron, 42*(3), 509–517.
- Zovetti, N., Rossetti, M. G., Perlini, C., Maggioni, E., Bontempi, P., Bellani, M., & Brambilla, P. (2020). Default mode network activity in bipolar disorder. *Epidemiology and Psychiatric Sciences, 29*, e166.
- Zubin, J. (1975). Vulnerability-a new view of schizophrenia. In *PsycEXTRA Dataset*.  
<https://doi.org/10.1037/e544502009-010>



## Acknowledgements

At this point, I would like to thank several people without whose support this work would not have been possible.

First, I would like to express my sincere gratitude to Philipp Sämann not only for his professional and constantly available support, but also for his genuine interest in brain functioning which was very inspiring and motivating. Moreover, I would like to thank Elisabeth Binder for her encouraging advice and professional guidance. Furthermore, I would like to thank Nikos Koutsouleris for his contribution as a member of my thesis advisory committee and his feedback. I also express my gratitude to Michael Czisch for his methodological advices and providing access to the MRI research facilities. Additionally, I would like to thank the technical assistants of the Neuroimaging Core Unit, particularly Ines Eidner and Anna Gallner, for their tremendous support and patience during the data collection phase.

My sincere thanks also go to my PhD colleagues for their help with the data acquisition, their advice, coffee breaks and discussions on both scientific and non-scientific topics. Special mention goes to my colleague Riya Paul who became a good friend of mine over the years and whose emotional support helped carrying me through my PhD. Similar, I owe a great debt of gratitude to all my friends for always having my back and providing a necessary balance to work.

Above all, I am deeply grateful to my parents for their constant and loving support on many levels.

Thank you all for the wonderful and exciting time which I will always keep in good memory!



## Affidavit



### Affidavit

Eberle, Christopher

Surname, first name

Nußbaumstraße 7

Street

80336, Munich, Germany

Zip code, town, country

I hereby declare, that the submitted thesis entitled:

Ventral striatal fMRI in affective and psychotic disorders:

A transdiagnostic approach using resting state and task functional resonance imaging, clinical and genetic data

is my own work. I have only used the sources indicated and have not made unauthorised use of services of a third party. Where the work of others has been quoted or reproduced, the source is always given.

I further declare that the submitted thesis or parts thereof have not been presented as part of an examination degree to any other university.

Munich, 20.09.2022

place, date

Christopher Eberle

Signature doctoral candidate



## Confirmation of congruency



**Confirmation of congruency between printed and electronic version of the doctoral thesis**

Eberle, Christopher

Surname, first name

Nußbaumstraße 7

Street

80336, Munich, Germany

Zip code, town, country

I hereby declare, that the submitted thesis entitled:

Ventral striatal fMRI in affective and psychotic disorders:  
A transdiagnostic approach using resting state and task functional resonance imaging, clinical and genetic data

is congruent with the printed version both in content and format.

Munich, 20.09.2022

place, date

Christopher Eberle

Signature doctoral candidate



## Publication

Eberle C, Peterse Y, Jukic F, Müller-Myhsok B, Czamara D, Martins J, et al. Endophenotype Potential of Nucleus Accumbens Functional Connectivity: Effects of Polygenic Risk for Schizophrenia Interacting with Childhood Adversity. *J Psychiatry Brain Sci.* 2019;4:e190011. <https://doi.org/10.20900/jpbs.20190011>